ABSTRACT

Title of Document:	SEISMIC RESPONSE OF ACCELERATION-SENSITIVE NONSTRUCTURAL COMPONENTS MOUNTED ON MOMENT-RESISTING FRAME STRUCTURES Ragunath Sankaranarayanan, Doctor of Philosophy, 2007
Directed By:	Assistant Professor Ricardo A. Medina, Department of Civil and Environmental Engineering

A statistical analysis of the peak acceleration demands for nonstructural components (NSCs) supported on elastic and inelastic regular moment-resisting frame structures is presented. The response of a variety of stiff and flexible frame structures (with 3, 6, 9, 12, 15, and 18 stories) subjected to a set of 40 far-field ground motions are evaluated. The NSCs under consideration are those that can be represented by single-degree-of-freedom systems with masses that are small as compared to the total mass of the supporting structure. The study evaluates and quantifies the dependence of peak component accelerations on the location of the nonstructural component in the structure, the damping ratio of the component, and the properties of the supporting structure such as its modal periods, height, stiffness distribution, and strength. The results show that current seismic code provisions will not always provide an adequate characterization of

peak component accelerations especially when the period of the NSCs fall in the higher modal period region of the supporting structure and the provisions do not address the inelastic action of the supporting structure. A parameter called as acceleration response modification factor (R_{acc}) is proposed to quantify the reduction in component amplification factors and inelastic FRS that is achieved due to the inelastic behavior of the building. A methodology that makes use of the R_{acc} factor to estimate the acceleration demands on NSCs mounted on inelastic supporting structures from that of elastic buildings is outlined. Separate R_{acc} factors are proposed for long-period, fundamental-period and short-period regions of the FRS at three different locations in the building namely roof, mid-height, and bottom-third location. A comparison of the proposed R_{acc} factors to that of results obtained from real multi-bay buildings show that the recommendations fall within 20% error range for both fundamental-period and short-period regions of FRS.

SEISMIC RESPONSE OF ACCELERATION-SENSITIVE NONSTRUCTURAL COMPONENTS MOUNTED ON MOMENT-RESISTING FRAME STRUCTURES

By

Ragunath Sankaranarayanan

Dissertation submitted to the Faculty of the Graduate School of the
University of Maryland, College Park, in partial fulfillment
of the requirements for the degree of
Doctor of Philosophy
2007

Advisory Committee:
Assistant Professor Ricardo A. Medina, Chair
Associate Professor Mark A. Austin
Associate Professor Peter C. Chang
Associate Professor David J. Lovell
Professor Norman M. Wereley

Dedication

Dedicated with gratitude to my parents and my spiritual gurus

Sri Sivaprabhakara Siddhayogi Paramahamsar,

Brahmasri Siddharajan Swami, and

Sri Kanakanpatti Mootai Swami.

Acknowledgements

I would like to thank all my instructors, colleagues, classmates, and friends at the University of Maryland (UMD) who have been invaluable sources of knowledge throughout my doctoral program. First and foremost, I wish to express my sincere appreciation and gratitude to my advisor Dr. Ricardo Medina for his patient guidance, encouragement and expertise throughout my graduate study. I am grateful to Dr. Mark Austin, Dr. Peter Chang, Dr. David Lovell and Professor Norman Wereley for serving on my committee and for providing their invaluable comments and suggestions.

I would like to record my deep sense of gratitude to my parents and my brothers, who had supported me morally and other ways during the period of my research. Their constant prayers and the blessings of my spiritual gurus had carried me through difficult times and I dedicate this dissertation to them.

I would like to thank my office-mates and fellow doctoral candidates Kyungha Park, and Antonio Rigato for their advice, understanding, help, and moral support. We had spent numerous hours discussing our research problems and had learnt a lot from each other.

The time that I had spent as a graduate assistant in learning technologies group of office of information technology had exposed me to effective teaching skills in both online and face-to-face environments. I thoroughly enjoyed the numerous workshops and support sessions that I had conducted with my supervisors and other members of the group. I am indebted to the group members for helping me to improve my instructional and communication skills: Ellen Borkowski, Michael Cain, William Dardick, Charles

Goldman, Ryan Harvey, Christopher Higgins, Mary Kot-Jansen, Deborah Mateik, Cherry Morgan, Sharon Roushdy, and David White. My special thanks to William Dardick, Charles Goldman, and Ryan Harvey for actively discussing my research problem from the computational point-of-view and for offering their expertise on optimizing my code in a cluster computing environment.

I thank Professor John Baras, Dionysus Blazakis, Kimberley Edwards, Althia Kirlew, and other staff members of Institute for Systems Research for their support and understanding when I worked on their website. I am thankful to Peg Jayant and Carlos Luceno for assisting me while using the Beowuf cluster for some of my simulations.

I would like to thank all my housemates and friends for their constant encouragement and support: Vishnu Arcot, Mr. & Mrs. Rakesh Bobba, Karthikeyan Chandrashekar, Mr. & Mrs. Jitamitra Karcherla, Mr. & Mrs. Karumbu Meyyappan, Mr. & Mrs. Aditya Naik, Mr. & Mrs. Akshay Naik, Mr. & Mrs. Patrick Pancras, Mr. & Mrs. Manikandan Ramasamy, and Kapil Sahasrabudhe.

I would like to thank the incredibly knowledgeable and helpful UMD librarians who always put in the extra effort to get me past reports and articles. In particular, I would like to thank Robert Kackley (EPSL), Jim Miller (EPSL), and Charles Wright (Interlibrary Loan Department).

I have received help directly and indirectly from many others for whom I am thankful. I have tried to acknowledge everyone who had helped me in my doctoral program. It is impossible to remember all and I apologize for those who have been inadvertently left out.

Table of Contents

List of Tables

List of Figures

Chapter 1: Introduction

1.1 MOTIVATION FOR THIS STUDY

Nonstructural Components (NSC) or Secondary Structures (SS) are those systems and elements housed on or attached to the floors, roofs and walls of a building or industrial facility that are not part of their main or intended load bearing structural system. They may also be subjected large seismic forces and must depend on their own structural characteristics to resist these forces (Villaverde 1991; 1997a). Although mostly ignored in current earthquake design methodology of buildings, the NSCs constitute a major part of damage in the event of an earthquake (Mckevitt et al. 1995; Myrtle et al. 2005). The damage costs of NSCs may account for 65% to 85% of the total construction cost of commercial buildings. In critical facilities like hospitals, the *indirect losses* due to damaged equipment, lost inventory and records, and revenue can be two to three times greater than the cost of replacing collapsed buildings or structures (Scholl 1984; Segal and Hall 1989; Naeim 2000; Taghavi and Miranda 2003). In the recent 2003 Bam earthquake almost all the NSCs in existing buildings suffered damage (Hosseini 2005). Moreover, the survival of NSCs during an earthquake is important for maintaining the operation of emergency services and the continuing functionality of a building. The damage to nonstructural components may also pose life safety concerns to the occupants (McKevitt 2004; Watts 2004).

Nonstructural portions of a building include every part of the building and all its contents that are not part of the building's structure i.e. everything except the columns,

floors, beams, load-bearing walls, etc. Examples of non-structural portions of a building are ceilings, windows, office equipment, furniture, inventory, appliances, heating, ventilation & air conditioning equipment, and electrical systems. In general NSCs are classified into three main categories: (1) architectural components, (2) mechanical and electrical equipment and systems, and (3) building contents and inventory (Villaverde 2004; Griffin 2006). Examples of the first category are building cladding systems, ceiling and lighting systems, interior partition walls, raised computer floors, and racks and shelving systems. Electrical power and distribution systems, heating, ventilation and cooling systems, fire protection systems, and emergency power systems are examples of the second category. Among some in the third category are production / manufacturing equipment and systems, computer equipment, record storage, supplies / inventory and furniture. Figure 1.1 shows some examples of acceleration-sensitive NSCs and damage to them in 1994 Northridge earthquake (Naeim and Lobo 1998; ATC 1999; Gould 2003).

Based on their primary types of failure, they can be classified either as displacement/deformation-sensitive components or acceleration-sensitive components. The displacement failures are mainly caused by excessive inter-story building displacements or drift. They can also be caused by incompatible stiffness or lack of proper detailing between the building structure and NSC. The inertial failures are caused by shaking of the component or rocking/sliding due to unanchored or marginally anchored conditions.

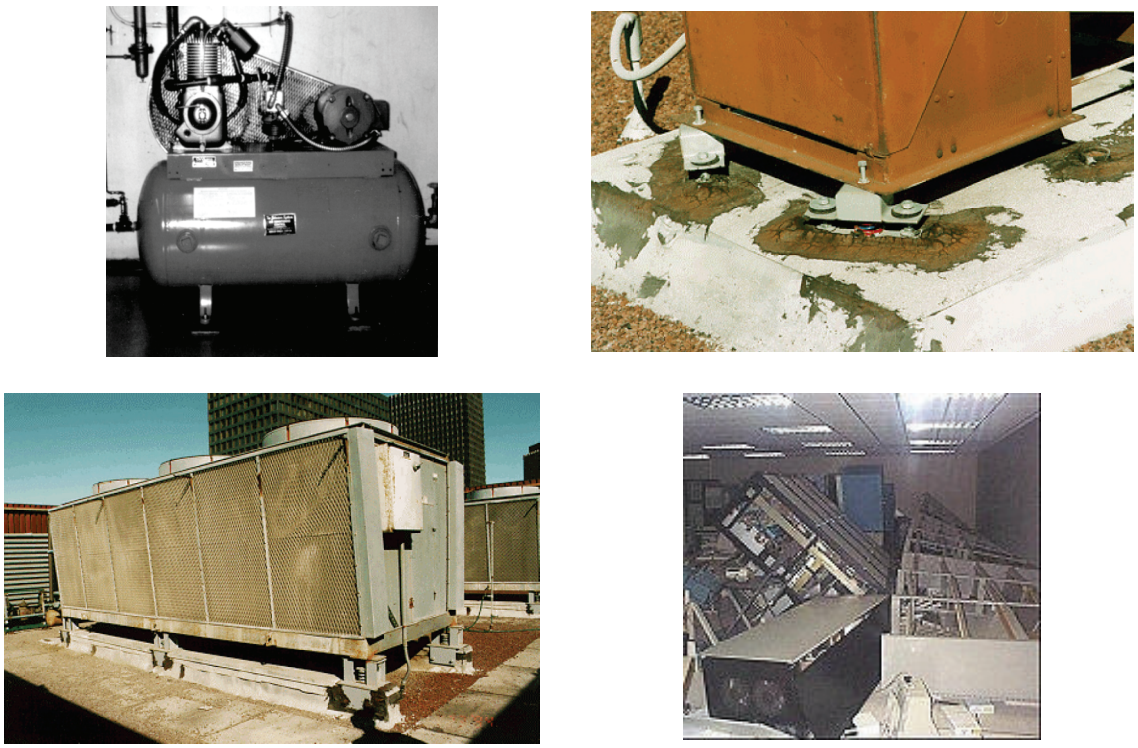

Figure 1.1 Examples of acceleration-sensitive nonstructural components and their damage (Naeim and Lobo 1998; ATC 1999; Gould 2003)

Based on their modeling, NSCs can be classified as rigid, flexible and hanging type systems. A component is rigid if its period is less than or equal to 0.06 sec (BSSC 2003). For rigid systems, the dynamic properties depend primarily on the ductility of its anchors. Engines and motors rigidly attached to floors are good examples. For flexible systems, it might be necessary to model the element as MDOF system with distributed mass and stiffness. These are typically attached to multiple points in the building. Examples are signboards and pipelines. For the third category of systems hanging from above, they may be modeled as single mass pendulum. Examples are lighting systems, cable trays and chandeliers. It can be said that when compared to the different

classifications of building systems, the types of NSCs are more diverse and hence they can be classified based on a variety of criteria. This makes the development of specific performance evaluation procedures for NSCs more challenging.

While more advanced and rational techniques for evaluating building structures have been developed under the framework of Performance Based Earthquake Engineering (PBEE), the advances in the area of NSCs are minimal. This is reflected in the ATC-58 project task 2.3 report (ATC 2004), which acknowledges the need to identify the Engineering Demand Parameters (EDPs) that would constitute the basis for next-generation Performance Based Earthquake Engineering guidelines. The term EDPs, denotes the structural response quantities that can be used to predict damage to structural and nonstructural components and systems. Thus, studies on NSCs are an important thrust area in PBEE.

Figure 1.2 shows the overview of the PBEE process (Moehle 2003). The first step is the identification of one or more ground motion Intensity Measures (IMs) that captures the important characteristics of earthquake ground motion that affect the performance of building and NSCs. For the assessment of the performance of a building system, some examples of IM are Peak Ground Acceleration (PGA), Peak Ground Velocity (PGV), Peak Ground Displacement (PGD) or a spectral response quantity such as spectral displacement (S_d), velocity (S_v) or acceleration (S_a). The NSCs are not directly affected by ground shaking. The building response acts like a filter that changes the earthquake characteristics for the NSCs. Hence for NSCs the IM should characterize not the intensity of ground shaking but rather the intensity of response motion of the building structure at the points of attachment of the NSCs.

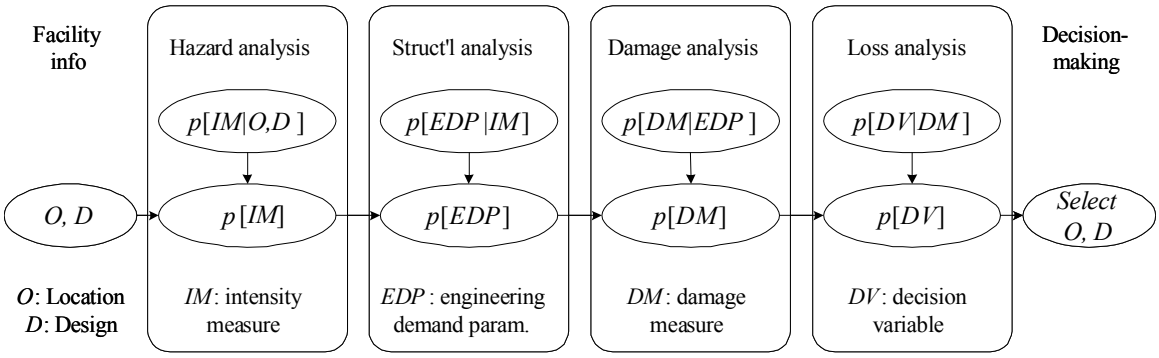

Figure 1.2 Overview of PBEE Process (Moehle 2003)

The second step is to determine the EDPs that describe the response of the structure as a whole and of its individual structural components. For NSCs this step means selecting the structural EDPs calculated from the predicted response of structures, which predict the severity of shaking the NSC is subjected to. Floor Response Spectrum (FRS) is a good example of EDP_{NSC}. The ATC-58 document specifically notes that the traditional code demand parameters for NSCs are based on indirect and unproven procedures. The reduced equivalent static values provided in codes and FEMA 273/274 are based on judgment and it is not known if they correlate well with actual performance (ATC 2004). Current EDP_{NSC} for NSCs are not directly linked to the nonlinear dynamic response of the actual building in which the components are located. As explained in the later sections, the current dissertation focuses on this step and aims to address some of the shortcomings in the step 2 of PBEE process.

The third step is to relate the EDPs to Damage Measures (DMs) that describe the physical condition of the components and contents. DMs include effective descriptions of damage state or condition, which are then used to estimate the effects on functionality,

occupancy-readiness, life safety consequences and necessary repairs of nonstructural components and systems. The product of this step are the conditional probabilities, p[DM|EDP], which are then integrated with p[EDP] to calculate the mean annual frequencies of exceedance.

The final step in the PBEE process is the calculation of Decision Variables (DVs) that serve to translate damage estimates into quantities that are useful to those tasked with making risk-related decisions. The decision variables relate to decision metrics namely dollar losses, downtime and deaths. This step results in getting the conditional probabilities, p[DM|EDP], which are then integrated with p[DM] to calculate the mean annual frequencies of exceedance for the DV, p[DV].

1.2 OBJECTIVES AND OUTLINE

The global objective of this study is to arrive at a methodology for the statistical quantification of acceleration (strength) demands of NSCs mounted on multi-story frames especially in the inelastic domain. Development of such a methodology requires the understanding and quantification of the demands imposed by ground motions on elastic acceleration-sensitive NSCs mounted on elastic and inelastic regular moment-resisting frames with different configurations and structural properties. Although vast amounts of information (sometimes closed form solutions) are available for estimating the acceleration demands on NSCs in the elastic domain, only sparse studies had attempted to estimate the demands on NSCs when the building behaves inelastically. Endeavors at estimating a response modification factors that can be applied to acceleration demands on NSCs mounted on elastic buildings to obtain the corresponding demands when the building behaves inelastically will subsequently enhance the understanding of the

acceleration demands on NSCs and lead to better estimation of acceleration demands. Hence, the approach in the study is geared towards establishing an acceleration response modification factor (R_{acc}) that can make use of the existing results in the elastic domain. This factor when combined with the equipment modification factor (R_p) in current building code provisions can address both the nonlinearity of the equipment and the supporting structure.

The specific objectives are summarized as follows

- To identify Nonstructural Engineering Demand Parameters (EDP_{NSC}) helpful to characterize response of NSCs,
- To evaluate the sensitivity of the EDP_{NSC} to variations in structural properties, analysis models, and location in the building, and
- To develop a methodology to estimate the peak acceleration demands of NSCs exposed to far-field ground motions.
- To establish an acceleration response modification factor that can be applied to scale acceleration demands of components in elastic structures to obtain the corresponding demands of components mounted on inelastic structures.

The NSCs under consideration are those that can be represented by single-degree-of-freedom systems with masses that are small as compared to the total mass of the supporting structure. The NSCs are assumed to be elastic SDOF systems with single point of attachment. Studies are also conducted to identify the range for which the results of the current study are applicable when dynamic interaction effects are present.

Chapter 2 includes the discussion on the generic frames and the analysis methodology. The peak acceleration demands for acceleration-sensitive nonstructural

components supported on elastic and inelastic regular moment-resisting frame structures are statistically analyzed. The responses of a variety of stiff and flexible frame structures (with 3, 6, 9, 12, 15, and 18-stories) subjected to a set of 40 ground motions are evaluated. This study evaluates and quantifies the dependence of peak component accelerations on the location of the nonstructural component in the structure, the damping ratio of the component, and the properties of the supporting structure such as its modal periods, height, stiffness distribution, and strength.

Chapter 3 focuses on the development of a methodology to estimate the acceleration demands of NSCs. In this chapter, the results of the previous chapter are analyzed vis-à-vis the current code guidelines. The results show that current seismic code provisions do not provide an adequate characterization of peak component accelerations. A methodology is developed to estimate peak acceleration demands for the design of nonstructural components mounted on inelastic frame structures with different stiffness and strength distributions along the height. A parameter called acceleration response modification factor (R_{acc}) is introduced in this dissertation that aids in the process of estimating the peak acceleration demands on NSCs mounted on inelastic buildings from that of results from elastic buildings. The properties of R_{acc} allow the FRS to be split into three separate regions namely long-period, fundamental-period and short-period regions respectively. Recommendations for R_{acc} values in these three zones are provided based on the results of a statistical analysis done on the results obtained from a large number of time-history analyses performed in this dissertation for different levels of inelastic behavior of the supporting structure. Separate statistical equations are provided for NSCs with damping ratios of 0.01%, 1%, 2% and 5%.

In Chapter 4 the utilization of a single-bay generic frame for seismic demand evaluation of NSCs is assessed by correlating its response with that of a "real" structure. The results for two structures namely SAC LA9-M1 model and VAN NUYS model are presented. The results from R_{acc} recommendations based on statistical models in the previous chapter are compared to the median R_{acc} values obtained from the multi-bay frames.

Chapter 5 summarizes the work and lists the main conclusions drawn in this study. Three appendices are included. Appendix I presents the effect of dynamic interaction on the acceleration demands of NSCs. Recommendations are provided for the range of application of non-interaction results obtained in this study to problems involving dynamic interaction. Appendix II investigates the FRS amplifications due to localized yielding of the supporting structure using building models in which inelastic action is allowed only in the first story of the building. Appendix III presents the peak acceleration demands of NSCs for near-fault ground motions. The classification of the near-fault ground motions is primarily based on the pulse period of the normal component of the ground motion at a given site. The appendix investigates whether the methodology outlined in this dissertation can be extended to include near-fault ground motions in future studies.

Chapter 2: Parameters that Influence the Response of NSCs

Most results in this chapter have been reproduced from the paper published in *Engineering Structures* (Medina et al. 2006).

2.1 INTRODUCTION

In view of both the safety and economic relevance of minimizing damage to NSCs in earthquakes, several research efforts have focused on

(a) assessing the behavior of NSCs as well as their dynamic interaction with the primary structure (Segal and Hall 1989; Gupta 1990; Singh 1990; Adam 2001), which is discussed in detail in appendix I of this dissertation, and

(b) prescribing simplified design methodologies for such components (Singh et al. 1993; Soong et al. 1993; Villaverde 1997a; Villaverde 2006).

State-of-the-art reviews on these subjects have been presented by various researchers (Chen and Soong 1988; Soong 1994; Phan and Taylor 1996; Villaverde 1997b; Villaverde 2004). However, as demonstrated in this chapter, a *better understanding of the seismic response of NSCs is called for, especially for those mounted on inelastic moment-resisting frame structures*.

The first studies on the response of NSCs were focused on the safety of critical components in nuclear power plants (Biggs and Roesset 1970; Villaverde 1997a). These

studies led to the development of the US Nuclear Regulatory Guide 1.22 (NRC 1978). Other code regulations for the design of NSCs mounted on buildings were developed at later dates and are included in current seismic code provisions for buildings (BSSC 2003; ICC 2003). Recent research on NSCs has dealt with estimating the Peak Floor Acceleration (PFA) of structures. For instance, Rodriguez et al. (Rodriguez et al. 2002) used a modal superposition approach to evaluate PFAs for elastic and inelastic buildings whose lateral-load resisting system is composed of structural walls. Taghavi and Miranda (Miranda and Taghavi 2005; Taghavi and Miranda 2005) utilized a simplified model of a multistory building to develop a procedure to estimate the PFAs of buildings. Peak floor acceleration demands are important in the context of this study because at any given floor level the PFA provides the "anchor" point for the development of Floor Response Spectra (FRS), i.e., the PFA is the maximum acceleration of an infinitely stiff NSC.

The goal of this chapter is to evaluate peak component acceleration demands for acceleration-sensitive NSCs supported on inelastic regular moment-resisting frame structures. The response of a variety of stiff and flexible framed structures (3- to 18-stories) subjected to a set of 40 far-field ground motions is studied, i.e., ground motions without near-fault, forward-directivity characteristics (effect of near-fault ground motion on NSCs are discussed in appendix III). The NSCs under consideration are those that can be represented by elastic single-degree-of-freedom (SDOF) systems. This chapter shows the dependence of peak component accelerations on the location of the NSC in the structure and its damping ratio, as well as the properties of the supporting structure such as its modal periods, height, stiffness distribution, and strength. These studies form the

basis for the next chapter namely recommendations to estimate peak component acceleration demands for the design of NSCs mounted on elastic and inelastic frames.

2.2 ANALYSIS METHODOLOGY

The methodology used in this study consists of performing dynamic simulations in which structural models (single-bay, two-dimensional frames) are exposed to a set of ground motions. For a given structural model and ground motion, the acceleration response at selected floor levels is obtained and used as input for a SDOF analysis program to develop its corresponding floor response spectrum. The damping ratios, ζ of interest for the NSCs are 0.01%, 1%, 2%, and 5%.

It is important to note that, although stochastic methods are computationally efficient in the analysis of elastic primary and secondary structures (Gupta 1990), time-history analyses were conducted in this study because of the need to account for the inelastic behavior of the primary structure. Time history analyses were performed using DRAIN-2DX computer program (Prakash et al. 1993). The time history analyses and corresponding FRS generation, demands enormous computational resources. This study required a trusted code that can be copied to numerous machines on the network on the fly so that the simulations can be done in a distributed computing environment. Numerous research studies have used the DRAIN-2DX code for time-history analyses on various building models and the results from DRAIN-2DX are well benchmarked with results from other computer codes (Inel et al. 2001).

2.2.1 Building Models

The building models with 3, 6, 9, 12, 15 and 18 stories utilized in this study correspond to moment-resisting frame structures with the same mass at all floor levels. Each building is a two-dimensional single-bay frame with a beam span of 24 feet and a constant story height of 12 feet. The frames are designed based on the strong column-weak girder philosophy, i.e., plastification only occurs at the beam ends and at the bottom of the first-story columns (all remaining columns are assumed to be infinitely strong). A desirable design is one in which column plastification is avoided, but in some cases this goal is not actually achieved (Medina and Krawinkler 2004). However, the deformation (and acceleration) demands in the structure are not expected to be significantly altered by plastification in columns unless a story mechanism develops. Member strengths are tuned such that simultaneous yielding occurs and a beam-hinge mechanism (BH) develops when the building is subjected to a parabolic load pattern, which corresponds to a $k = 2$, NEHRP load pattern (BSSC 2003). These hinges are modeled with rotational springs whose hysteretic behavior is defined by a peak-oriented, moment-rotation relationship, with 3% strain-hardening. Five percent Rayleigh damping is assigned to the first mode and the mode at which the cumulative mass participation exceeds 95%. While the accelerations on each floor of the 3- and 6-story structures are recorded, only five floors from the 9- and 18-story frames are studied. The selected floors from the 9- and 18-story frames are uniformly distributed throughout the height of the building to provide a near-complete picture of the distribution of floor accelerations over the height of the building. Each building model and the floors for which the data are recorded are shown in figure 2.1.

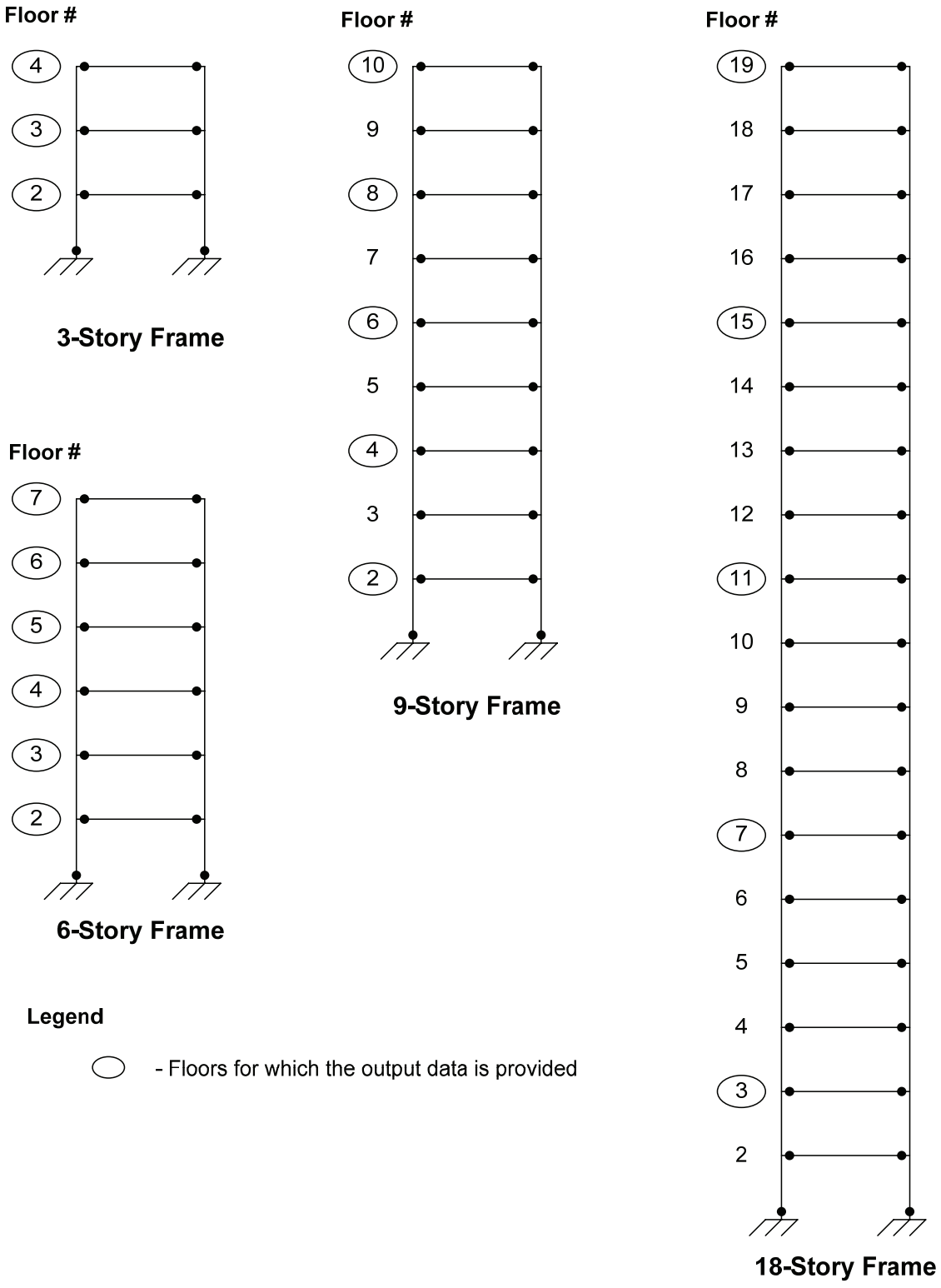

Figure 2.1 Building models and levels for which floor acceleration data was recorded

The absolute stiffness of each building model is assigned such that the first mode period (T_{B1}) is equal to either *0.1N* (stiff frame) or *0.2N* (flexible frame), where *N* is the number of stories in the structure. These T_{B1} values are considered to be reasonable bounds for reinforced concrete and steel-moment-resisting frames (Goel and Chopra 1997; 1998; Crowley and Pinho 2004; Medina and Krawinkler 2004). Two different beam-to-column stiffness ratios are used namely, one that corresponds to a linear first-mode shape, and a second one that corresponds to a nonlinear first-mode shape. Both these frames have nonlinearity distributed throughout the height of the frame. A separate study was also conducted with frame modes that have localized nonlinearity (Weak Story or WS models). The properties of these WS frames and the results obtained are discussed in Appendix II. Nonlinear first mode shape frames were used for all the studies (12 building models in total). The fundamental period of these frames cover the range from 0.3 sec. to 3.6 sec. Only a limited set of linear first mode shape frames were used. Their application is limited to understanding the difference in NSC response from that of nonlinear first mode shape frame. Hence their results were restricted to 3-, 9- and 18-story stiff / flexible frames and one stiff 6-story frame (7 building models in total). The mode shapes of linear first mode frames are presented in figures 2.2 and 2.3. Figures 2.4 to 2.6 show the mode shapes of all the nonlinear first-mode frames used in this study. The modal periods of the buildings are presented in Table 2.1.

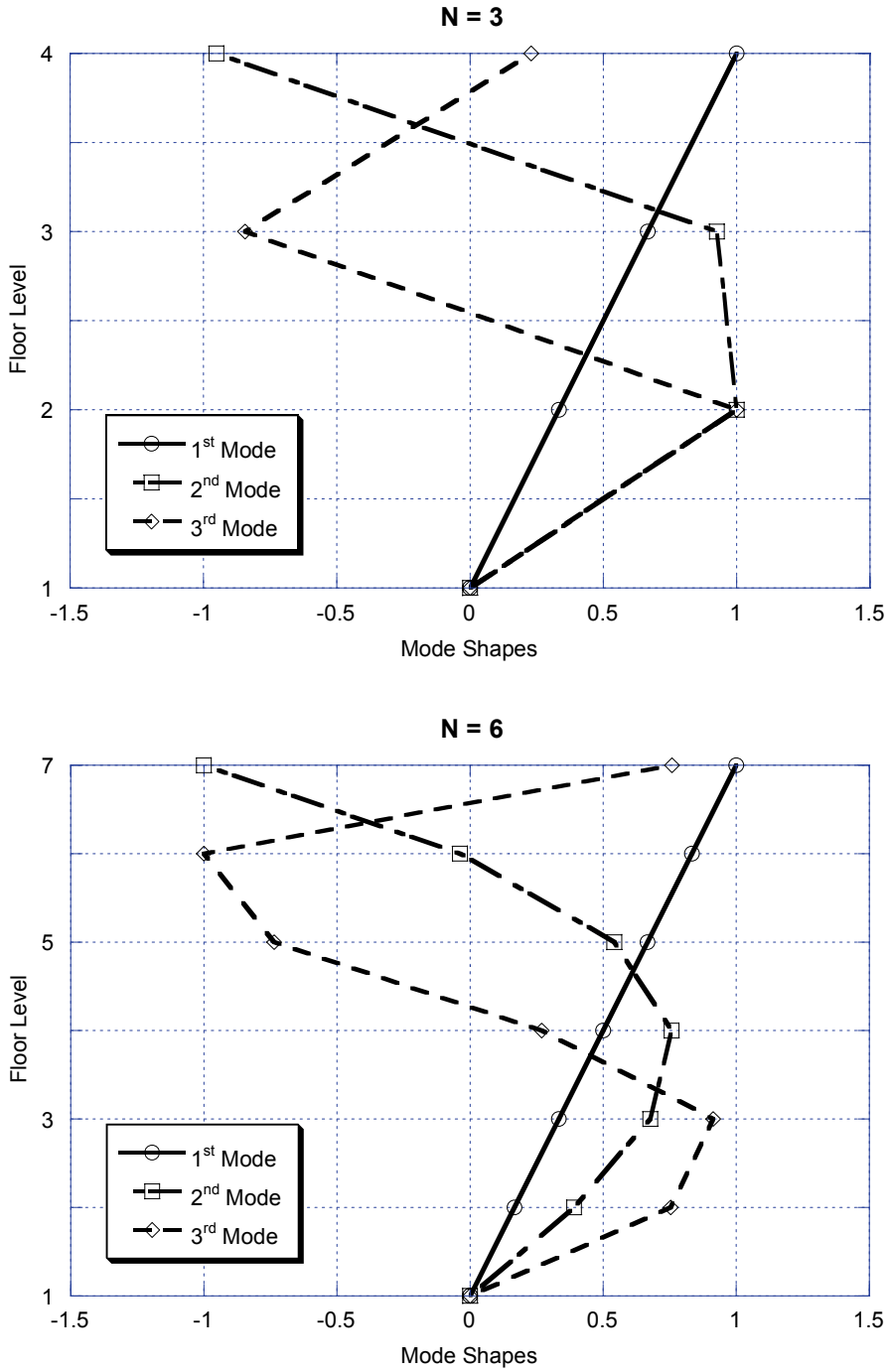

Figure 2.2 Mode shapes of *N*= 3 and *N*= 6 linear first-mode building models

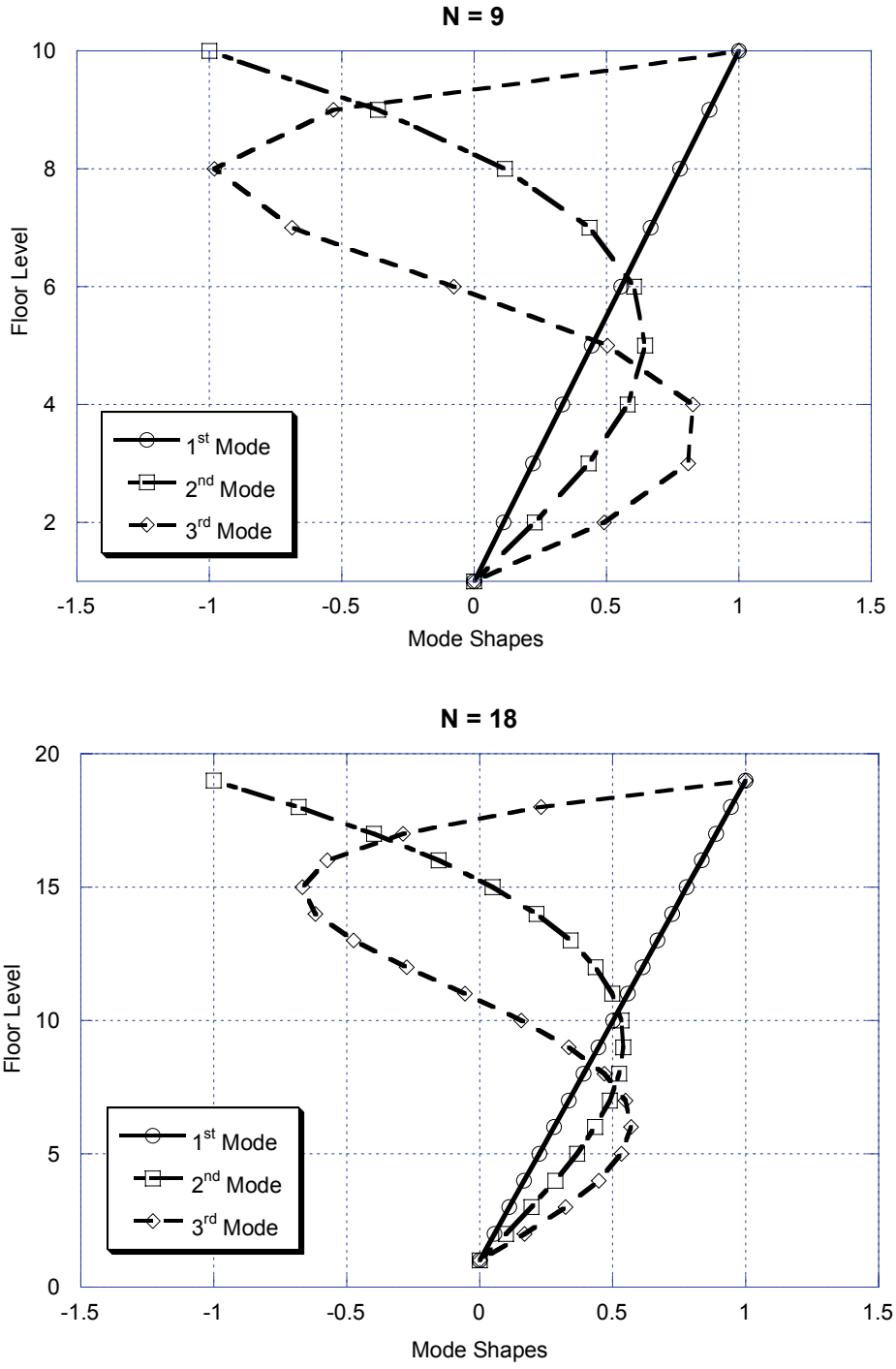

Figure 2.3 Mode shapes of *N*= 9 and *N*= 18 linear first-mode building models

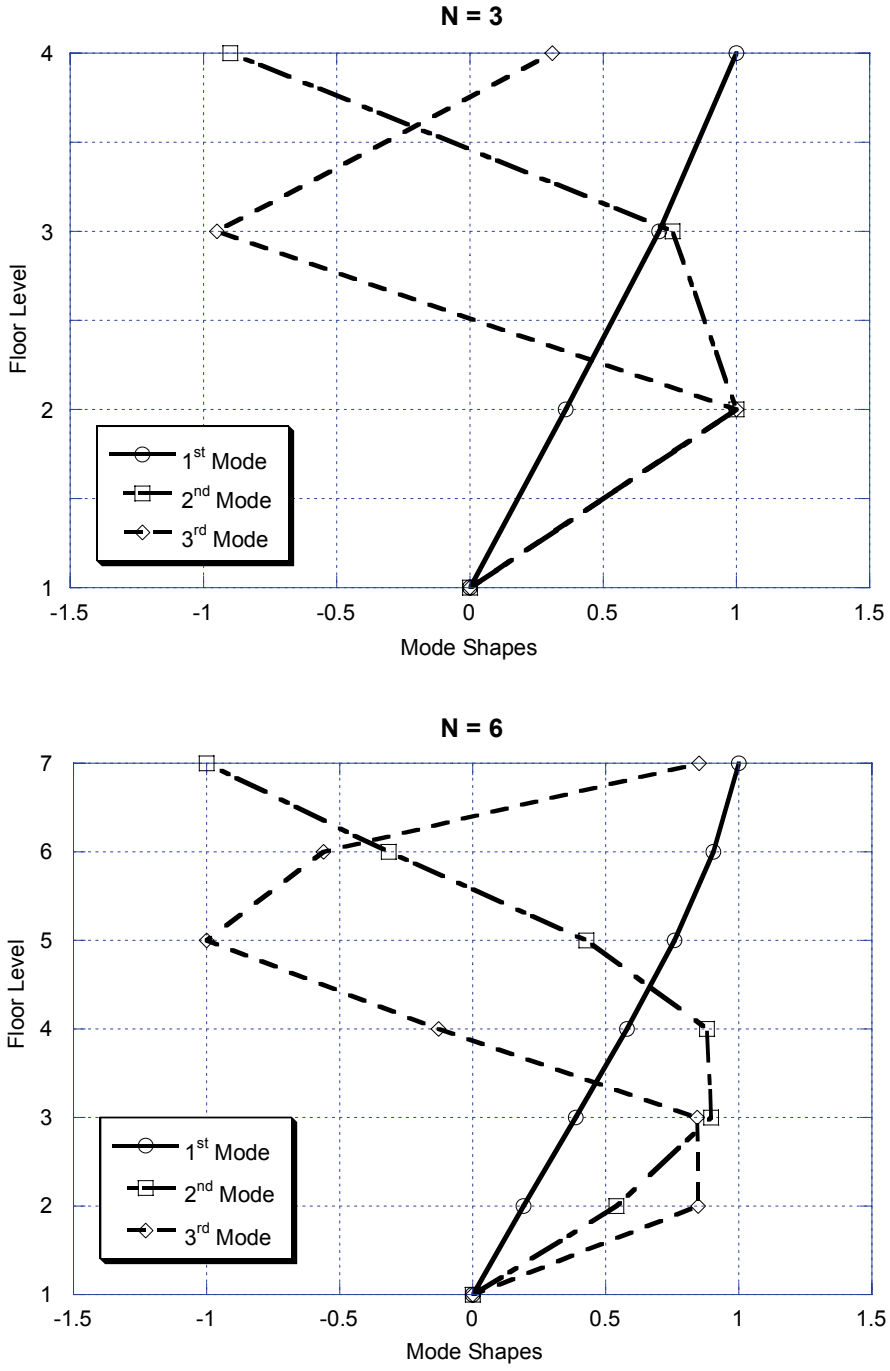

Figure 2.4 Mode shapes of *N*= 3 and *N*= 6 nonlinear first-mode building models

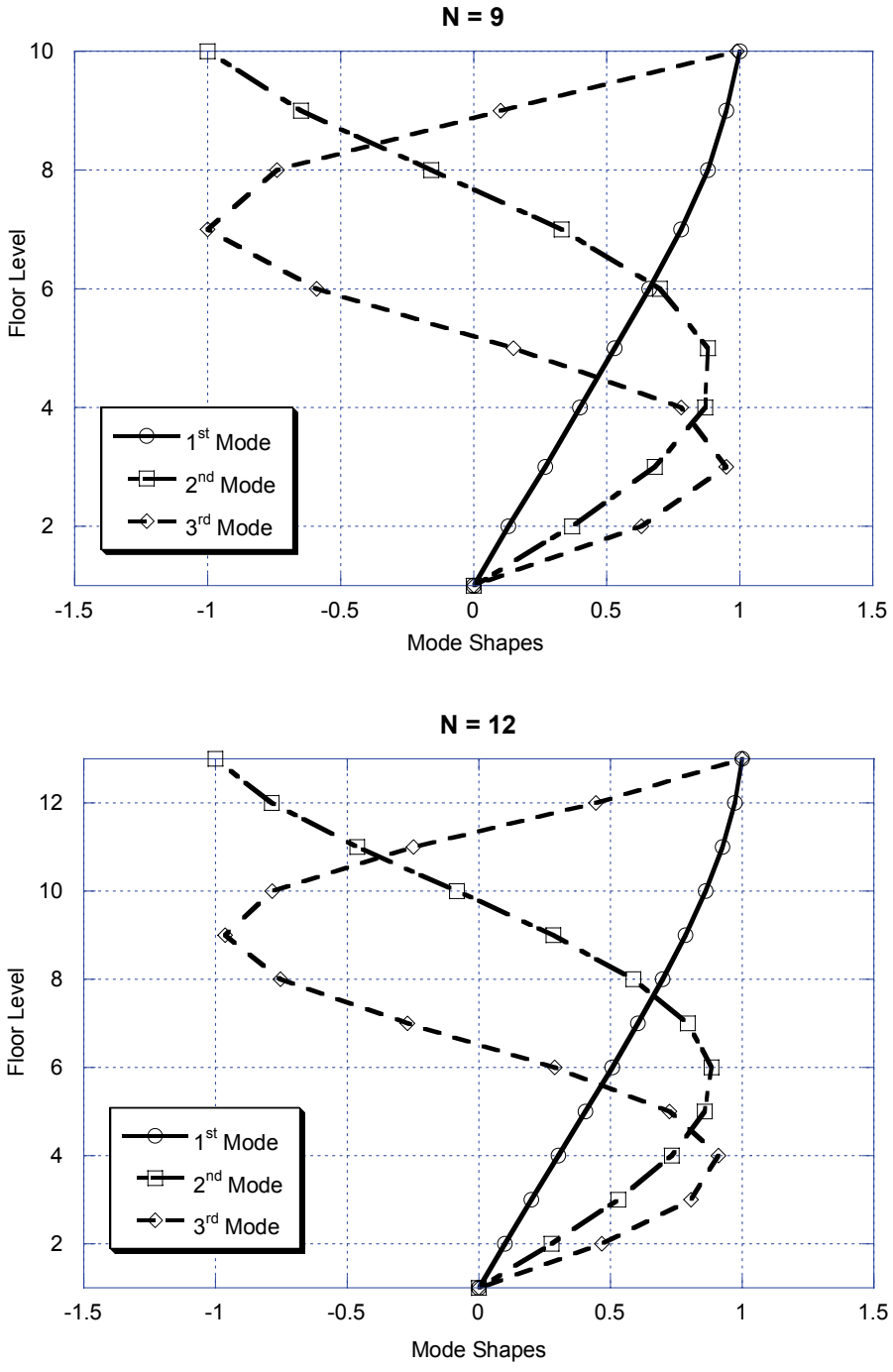

Figure 2.5 Mode shapes of *N*= 9 and *N*= 12 nonlinear first-mode building models

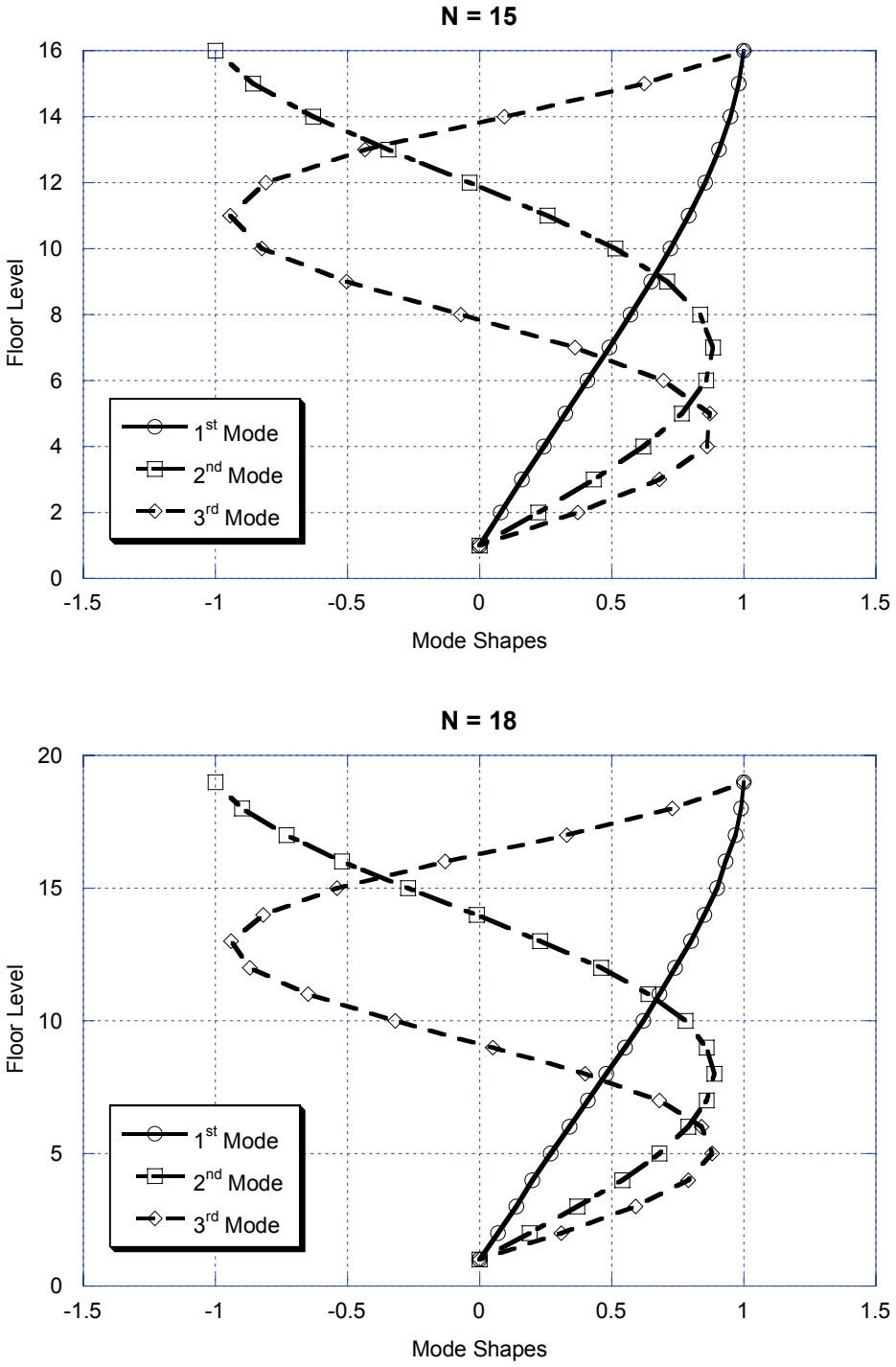

Figure 2.6 Mode shapes of *N*= 15 and *N*= 18 nonlinear first-mode building models

(a) Linear first-mode shape structures

# Stories	Stiff frame periods (sec.)			Flexible frame periods (sec.)		
	T_{B1}	T_{B2}	T_{B3}	T_{B1}	T_{B2}	T_{B3}
3	0.300	0.100	0.047	0.600	0.201	0.093
6	0.600	0.228	0.126	----------		
9	0.900	0.354	0.207	1.800	0.708	0.414
18	1.800	0.727	0.447	3.600	1.454	0.894

(b) Nonlinear first-mode shape structures

# Stories	Stiff frame periods (sec.)			Flexible frame periods (sec.)		
	T_{B1}	T_{B2}	T_{B3}	T_{B1}	T_{B2}	T_{B3}
3	0.300	0.094	0.045	0.600	0.187	0.091
6	0.600	0.203	0.110	1.200	0.406	0.221
9	0.901	0.312	0.177	1.801	0.623	0.354
12	1.200	0.419	0.244	2.400	0.839	0.487
15	1.500	0.527	0.310	3.000	1.054	0.619
18	1.800	0.634	0.375	3.600	1.268	0.751

Table 2.1 Modal periods of supporting structures

For each period and number of stories, frames with nine different base shear strength values are designed, one for elastic behavior and eight for inelastic behavior. The parameter utilized to quantify the strength of the structure is the base shear coefficient, γ, which is equal to the base shear strength normalized by the seismically effective weight, V_y/W. The base shear coefficient is based on the ratios $[S_a(T_{B1})/g]/\gamma = 0.25$ (for elastic behavior) and 1 to 8 (in increments of 1) for inelastic behavior, where $S_a(T_{B1})$ is the 5% damped spectral acceleration at the fundamental period of the supporting structure. In this study, the ratio $[S_a(T_{B1})/g]/\gamma$ is denoted as the Relative Intensity (*RI*). Generic models of

the type used in this study are adequate to represent the global seismic response of multi-bay regular frame structural models as shown by Medina (Medina and Krawinkler 2004).

2.2.2 Ground Motions

The set of 40 ground motions used in this study do not exhibit near-fault, forward-directivity characteristics. The far-field (non near-fault or ordinary) ground motions used in this study were recorded in stiff soils, i.e., NEHRP site class D, have a moment magnitude that varies from 6.5 to 6.9, and closest distances to the fault rupture are in the range of 13 km to 30 km. Table 2.2 gives the details about the 40 ground motions used in this study. Detailed information about the ground motions can be obtained from references (PEER 2003; Medina and Krawinkler 2004). Soft soil effects and effects of large magnitude ground motions ($M_w \geq 7.0$) are not considered in this study.

The median spectrum for this set of ground motions is comparable in shape to the IBC 2003 response spectrum for a coastal region in California as shown in figure 2.7. It is assumed that, on average, the frequency content of the ground motions is an adequate characterization of the ground motion hazard represented by the IBC 2003 response spectrum. The results presented in this study are applicable to ground motions with frequency content characteristics similar to those described above. To understand the effects of near-fault ground motions, a separate study was conducted with 64 recorded near-fault forward-directivity ground motions. Their results are presented in appendix III.

Earthquake	Year	M_w	Station
Imperial Valley	1979	6.5	Calipatria Fire Station
			Chihuahua
			Compuertas
			El Centro Array #1
			El Centro Array #12
			El Centro Array #13
			Niland Fire Station
			Plaster City
			Cucapah
			Westmorland Fire Station
Loma Prieta	1989	6.9	Agnews State Hospital
			Capitola
			Gilroy Array #3
			Gilroy Array #4
			Gilroy Array #7
			Hollister City Hall
			Hollister Differential Array
			Halls Valley
			Salinas - John & Work
			Palo Alto - SLAC Lab.
			Sunnyvale - Colton Ave.
Northridge	1994	6.7	LA - Centinela St.
			Canoga Park - Topanga Can.
			LA - N Faring Rd.
			LA - Fletcher Dr.
			Glendale - Las Palmas
			LA - Holywood Stor
			Lake Hughes #1
			Leona Valley #2
			Leona Valley #6
			La Crescenta-New York
			LA - Pico & Sentous
			Northridge - 17645 Saticoy St.
			LA - Saturn St
			LA - E Vernon Ave
San Fernando	1971	6.6	LA - Hollywood Stor Lot
Superstition Hills	1987	6.7	Brawley
			El Centro Imp. Co. Cent
			Plaster City
			Westmorland Fire Station

Table 2.2 Ground motion records

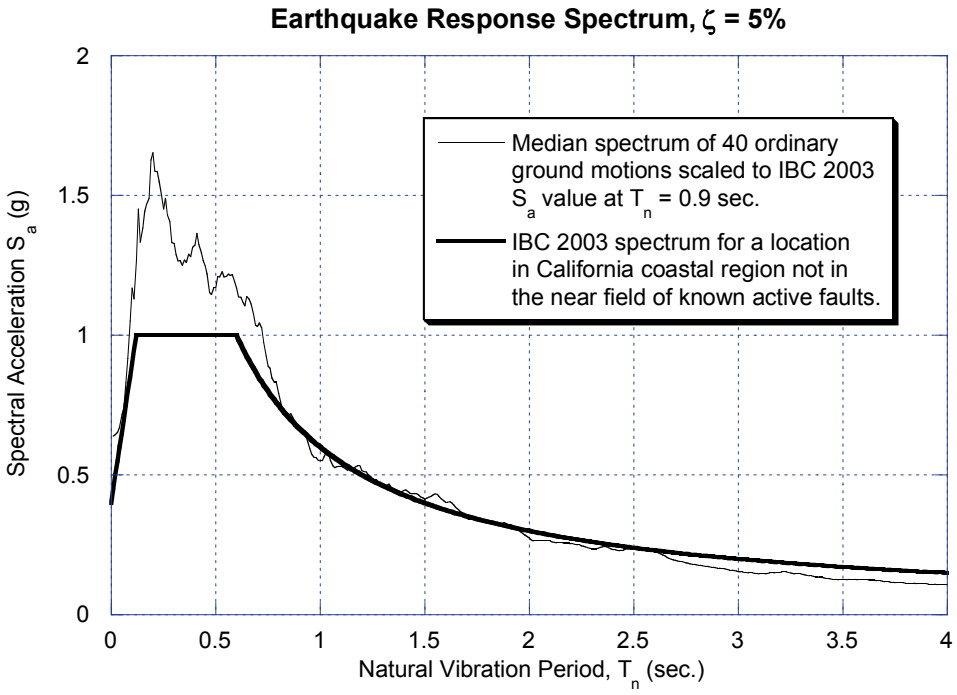

Figure 2.7 Median spectrum of far-field (ordinary) ground motions and IBC 2003 spectrum for site class D

2.3 PEAK FLOOR ACCELERATION DEMANDS

By definition, the peak component acceleration demand at $T_C/T_{B1} = 0$, where T_C/T_{B1} is the ratio of the period of the NSC (T_C) to the fundamental period of the supporting structure (T_{B1}), is the PFA response of the primary structure, i.e., the maximum acceleration demand of very stiff NSCs. PFA values are the "anchor" point for floor response spectra and also represent the normalizing parameter when the component amplification factor (defined as the peak nonstructural component acceleration normalized by the peak floor acceleration of the elastic frame (see equation (2.1) and figure 2.8) is utilized. Therefore, understanding and quantifying the distribution of PFAs

for various frames can lead to better predictions of the acceleration responses of NSCs. The evaluation of the variation in PFAs with height and procedures to estimate these demands have been the subject of several studies (Singh et al. 1993; Rodriguez et al. 2002; Miranda and Taghavi 2003; Taghavi and Miranda 2003; Chaudhuri and Hutchinson 2004; Medina and Krawinkler 2004; Taghavi and Miranda 2005) and a good understanding of the PFA demands on elastic buildings is available in the literature.

$$a_p = S_{aC} / PFA_e \tag{2.1}$$

Figures 2.9, 2.10, and 2.11 shows representative results for the family of frame models used in this study in which statistical information (i.e., median and 84th percentile values) on the ratio of peak floor acceleration to peak ground acceleration, PFA/PGA, is presented. As shown in these figures, current seismic design provisions in the United States (ICC 2003) do not account for variation of the ratio PFA/PGA as a function of the fundamental period and the level of inelastic behavior of the primary structure. It is important to note that for the inelastic $N = 18$, $T_{B1} = 3.6$ sec. frame, median values are not reported in figure 2.11. For this building several ground motion records caused the system to undergo dynamic instability because of P-delta effects; thus, statistical values could not be readily computed. The general conclusion is that alternative methods to estimate more accurately the variation of PFA with height are needed. The reader is referred to the work in literature (Singh et al. 1993; Miranda and Taghavi 2003; Taghavi and Miranda 2003; Medina and Krawinkler 2004; Taghavi and Miranda 2005) for additional information on this topic.

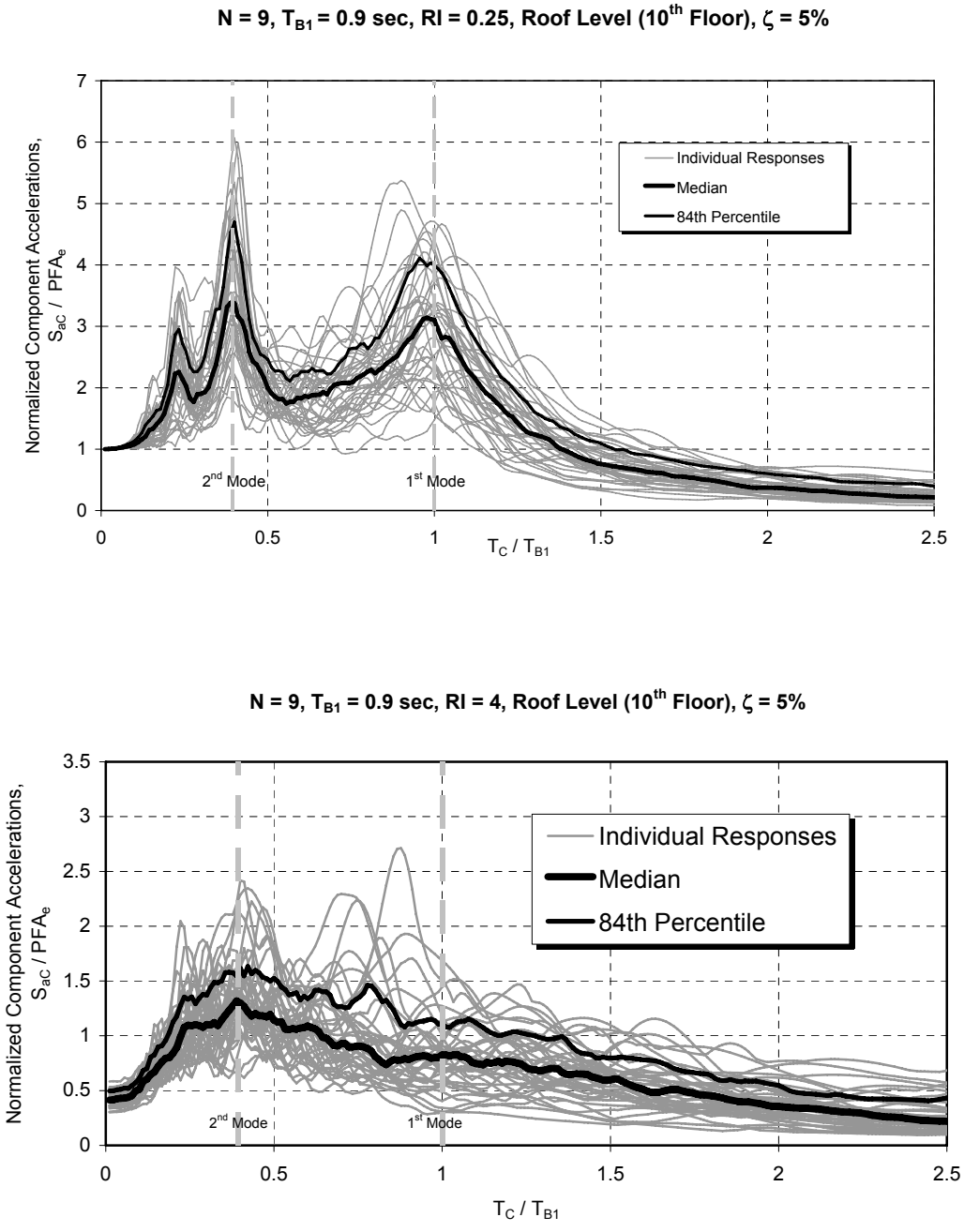

Figure 2.8 Normalized peak component accelerations (component amplification factors) as a function of the ratio T_C/T_{B1}, 9-story frames, component damping ratio = 5%, RI = 0.25 and 4

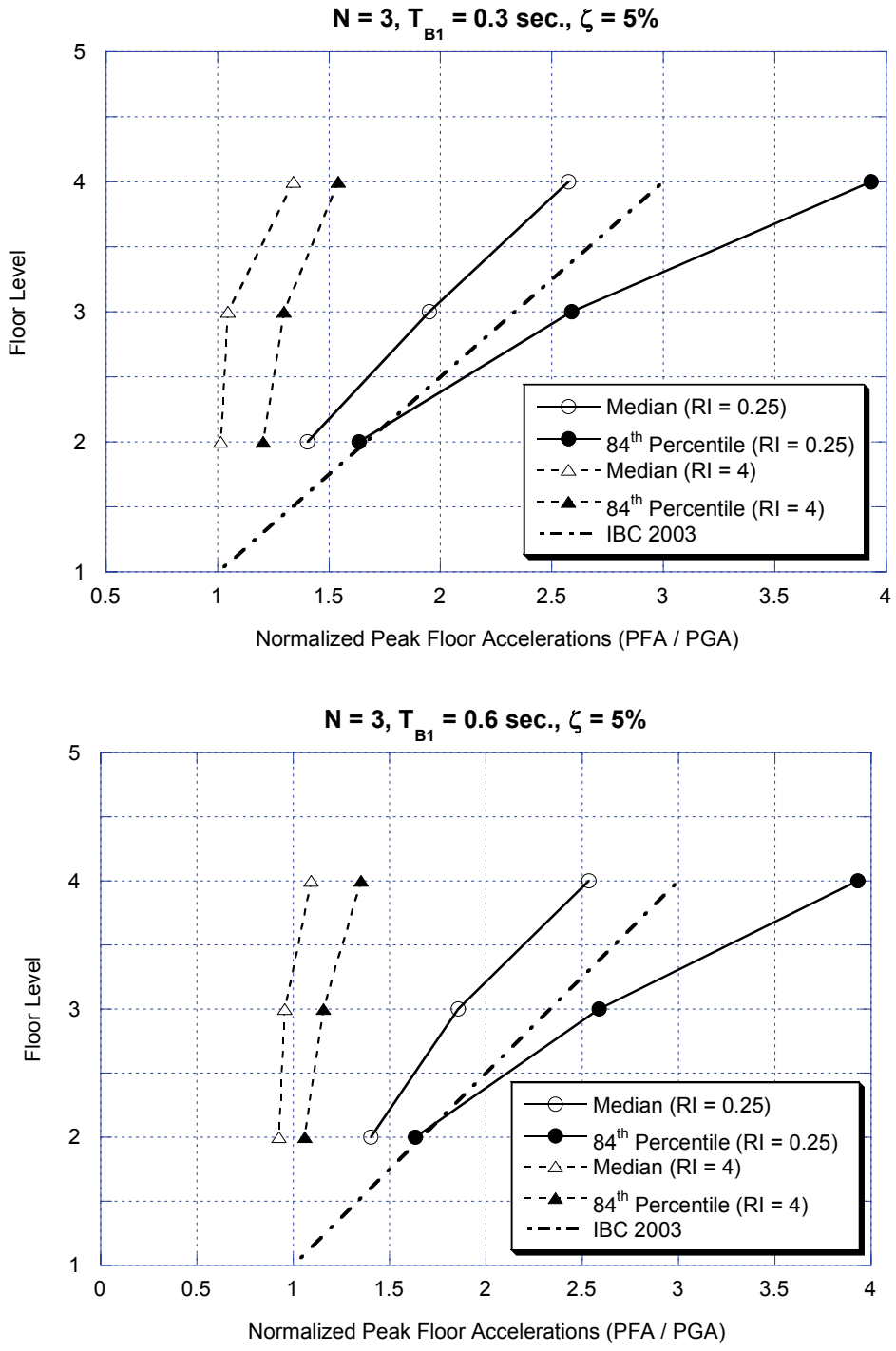

Figure 2.9 Normalized peak floor accelerations of 3-story frames, component damping ratio = 5%, *RI* = 0.25 and 4.0

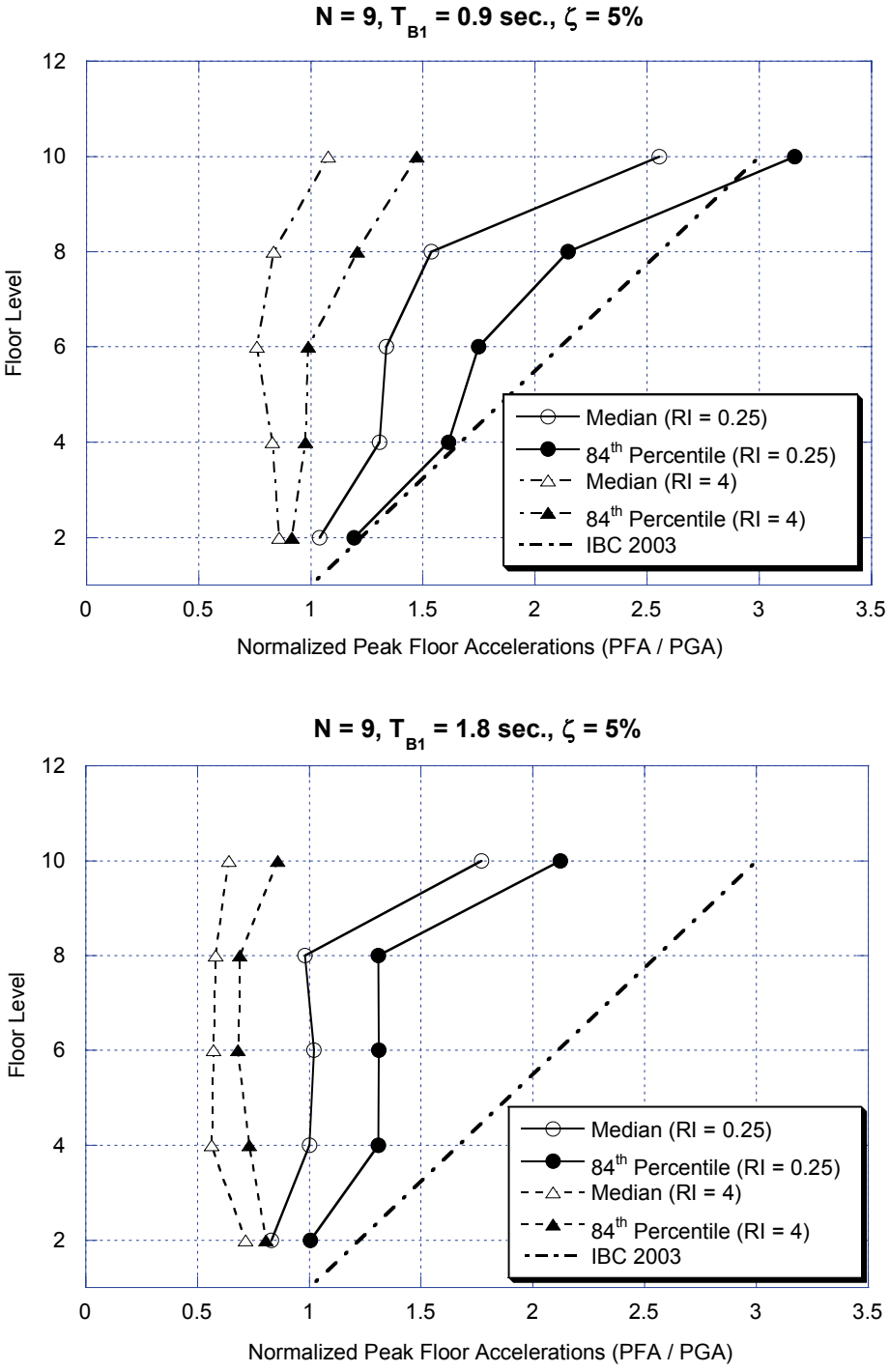

Figure 2.10 Normalized peak floor accelerations of 9-story frames, component damping ratio = 5%, *RI* = 0.25 and 4.0

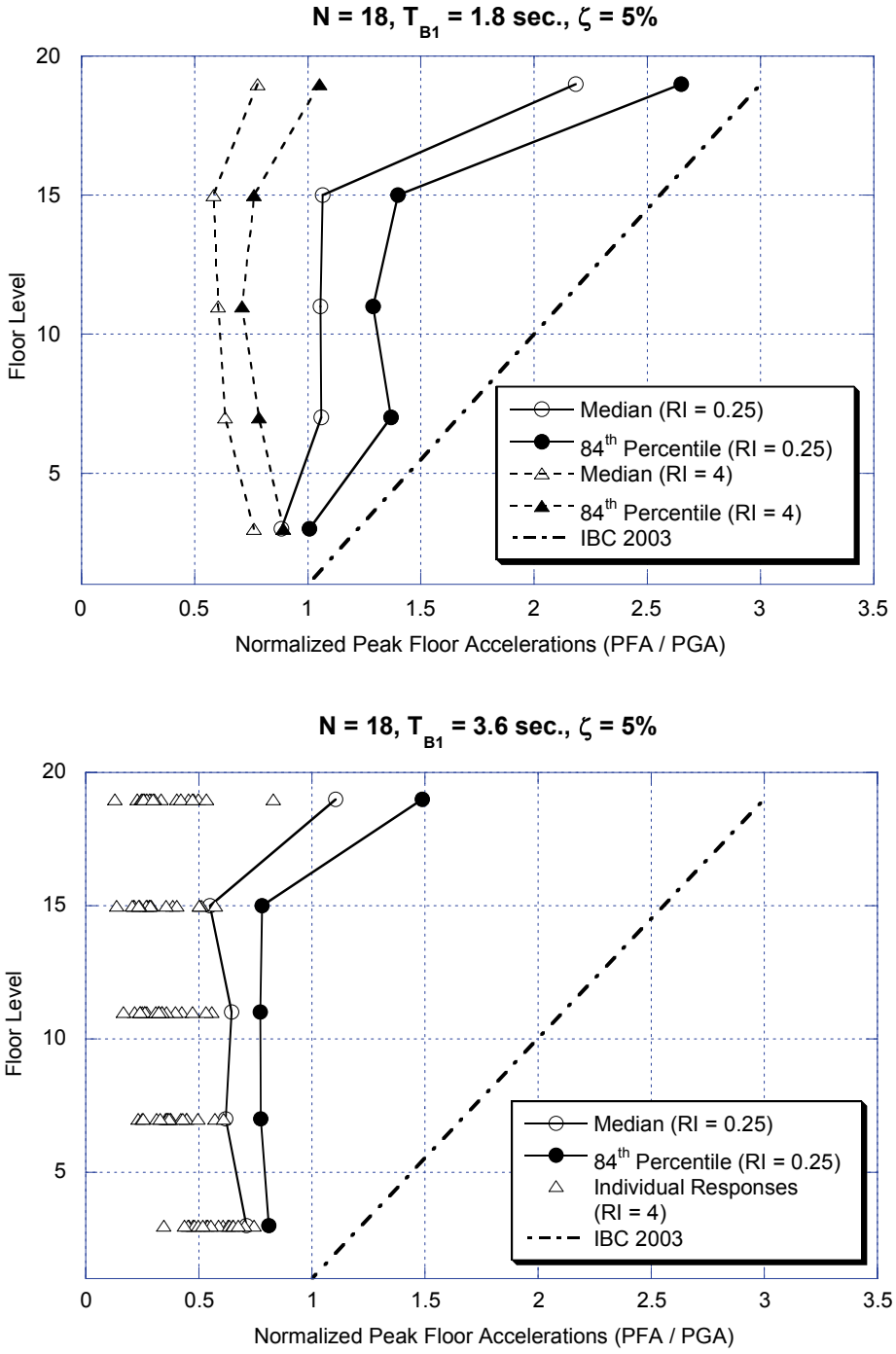

Figure 2.11 Normalized peak floor accelerations of 18-story frames, component damping ratio = 5%, *RI* = 0.25 and 4.0

2.4 EVALUATION OF PEAK COMPONENT ACCELERATIONS

The analyses demonstrate that the maximum acceleration response of the 5%-damped elastic SDOF systems used to represent NSCs ranges between 0.24 and 34.7 times the PGA and up to 8.3 times the PFA. Due to this wide range of amplification values, there is a need to identify and provide quantitative information on the key drivers of NSC acceleration response to understand the behavior of such systems and compute peak component acceleration demands. The appropriate quantification of peak component acceleration demands is of paramount importance in order to develop simplified recommendations for the design of NSCs and their attachments. The dependence of peak component accelerations on parameters such as the modal periods of the supporting structure, the location of the NSC along the height of the structure, the height of the supporting structure, its stiffness distribution, its strength, and the damping ratio of the NSC is discussed next for the set of frames and ground motions used in this study.

2.4.1 Modal periods of the supporting structure

The modal periods of a building significantly influence the response of NSCs, as can be observed in figure 2.8, which depicts information on the normalized 5%-damped roof response spectra for the elastic (RI = 0.25) and inelastic (RI = 4) 9-story frame with a fundamental period of 0.9 sec. The gray lines in figure 2.8 represent floor response spectra for each one of the 40 ground motions, while the black lines represent median and 84th percentile values. The stiffness distribution for this frame structure corresponds to a linear first-mode shape. The maximum normalized

component acceleration (S_{aC}/PFA_e) is plotted as a function of the ratio T_C/T_{B1}. Peak S_{aC}/PFA_e values occur when the component is in tune with one of the modal periods of the supporting structure. This is representative of the behavior observed along the height of all the building models used in this study. This behavior highlights the importance of the parameter T_C/T_{Bi}, where T_{Bi} is the period of vibration of the i^{th} mode, in the quantification of the maximum acceleration response of NSCs. These observations are consistent with those discussed in other studies (Lin and Mahin 1985; Sewell et al. 1987; Bachman et al. 1993; Singh et al. 1993; Bachman 2003; Miranda and Taghavi 2005).

2.4.2 Location of the NSC in the building

The location of the NSC in the building has a significant influence on the S_{aC} values. Maximum component accelerations are generally larger at the top floors, as shown in Figure 2.12 for 9-story frames with a fundamental period of 0.9 sec., and *RI* values of 0.25 and 4. This behavior is consistent with the variation in PFAs shown in figures 2.9, 2.10, and 2.11, and representative of results obtained for other frame structures used in this study. Another important observation is the variation of the shape of the FRS with height. For instance, as the height of the location of the NSC decreases, the S_{aC} values that correspond to the fundamental period of the supporting structure, $S_{aC}(T_C/T_{B1} = 1)$ decrease more rapidly than the S_{aC} values that correspond to the structure's higher-mode periods. Moreover, it can be observed that the differences between the median maximum component accelerations and the median ground motion spectral accelerations increase with height. This difference is more pronounced when the NSC has a period near the fundamental period of the primary

structure. The conclusion is that a reliable evaluation of peak component acceleration demands for seismic design should address the changes in floor acceleration spectral shape due to the location of the NSC in the structure.

2.4.3 Height of the supporting structure

In order to evaluate the effect of the height of the supporting structure on the peak component acceleration demands, statistics of the ratio $S_{aC}(T_{B1}) / S_{aC}(T_{B2})$ (for NSCs with 5% damping) are shown in figures 2.13 and 2.14 for selected elastic and inelastic (RI = 4) frames with a linear first-mode shape. This ratio represents a quantitative measure of the variation of the shape of the floor response spectrum with height around the first two modal periods of the supporting structure. The ratio values smaller than 1.0 indicate a larger component acceleration response when the NSC is in tune with the second mode period of the supporting structure. The frames under consideration are the N = 3- and 6-story frames with T_{B1} = 0. 6 sec. (3/6 set) and the N = 9- and 18-story frames with T_{B1} = 1.8 sec. (9/18 set). For the 9/18 set, the $S_{aC}(T_{B1}) / S_{aC}(T_{B2})$ ratios are similar, which implies that given the fundamental period and relative height, the shape of FRS around the modal periods of the supporting structure are consistent. This behavior is attributed to the fact that the first and second mode shapes of the 9- and 18-story structures (see figure 2.3) as well as their modal periods (see Table 2.1) match very closely. However, the second mode shapes of the 3-story flexible frame and 6-story stiff frame are dissimilar, although their modal periods are comparable (see figure 2.2). Because of this difference, the plots in figure 2.13 vary significantly.

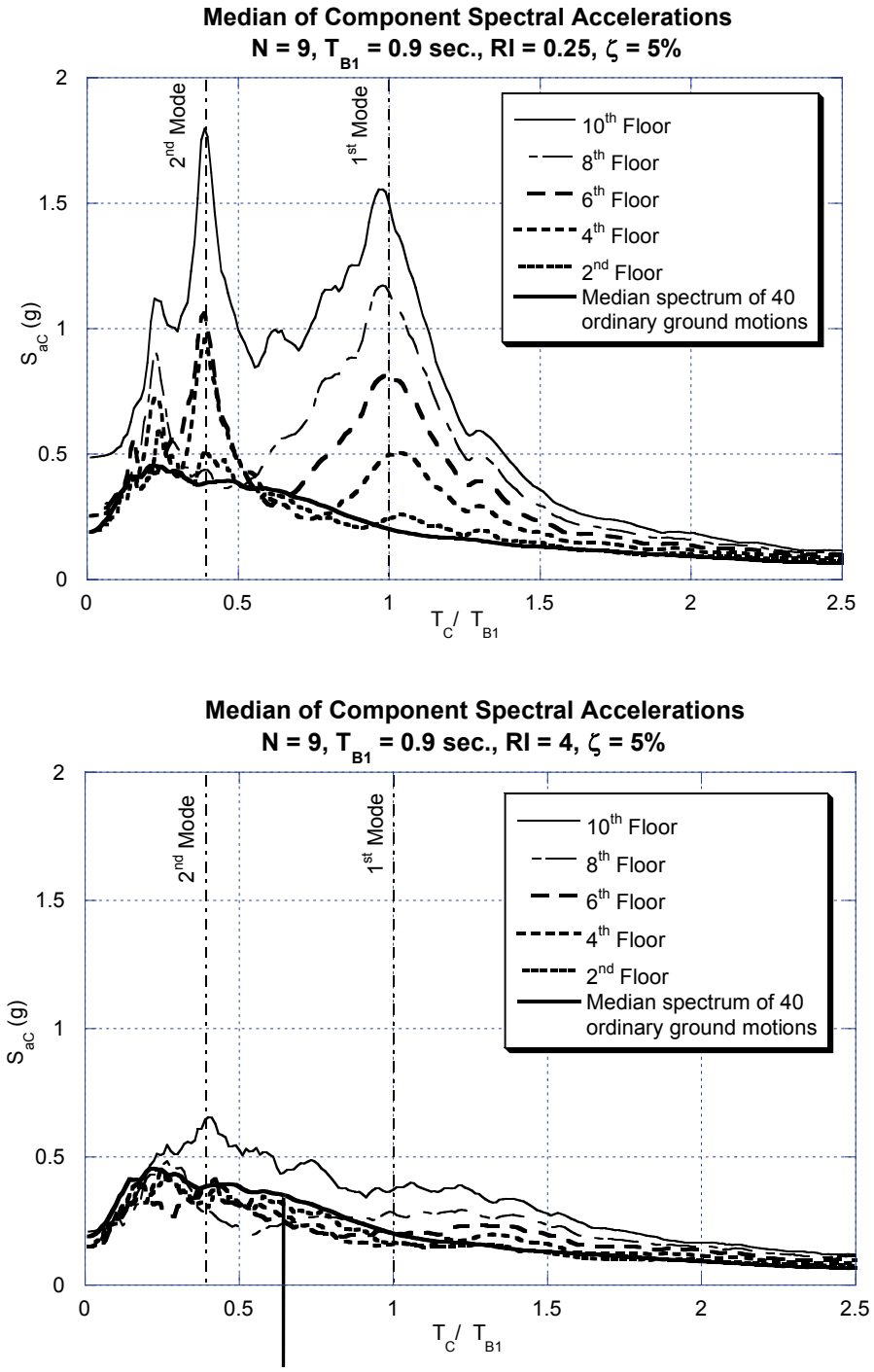

Figure 2.12 Median of peak component accelerations, 9-story frames, T_{B1} = 0.9 sec., component damping ratio = 5%, *RI* = 0.25 and 4.0

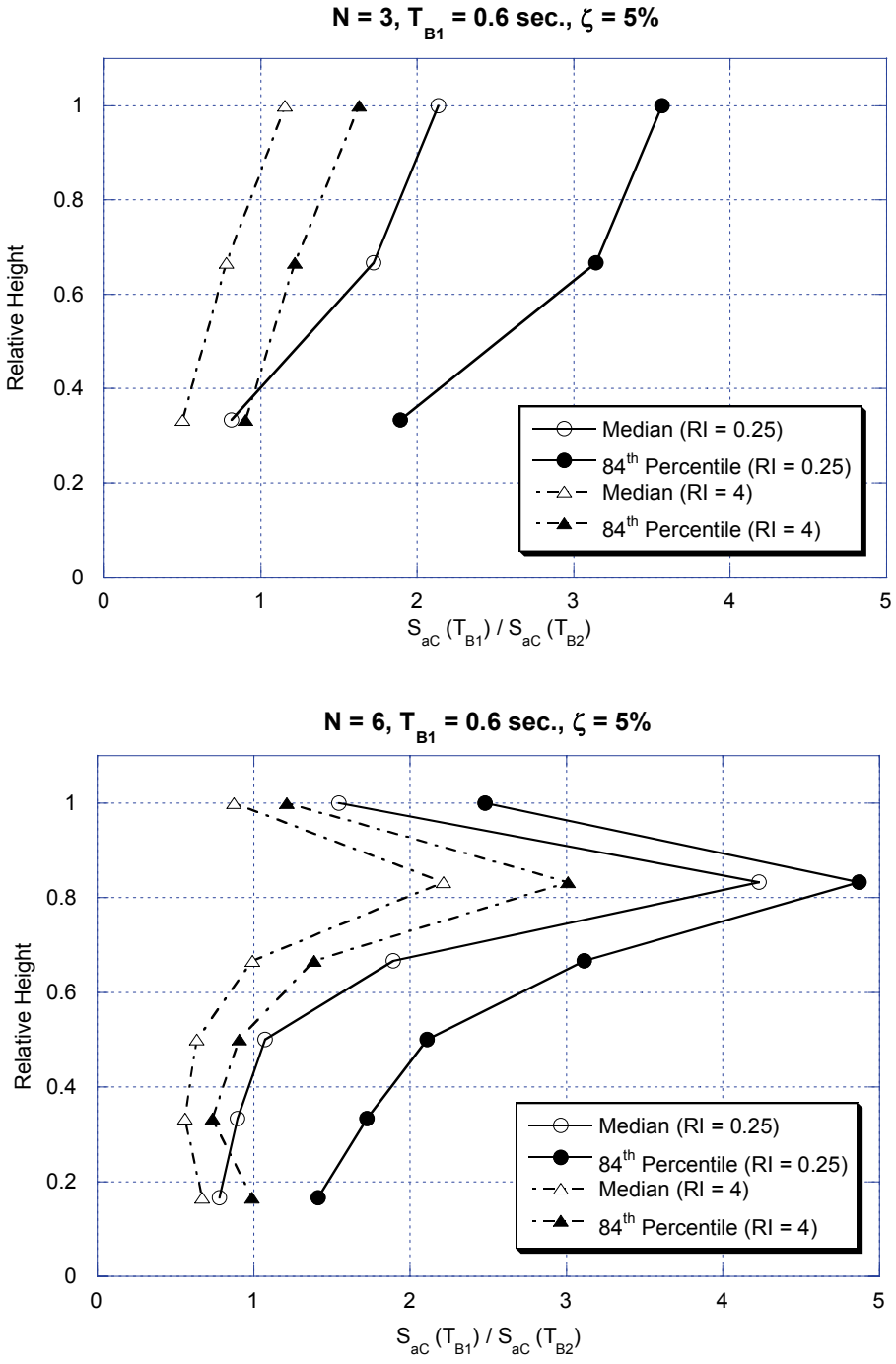

Figure 2.13 Effect of building height on the ratio of peak component acceleration at $T_C = T_{B1}$ to the peak component acceleration at $T_C = T_{B2}$, T_{B1} = 0.6 sec., component damping ratio = 5%, *RI* = 0.25, and 4

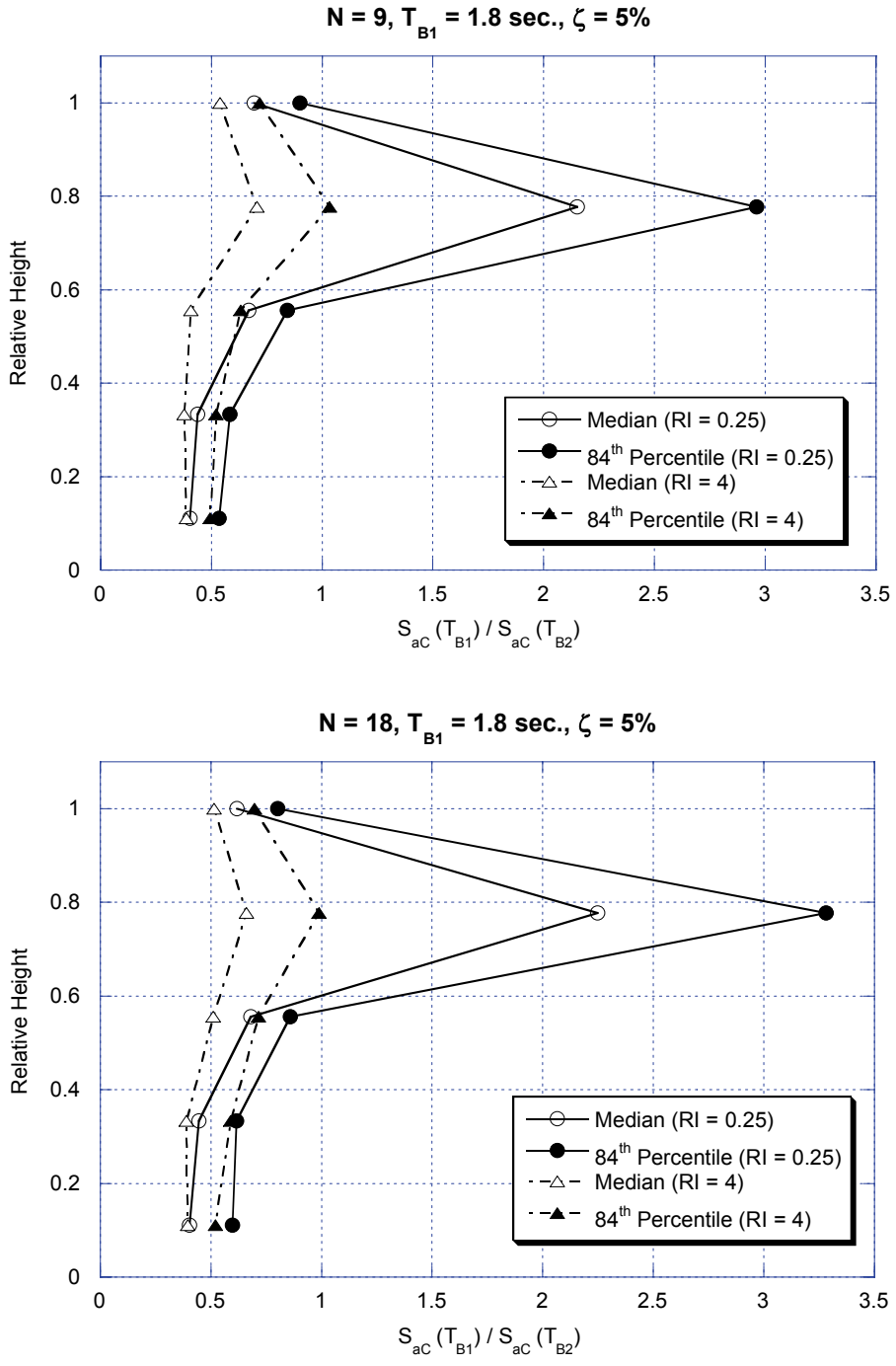

Figure 2.14 Effect of building height on the ratio of peak component acceleration at $T_C = T_{B1}$ to the peak component acceleration at $T_C = T_{B2}$, T_{B1} = 1.8 sec., component damping ratio = 5%, RI = 0.25, and 4

Hence, it can be said that

(1) the influence of higher modes on peak component acceleration values is highly dependent on the mode shapes of the structure, and

(2) for moderate-to-long period structures, given T_{BI}, the variation of floor-response spectral shapes with relative height are weakly dependent on the height (i.e., number of stories) of the frame.

2.4.4 Stiffness distribution of the supporting structure

The influence of various stiffness distributions over the height on the peak component acceleration demands was also investigated. Representative results corresponding to elastic (RI = 0.25) and inelastic (RI = 4.0) nine-story building models with linear and nonlinear first-mode shapes are discussed. Structures with different stiffness distributions are tuned so that their fundamental periods are equal to 0.9 sec. The mode shapes are shown in figures 2.3 and 2.5 and the modal periods in Table 2.1. The ratios of the 5%-damped peak component acceleration of the nonlinear first-mode shape models to that of the linear first-mode shape models are shown in figure 2.15. This ratio is characterized by a significant number of spikes in the higher-mode period range, which are caused by differences in the values of higher mode periods between the models. These differences combined with the discretization of component period values in the generation of FRS accentuate the spikes (spectral quantities are calculated with an interval of ΔT_C = 0.01 sec. for periods from 0 to 5 sec., which results in 500 points for each response spectrum).

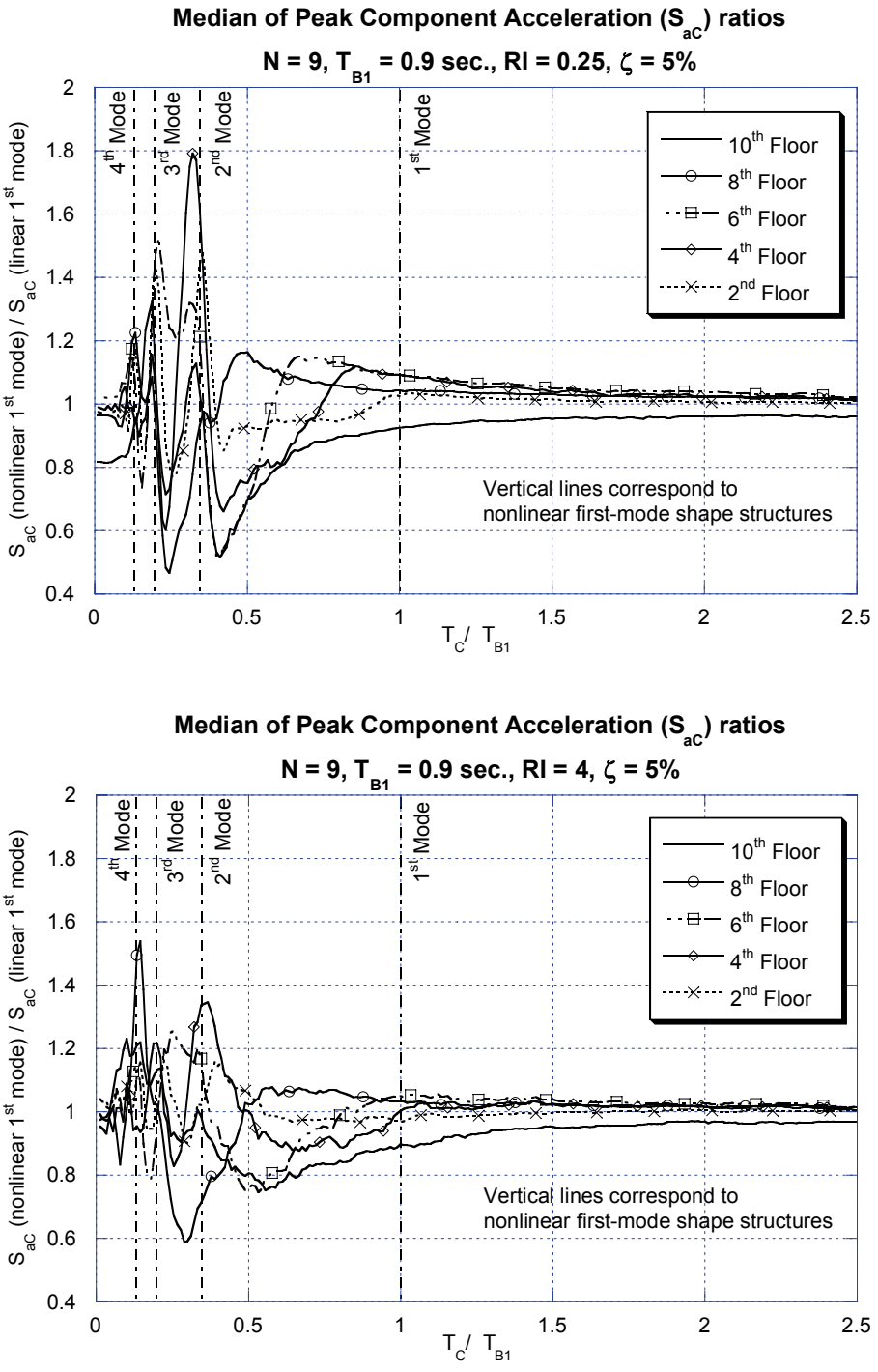

Figure 2.15 Median of peak component acceleration ratios, 9-story frame, T_{B1} = 0.9 sec., component damping ratio = 5%, *RI* = 0.25, and 4

In the median, away from the spikes, differences in peak component acceleration demands caused by variations in the stiffness distribution of the primary structure are on the order of 10%. These results are representative of those obtained for all other frames and different damping ratios for the NSCs.

2.4.5 Strength of the supporting structure

A fundamental aspect of FRS that is not currently addressed in seismic code provisions is the dependence of peak component acceleration demands on the strength of the supporting structure, i.e., its degree of inelastic behavior. In general for both stiff and flexible frames, median FRS for inelastic frames do not exhibit significantly sharp acceleration peaks as observed in median FRS for elastic frames (see figure 2.8). The exception is the short-period structures (T_{B1} = 0.3 sec), for which peaks in the floor acceleration response are evident for both the elastic and inelastic frames.

Once the primary structure experiences inelastic behavior, the deamplification of peak component acceleration demands is more pronounced near the first mode period of the primary structure (see figures 2.9 to 2.11, and figure 2.16). Peak component acceleration demands that correspond to higher modes are also deamplified but by a smaller amount. Studies by other researchers also indicated that the inelastic action for other types of supporting structures, e.g., one-story frames and structural walls, significantly reduces the acceleration near the fundamental period of the supporting structure (Lin and Mahin 1985; Rodriguez et al. 2002).

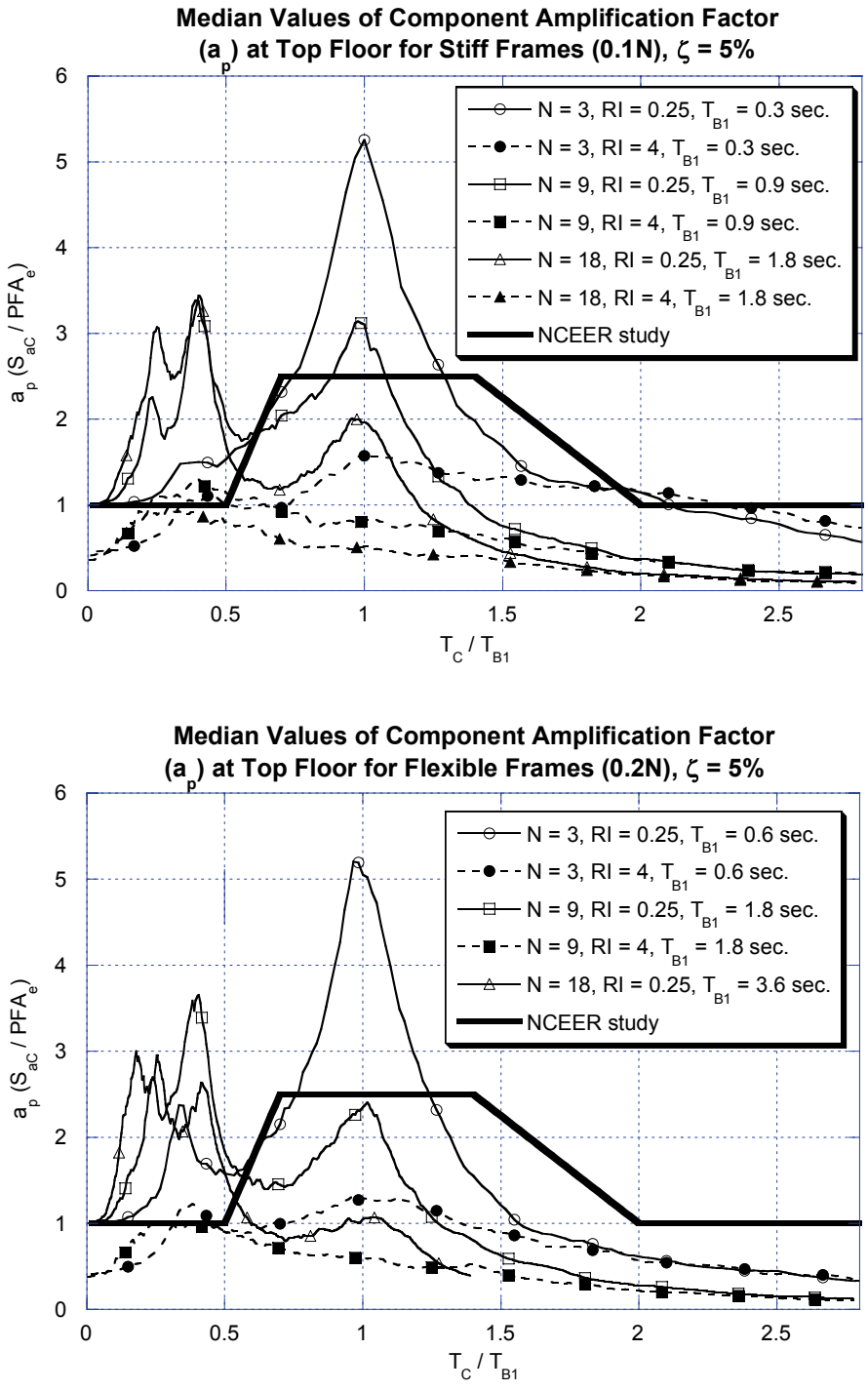

Figure 2.16 Median of component amplification factor for stiff and flexible frames, component damping ratio = 5%, *RI* = 0.25 and 4

It is important to note that an amplification of peak component accelerations mounted on inelastic structures can occur when a building experiences localized inelastic behavior (Sewell et al. 1986; Singh et al. 1996). The effect of localized nonlinearity and corresponding amplification in FRS are discussed in detail in Appendix II These results can also be evaluated in a more comprehensive manner from figures 2.13 and 2.14, which shows the variation along the height of the ratio $S_{aC}(T_{B1}) / S_{aC}(T_{B2})$ for NSCs with 5% damping. Overall, the figure indicates smaller ratios for inelastic structures, although, at most floor levels, the ratios for inelastic and elastic frames approach the same value as the fundamental period of the structure increases. These observations imply that for frame structures with distributed inelasticity an additional benefit of allowing the primary structure to dissipate energy through inelastic action is the reduction in the maximum acceleration demands experienced by the NSCs. This would allow the design of NSCs and/or their attachments to the primary structure to be based on smaller force demands, which translates into more economical attachments or connections.

2.4.6 Damping ratio of NSCs

An evaluation of the effect of component damping in the estimation of peak component accelerations is important to provide a reasonable quantification of the absolute value of accelerations, which are sensitive to the level of damping of the component. Here, damping ratios equal to 0.01%, 2%, and 5% were considered. This range is deemed to be appropriate for the characterization of NSCs. Most of the results discussed in this chapter pertain to NSCs with a damping ratio equal to 5%. The purpose of this section is to evaluate and quantify the sensitivity of the results to

the component damping ratio. For this purpose, variations in component damping are presented for the elastic and inelastic (RI = 4) 9-story frame with a linear first-mode shape, and fundamental periods of 0.9 sec, and 1.8 sec exposed to the set of 40 ordinary ground motions. Median values of the ratio of the roof peak component accelerations for damping ratios equal to 0.01% and 2% to the roof peak component accelerations for a damping ratio of 5% are shown in figure 2.17. As expected, less damping causes more amplified and sharper FRS than those corresponding to 5% damping, especially for component periods near the modal periods of the primary structure. It can be concluded that lower damping causes amplifications in the acceleration response of the NSC, with maximum amplifications (with respect to values for 5% damping) on the order of 1.5 for 2% damping and 2 to 3 for 0.01% damping. Similar trends are observed for the 3-, 6- , and 18-story frames used in this study.

2.5 SUMMARY

This chapter evaluates and quantifies the dependence of peak component accelerations on the location of the nonstructural component in the structure, the damping ratio of the component, and the properties of the supporting structure such as its modal periods, height, stiffness distribution, and strength. This step is necessary before any attempt to propose a methodology for the estimation of acceleration demands on NSCs mounted on inelastic frames (see Chapter 3). The summary of most salient results obtained from this study is presented next.

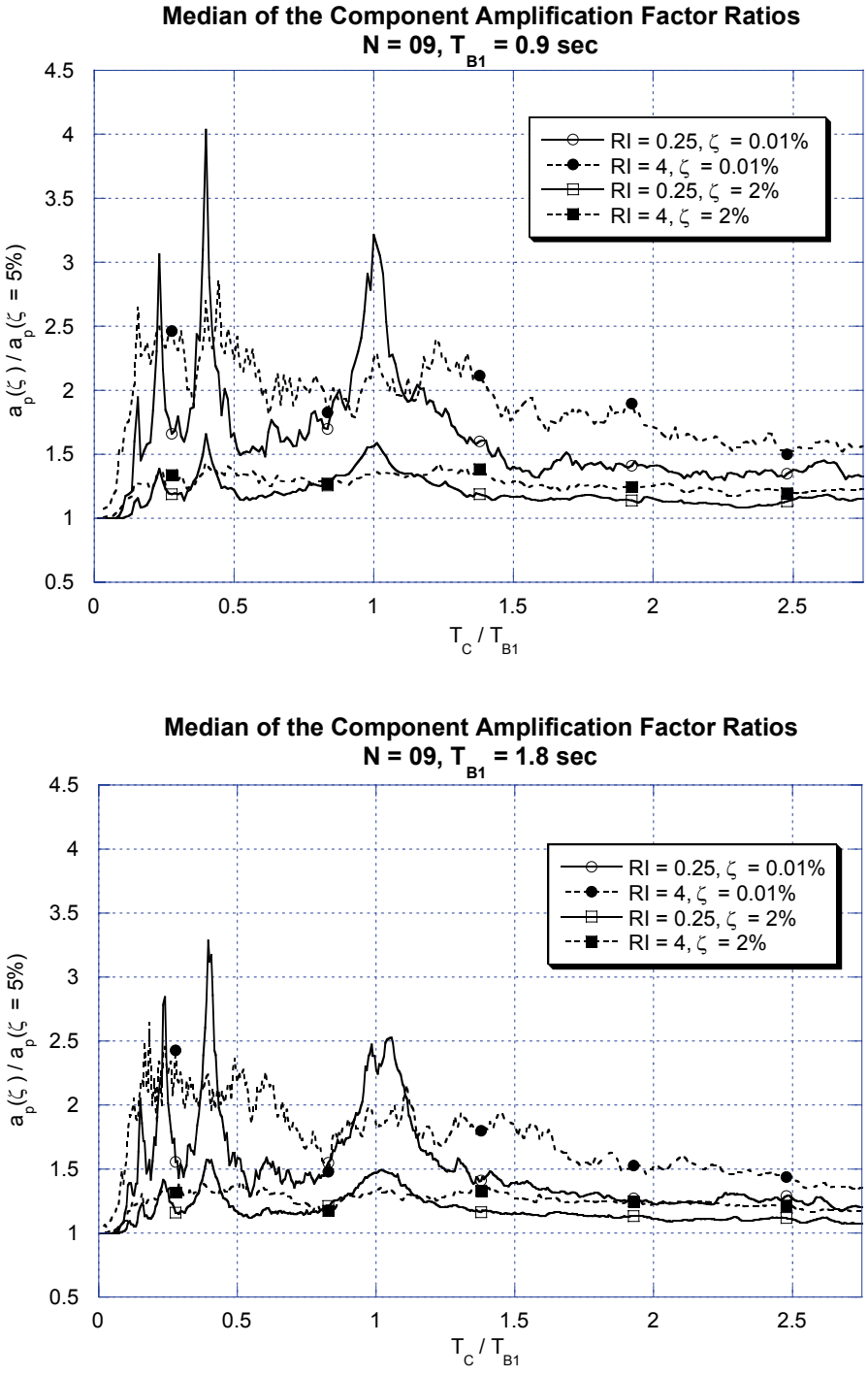

Figure 2.17 Median of component amplification factor ratios at top floor of 9-story frames for different component damping ratios for stiff and flexible frames, *RI* = 0.25 and 4

- The variation of peak floor accelerations with height is strongly dependent on the fundamental period of the supporting structure and its strength. Moreover, for a given fundamental period, the variation of PFA with respect to the relative height of the structure is weakly dependent on the number of stories. These patterns of behavior are not adequately represented by current seismic design provisions, which assume a linear variation with height regardless of period or level of inelastic behavior of the supporting structure. The variation of PFA along the height of the frame is mostly non-linear. For longer period structures, the PFA values provided in current provisions are conservative.
- The parameter T_C/T_{Bi}, where T_C is the period of the NSC and T_{Bi} the period of vibration of the i^{th} mode of the supporting structure, is an important parameter in the quantification of the maximum acceleration response of NSCs. The maximum acceleration response of NSCs generally occurs when $T_C = T_{Bi}$. However, for moderate to longer period frames with higher mode effects, the maximum acceleration response occurs at the second or higher modal period.
- The reliable quantification and evaluation of FRS for seismic design should address the changes in spectral shape due to the location of the NSC in the structure. NSC acceleration demands in the fundamental period region are generally higher at the top stories of the frame. However, the acceleration demands at higher modal period region are weakly dependent on the location of the NSCs.

- For a given T_{B1} and relative height, moderate- and long-period frame structures exhibit floor response spectral shapes that are weakly dependent on the number of stories.
- Variations in stiffness distribution along the height for frames with same T_{B1} values, cause differences in the values of component amplification factors at higher modal periods when only the fundamental periods are matched. The differences reflect in the locations of the peaks of FRS. In the median, away from the peaks, differences in peak component acceleration demands caused by variations in the stiffness distribution (straight-line first mode versus nonlinear first-mode) of the primary structure are on the order of 10%.
- A benefit of allowing the primary structure to dissipate energy through inelastic action is the reduction in the maximum acceleration demands experienced by the NSCs. This implies that NSCs and their attachments to the primary structure can be designed based on smaller forces, which translates into more economical connections or attachments. This deamplification of component accelerations with a decrease in the strength of the supporting structure is more pronounced for component acceleration values near the modal periods of the supporting structure. As explained in the next task, this deamplification may not be applicable for buildings with concentrated inelasticity where only the bottom stories fail in the inelastic range (see Appendix II) or when the damping ratio of the NSCs are very small.
- Smaller values of NSC damping ratios produce higher acceleration demands. The maximum amplifications around the modal periods when compared to the

demands obtained for NSCs with 5% component damping ratio are of the order of 1.5 for 2% damping and 2 to 3 for 0.01% damping.

- Although simple and rational, the design provisions in the current building codes for the estimation of acceleration demands on NSCs do not account for the inelastic action of the supporting structure and also are not adequate in representing the acceleration demands in the short-period region of the FRS for both elastic and inelastic buildings.

Chapter 3: Methodology for the Estimation of NSC Demands

3.1 INTRODUCTION

In the previous chapter, the factors influencing the acceleration demands of NSCs were studied with main focus on identifying the most important parameters that should be considered in developing the next-generation guidelines for the analysis and design of NSCs. This dissertation attempts to develop a methodology to provide better estimates of peak acceleration demands for the design of nonstructural components mounted on inelastic frames. For this goal, it is important to understand the strengths and weaknesses of current seismic design provisions in building codes. Hence, the first part of the chapter provides an overview of the current seismic provisions in the US. The second part of the chapter deals with the development of a methodology to estimate the seismic demands of NSCs.

3.2 ASSESSMENT OF CURRENT SEISMIC DESIGN PROVISIONS

Current U.S. building code requirements for the seismic design of NSCs are based on 2003 NEHRP Provisions (BSSC 2003). The seismic design forces and the amplification factors proposed in the building codes originated with a study and workshop sponsored by the National Center for Earthquake Engineering Research, NCEER (Singh et al. 1993). These design guidelines for NSCs in building codes are based on past experience, intuition and engineering judgment rather than on experimental and analytical results (Filiatrault et al. 2004b). Hence, in recent times, many researchers have attempted to characterize the seismic behavior of nonstructural

components both analytically and experimentally so that effective mitigation measures can be developed. University of Buffalo (UB-NEES) had commissioned a Nonstructural Component Simulator (UB-NCS) to evaluate the seismic performance of NSCs and quantify their experimental fragility for both acceleration-sensitive and displacement-sensitive NSCs (Filiatrault et al. 2004a; Filiatrault et al. 2004b; Retamales et al. 2006). Recent analytical work is focused on estimating the PFA and peak acceleration demands on stiff and flexible NSCs mounted primarily on elastic buildings (Singh et al. 2006a; 2006b) and on developing approximate but rational methods that account for nonlinear behavior of NSCs and supporting structure (Villaverde 2005; 2006). This has been discussed in brief in the previous chapter (see section 2.3) and NSC acceleration demand estimation for equipment mounted on inelastic buildings is discussed in the later part of this dissertation (see section 3.4.1).

The current provisions attempt to simplify the calculations while maintaining the analytical rationality. They are aimed to achieve the objectives without unduly burdening the practitioner with complicated formulations. However, these simple guidelines are non-conservative especially when the period of the NSC is around or matches one of the higher modal periods of the building (Medina et al. 2006) and economic losses due to the failure of NSCs had been observed in most earthquakes including the recent 2006 Hawaii region earthquake. As per the 2003 NEHRP provisions, SEI/ASCE 7-02 standard (ASCE 2003) and IBC 2003 (ICC 2003), the following equations are used to determine the force transferred to a component and/or its attachment to the supporting structure (F_p):

$$F_p = \frac{0.4 a_p S_{DS} W_P}{R_P / I_P}\left(1 + 2\frac{z}{h}\right) r \tag{3.1}$$

except that F_p need not be greater than

$$\left(F_p\right)_{\max} = 1.6 S_{DS} I_P W_P r \tag{3.2}$$

and must not be less than

$$\left(F_p\right)_{\min} = 0.3 S_{DS} I_P W_P \tag{3.3}$$

in which a_p is the component amplification factor; W_P is the operating weight of the component; S_{DS} is the short period spectral acceleration parameter; h is the average roof height of the structure above the base; z is the height above the base of the point of attachment of the component, but z shall not be taken less than 0 and the value of z/h need not exceed 1.0; I_p is the component importance factor, and R_p is the component response modification factor. The factor r in equation (3.1) was first introduced in the 2003 NEHRP provision by means of an exception clause. The clause states that:

$$r = 1 \text{ if } T_p \le T_{flz} \tag{3.4}$$

$$r = \frac{T_{flx}}{T_p} \text{ if } T_p > T_{flz} \tag{3.5}$$

where, T_{flx} is defined as

$$T_{flx} = \left(1 + 0.25\frac{z}{h}\right)\frac{S_{D1}}{S_{DS}} \tag{3.6}$$

This means that if the component period T_p, is greater than $T_{flx,}$ the value of F_p may be reduced by the ratio of T_{flx}/T_p. S_{D1} is the design, 5% damped, spectral response acceleration parameter at a period of 1 second.

3.2.1 Component Importance Factor

The component importance factor, I_p represents both the life-safety importance of the component and the hazard-exposure importance of the structure. I_p shall be taken as 1.5 if

a) the component is required to function after the earthquake, or

b) the component contains hazardous materials, or

c) the component is needed for the continued operation of the facility or its failure could impact the continued operation of the facility.

All other components shall be assigned an I_p value of 1.0. NSCs such as parapets, cornices, canopies, marquees, glass, and precast concrete cladding panels could fall from the structure and they are among the most hazardous NSCs. Special consideration should also be given to NSCs that could block means of egress or exit ways by falling during an earthquake. NSCs in seismic use group III and in seismic design category C or higher should also be designed with an I_p value of 1.5.

3.2.2 Component Response Modification Factor

The component response modification factor, R_p accounts for the overstrength and the inelastic deformation capability of the NSC and/or its anchors. R_p represents the energy absorption capability of the component without considering the yielding of the supporting structure. R_p values provided in tables in the 2003 NEHRP provisions vary from 1.0 to 3.5 for architectural components and from 1.5 to 5.0 for mechanical and electrical components. In general a value of R_p = 1.5 is considered for low deformability element, R_p = 2.5 for limited deformability element and R_p = 3.5 for high deformability element.

3.2.3 Component Amplification Factor

The component amplification factor (a_p) accounts for the dynamic amplification of the NSC acceleration response, especially near the point of resonance with the fundamental period of the supporting structure, T_{B1} (i.e. when $T_C = T_{B1}$). This factor is designed to address NSC weight and mass distribution, including the dynamic properties of the NSC. Because of the dependence of the peak NSC acceleration demands and a_p on the ratio of T_C/T_{B1} (see 2.4.1), an accurate determination of both the modal periods of the building and NSC is needed for the estimation of demands on NSCs for a specific building-NSC combination. The period of the building T_{B1}, may not be readily available when the NSCs are designed or selected. Moreover, the period of the NSC namely T_C is usually only obtained by expensive shake-table or pull-back tests. Hence, the ratio, T_C/T_{B1} may not be readily available. To address this issue, current provisions provide a listing of a_p values in tables based on the expectation that the component will predominantly behave in a stiff or flexible manner (Drake and Bachman 1996). If the fundamental period of the NSC is less than 0.03 sec, no dynamic amplification is expected and hence $a_p = 1.0$. In current provisions, NSCs with fundamental period less than 0.03 sec are called rigid components / rigidly attached components and NSCs with fundamental period greater than 0.03 sec. are named flexible components / flexibly attached components.

The following equations describe the values of a_p in different regions of T_C/T_{B1} (see Figure 2.16).

$$a_p = 1.0 \text{ for } T_C / T_{B1} \leq 0.5 \tag{3.7}$$

$$a_p = 2.5 \text{ for } 0.7 \leq T_C / T_{B1} \leq 1.4 \tag{3.8}$$

$$a_p = 1.0 \text{ for } T_C / T_{B1} \geq 2.0 \tag{3.9}$$

Thus, a maximum a_p value of 2.5 is assumed for flexible components with periods around the fundamental period of the building and a minimum a_p value of 1.0 is assumed for regions with $T_C / T_{B1} \leq 0.5$ and $T_C / T_{B1} \geq 2.0$. For other regions of T_C/T_{B1}, namely $0.5 \leq T_C / T_{B1} \leq 0.7$ and $1.4 \leq T_C / T_{B1} \leq 2.0$, the a_p values are linearly interpolated from 1.0 to 2.5 (BSSC 2003). Equation (3.1) assumes a constant shape for the floor response spectrum (FRS) regardless of where the NSC is located in the supporting structure, i.e., a_p, does not depend on the location of the component in the supporting structure. In the provisions, the variation of the magnitude of the FRS with height is indirectly addressed by the variation of the factor PFA/PGA which stands for the Peak Floor Acceleration (PFA) normalized by the Peak Ground Acceleration (PGA). This factor varies from 1.0 at the ground to 3.0 at the roof and this had already been discussed in detail in the previous chapter (see section 2.3). The a_p factor scales the PFA values depending on the nature of the component. Thus, the current provisions represent a trapezoidal distribution of floor accelerations within the structure, linearly varying from the acceleration at the ground ($0.4S_{DS}$) to the acceleration at the roof ($1.2S_{DS}$).

The design spectrum for the building beyond period T_s ($T_s = S_{D1}/S_{DS}$) reduces in proportion to the ratio of T_s/T_{B1}. The primary structure is subjected to reduction in design forces for T_{B1} values higher than T_s. Hence, the current provisions justify similar reduction in design forces for NSCs (BSSC 2003). This reduction is addressed by the recently introduced exception clause as described previously by equations (3.4) and (3.5). Data from acceleration recordings measured at the roof level for buildings

show that the reduction in response begins at periods about 25% greater than S_{D1}/S_{DS}. Hence, the transition period T_{flx} in provisions has been increased by 25%. At the ground level, the effect of the structure response has no influence on the NSCs and hence the adjustment is zero. A linear interpolation is used between the top and bottom of the structure.

In brief, the current provisions are very simple and they are primarily aimed to address the NSC acceleration demands around the fundamental period region ($0.7 \le T_C / T_{B1} \le 1.4$). The R_p factor addresses the nonlinear action of the NSC. However, they do not address the effect of higher modes that can cause variations in the pattern of acceleration distribution along the height of the frame, the demands in the higher modal regions and effect of nonlinearity of the supporting structure on the demands on NSCs. The use of linear methods in the analysis of NSCs may often lead to unrealistic designs when the supporting structure behaves inelastically (both underestimation and overestimation of NSC acceleration demands).

3.3 COMPONENT AMPLIFICATION FACTORS FOR NSCS MOUNTED ON ELASTIC FRAMES

The focus of this dissertation is to estimate the acceleration demands on NSCs mounted on inelastic buildings. However, it is necessary to understand the acceleration demands on NSCs mounted on elastic frames before an attempt can be made to understand the behavior of NSCs mounted on inelastic buildings, which is described in the later part of this chapter (see section 3.4). Moreover, most building-structures behave in the linear structural force-displacement region for frequent but

small-magnitude earthquakes. Hence, it is necessary to understand the NSC demands when the building behaves elastically.

3.3.1 Overview

Extensive results are available in the public domain that enumerates the acceleration demands on NSCs mounted on elastic frames. One of the earliest and most popular method of calculating the response of NSCs is using Floor Response Spectrum (FRS) method (Biggs and Roesset 1970; Amin et al. 1971; Singh 1975). FRS method is similar to typical ground motion response spectra which quantifies the excitation of the base of the supporting structure. In the case of FRS the response spectrum for the excitation at the base of the NSC is generated giving it the name instructure response spectrum or systems-in-cascade. Earlier FRS methods required the analysis of combined primary (structural) – secondary systems. The validity of the FRS method is well established when the mass of the NSC is very small when compared to that of the supporting structure. Addressing the interaction effects (when mass of the NSC is larger) and non-classical damping effects (when the damping ratios of building and NSC are significantly different) in the analytical closed form solutions of original FRS method is very complex and impractical. Hence, alternate methods have been developed specifically to address these issues. These methods typically fall into two broad categories (Gupta 1990; Villaverde 2004):

a) FRS correction methods which employ modifications to address the effect of interaction and nonclassical damping, and

b) approximate modal or random vibration analysis of the combined structural-nonstructural system using modal synthesis.

Detailed information on FRS methods is available in references (Gupta 1990; Singh 1990; Soong 1994; Dey and Gupta 1998; Villaverde 2004). This dissertation makes use of the FRS approach wherein a large number of finite-element based elastic (and inelastic) building models are subjected to time-history analyses. The estimation of elastic NSC demands is a very important step in the proposed methodology which makes use of the demands on NSCs mounted on elastic buildings to estimate the demands on NSCs mounted on inelastic buildings (see section 3.6). The results for NSCs mounted on elastic buildings presented in this section are aimed for two additional reasons namely:

a) to complement the understanding of the problem (namely quantification of acceleration demands on NSCs mounted on elastic frames), and

b) to aid researchers attempting to compare / validate the results of the current dissertation to that of existing results obtained by different methods.

The interaction effects that are not considered in the broader part of this dissertation are discussed in detail in appendix I.

3.3.2 Representation of FRS Results

As explained in the previous chapter, FRS is the plot of the peak value of the response quantity as a function of the period of the NSC (T_C). The component amplification factor (a_p) for NSCs mounted on elastic frames is the ratio of peak component acceleration to that of the peak floor acceleration (see equation (3.10)).

$$a_p = \frac{S_{aC}(elastic)}{PFA_e} \tag{3.10}$$

This value being an alternate representation of FRS is also a continuous response quantity. Hence, it is necessary to categorize the FRS at salient modal periods and locations in the supporting structure, so that a near complete picture of the FRS can be obtained from the data at a multiple number of locations and modal periods/modal period ranges of the supporting structure. The results of the sensitivity study performed in the pervious chapter helps towards this goal.

It has been clearly demonstrated in the previous chapter that the a_p values are strongly dependent on the modal periods (T_C / T_{Bi} ratio) and the location of the NSC in the building (see sections 2.4.1 and 2.4.2). The peak values of a_p for elastic frames occur around the modal periods of the building. These values are named as a_{pi}, where the subscript i stands for the number of the modal period. Thus, a_{p1}, a_{p2} and a_{p3} stand for the a_p values at the first, second, and third modal periods of the building, respectively (see equation (3.11)). Due to the numerical nature of time-history analyses performed in the current dissertation, FRS values are computed at component periods (T_C) spaced in 0.01 sec intervals. Hence, a tolerance of 5% of the modal period is used while picking the a_p values at a particular modal period (see equation (3.12)). Consequently, the a_{pi} values (a_{p1}, a_{p2} and a_{p3}) represent the peak a_p values in the interval $0.95T_{Bi} \le T_C \le 1.05T_{Bi}$.

$$\begin{aligned} a_{p1} &= \max(a_p) \text{ at } T_C / T_{B1} = 1.0 \\ a_{p2} &= \max(a_p) \text{ at } T_C / T_{B2} = 1.0 \\ &\vdots \\ a_{pi} &= \max(a_p) \text{ at } T_C / T_{Bi} = 1.0 \end{aligned} \tag{3.11}$$

$$a_{pi} = \max(a_p) \text{ in the interval } 0.95T_{Bi} \le T_C \le 1.05T_{Bi} \tag{3.12}$$

The magnitudes of a_{pi} values are a function of periods of the primary structure, the location of the NSC in the building, and the damping ratio of the NSC. To address the variation of a_p values with respect to the location of NSC in the building, a_p values are presented at three locations in the building namely, roof, mid-height, and a height equal to one third of the total height of the frame (bottom-third). These values correspond to relative height (*RH*) values of 1, 0.5, and 0.33, respectively. For each building, the floors are spaced at *RH* values of the order *1/N*, where *N* is the number of stories of the building. Thus, the FRS value recorded at a floor closest to location of interest is used while picking the values at mid-height and bottom-third location.

Any robust methodology should consider a wide range of building and NSC properties so that the results can be applied in the broader context and be generalized for most buildings. To address the variation in modal properties for the type of systems (due to variations in stiffness) considered in this dissertation, a wide range of frames with periods ranging from 0.3 sec to 3.6 sec have been used. The building models used in this study have T_{B1} that correspond to both stiff and flexible type buildings. The effect of variation in stiffness on the building models (straight-line first mode shape buildings versus nonlinear first-mode type buildings) had also been discussed (see section 2.4.4). The results in this study are aimed to address most types of moment-resisting frame structures with small to large fundamental periods of vibration.

To represent the FRS, both the a_p values and the location of first and higher modal periods (values of T_{Bi}) are necessary. An understanding of the ratio of the second period of vibration to the fundamental period of vibration (T_{B2}/T_{B1}) and the third period of vibration to the fundamental period of vibration (T_{B3}/T_{B1}), allows the simplified representation of all the salient periods of FRS as a function of T_{B1}. These ratios also help to find the location of the second and third peaks in the FRS when only the value of T_{B1} is known. The T_{Bi}/T_{B1} values are strongly dependent on the type of lateral load resisting system, i.e., flexural type system (e.g. walls and braced-frames) or shear type system (e.g. frames). For a pure flexural beam, the T_{B2}/T_{B1} and T_{B3}/T_{B1} ratios are on the order of 0.16 and 0.06, respectively, and they approach values of 1/3 and 1/5 for a pure shear beam (Miranda and Taghavi 2005). Chrysanthakopoulos (Chrysanthakopoulos et al. 2006) has presented approximate formulas for computing the first three modal periods of plane steel frames. The T_{B2}/T_{B1} and T_{B3}/T_{B1} ratios are order of 0.3 and 0.18 for unbraced frames with constant sections per height. The corresponding values of these ratios vary from 0.16 to 0.32 and 0.06 to 0.19 for braced frames. The T_{B2}/T_{B1} ratio for the frames used in this study varies from 0.31 for 3-story frame to 0.35 for 18-story frame. The T_{B3}/T_{B1} ratio has values of 0.15 for 3-story frame and 0.21 for 18-story frame. The T_{B2}/T_{B1} ratios for moment-resisting frames and wall type structures used in the study by Seneviratna (Seneviratna and Krawinkler 1997) are around 0.4 and 0.16, respectively. The corresponding T_{B3}/T_{B1} values are 0.26 and 0.06. Periods reported in other studies also show that the T_{B2}/T_{B1} values are lower than 0.5 (Singh et al. 1993; Wang and Wang 2005).

The T_{Bi} values reported in the above studies show that the higher modes of the supporting structure are more closely spaced when compared to the first two modes. Hence, it is worthwhile to group the response of higher modes by one value. The current code provisions which does not adequately address the NSC demands in the higher modal region, also indirectly group this region into one entity and specifies a value of $a_p = 1.0$ for $T_C / T_{B1} \leq 0.5$. The region from $0 \leq T_C \leq 0.5T_{B1}$ is usually called as the short period or High Frequency (*HF*) region. As all the higher modes fall in this region for typical building configurations, it is important to understand the maximum values of a_p for NSCs that have periods in this high frequency (*HF*) region (see equation (3.13)). This value allows categorizing all the peaks in this region by one envelope value. The current study recognizes the importance of this region and groups the NSC demands into a single value representative of the entire region. The envelope value that represents the maximum value of a_p in this region is called as $(a_{p\text{-}HF})_{max}$.

$$(a_{p-HF})_{\max} = \max(a_p) \text{ in the interval } 0 \leq T_C \leq 1.05T_{B2} \tag{3.13}$$

Although the definition of $(a_{p\text{-}HF})_{max}$ in equation (3.13) includes only the higher modes, the High Frequency (*HF*) region can be generalized as the region with $T_C / T_{B1} \leq 0.5$, based on the published period formulae available in the literature that has been discussed above. This generalization also helps to address inaccuracies in computation / determination of higher modal periods.

The maximum a_p value, $(a_p)_{max}$, observed for the entire period range of the FRS (see equation (3.14)) is usually the maximum of a_{p1} and $(a_{p\text{-}HF})_{max}$. This value allows one to find the maximum amplification irrespective of the corresponding

period in the FRS. This value is useful when one does not know the period of the NSC or the location of the NSC in the supporting structure (see section 3.3.4), but only the period of the supporting structure. Some recent studies have recommended equivalent a_p values or floor spectrum coefficients that covers all the peaks (both fundamental and higher modal peaks) by an envelope curve (Singh et al. 2006b). An understanding of $(a_p)_{max}$ also aids researchers following the above approach.

$$(a_p)_{\max} = \max(a_p) \text{ in the interval } 0 \le T_C \le \infty \tag{3.14}$$

3.3.3 a_p Values at First Three Modal Periods of the Supporting Structure

In this subsection, the quantification of the a_p values is presented for NSCs that have periods around the first three modal periods of the building (a_{p1}, a_{p2} and a_{p3}). Figure 3.1 shows the median a_{p1} and a_{p2} values recorded at the roof for all the frames. It can be seen that a_{p1} values decrease with an increase in the fundamental period of the building. This behavior is similar to the $1/T_{B1}$ variation reported in other studies (Singh et al. 2006a). Higher values of a_p are obtained for lower values of component damping. The median a_{p1} values vary from 9.4 to 1.9 and from 5.5 to 1.3 for $\zeta = 2\%$ and $\zeta = 5\%$ damping ratio of NSC, respectively. For a given fundamental period of the frame, a_p values are weakly dependent on the height of the structure (i.e., the number of stories).

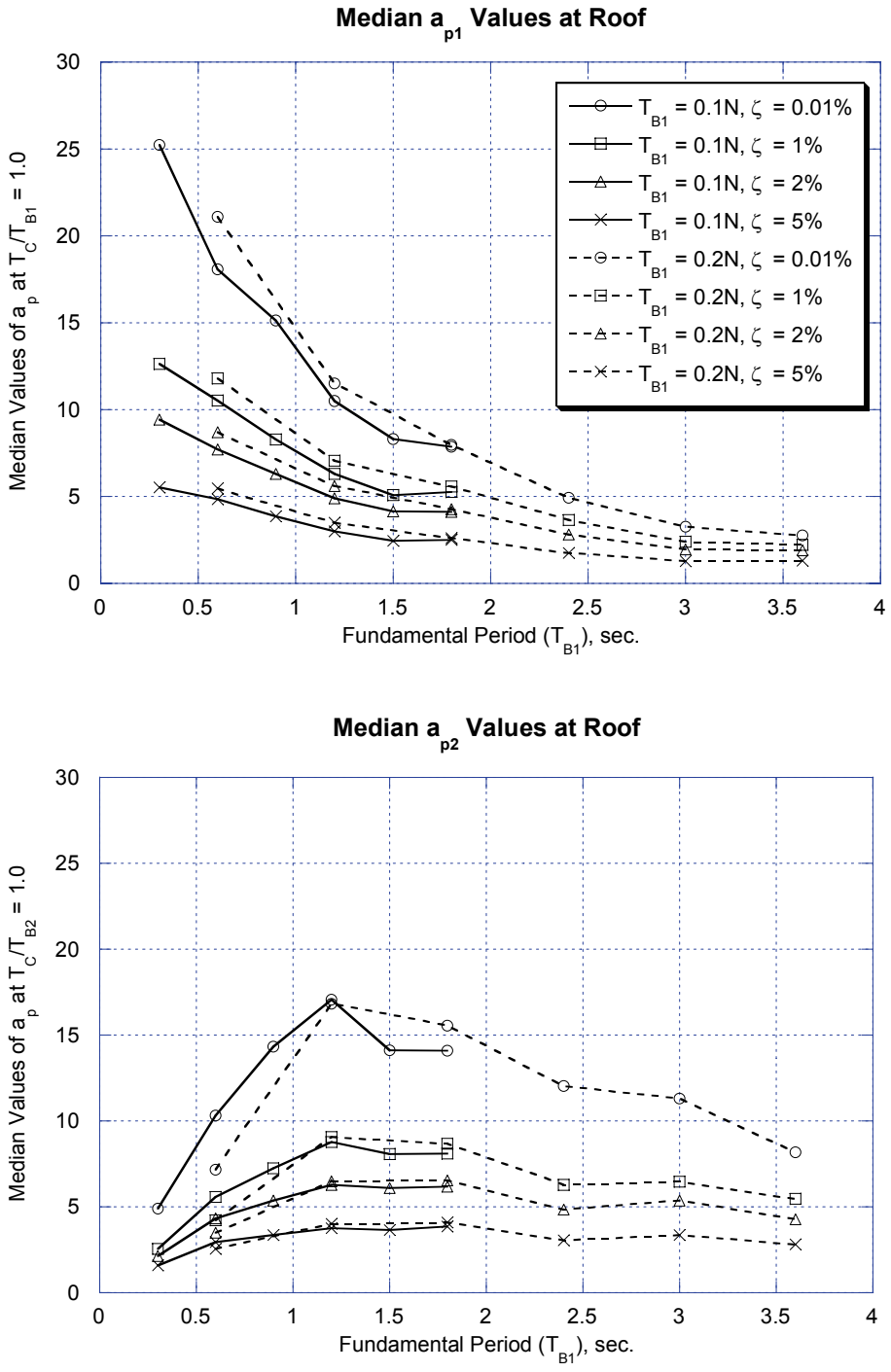

Figure 3.1 a_p values at first two modal periods of the building at roof location

Figures 3.2 and 3.3 show the corresponding values at mid-height and at 1/3rd height of the frame, respectively. These plots show the medians of the peaks of the FRS around the first and second modal periods for the buildings considered in this dissertation. For a given T_{B1}, the values of a_{pi} are strongly dependent on the mode shape and the participation factor of the i^{th} mode. Hence, it can be seen that the a_{p1} values at roof are higher than the values at the lower floors. The a_{p2} values at mid-height and 1/3rd height of the frame are higher than a_{p2} values at roof. For building periods higher than 0.9 sec, the median a_{p2} values at mid-height location are approximately equal to 7.9, 5.9, and 3.6, for 1%, 2%, and 5%, NSC damping ratios, respectively. It should also be noted that the FRS values are recorded only at fixed, equally spaced floor levels for taller frames ($N \geq 9$). This combined with selection of floor of interest that are spaced in increments of *1/N*, produces a zigzag pattern (see figure 3.2 around T_{B1} = 1.5 sec.) for a_{p2} values at mid-height of the frames. The *RH* at mid-height location has values of 0.67, 0.5, 0.56, 0.5, 0.6 and 0.56 for 3-, 6-, 9-, 12-, 15- and 18- story frames, respectively. The *RH* values at bottom-third location are closer and they vary from 0.33 to 0.4.

Figure 3.4 shows the variation of a_{p3} values at the roof and bottom-third location for the frames used in this study. It can be seen that a_{p3} values increase with the fundamental period of the frames till about 1.2 sec., and with further increase in the fundamental period, the values remain constant. After this transition period, the median a_{p3} values at the roof are of the order of 10, 6, 5 and 3 for NSC damping ratios of 0.01%, 1%, 2% and 5%, respectively.

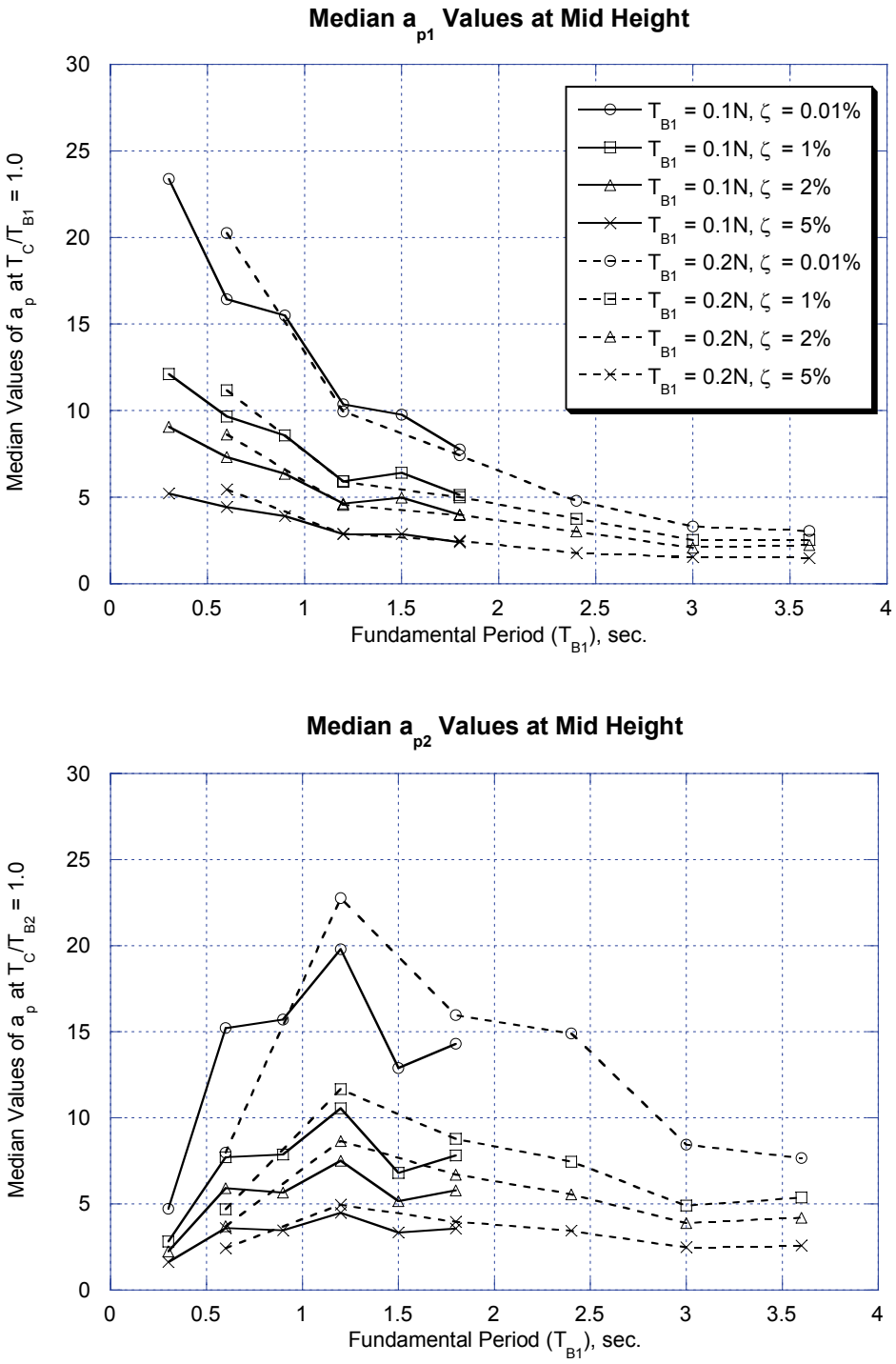

Figure 3.2 a_p values at first two modal periods of the building at mid-height location

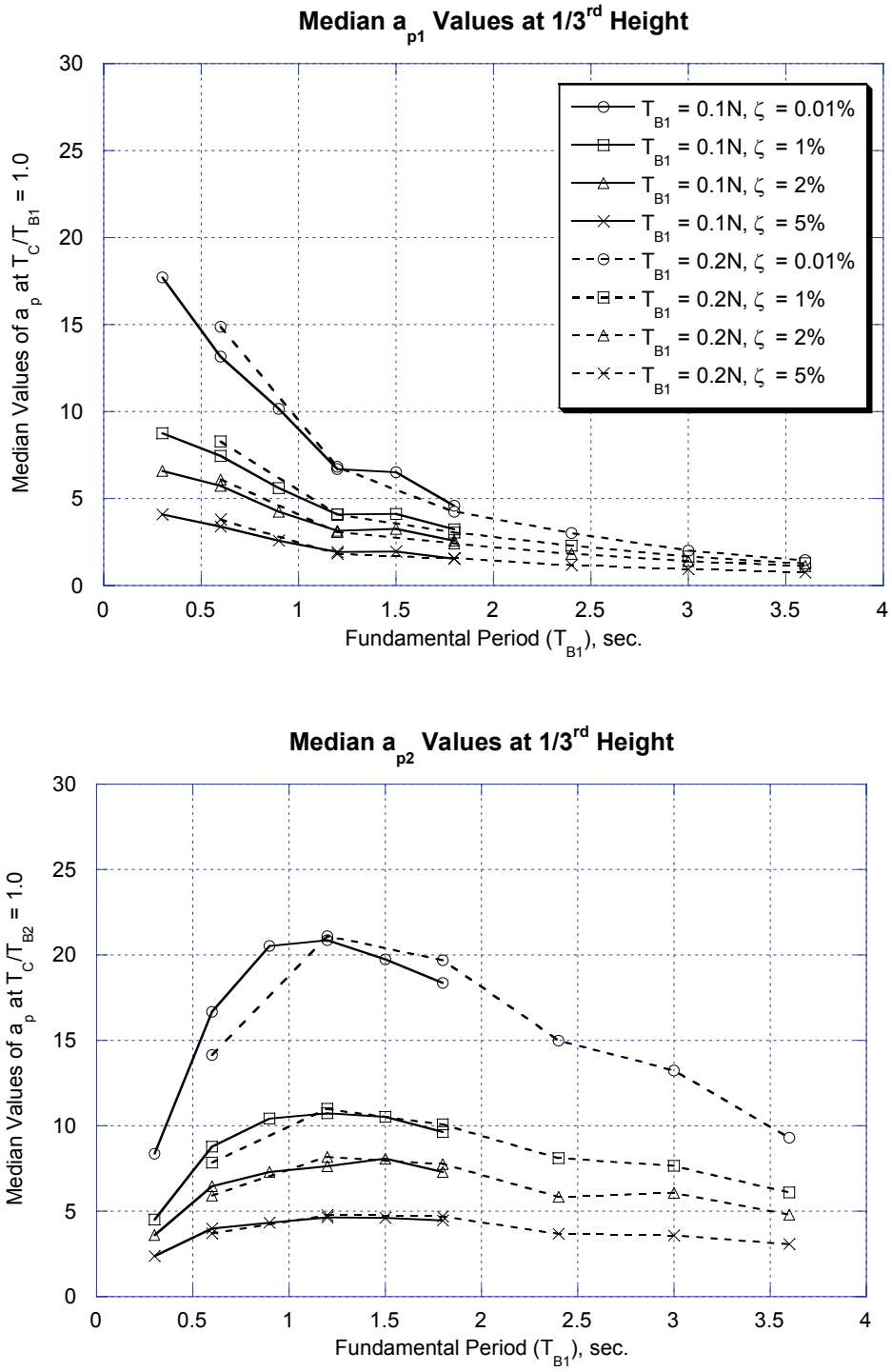

Figure 3.3 a_p values at first two modal periods of the building at 1/3rd height

The average of a_{p3} values for each individual case in figure 3.4 reported at the bottom-third location is similar to the corresponding values at the roof. These plots show that the median values of a_{pi} reported for the first three modal periods are consistently higher than the values of 1.0 and 2.5 used in the current provisions even for high damping ratios of NSCs (5% and 2%).

3.3.4 Maximum Values of a_p and Values at Higher Modal Region

Figures 3.5 to 3.7 show the median $(a_p)_{max}$ and $(a_{p\text{-}HF})_{max}$ values recorded at roof, mid-height, and bottom-third height of the frame, respectively. Similar to the previous results, the $(a_p)_{max}$ values are sensitive to very low values of component damping. The magnitudes of the median $(a_p)_{max}$ values at roof and at bottom-third height are nearly equal for component damping values of 1% and above, thus showing a weak dependence of $(a_p)_{max}$ on the location of NSC in the structure. The $(a_p)_{max}$ variation is very different when compared to the inverse variation of a_{p1} with respect to T_{B1} at the roof and other locations (see figure 3.1). For damping ratios of 1% and higher, the median $(a_p)_{max}$ values at roof are nearly constant for periods beyond 0.6 sec. As the fundamental period increases, the a_{p1} values decrease (see figures 3.1 to 3.3) but a_{p2}, a_{p3} and higher mode a_{pi} values increase (see figure 3.4). Although the shape of the FRS varies for different T_{B1} values, the $(a_p)_{max}$ values are nearly the same. It can be seen that $(a_p)_{max}$ values are consistently higher than the maximum value of 2.5 prescribed in current code provisions.

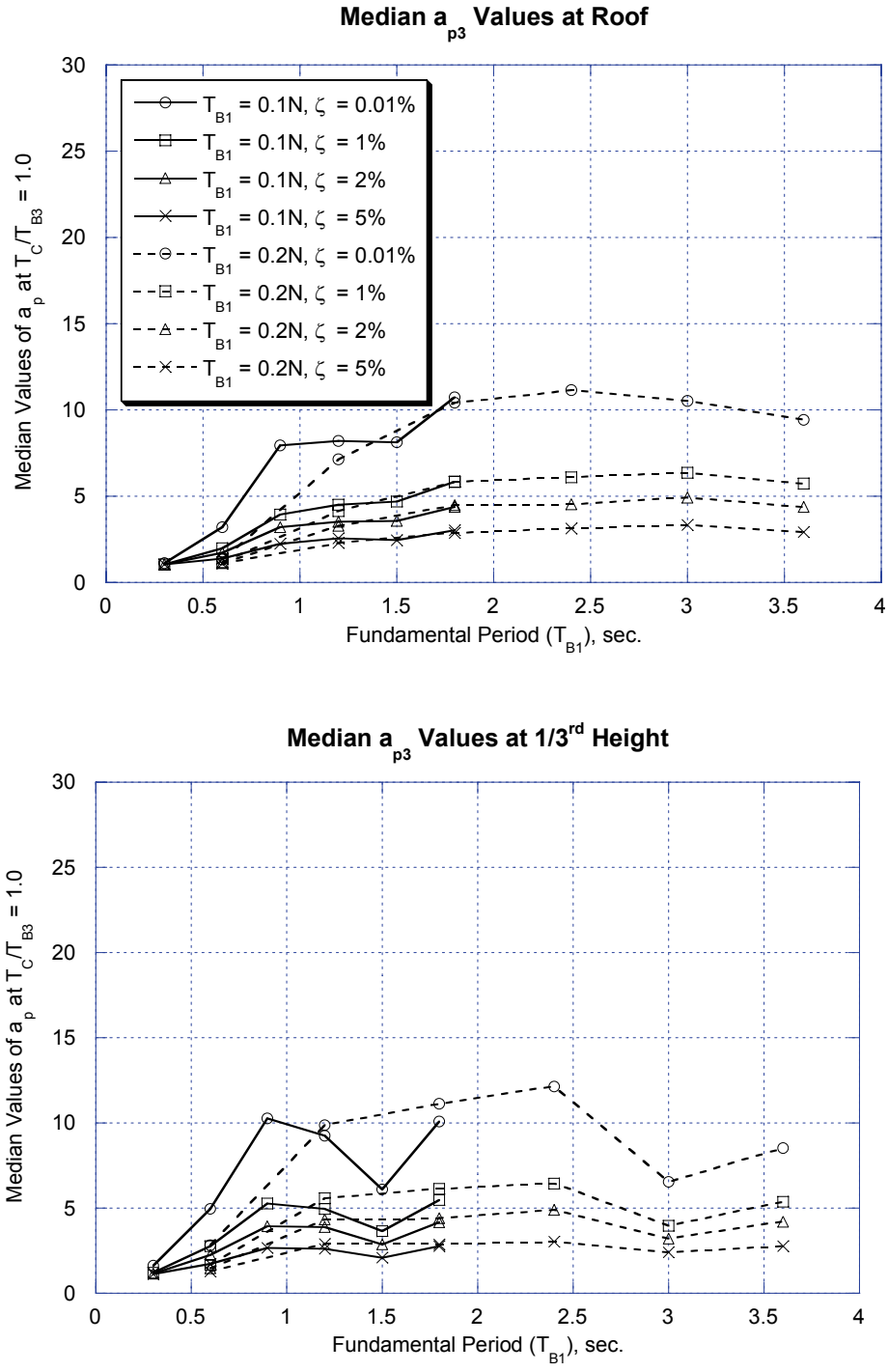

Figure 3.4 a_p values at third modal period for roof and mid-height location

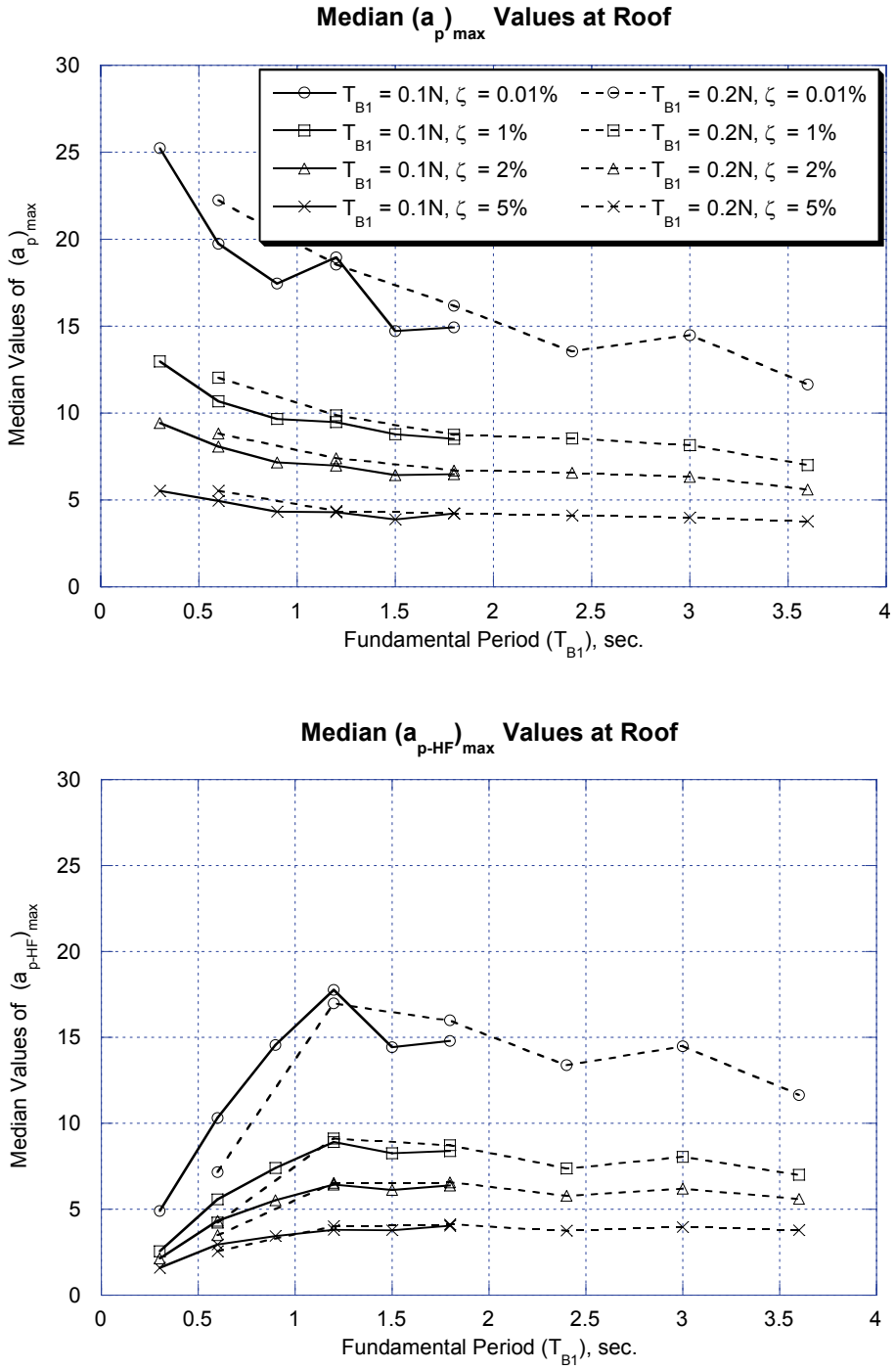

Figure 3.5 Maximum values of component amplification factor at roof for elastic buildings

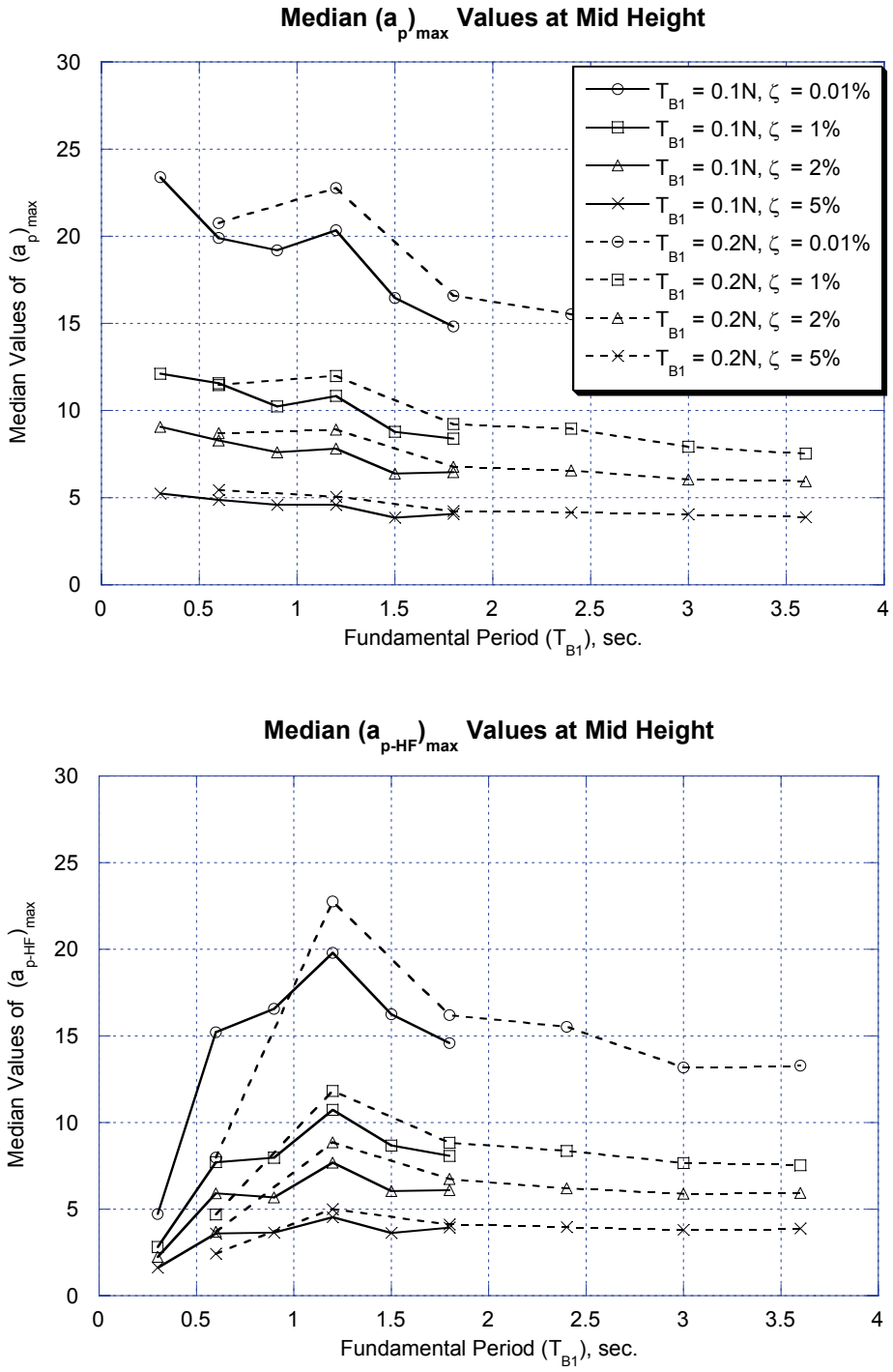

Figure 3.6 Maximum values of component amplification factor at Mid-height for elastic building

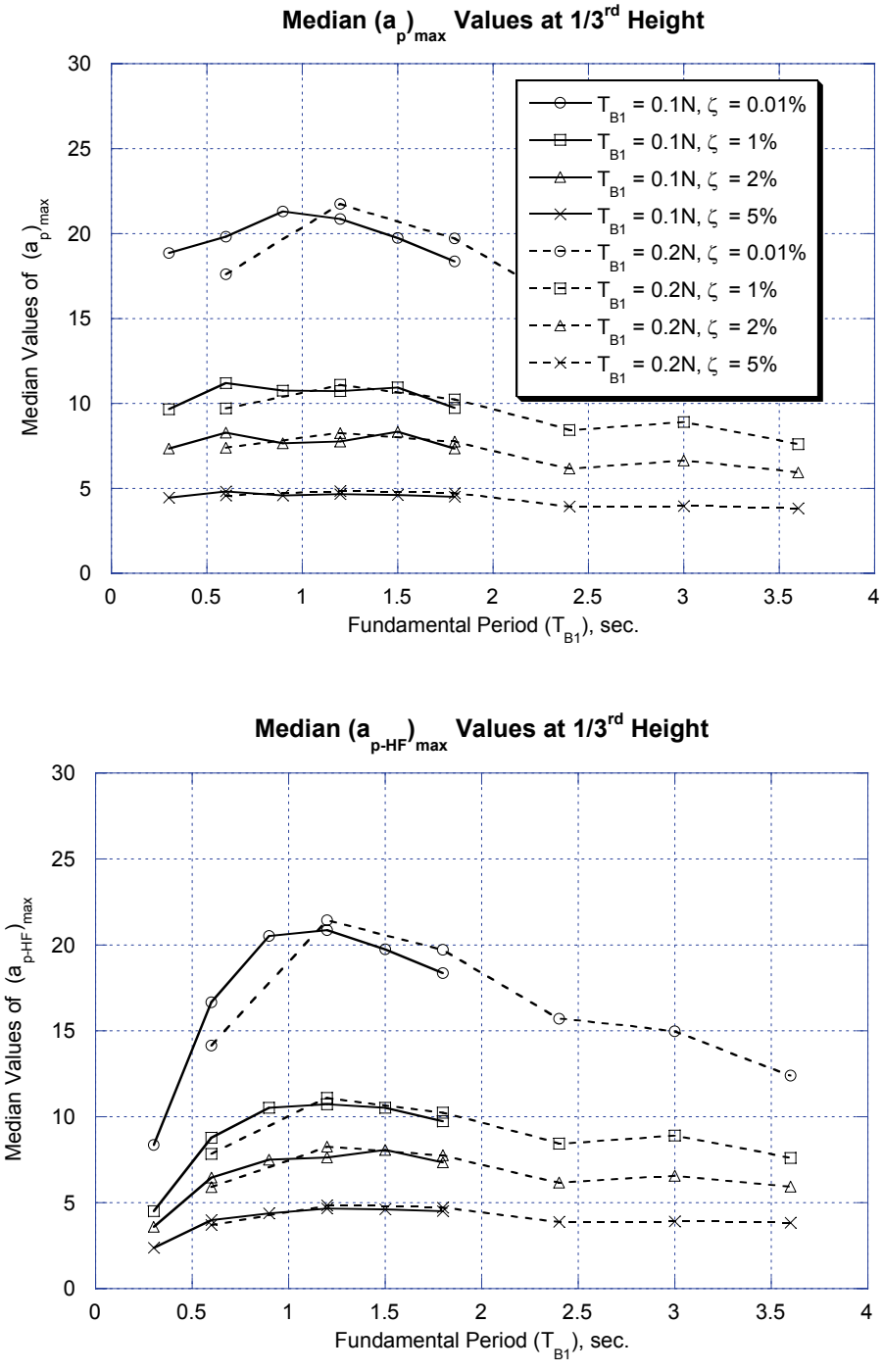

Figure 3.7 Maximum values of component amplification factor at bottom-third height for elastic buildings

The weak dependence of $(a_p)_{max}$ on the location of the NSCs can be attributed to the fact that maximum values of a_{pi} corresponding to i^{th} modal period occur at lower floor locations for higher modal periods. However, a_{p1} has maximum value around $RH = 1$ (see section 3.3.3). Hence, $(a_p)_{max}$ being the greater value of both a_{p1} and a_{pi} at higher modes is weakly dependent on the location of NSC and hence a single value of $(a_p)_{max}$ can be provided for elastic buildings. The $(a_p)_{max}$ value represents the maximum component amplification value for a supporting structure with a given T_{B1}. Hence, this value is useful when the period of the NSC is not known to the designer aiming to design the supports for NSCs mounted on a building. However, this value might be overly conservative when the period of the NSCs are sufficiently away from the peak acceleration response regions of the FRS (e.g. when the period of the NSC is much larger than T_{B1}). Recently some researchers have attempted to provide equivalent a_p values or response spectrum coefficients which have single envelope value that covers both the fundamental and higher modal period regions (Singh et al. 2006b). The $(a_p)_{max}$ values provided in this study are useful for future works that follow that approach.

The $(a_{p\text{-}HF})_{max}$ values are nearly constant for T_{B1} values higher than 0.9 sec. Beyond this period, the higher mode periods dominate the a_p values and the a_p peaks at higher modes are significantly higher than a_{p1} values. The median $(a_{p\text{-}HF})_{max}$ values are of the order of 15, 9, 7 and 4 for 0.01%, 1%, 2% and 5% damping of NSCs, respectively. The median $(a_{p\text{-}HF})_{max}$ in the *HF* region are significantly higher than the value of 1.0, prescribed in the current code provisions.

The current results clearly demonstrate the need for considering the component amplification factors at higher modal periods of the supporting structure and the importance of the higher frequency region in defining the shape of the FRS. Moreover the $(a_{p\text{-}HF})_{max}$ values by definition being the combined response of all higher modes are not dependent on the location of the NSC. Median $(a_{p\text{-}HF})_{max}$ values are consistently greater than 1. The results clearly show that the current provisions are inadequate in the low period region.

3.4 ACCELERATION RESPONSE MODIFICATION FACTOR FOR NSCs MOUNTED ON INELASTIC FRAMES

The inelasticity of a building modifies the floor motions and the forces to which the NSCs are subjected as compared to the motions and forces for elastic structural behavior. At present, there is no clear understanding as to how inelastic behavior may affect a FRS (Villaverde 2004). In general, it is perceived that this structural nonlinearity will greatly benefit the NSC response, under most situations (Lin and Mahin 1985; Sewell et al. 1986; Singh et al. 1993) i.e, the acceleration demands on NSCs mounted on inelastic buildings are smaller than that mounted on elastic buildings. To understand the behavior of NSCs in inelastic building structures, this study exposes the structure to different levels of inelasticity as defined by the Relative Intensity (RI) parameter and then quantifies the response of NSCs attached to them. To facilitate the comparison of the results for NSCs when the building behaves inelastically to that when the building behaves elastically, a parameter called acceleration response modification factor (R_{acc}) is introduced in this dissertation. The R_{acc} factor is defined as the FRS for linear structural response normalized by the FRS

for a certain level of nonlinear structural behavior (see equation (3.15)). As described earlier (section 3.2.2), current provisions address the effect of nonlinearity of the equipment through R_p factor. However, many types of conventional structures are designed to resist strong earthquakes and can be expected to experience significant inelastic deformations when subjected to severe levels of earthquake ground motions. This nonlinear behavior of the supporting structure will influence the NSCs significantly. The R_{acc} factor is proposed to address this specific issue, i.e. the influence of inelasticity of the supporting structure on the peak acceleration demands for NSCs.

$$R_{acc} = \frac{S_{aC}(elastic)}{S_{aC}(inelastic)} \tag{3.15}$$

The R_{acc} factor can be used to scale the response of NSCs mounted on elastic structures to obtain the acceleration demands on NSCs mounted on inelastic structures (see section 3.6). Although, the proposed methodology makes use of the elastic a_p values obtained using the FRS method in this dissertation, the R_{acc} factors can be used regardless of the method used to obtain the peak response of NSCs on elastic buildings. Moreover, the R_{acc} factors can be combined with the R_p factor (see equation (3.1)) currently used in the building so that the building codes can account for both the nonlinearity of the buildings and that of NSC.

3.4.1 Overview of Previous Research Efforts

Literature dealing with the influence of nonlinear MDOF structural behavior on NSC response has primarily been limited to case studies of typical nuclear power plant structures (Kawakatsu et al. 1979). Due to the complexities in obtaining an

analytical solution, most of the efforts have been directed towards the development of reduction and amplification factors by which a linear floor response spectrum should be modified to approximately take into account such nonlinearity. Some of these works use the same approach in this dissertation; however, most works use different measures for quantifying the nonlinearity of the building (e.g structure displacement ductility). Kennedy (Kennedy et al. 1981) evaluated a typical MDOF Pressurized Water Reactor auxiliary building modeled with a series of lumped masses and beam elements considering soil-structure interaction effects. That study used a FRS ratio factor that is an inverse of R_{acc}. The study concluded that the inelastic behavior has the effect of reducing the in-structure response for most frequencies from elastically calculated spectral values. In a comparison of inelastic to elastic FRS at various locations of the structure, Wesley (Wesley and Hashimoto 1981) found that structural nonlinearity often caused increases in High-Frequency region of the spectra. Bumpus (Bumpus et al. 1980) undertook a systematic effort at examining the influence of ground motions and MDOF structural nonlinearity on equipment under the seismic safety margins research program (LLNL 1980). The FRS results for a simple ten-mass stick model (shear beam) subjected to 45 different input time histories were presented. This study used a factor called *Factor of Conservatism* (*FOC*) which is equivalent to the R_{acc} factor. The study reports a substantial increase in *FOC* near the elastic first mode structural frequency and a decrease in *FOC* at higher frequencies. Lin and Mahin (Lin and Mahin 1985) undertook a parametric study on the influence of structural nonlinearity on equipment response primarily with SDOF elastic equipment mounted on a SDOF structure. The FRS of an inelastic structure was

obtained by reducing the structure's yield displacement until the desired ductility was achieved. Their study used a parameter called *amplification factor*, which is equivalent to the inverse of the R_{acc} factor used in this study. Sewell (Sewell et al. 1986; Sewell et al. 1987) used the ratio of FRS for the inelastic structure normalized by the FRS of the corresponding elastic structure to quantify the nonlinear behavior. This ratio was called as *Floor Response Spectra Ratio (FRSR)*, and is equivalent to the inverse of the R_{acc} factor. Singh (Singh et al. 1993), defined a *response reduction factor* or *R-factor* which is the ratio between the elastic and inelastic absolute accelerations of the subsystem. The study concluded that for normal equipment, the use of *R-factor* provides a practical and simple approach to include the effect of yielding in the calculation of forces on NSCs. For more details on the different methods of analysis and overview of existing literature, the reader is referred to the literature reviews presented in works by Sewell (Sewell et al. 1986; Sewell et al. 1987), Chen and Soong (Chen and Soong 1988), Soong (Soong 1994), Phan and Taylor (Phan and Taylor 1996), Villaverde (Villaverde 1997b; Villaverde 2004) and Gupta (Gupta 1990).

The previous research efforts focused mostly on establishing the elastic FRS. Due to the large computational requirements and difficulties in solving the problem analytically, only isolated studies were done for quantifying the demands in the inelastic domain of supporting structure. These works mostly aimed to demonstrate the deamplification of demands around the fundamental period region with a few case studies. Although Sewell (Sewell et al. 1986; Sewell et al. 1987) attempted to understand the factors influencing the equipment response mounted on nonlinear

structures and also FRS amplification that can occur in some regions of FRS, the application of their results to typical regular moment-resisting frame type building considered in this dissertation is limited, because of two primary reasons:

a. The reference shear beam (stick) structural model used is representative of a typical, fixed-base, stiff Nuclear Power Plant (NPP) structure with a period of 0.33 sec. (3 Hz).
b. The size of the ground motion sample considered is too small to establish any firm correlations between input motions and the results. Their study used 4 near-fault ground motions (whose closest distances to the rupture fault area are less than 5 km) and one far-field ground motion.

Recent research works (Singh et al. 2006b; Villaverde 2006) that attempted to propose simplified methodologies for estimating the seismic design forces acknowledge the need for in-depth studies on quantifying the R_{acc} factor or other factors as a function of different properties of the supporting structure and equipment. The R_{acc} factor proposed in this study depends on the modal periods of the supporting structure, height of the supporting structure, location of NSC, damping ratio of NSC, and level of inelasticity of building. The large number of building and ground motion parameters used in the study allows the robust determination of R_{acc} values and their associated uncertainties.

3.4.2 Properties of R_{acc}

Figure 3.8 shows a typical plot of R_{acc} with both the elastic and inelastic FRS drawn for convenience. Representative plots for median of R_{acc} values at various

locations in the building are depicted in figures 3.9 and 3.10 for the 9-story frame with a fundamental period of 0.9 sec. and RI values of 2 and 4. In these figures, the damping ratios of the NSCs are 1% and 5%, respectively. As expected, R_{acc} increases with the value of *RI*, and larger values of R_{acc} are observed for NSCs with periods near the modal periods of the supporting structure. This implies that deamplifications of peak component accelerations caused by the inelasticity of the primary structure are more pronounced when the period of the NSC is close to the modal periods of the primary structure. It is important to note that the values of R_{acc} are much larger in the upper half of the structure, i.e., R_{acc} for the 2nd, and to some extent, the 4th floor of the structure are relatively small (i.e., closer to one). Increased equipment damping tends to reduce and smooth the R_{acc} values.

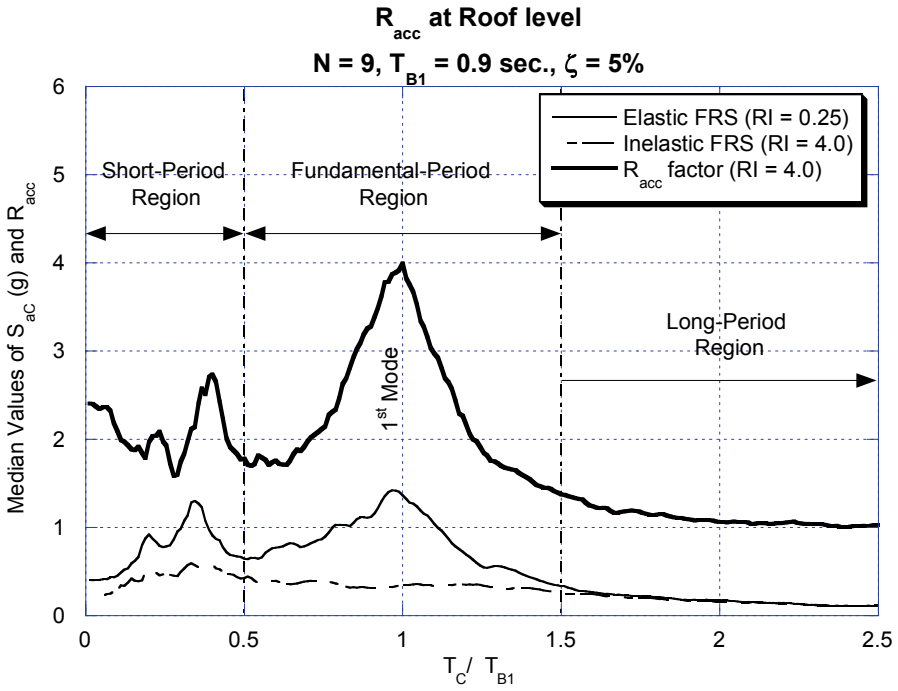

Figure 3.8 Acceleration response modification factor showing different FRS regions

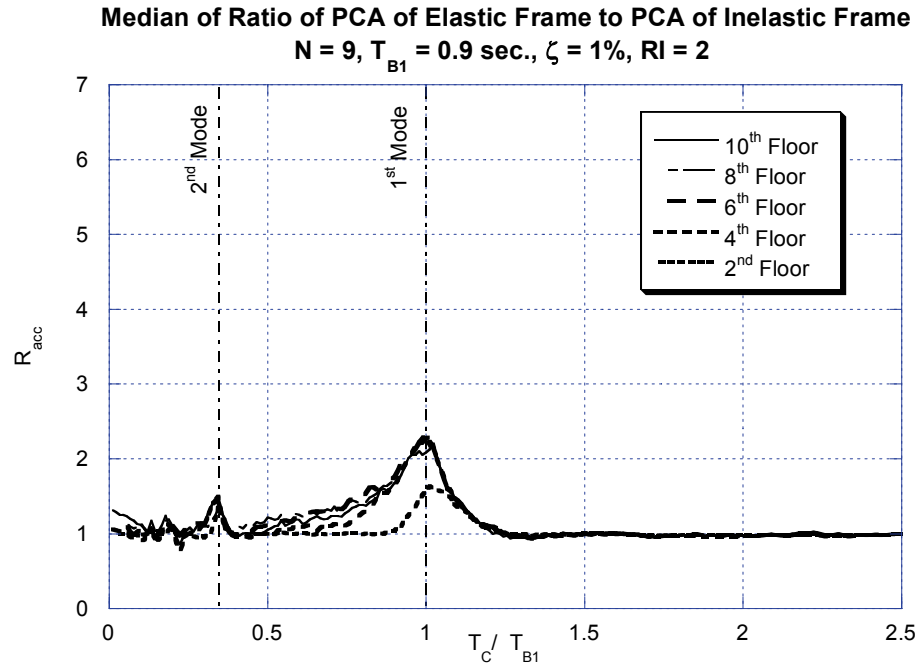

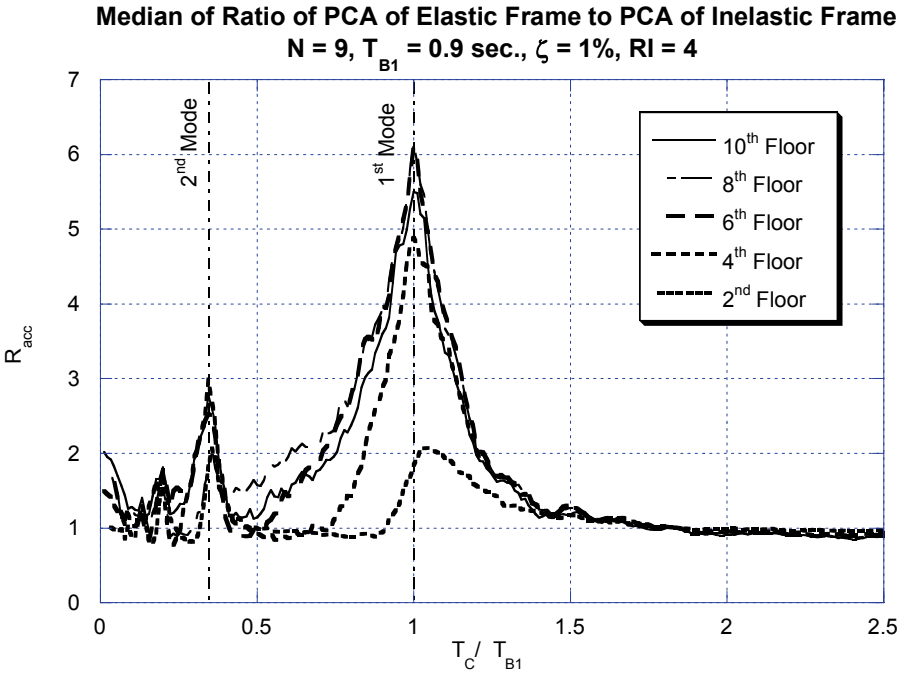

Figure 3.9 R_{acc} factor for 9-story frame with T_{B1} = 0.9 sec., various relative intensities and component damping ratio = 1%

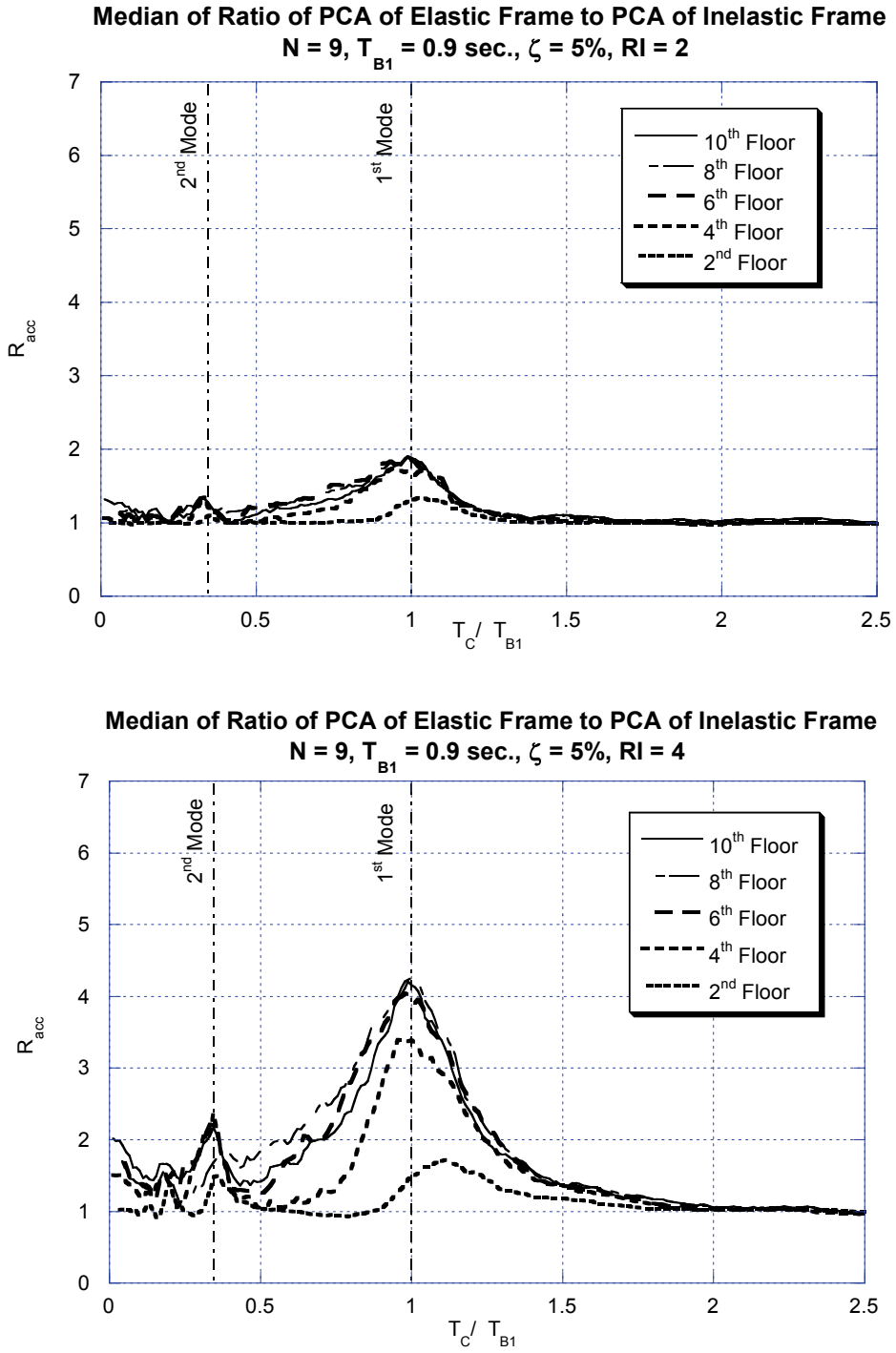

Figure 3.10 R_{acc} factor for 9-story frame with T_{B1} = 0.9 sec., various relative intensities and component damping ratio = 5%

The locations of the spectral peaks are weakly dependent on the level of equipment damping values considered in this study. These patterns are consistent across all structures and components used in this study. Three different period ranges are demarcated, and the behavior of R_{acc} in these ranges is discussed below.

1. Long-Period (Low Frequency) Region ($T_C / T_{B1} > 1.5$)
2. Fundamental-Period Region ($0.5 \le T_C / T_{B1} \le 1.5$)
3. Short-Period (High Frequency) Region ($T_C / T_{B1} < 0.5$)

3.4.2.1 Long-period region

The median R_{acc} values are slightly higher than unity. In the long period region the values fluctuates about unity, sometimes being greater than unity and sometimes slightly less than unity. R_{acc} values less than unity mean that the inelastic FRS values at a given period are higher than the elastic FRS values. The reason for amplification in this region is that the structure softens with higher *RI* values and the predominant period of vibration shifts or lengthens. The nonlinear FRS tends to flatten, broaden and sometimes shifts across the right of the elastic FRS, resulting in marginal decrease in FRS values below one.

3.4.2.2 Fundamental-period Region

In the vicinity of the elastic fundamental period, a substantial increase in R_{acc} is seen. This increase is higher for higher RI values and lower values of component damping. The increase can be attributed to two primary causes:

a) an increase in the damping ratio of the structure as a result of its energy absorbing nonlinear behavior and

b) a shift of the fundamental natural period of the structure away from the period of the nonstructural element, as defined earlier.

This reduction in inelastic FRS is quantified by higher R_{acc} values which in-turn yields considerable benefits for acceleration-sensitive equipment in this period range. This behavior is similar to that consistently seen in SDOF systems (Lin and Mahin 1985).

3.4.2.3 Short-period Region

The behavior of R_{acc} in this region is dependent on the location of NSC in the building and the effect of higher modes. Figure 3.11 shows the R_{acc} values at short-period region for the 0.9 sec. frame with NSC damping ratio of 0.01%. The figure shows $R_{acc} \geq 1.0$ at the 2nd and 3rd modal periods. This means that the higher modal periods also experience FRS deamplification when the structure transitions from elastic to inelastic behavior under the effect of ground motion. At the lower floor locations and near the higher modal periods, R_{acc} values less than one are observed. This behavior was observed for frames with 0.01%, 1% and 2% component damping ratios. However, for NSC damping ratio of 5%, the values are nearly equal to one for the models used in this dissertation. For very short periods, the R_{acc} value stabilizes to a constant value. This value is given by the ratio of the Peak Floor Acceleration (PFA) of the elastic structure response to the PFA of the inelastic structure response ($PFA_{elastic}$ / $PFA_{inelastic}$). An increase in *RI* values also produces a corresponding increase in the PFA ratios.

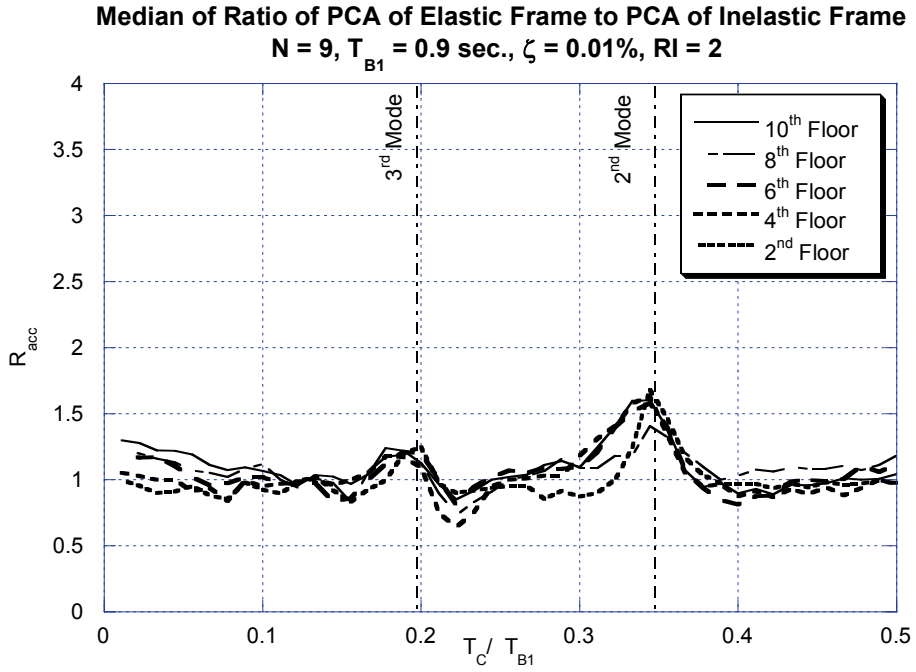

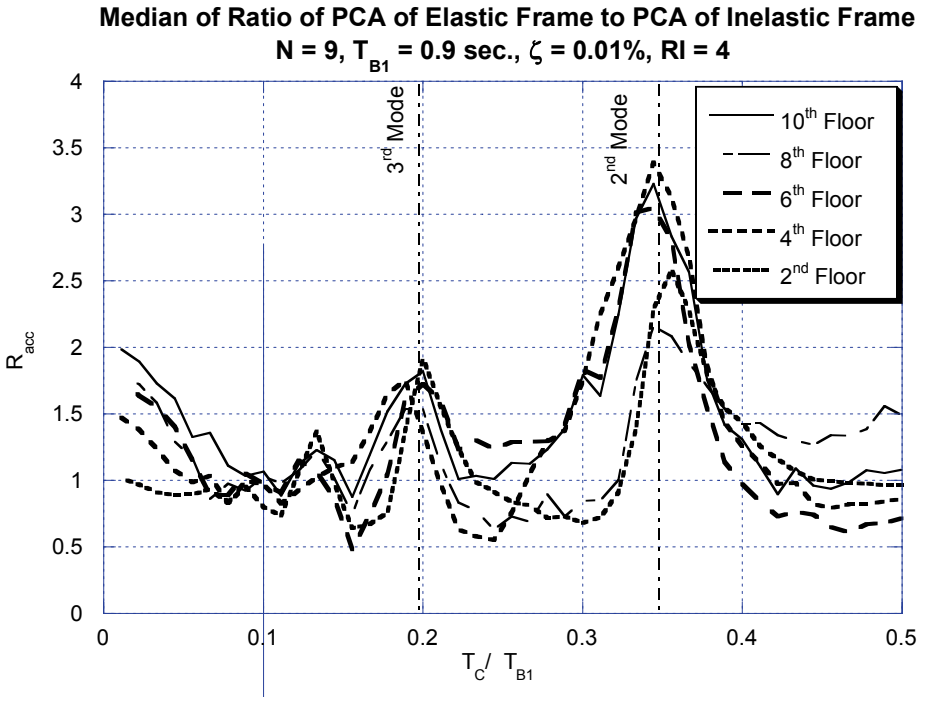

Figure 3.11 R_{acc} factor for 9-story frame with T_{B1} = 0.9 sec., various relative intensities and component damping ratio = 0.01%

Some numerical studies have shown that the FRS for nonlinear structure may actually increase in comparison to those obtained when the structure is assumed to remain linear at all excitation levels (Bumpus et al. 1980; Sewell et al. 1986; Sewell et al. 1987; Cornell and Sewell 1989; Singh et al. 1993; Singh et al. 1996; Villaverde 2004). Moreover, these studies have also shown that this increase is particularly noticeable at high frequencies and it depends on the properties of ground motion, supporting structure, the location of NSC in the building, and the level of inelasticity. The results obtained in this study are consistent with this observation. Median R_{acc} values less than one in this region, vary erratically with period and occur for lower and higher RI values. These values do not necessarily occur at the modal frequencies or at the peaks in the input ground motion. Figure 3.11 shows that $R_{acc} \leq 1.0$ occur in between two peak values of R_{acc}. This dissertation does not attempt to quantify the FRS amplification in this region, rather on the deamplification that occurs consistently around the first and higher modes of the building for all the damping ratios of NSCs. FRS amplification is discussed in more detail in appendix II.

3.5 FACTORS AFFECTING R_{acc}

It is important to understand the various parameters that affect the acceleration response modification factor (R_{acc}) before an attempt can be made to generalize its behavior. For this purpose, the R_{acc} values at the first and higher modal periods are investigated. The R_{acci} values stand for R_{acc} values at i^{th} modal period and are defined in equations (3.16) and (3.17). The maximum R_{acc} value at the short-period region can be represented by $(R_{acc\text{-}HF})_{max}$ parameter (see equation (3.18)). The effect of factors such as modal periods of the supporting structure, location of the NSC in the building,

height of the supporting structure, damping ratio of the NSCs, fundamental period of the supporting structure, and the level of Relative Intensity (*RI*) is investigated in the current section.

$$\begin{aligned} R_{acc1} &= \max(R_{acc}) \text{ at } T_C / T_{B1} = 1.0 \\ R_{acc2} &= \max(R_{acc}) \text{ at } T_C / T_{B2} = 1.0 \\ &\vdots \\ R_{acci} &= \max(R_{acc}) \text{ at } T_C / T_{Bi} = 1.0 \end{aligned} \tag{3.16}$$

$$R_{acci} = \max(R_{acc}) \text{ in the interval } 0.95T_{Bi} \le T_C \le 1.05T_{Bi} \tag{3.17}$$

$$(R_{acc-HF})_{\max} = \max(R_{acc}) \text{ in the interval } 0 \le T_C \le 1.05T_{B2} \tag{3.18}$$

3.5.1 Modal Periods of the Supporting Structure

In the previous chapter, the effect of modal periods of the supporting structure on the FRS values was evaluated (see section 2.4.1). The R_{acc} factor being the ratio of two floor response spectra quantities is also significantly influenced by the changes to FRS in both the elastic and inelastic domains. From figures 3.9 and 3.10, it can be seen that maximum values of R_{acc} occur at or around the modal periods. These plots reiterate the importance of the parameter T_C/T_{Bi} where T_{Bi} is the period of vibration of the i^{th} mode in the quantification of acceleration demands on NSCs mounted on inelastic frames. Unlike the elastic a_{pi} values at higher modes, which sometimes exceed the a_{p1} values, the R_{acci} values are not significant at higher modal periods when compared to the R_{acc1} values. However, R_{acci} values are greater than one at higher modal periods and values less than one occurs in between two modal periods (see figure 3.11). One of the possible factors is the modal interaction or internal resonance of the modes of the nonlinear system that causes R_{acc} values in the higher mode regions to reduce drastically (Nayfeh and Mook 1979), sometimes resulting in

R_{acc} values lesser than one. Hence, to calculate the benefit (reduction in acceleration demands) to NSCs due to inelastic action of the supporting structure in the fundamental-period region and short-period region, R_{acc1} and $(R_{acc\text{-}HF})_{max}$ respectively, are sufficient.

3.5.2 Height of the Supporting Structure

The effect of height of the supporting structure can be studied by looking into the R_{acc} plots for two frames with same fundamental period but different number of stories (N). The stiff and flexible frames used in this dissertation have fundamental periods of $0.1N$ and $0.2N$, respectively, and thus allow this comparison to be made for a set with identical T_{B1} values. Figures 3.12 and 3.13, show the results for sets of frames with T_{B1} values of 0.6 sec and 1.8 sec, respectively. The NSCs have 2% damping ratio and frames have RI values of 4. For the 1.8 sec frame set, the R_{acc} values and the shape of the R_{acc} plots, match very closely due to the close resemblance of the mode shapes (see figures 2.5 and 2.6). However, for the 0.6 sec frame set, the R_{acc} values match closely only at the first mode (see figure 2.4). At the short-period region, due to the larger participation of higher modes in the 6-story frame, R_{acc} values are slightly higher than that of the 3-story frame. Moreover, R_{acc} values less than one occur for a small short-period region in the bottom-most story of the 0.6 sec. frames (see figure 3.12). In the very high frequency region where the values approach the ratio of the PFAs ($PFA_{elastic} / PFA_{inelastic}$), median values are also similar in both frames. Thus it can be generalized that the R_{acc} values are more dependent on the T_{B1} values than the number of stories of the supporting structure.

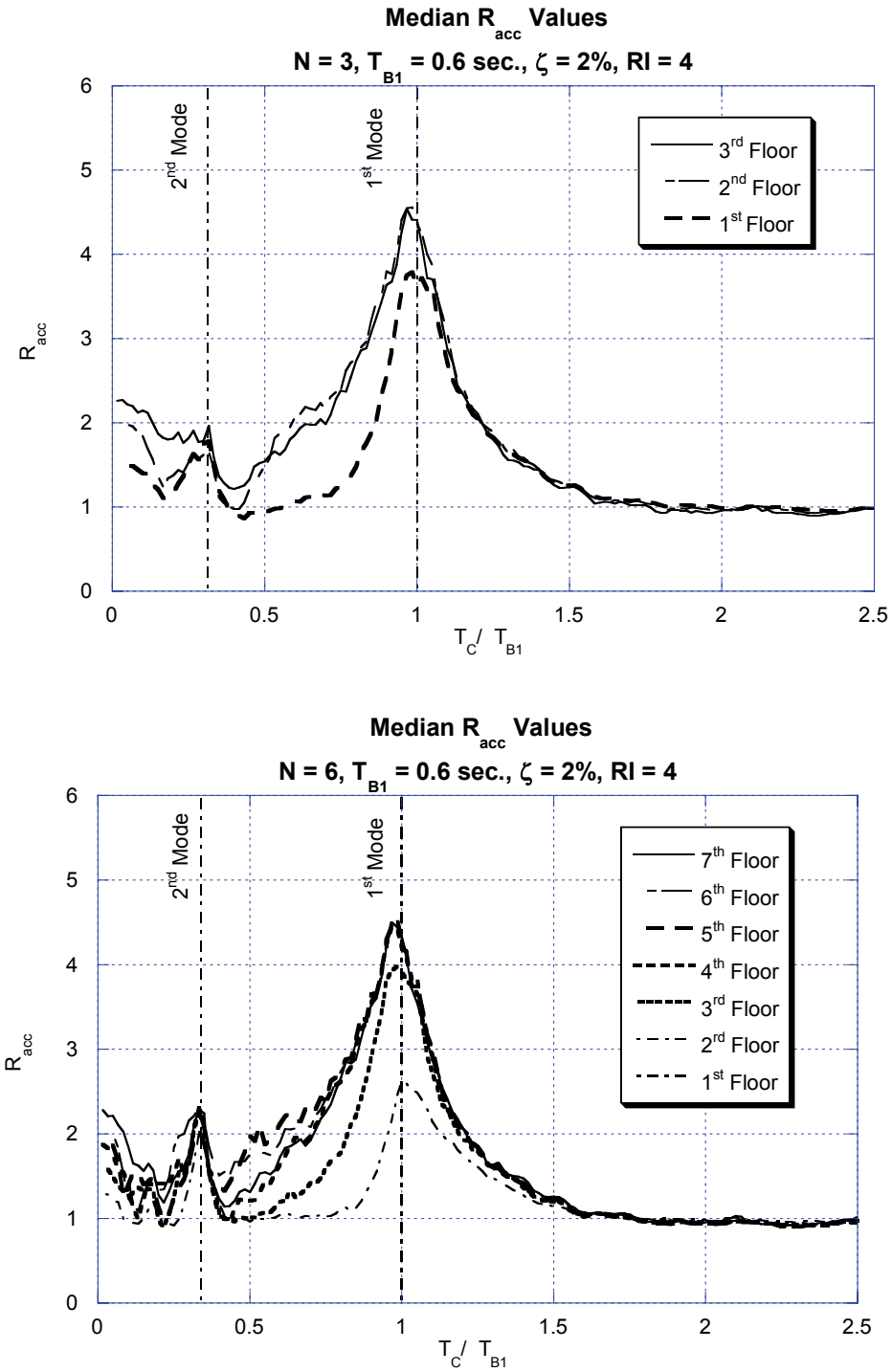

Figure 3.12 Effect of building height on R_{acc}; component damping ratio = 2%, RI = 4, T_{B1} = 0.6 sec.

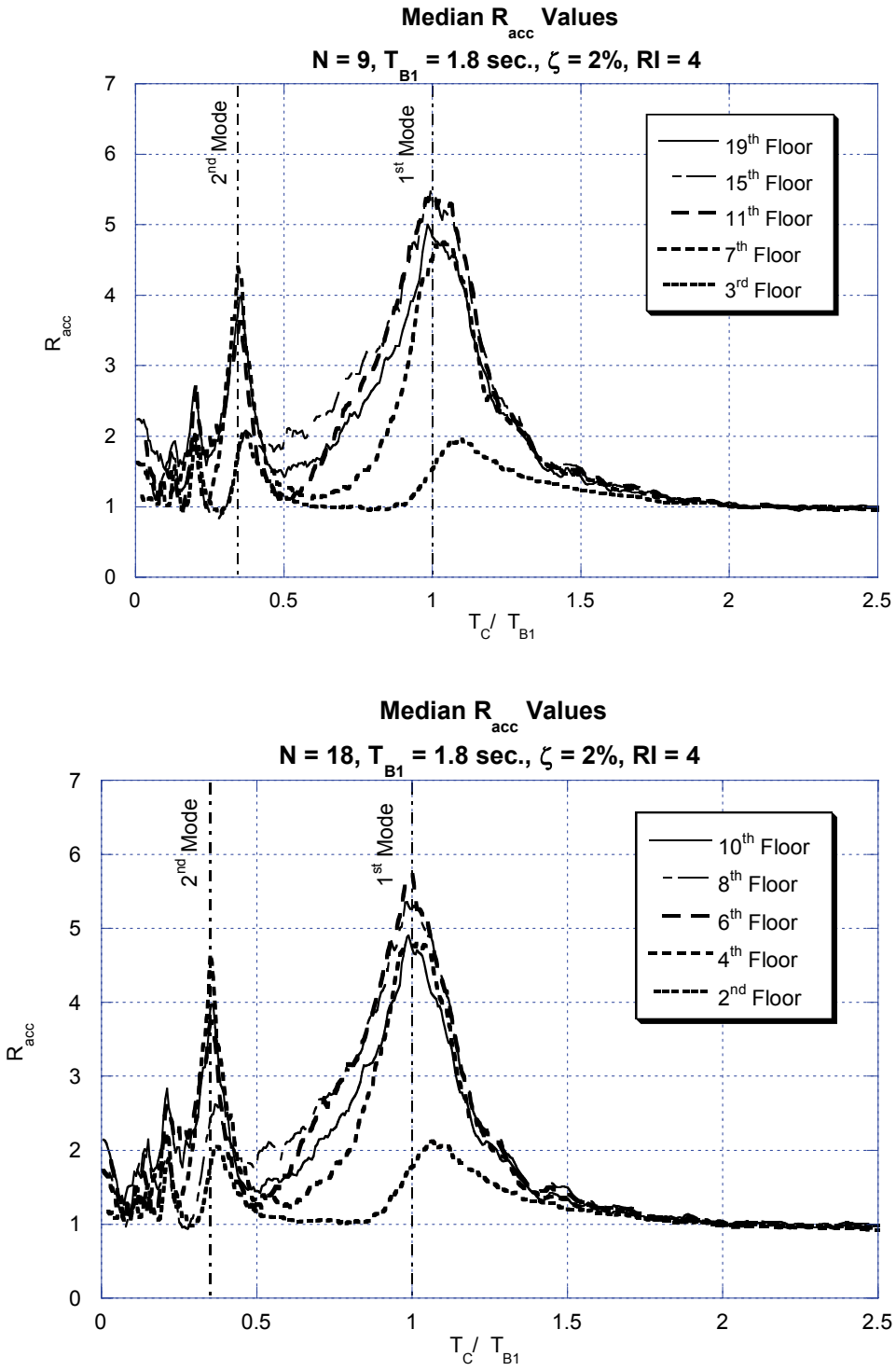

Figure 3.13 Effect of building height on R_{acc}; component damping ratio = 2%, RI = 4, T_{B1} = 1.8 sec.

3.5.3 Location of NSC in the Building

It has been previously discussed that in general, the R_{acc} values at higher floors are much larger than the corresponding values at lower floors of the building for the entire range of the spectra. Figure 3.14 shows the median R_{acc1} values for 1% and 2% damped NSCs along the height for all the stiff frames ($T_{B1} = 0.1N$) used in this study. The corresponding values for flexible frames ($T_{B1} = 0.2N$) are shown in figure 3.15. R_{acc1} values vary linearly from the base to a location just below the mid-height of the frame. The maximum value of R_{acc1} occurs at a location between the roof and mid-height of the building. The R_{acc1} values at the roof can be taken to approximately represent the average values of R_{acc1} at the top half of the frame. This variation of the R_{acc1} along the height is maintained for all the frames and is independent of the damping of the NSC. The contribution of the higher modes in the 3-story frame is much less when compared to other higher storied frames and hence the R_{acc1} values for that frame are different. However, the shape of the R_{acc1} curve along the height is still maintained for the 3-story frame. For flexible frames with $N \geq 15$, P-delta effects caused most of the analyses (greater than 50%) to undergo dynamic instability. Due to the reduction in the sample size, statistical measures of R_{acc1} values could not be obtained with sufficient confidence and hence are not presented in figure 3.15.

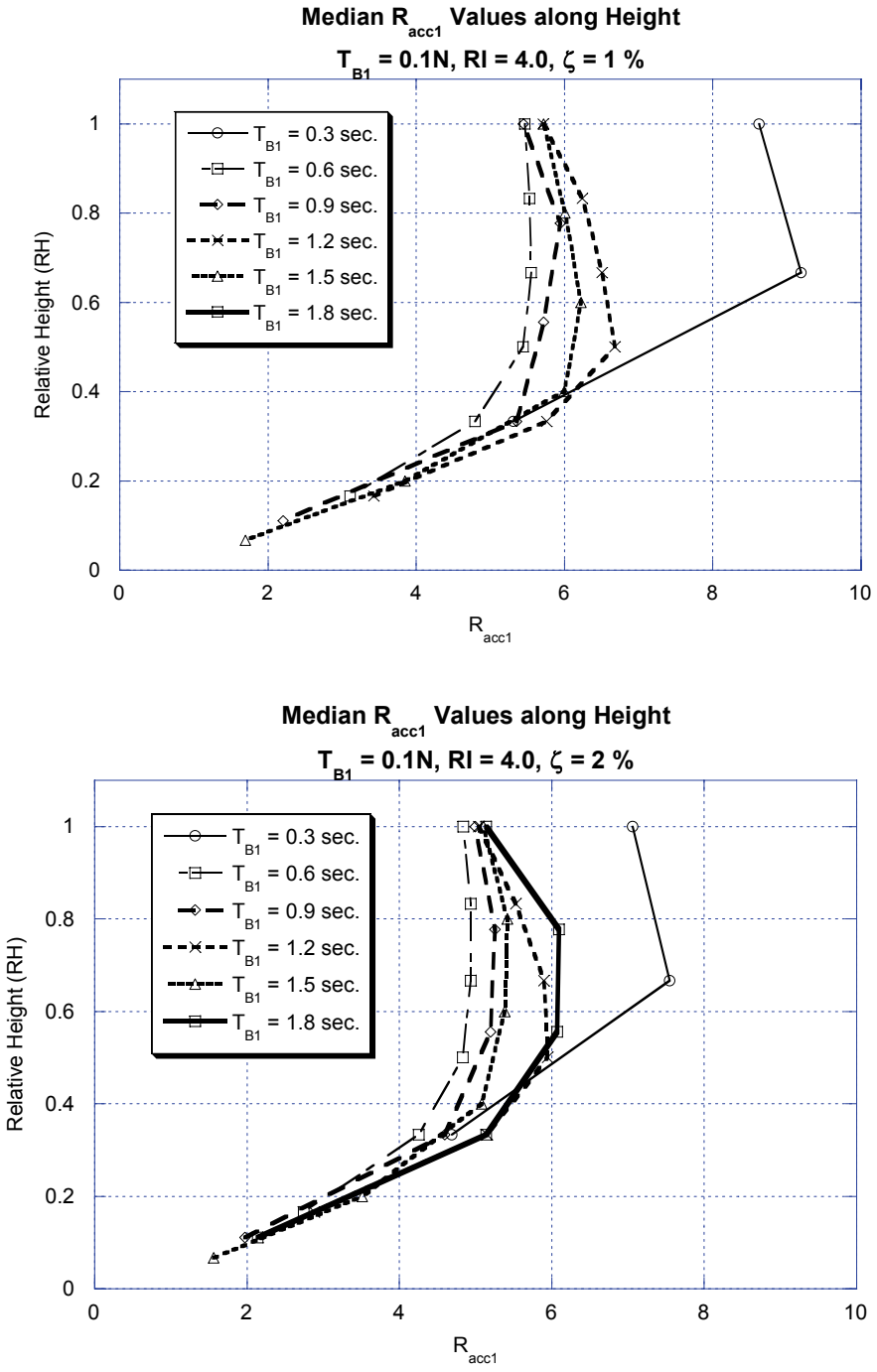

Figure 3.14 R_{acc1} values along the height of the building; RI = 4, T_{B1} = 0.1N sec.

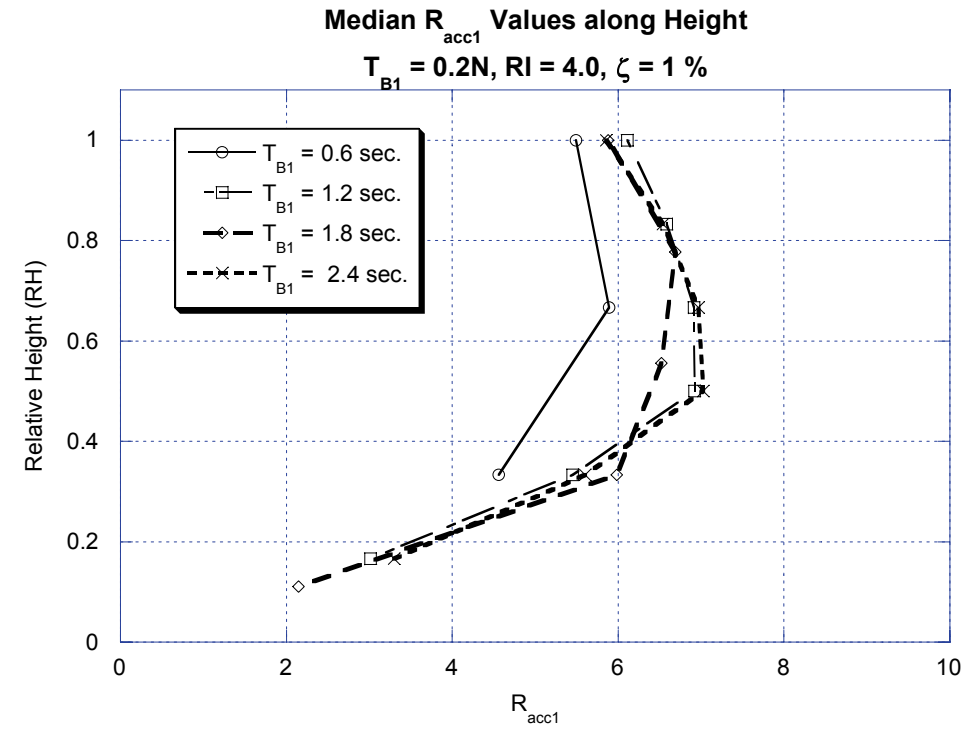

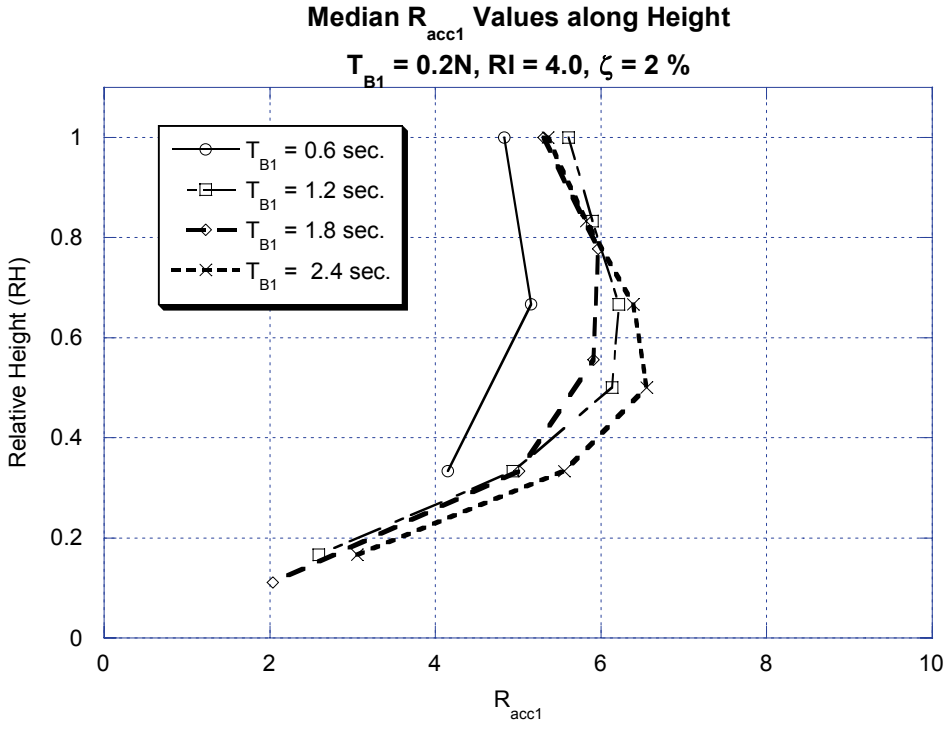

Figure 3.15 R_{acc1} values along the height of the building; RI = 4, T_{BI} = 0.2N sec.

Figures 3.16 and 3.17 show the R_{acc2} and $(R_{acc\text{-}HF})_{max}$ values, respectively along the height for all the frames for NSCs with damping ratios of 2%. The R_{acc2} values and $(R_{acc\text{-}HF})_{max}$ values match very closely for most cases. This means that the $(R_{acc\text{-}HF})_{max}$ values are dominated by the peaks in the R_{acc} values around the second modal period and hence R_{acc2} values can be representative of the entire HF region. The $(R_{acc\text{-}HF})_{max}$ parameter defines the maximum deamplification of the inelastic FRS with respect to the corresponding elastic FRS in the short-period region. In contrast to the regular pattern in the shape of R_{acc1}, the shape of the $(R_{acc\text{-}HF})_{max}$ values along height in the short-period region has an irregular (zigzag) pattern (see figure 3.17). The maximum and minimum values occur either at the top-third or at the bottom-third height of the building. The values at roof and mid-height location of the building are representative of the average values at the top half of the frames. The bottom most story has the minimum value of $(R_{acc\text{-}HF})_{max}$ values.

3.5.4 Damping Ratio of NSCs

In this study, the NSCs are modeled as elastic SDOF systems with dynamic responses uncoupled from the supporting structure. As the benefits of the NSC going nonlinear are not in the scope of this study, the only variable besides the period of vibration of the NSCs influencing the FRS and R_{acc} is the amount of damping in the NSCs. It is well understood that smaller values of component damping lead to an increase in S_a values of response spectra (both ground motion spectra and floor response spectra).

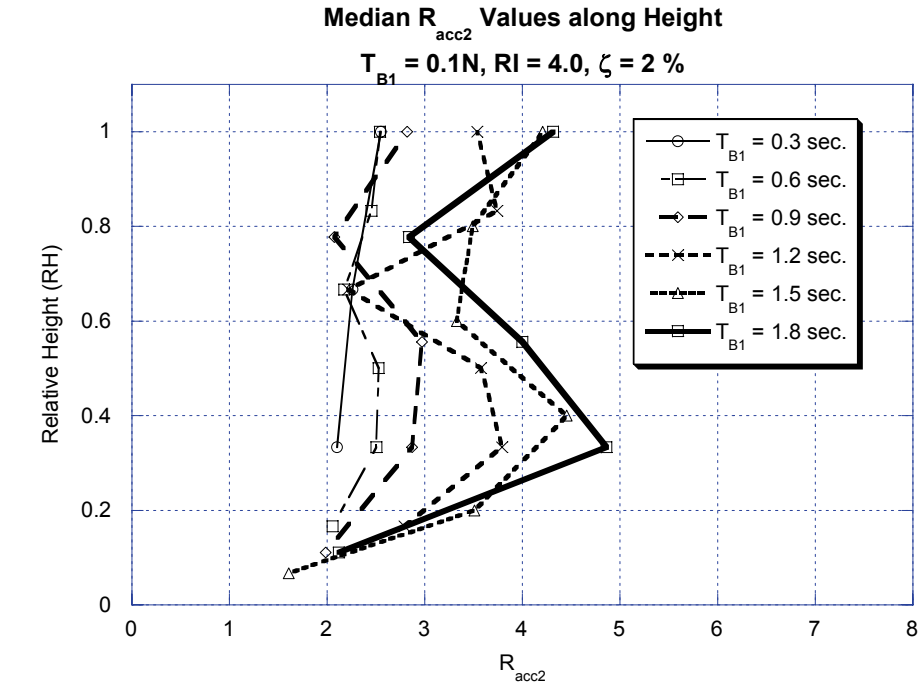

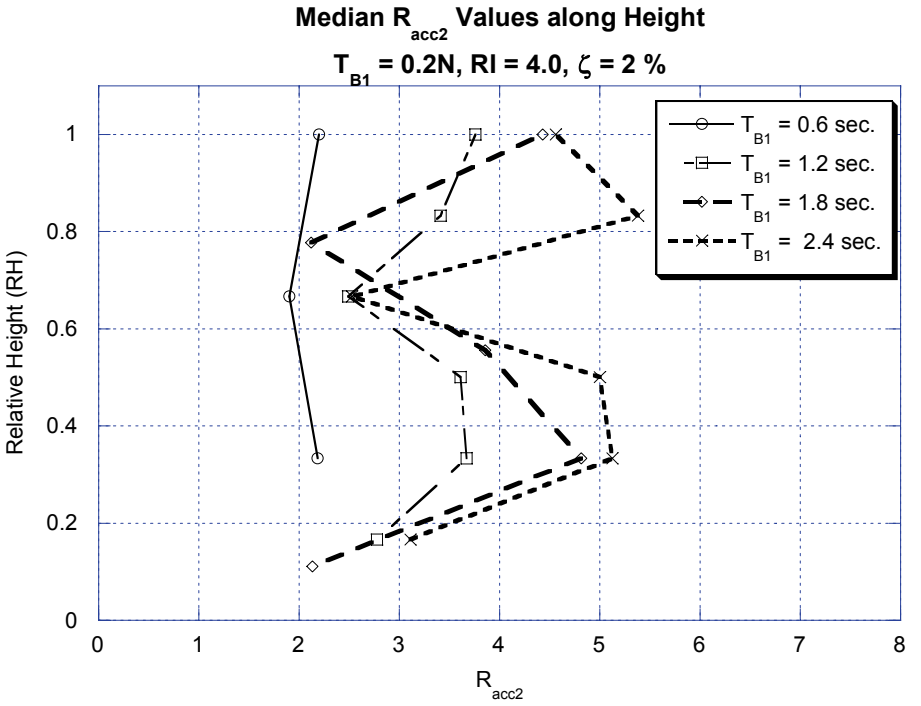

Figure 3.16 Maximum R_{acc2} values along the height; component damping ratio = 2%, RI = 4

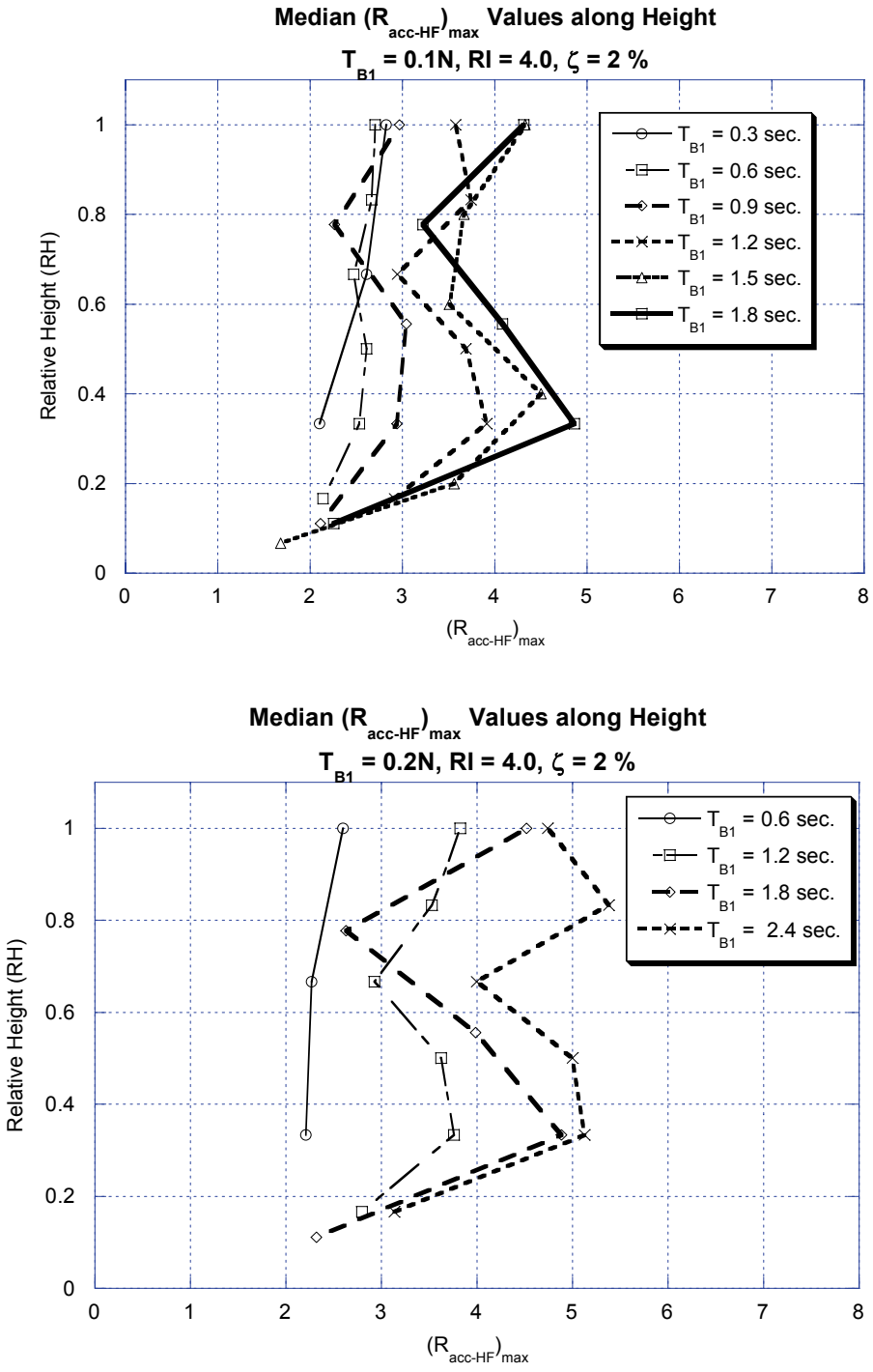

Figure 3.17 Maximum $R_{acc\text{-}HF}$ values in the low period region; component damping ratio = 2%, RI = 4

A decrease in damping values should produce higher FRS values for both elastic and inelastic behavior of supporting structure. However, this statement is true only in regions away from the short-period region. In the short-period region, the inelastic FRS values can get locally amplified and show larger spikes in inelastic FRS when compared to elastic FRS for lower values of component damping. Hence, R_{acc} values change with component damping values.

Figure 3.18 shows the median R_{acc} values at roof and bottom-third height for a 9-story frame with a fundamental period of 0.9 sec and varied component damping ratios. The component damping ratios of interest are 0.01%, 1%, 2% and 5%. It can be seen that the R_{acc} for smaller damping ratios of NSC are more amplified and contain sharper and more pronounced peaks than R_{acc} for higher damping values. This effect is also reflected on the FRS, where sharp spikes in FRS occur at or near modal structural frequencies. Thus, equipment damping can suppress or enhance the values of R_{acci}. With lower values of component damping, the R_{acc} values in the short-period region achieve values less than one. Away from the fundamental and short-period regions (i.e. at the long-period region), the R_{acc} values are very close for various values of component damping.

Figure 3.19 shows the R_{acc1} values along height as a function of component damping. It can be seen that the R_{acc1} values along the height are consistently higher for smaller damping values due to the enhancement of the FRS peaks. The general shape of the R_{acc1} variation along height is maintained for all the values of component damping. This behavior is also maintained in the short-period region as seen in figure 3.20.

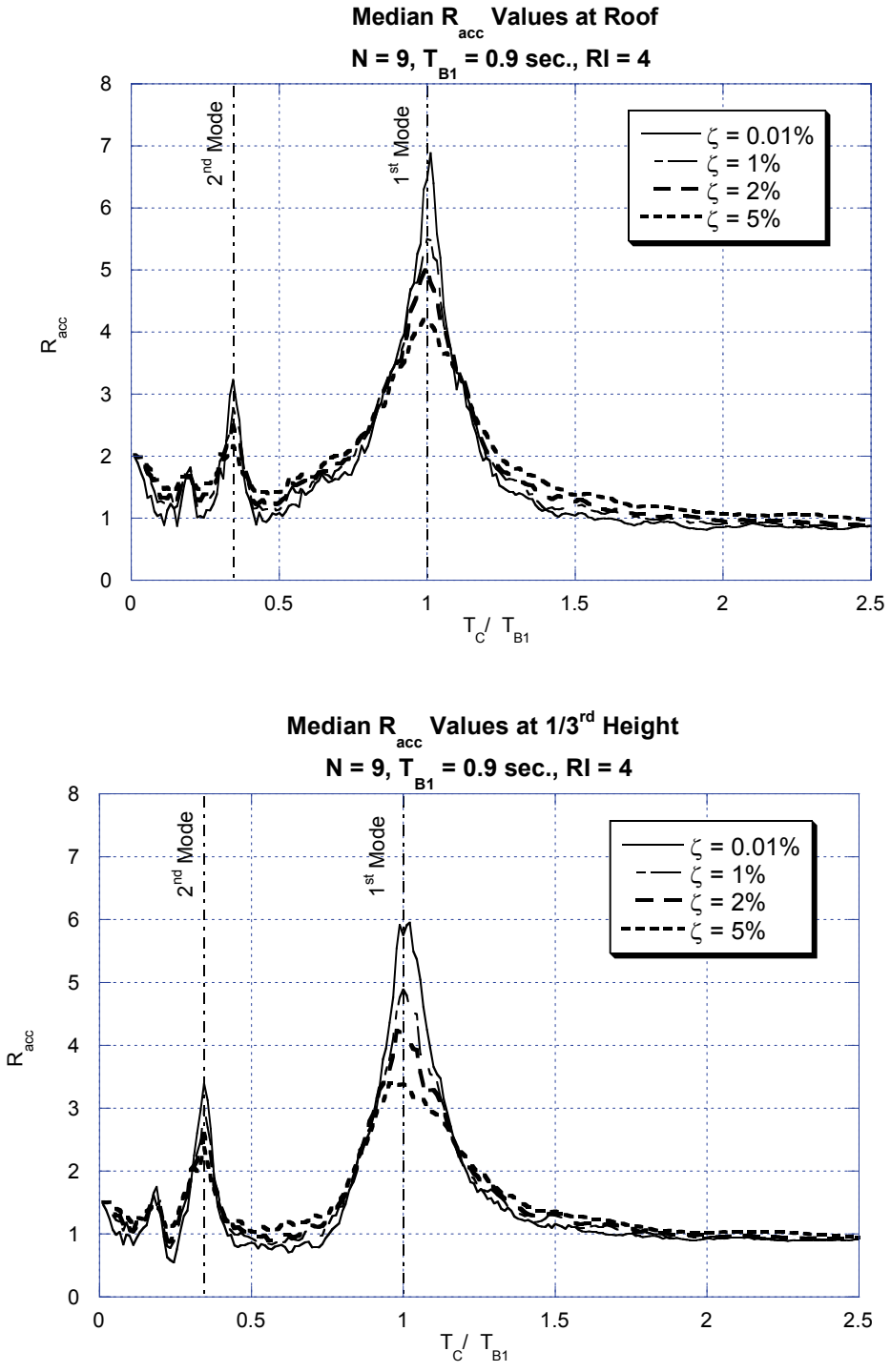

Figure 3.18 Effect of damping on R_{acc} values; component damping ratio = 2%, RI = 4

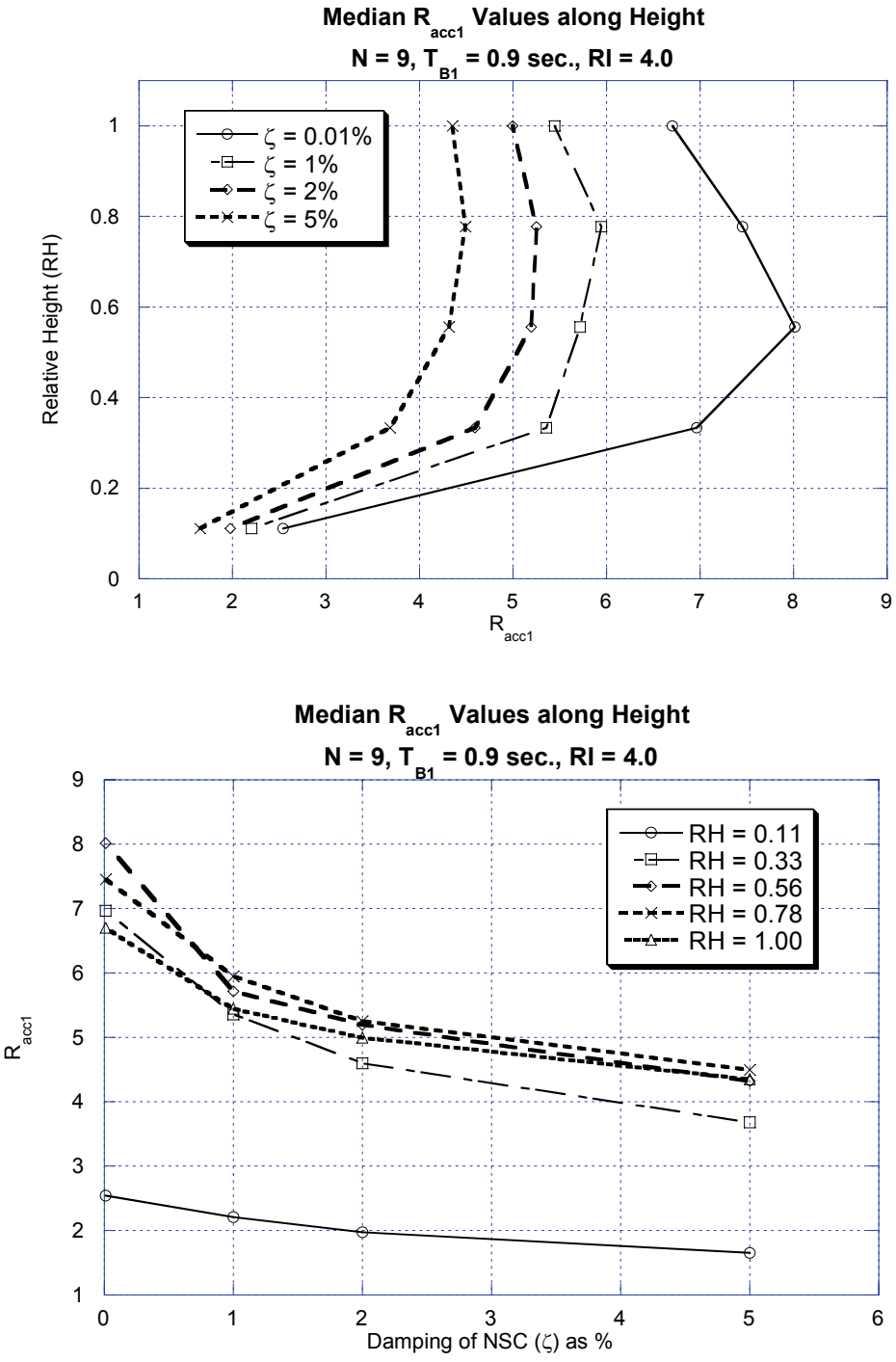

Figure 3.19 R_{acc1} values along height for various values of component damping ratios; T_{B1} = 0.9 sec., RI = 4

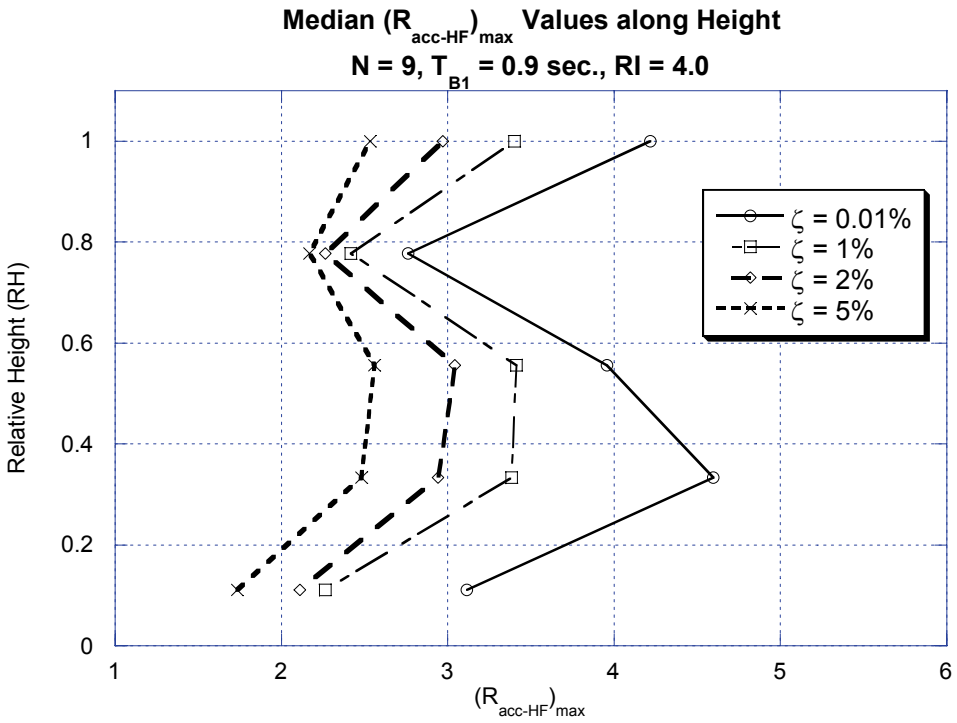

Figure 3.20 Maximum R_{acc} value along height in the low period region for various values of component damping; T_{B1} = 0.9 sec., RI = 4

3.5.5 Fundamental Period of the Supporting Structure

Figures 3.21 to 3.23 show the variation of median values of R_{acc1} and $(R_{acc\text{-}HF})_{max}$ values at roof, mid-height, and bottom-third locations, respectively for RI = 2 for all the stiff and flexible frames for NSC damping ratios of 0.01%, 1%, 2% and 5%. For a given damping ratio, the R_{acc1} values are nearly constant for fundamental periods beyond 0.3 sec. This behavior has also been observed for higher RI values (RI > 2).

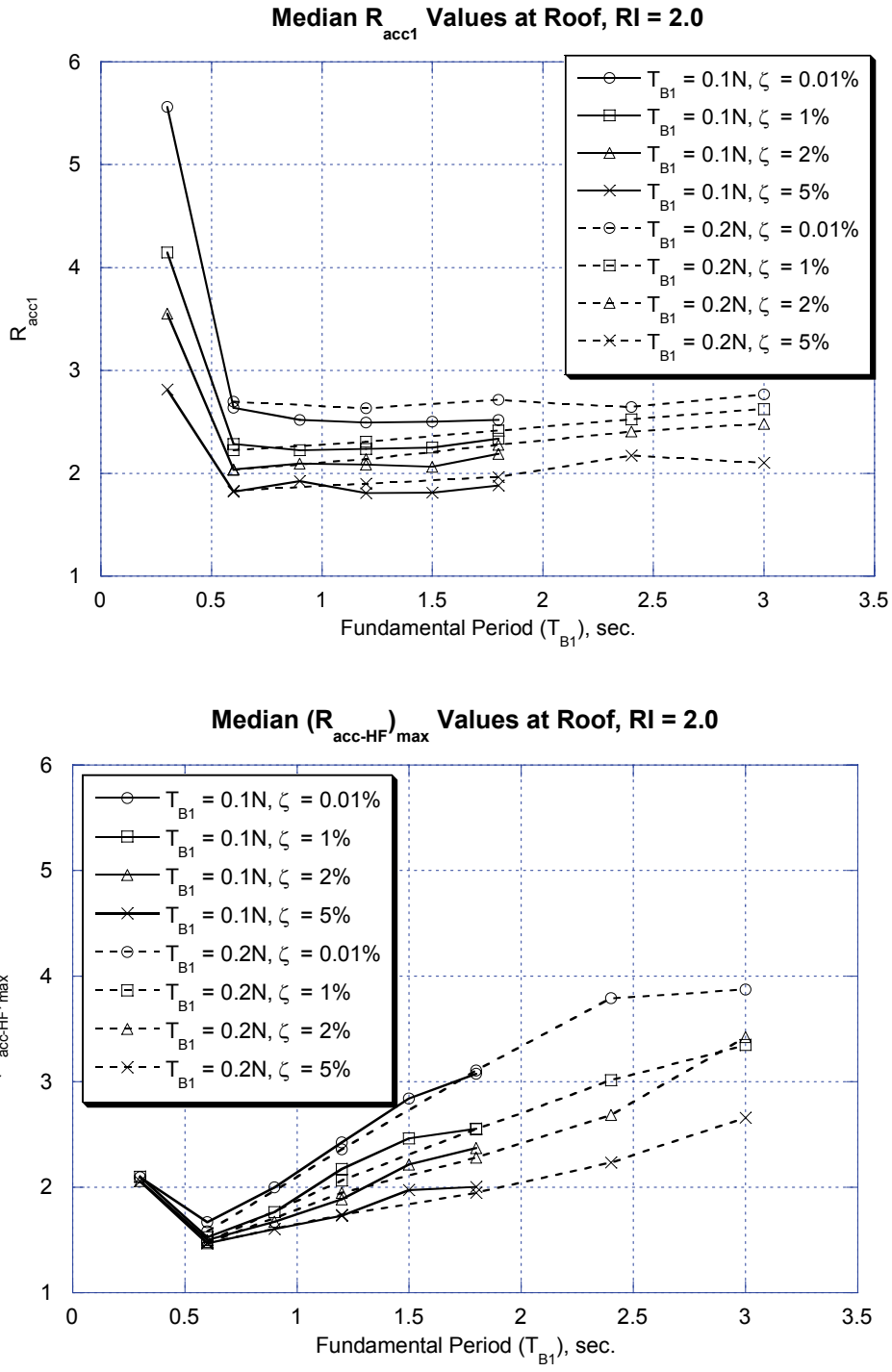

Figure 3.21 R_{acc} variation at roof location for different fundamental periods of the building, RI = 2.0

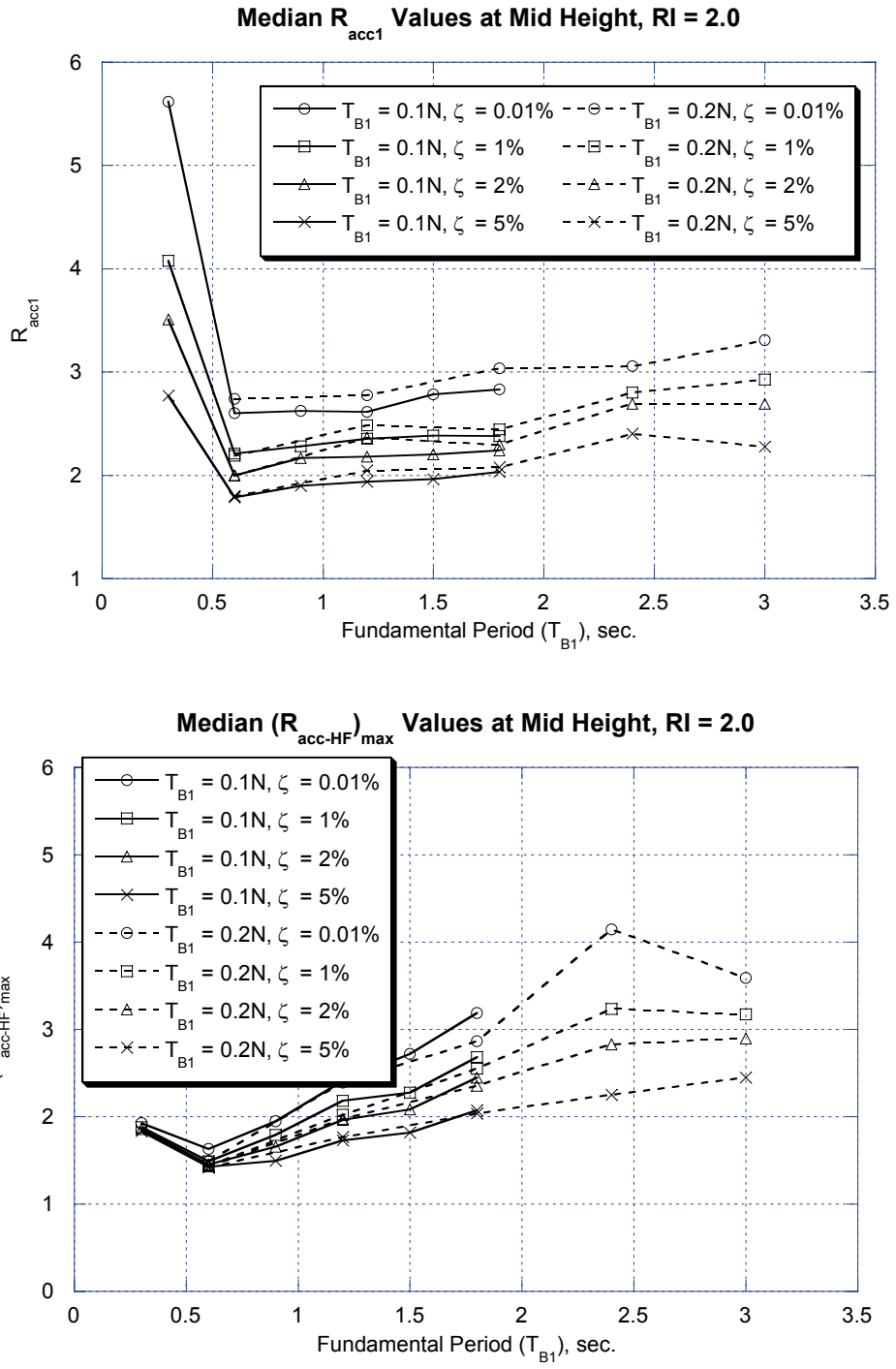

Figure 3.22 R_{acc} variation at mid-height location for different fundamental periods of the building, RI = 2.0

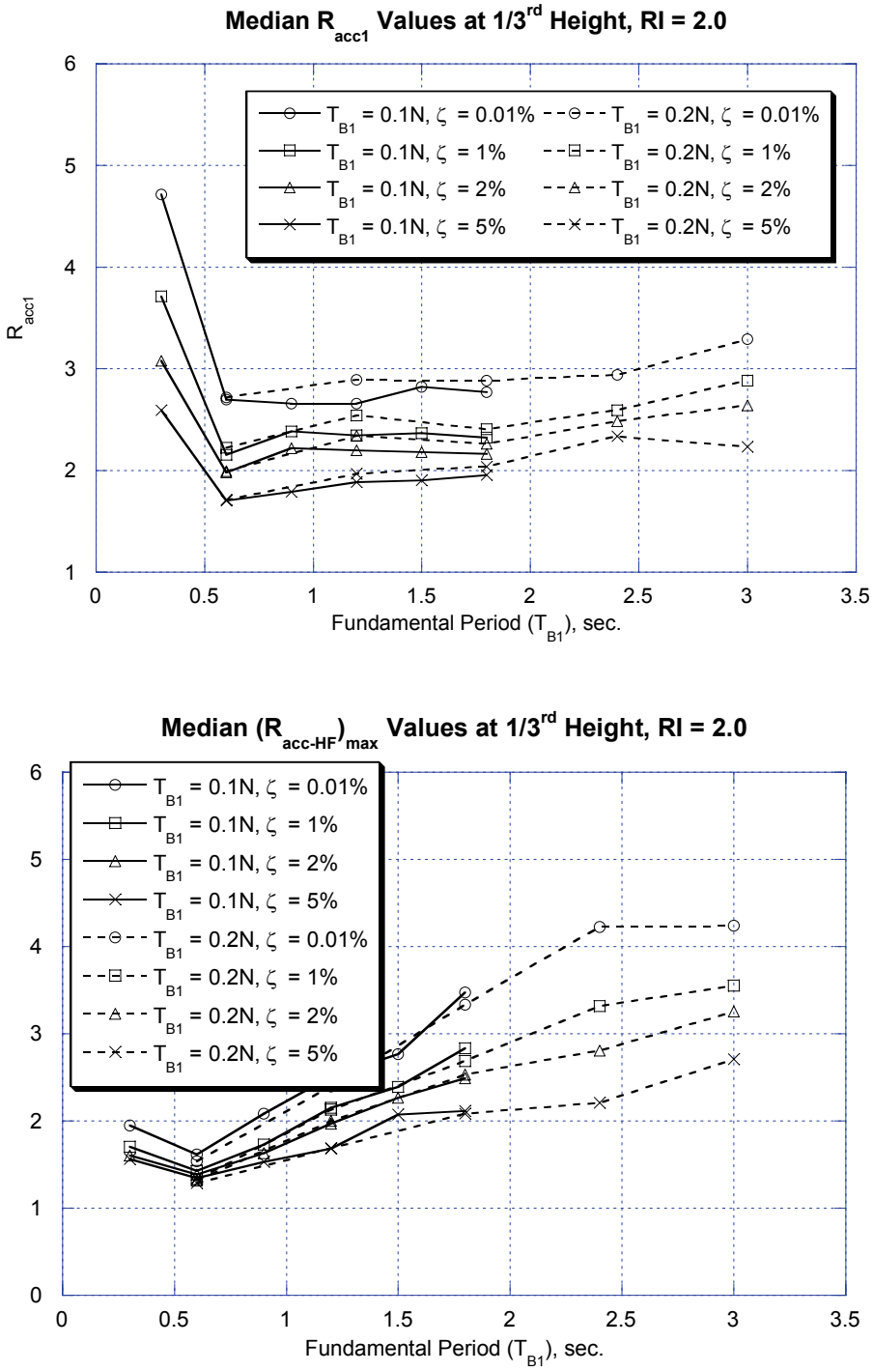

Figure 3.23 R_{acc} variation at bottom-third location for different fundamental periods of the building, RI = 2.0

This implies that the R_{acc1} values are independent of T_{B1} values, except for short-period frames (3-story frame with T_{B1} = 0.3 sec.). An equivalent nonlinear SDOF system at this period is a small period system governed by the equal-energy rule. The inelastic behavior in this region is distinctly different from systems with T_{B1} ≥ 0.5 sec (Ye and Otani 1999). For larger T_{B1} values, the inelastic peak displacements remain the same as maximum elastic displacements for different levels of nonlinearity (strengths) of the supporting structure (equal-displacement rule). This behavior can also be seen from figure 3.14 and 3.15, where the shape of the R_{acc1} curve remains the same for all buildings except for the 3-story frame. This property is relevant in the sense that it allows the generalization of the behavior of R_{acc1} for all buildings with medium to long periods of vibration in the fundamental mode, i.e. $T_{B1} \geq 0.6$ sec. As the T_{B1} values increase, the a_{p1} values decrease for both elastic and inelastic buildings. Hence, the R_{acc1} values are constant for all higher T_{B1} values as the rate of decrease of elastic and inelastic FRS is similar.

In the higher modal period region, the $(R_{acc\text{-}HF})_{max}$ values are dominated by the R_{acc2} mainly to the unique property of internal resonance between modes in the short-period region (Nayfeh and Mook 1979). The median $(R_{acc\text{-}HF})_{max}$ values increase with increase in T_{B1} values. The corresponding values in the elastic domain are constant as 3rd and 4th modes start contributing to the elastic response with increasing T_{B1} values (see figures 3.5 and 3.7). In other words, the inelastic FRS in the short-period region gets flatter and decrease with increase in T_{B1} values. The magnitude of $(R_{acc\text{-}HF})_{max}$ values beyond T_{B1} values of 1.5 are higher than that of R_{acc1} values.

The behavior of R_{acc} in the fundamental-period range and short-period range is similar for all locations of the building. Greater deviation in this behavior is seen at the mid-height location due to the approximations in selecting the results at mid-height location where the *RH* values vary from 0.5 to 0.67 or greater changes in the higher mode shape values around the mid-height location or a combination of both.

3.5.6 Level of Inelastic Behavior of Supporting Structure

Figure 3.24 shows the variation in shape of R_{acc1} and $(R_{acc\text{-}HF})_{max}$ along height for various values of Relative Intensity for all locations of 9-story, 0.9 sec. building with NSC damping ratios of 2%. Figure 3.25 shows the variation of R_{acc} with increase in *RI* values for the same building. As expected, R_{acc} increases with the values of *RI*. For smaller values of *RI*, the R_{acc} values are more uniformly distributed throughout the entire height of the building. The variations in R_{acc} values along the height are apparent only for *RI* values of 4.0 or higher. This is also reflected in figure 3.25, where the values are closer to the straight line variation at the roof for $RI \leq 4.0$. It is important to note that the values of R_{acc} are much larger in the upper half of the structure, i.e., R_{acc} for the 2nd, and to some extent, the 4th floor of the structure are relatively small (i.e., closer to one). These patterns are consistent across all structures and components used in this dissertation. The magnitude of R_{acc1} value are closer to twice the values of $(R_{acc\text{-}HF})_{max}$, which clearly show that the greater equipment benefit due to nonlinearity of the supporting structure is achieved for equipment with periods near fundamental period of the building. Figure 3.26 reiterates the weak dependence of R_{acc1} on T_{B1} for different *RI* values.

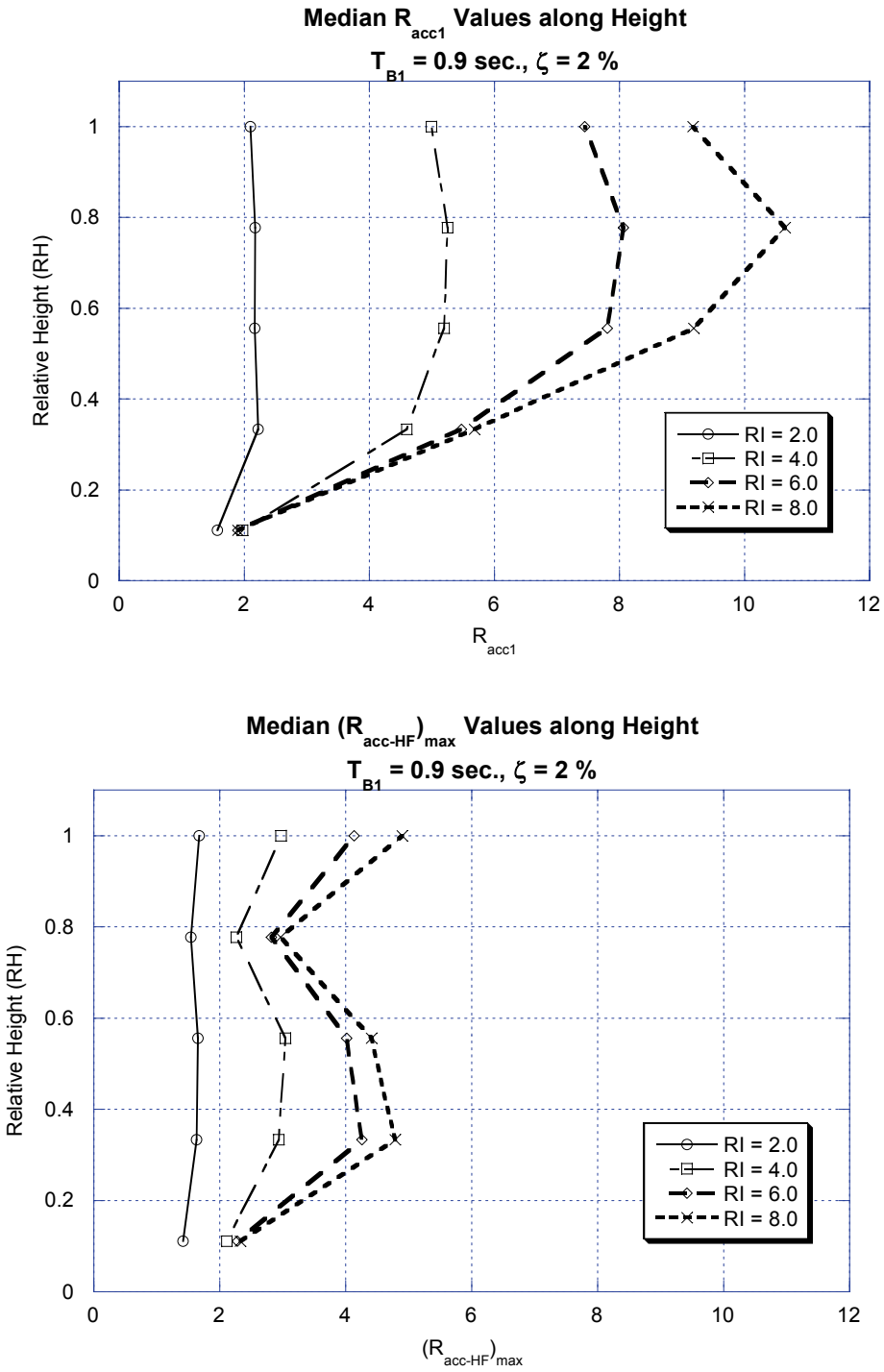

Figure 3.24 Shape of the R_{acc} variation at along height for various *RI* values; component damping ratio = 2%, T_{B1} = 0.9 sec.

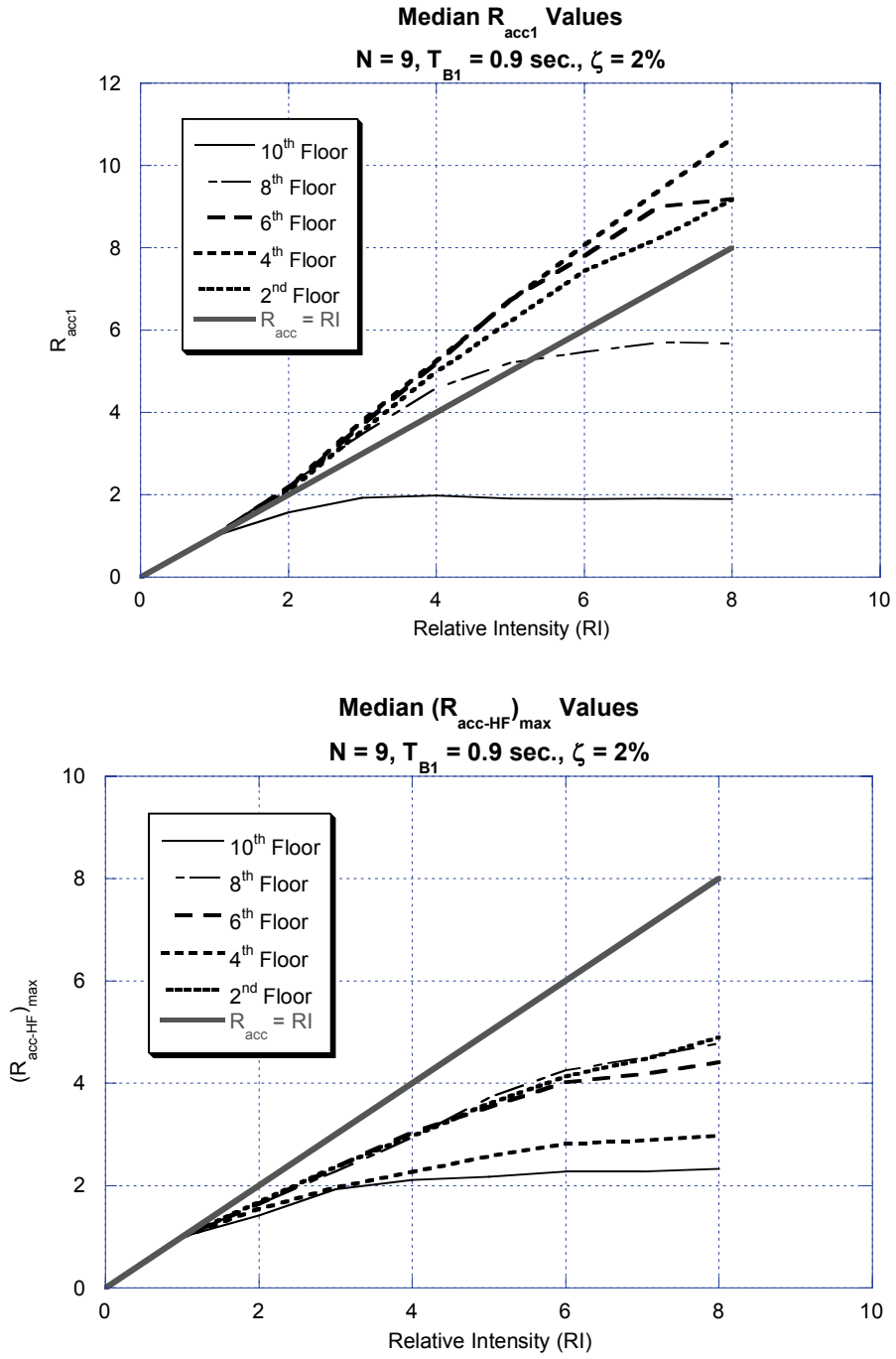

Figure 3.25 R_{acc} variation along height for various *RI* values; component damping ratio = 2%, T_{B1} = 0.9 sec.

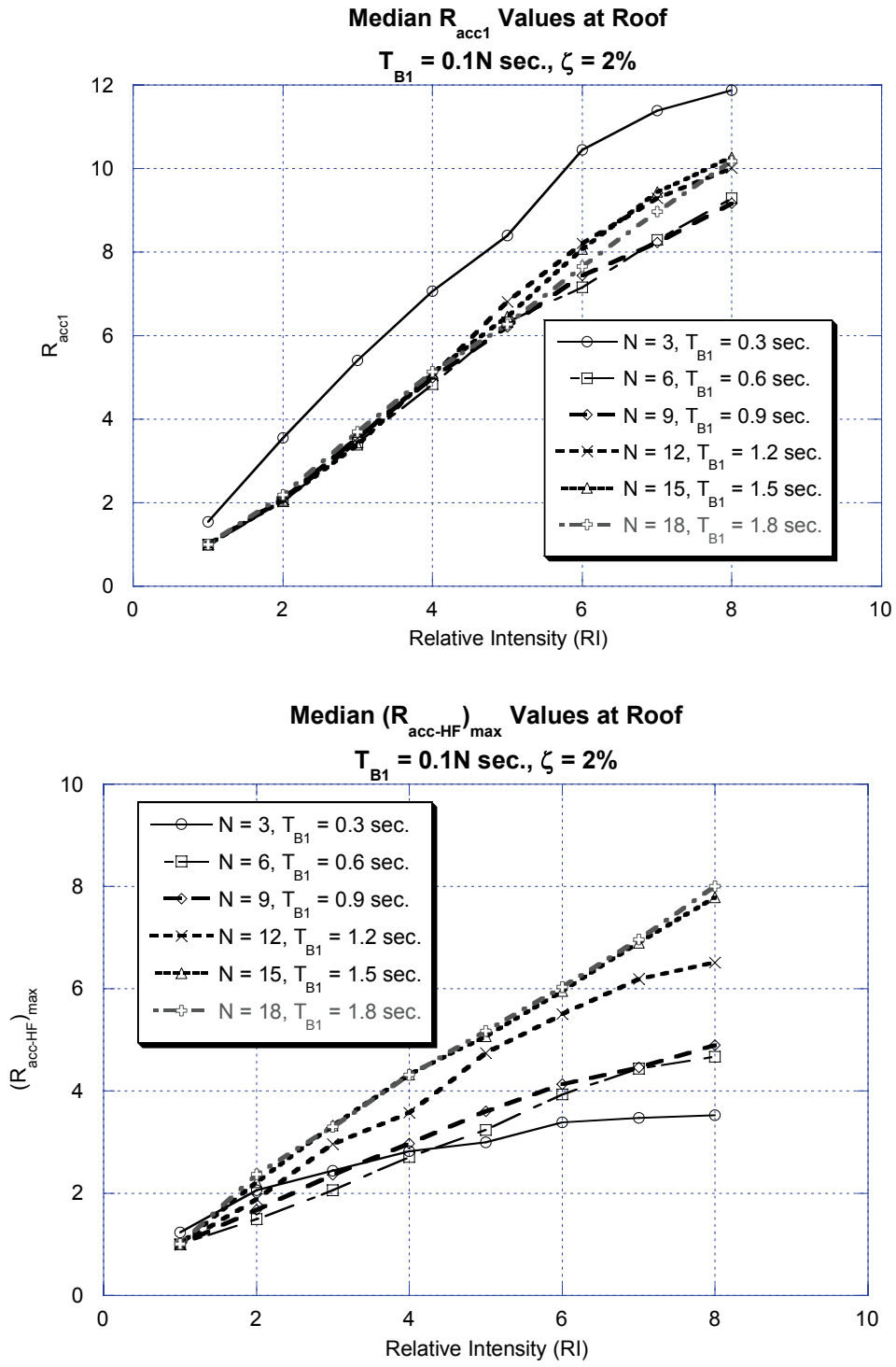

Figure 3.26 R_{acc} variation at roof for various *RI* values of stiff frames; component damping ratio = 2%

The R_{acc1} and $(R_{acc\text{-}HF})_{max}$ values are plotted for all stiff frames with component damping of 2%. It can be seen that the slope of the $(R_{acc\text{-}HF})_{max}$ are different for various buildings and hence it is dependent on T_{B1}. The slope of the longer period frames is greater and hence the $(R_{acc\text{-}HF})_{max}$ values at a specific location increase with T_{B1}. At higher values of *RI*, the deviation from straight line (represented by $R_{acc} = RI$ line) is higher. The behavior of the 3-story frame is distinctly different from other buildings.

3.6 METHODOLOGY FOR THE ESTIMATION OF PEAK COMPONENT ACCELERATION DEMANDS

An important objective of this dissertation is to quantify the acceleration demands on NSCs mounted on inelastic frames. With the behavior of R_{acc} in the three regions of interest well understood, an attempt can be made to use the proposed acceleration response modification factor (R_{acc}) to estimate the acceleration demands of NSCs in inelastic buildings using the results for elastic buildings. Given the degree of inelastic behavior of the primary structure, the T_C/T_{B1} range of interest, the location of the NSC in the primary structure, and the damping ratio of the nonstructural component, floor response spectra for inelastic frames can be estimated from floor response spectra for elastic frames using the following steps:

1. Calculate component amplification factors, a_p, for elastic frames, $S_{aC}(elastic)/PFA_e$, where the terms 'elastic' refers to the strength of the primary structure.
2. Estimate the value of the acceleration response modification factor, $R_{acc} = S_{aC}(elastic)/S_{aC}(inelastic)$.

3. Divide S_{aC}*(elastic)*/PFA_e by R_{acc} to obtain the component amplification factors, a_p, for inelastic frames, S_{aC}*(inelastic)*/PFA_e.
4. Multiply S_{aC}*(inelastic)*/PFA_e by PFA_e to obtain S_{aC}*(inelastic)*.

If the S_{aC}*(elastic)* values are known instead of the a_p values, then a simple division of S_{aC}*(elastic)* by R_{acc} factor gives the S_{aC}*(inelastic)* results. Thus the focus is to estimate the R_{acc} values for a given criterion (combination of T_{B1}, T_C, *RI*, ζ and *RH*). Recommendations for R_{acc} values are provided based on the statistical analyses (regression) of R_{acc} values obtained for different combinations of above parameters obtained for the set of ground motions used in this study. The distribution of R_{acc} values is lognormal. Hence, the recommendations are based on central values (medians) for a large number of nonlinear analyses. Considering the large sample size used in this study, the division of median values of S_{aC}*(elastic)* values by median values of R_{acc}, yields median values of S_{aC}*(inelastic)*. The dispersion (standard deviation) of R_{acc} and a_p*(inelastic)* values is presented separately and these values can be used to obtain the percentile values (e.g. 84th percentile values). The methodology can be adapted easily to find the S_{aC}*(inelastic)* values depending on the availability of a_p*(elastic)* or S_{aC}*(elastic)* or both of these values. In the proposed approach, the R_{acc} value is a function of:

1. the degree of inelastic behavior of the primary structure (i.e., *RI*);
2. the ratio of the period of the NSC to the fundamental period of the primary structure (i.e., T_C/T_{B1} ratios in three primary ranges of interest: $T_C / T_{B1} > 1.5$, $0.5 \le T_C / T_{B1} \le 1.5$ and $T_C / T_{B1} < 0.5$);

3. the location of the NSCs in the building (i.e., NSCs located in the upper half and the bottom half of the frame structure); and
4. the damping ratio of the NSC (i.e., from 0.01% to 5%).

It should be noted that the proposed R_{acc} factor is designed to show only a relative comparison of equipment response for nonlinear as compared to linear structures. No absolute measure of equipment response can be obtained from R_{acc} alone. Combined with FRS of elastic building or a_p values of an elastic building, R_{acc} can be used to reconstruct the inelastic FRS.

3.7 RECOMMENDATIONS FOR ACCELERATION RESPONSE MODIFICATION FACTOR VALUES

The focus of this section is on providing quantitative data to estimate the parameters $S_{aC}(elastic)/PFA_e$ and R_{acc} based on statistical results based on the family of frame structures and the ensemble of ordinary (far-field) ground motions used in this study. Median estimates of PFA_e can be obtained from section 2.3 of this dissertation and/or the work presented in references (Singh 1975; Singh et al. 1993; Medina and Krawinkler 2004; Miranda and Taghavi 2005; Taghavi and Miranda 2005; Singh et al. 2006a). P-Delta effects caused dynamic instability in flexible frames ($T_{BI} = 0.2N$) with 9- or more stories for higher levels of relative intensity ($RI \geq 3.0$) for some ground motions. For the 15- and 18-story frames with fundamental period of 3.0 sec., and 3.6 sec., respectively, more than half of the cases exhibited dynamics instability for $RI = 4$. Hence, quantitative information on the 15- and 18-story story flexible frames for all RI values and the 9-, 12- and 15-story flexible frames for higher RI values that caused dynamic instability are not considered

in the statistical analysis. For $RI = 1$, $R_{acc} > 1.0$ is achieved only for a very few cases and the R_{acc} distribution fails the Kolmogorov-Smirnov test (K-S test) for lognormal distribution for a level of significance of 0.05. Hence, results for $RI = 1$ are not included in the statistical analysis and the median R_{acc} values for this case can be considered as one.

As discussed previously, the behavior of 3-story frame is distinctly different from the medium to long period frames used in this study. Moreover, its exclusion allows the computation of R_{acc1} values independent of T_{B1} values for other frames used in this study. Hence, the results for this frame are presented separately and not included in the main set of data used to determine statistical models for median R_{acc} values. Figures 3.27 to 3.29 show the median R_{acc1} and $(R_{acc\text{-}HF})_{max}$ values for the 3-story frames (both stiff and flexible) at roof, mid-height, and bottom-third height, respectively. The dependence of $(R_{acc\text{-}HF})_{max}$ on T_{B1} values in this narrow short period region for periods of 0.3 sec. and 0.6 sec., is weaker when compared to the other frames. Hence, the median values presented in the plots for both the fundamental period and short-period regions are presented independent of T_{B1}. These values can be used as reduction factors for short-period frames. The R_{acc1} values for 3-story frames are much larger than $(R_{acc\text{-}HF})_{max}$ values and corresponding R_{acc1} values for the other set of frames. This can be attributed to the higher dominance of the first mode in the response of short-period frames. For NSCs mounted on inelastic short-period frames, great benefit can be achieved by tuning their periods to match that of supporting structure. However, these frames are more prone to FRS amplification due to the inelastic action of the supporting structure under special situations in short-period

region (e.g. when the damping ratios of NSCs are very small, when the inelasticity is concentrated at a story level, etc.). This is discussed in appendix II.

The R_{acc} results from the following building models in the medium to long fundamental period range with stiffness distribution consistent to nonlinear first mode shape are considered in the statistical analysis:

- Stiff Frames ($T_{B1} = 0.1N$)
  - N = 6, 9, 12, 15, and 18
  - RI = 2.0 to 4.0
  - RH = at least 5 locations that are uniformly distributed throughout the height of the building
  - ζ = 0.01%, 1%, 2% and 5%
- Flexible Frames ($T_{B1} = 0.2N$)
  - N = 6, 9, and 12
  - RI = 2.0 to 4.0; Results from frames that experienced dynamic instability due to P-Delta effects are not included.
  - RH = at least 5 locations that are uniformly distributed throughout the height of the building
  - ζ = 0.01%, 1%, 2% and 5%

It should be noted that although no failure due to P-Delta effects was observed for stiff frames, higher RI values are omitted for stiff frames for maintaining the data consistent with that of flexible frame results.

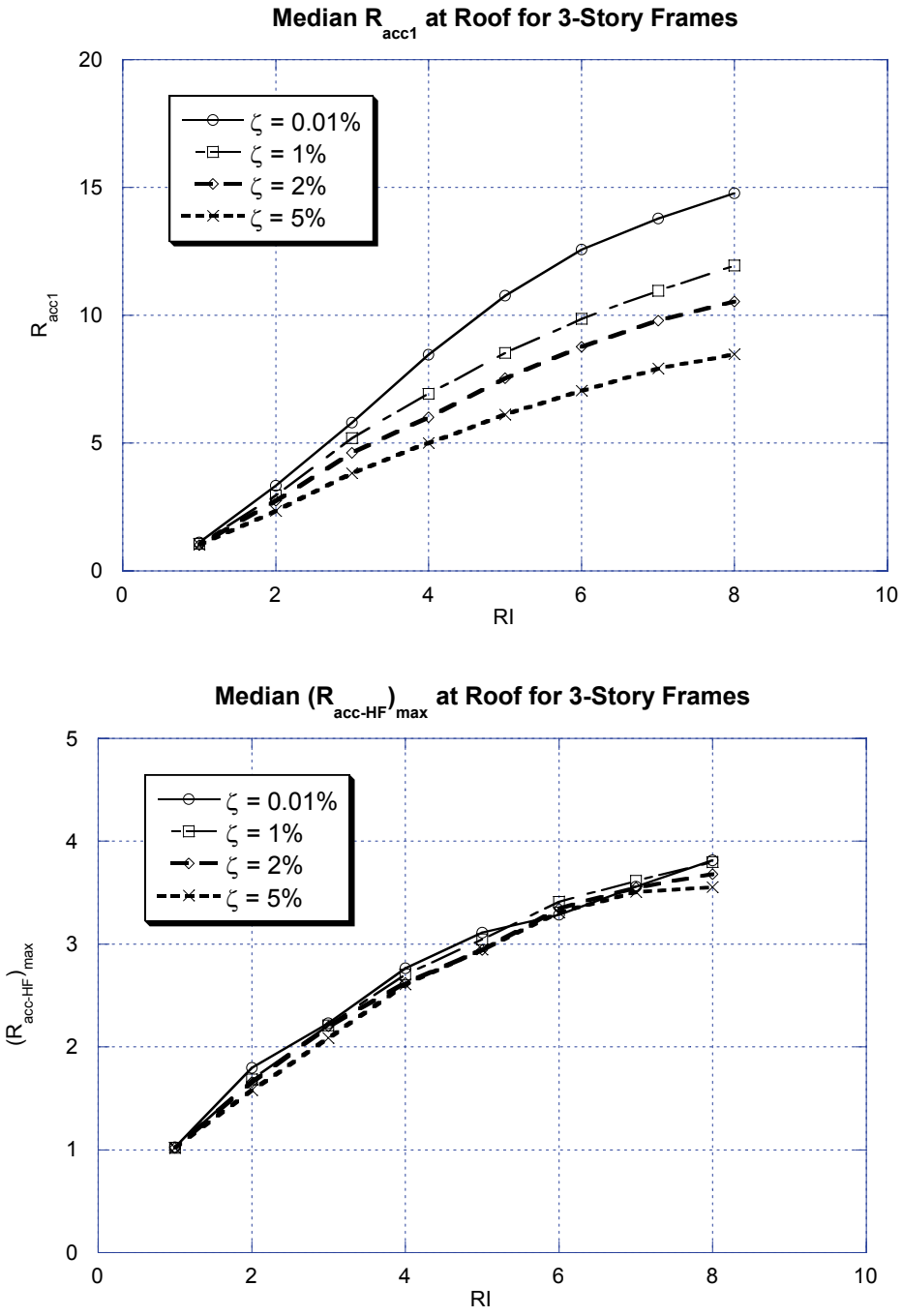

Figure 3.27 R_{acc} values at roof for various *RI* values of 3-story frame

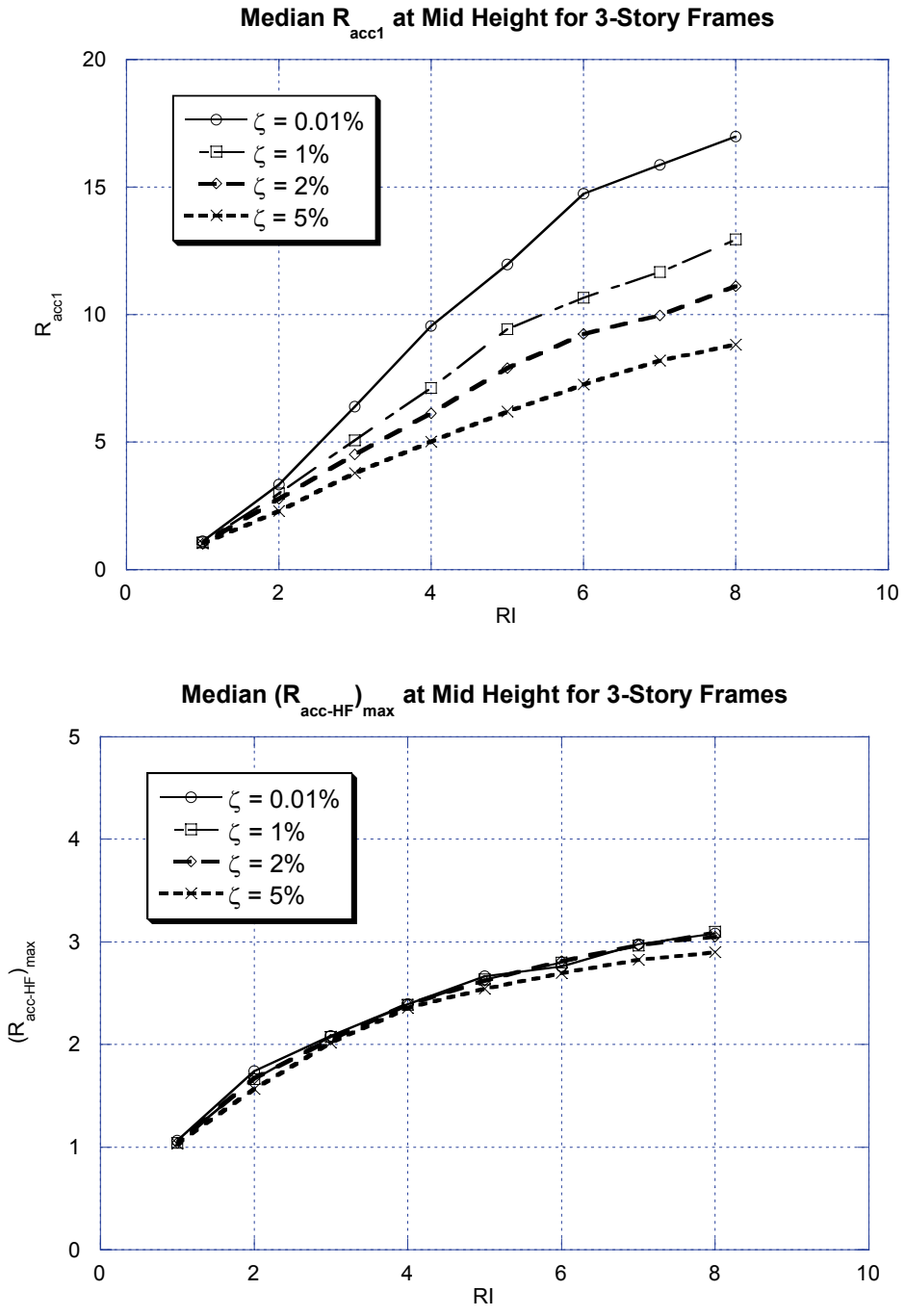

Figure 3.28 R_{acc} values at mid height location for various *RI* values of 3-story frame

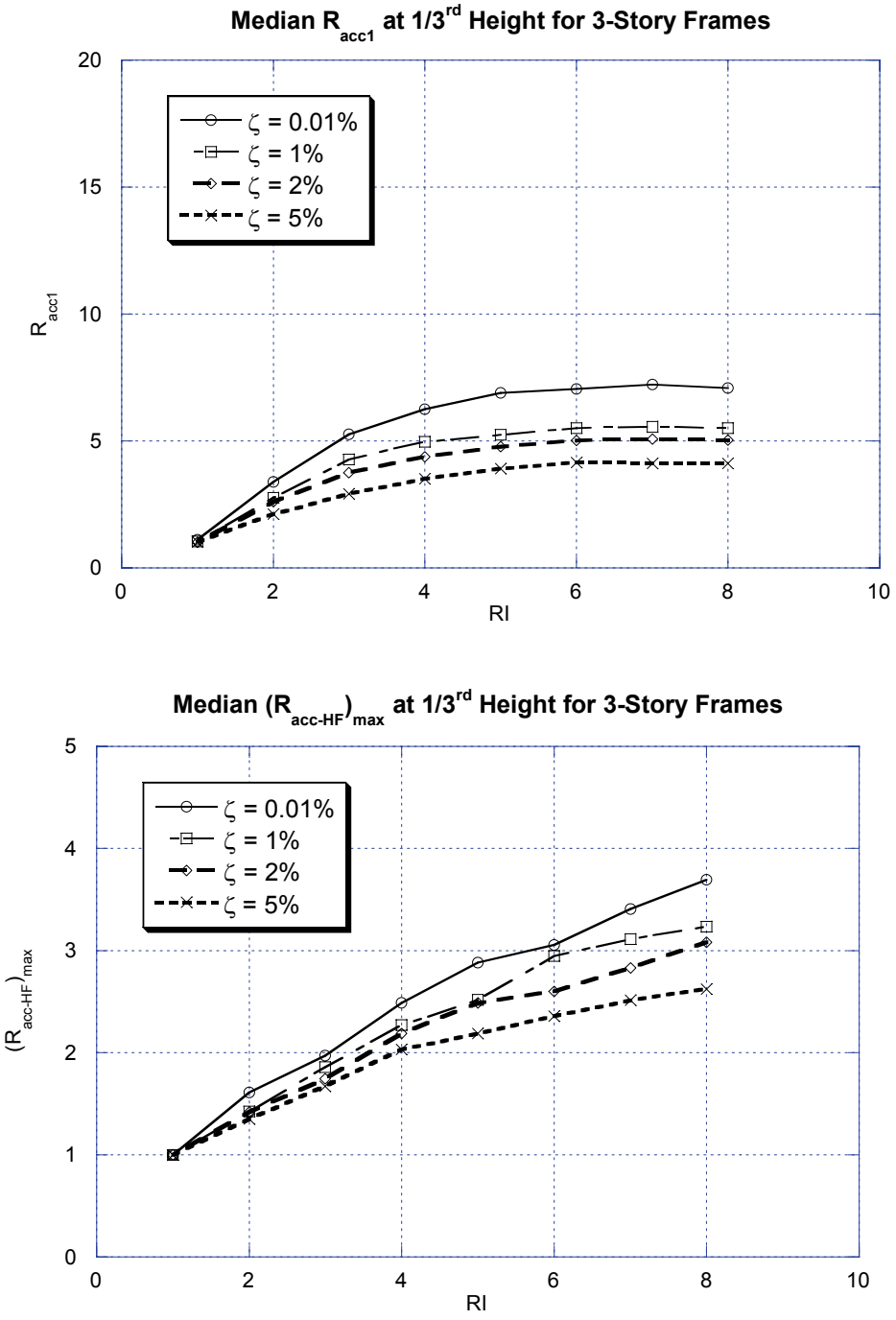

Figure 3.29 R_{acc} values at bottom third location for various *RI* values of 3-story frame

Thus, the estimates proposed in this study are applicable to frame structures with *RI* from 2 to 4, number of stories (*N*) from 6 to 18, fundamental periods (T_{B1}) from 0.6 sec. to 2.4 sec., and NSC damping values from 0.01% to 5%.

3.7.1 R_{acc} Values along the Height of the Building

Previous discussions focused on R_{acc} values at three distinct locations in the building namely roof (*RH = 1.0*), mid-height (*RH = 0.5*) and bottom-third (*RH = 0.33*) location. As discussed before, the R_{acc} distribution in the bottom half of the structure is linear and the values are small compared to the top-half of the building. Thus the bottom-half of the building has very low deamplification from elastic to inelastic FRS. The FRS ratios computed by other researchers for limited cases (Sewell et al. 1986; Singh et al. 1993) and the R_{acc} values obtained from the current results for small NSC damping ratios show that any amplification in inelastic FRS (shown by $R_{acc} < 1.0$) in the short-period region is predominant in the bottom-half of the building. This behavior is also observed in the results presented in appendix II. Moreover, in the current code provisions (see section 3.2), the PFA values that govern the acceleration demand of NSCs have a minimum value of $PFA = PGA$ at the base. Thus it is recommended that, $R_{acc} = 1.0$ is to be used for the bottom-half of the building. Although, the region from 1/3rd height to mid-height of the building shows deamplification, for conservatism in the results no deamplification is recommended. Thus, no reduction of forces is recommended in the bottom half of the building for the inelastic response. The top-half of the building shows significant reduction in FRS for inelastic behavior. Hence, $R_{acc} \geq 1.0$ are recommended for the top-half of the

structure. However, for completeness of results and as a reference for future studies, the R_{acc} values are provided in bottom-third location as well as at mid-height and roof of the building.

3.7.2 R_{acc} Values in Different FRS Regions

As explained in section 3.4.2, the FRS can be classified into three distinct regions namely long-period, fundamental-period, and short-period regions. The deamplification of inelastic FRS peaks in each of these regions can be represented by a single R_{acc} value. R_{acc1} and $(R_{acc\text{-}HF})_{max}$ represent the deamplifications in the fundamental-period and short-period regions respectively. The fundamental period region is characterized by a single FRS peak. The R_{acc1} value being the representative of this peak exemplifies the entire fundamental-period region. In the short-period region, the $(R_{acc\text{-}HF})_{max}$ is characteristic of all the peaks. Because the elastic FRS in this region is represented by the maximum value $a_p(elastic)$ in the entire region (see equation (3.13)), the corresponding R_{acc} value in the region (i.e. $(R_{acc\text{-}HF})_{max}$) represents the inelastic FRS envelope in this region. Hence, only one value of R_{acc} is provided per region. The recommended values of R_{acc} in these regions are discussed below.

3.7.2.1 Long-period Region

In the long-period region $(T_C / T_{B1} > 1.5)$, the R_{acc} values are closer to one and both the elastic and inelastic FRS has similar S_{aC} values. $R_{acc} < 1.0$ occur for few cases with small values of component damping ratios. For NSC damping ratios of 1%

to 5%, these values are close to one. Hence, $R_{acc} = 1.0$ is recommended for this region.

3.7.2.2 Fundamental-period Region

The inelastic FRS in the fundamental period is governed by the R_{acc1} factor. The R_{acc1} factor depends on location (*RH*), relative intensity of ground motion (*RI*), and NSC damping ratio (ζ). A statistical model is developed based on the results of both stiff and flexible frames to estimate the R_{acc1} values as a function of *RI* and NSC damping (ζ) ratio. Different equations are provided for roof and mid-height location in the building. The proposed R_{acc1}-*RI* relationship is of the form:

$$R_{acc1}(RH, RI, \zeta) = a\ RI^{b}, \text{ where } 2 \le RI \le 4 \tag{3.19}$$

This power function is a good representative of the variation of R_{acc} for different *RI* values. The results from a linear regression analysis with the natural logarithm of the values are provided in Table 3.1. The correlation coefficients for the simple statistical model are greater than 0.7 and it indicates a strong positive correlation of R_{acc1} with *RI* values. The standard errors of the estimate that are a measure of the accuracy of predictions made with the regression line are of the order of 0.3. This means that the R_{acc1} values predicted by the model fall in the range of ±0.3. Thus, the simple model used in the regression is capable of accurately predicting the median R_{acc1} values. Figure 3.30 shows a sample regression with the actual data points for R_{acc1} values at roof for both stiff and flexible frames with NSC damping ratios of 2%.

RH	ζ	*a*	*b*	Correlation Coefficient	Standard Error
1.0	0.0001	1.079	1.335	0.738	0.347
1.0	0.01	1.015	1.259	0.752	0.314
1.0	0.02	0.981	1.208	0.758	0.296
1.0	0.05	0.932	1.105	0.763	0.264
0.5	0.0001	1.107	1.410	0.750	0.354
0.5	0.01	1.037	1.326	0.756	0.327
0.5	0.02	0.991	1.278	0.759	0.312
0.5	0.05	0.943	1.161	0.761	0.280
0.33	0.0001	1.229	1.257	0.740	0.326
0.33	0.01	1.134	1.167	0.744	0.298
0.33	0.02	1.079	1.113	0.746	0.282
0.33	0.05	1.024	0.976	0.737	0.253

Table 3.1 R_{acc1} values at three locations based on regression models

RH	ζ	*d*	*e*	*f*	Correlation Coefficient	Standard Error
1.0	0.0001	1.147	1.018	0.552	0.666	0.413
1.0	0.01	1.051	0.931	0.467	0.664	0.369
1.0	0.02	1.012	0.890	0.432	0.658	0.355
1.0	0.05	0.982	0.809	0.364	0.635	0.318
0.5	0.0001	1.181	0.929	0.556	0.665	0.393
0.5	0.01	1.060	0.873	0.483	0.660	0.363
0.5	0.02	1.020	0.832	0.465	0.653	0.353
0.5	0.05	1.010	0.732	0.393	0.615	0.320
0.33	0.0001	1.215	0.984	0.635	0.651	0.447
0.33	0.01	1.079	0.906	0.556	0.644	0.409
0.33	0.02	1.034	0.853	0.539	0.640	0.395
0.33	0.05	0.960	0.787	0.498	0.623	0.360

Table 3.2 $(R_{acc\text{-}HF})_{max}$ values at three locations based on 2-parameter regression models

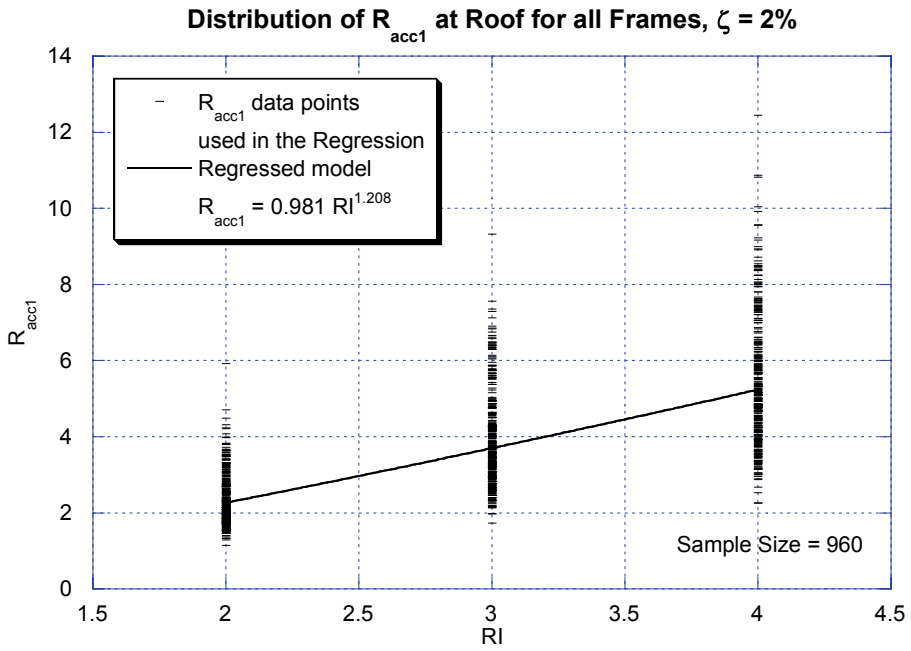

Figure 3.30 Sample regression showing the data points and the regressed equation; component damping ratio = 2%

The dispersion of data points increases with higher values of *RI*. Figure 3.31 shows the regressed R_{acc1} line defined by the parameters in Table 3.1 along with the median values of actual data from the nonlinear time-history runs. The results for all stiff frames with component damping ratio of 2% are shown in the above figure. The coefficient, *a* in the regression model dominates for lower values of *RI*.

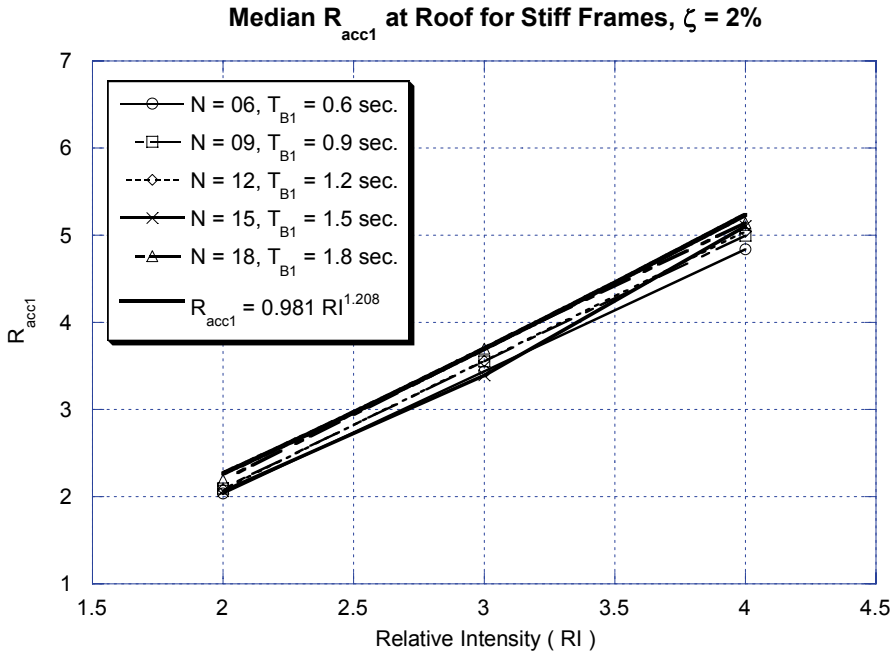

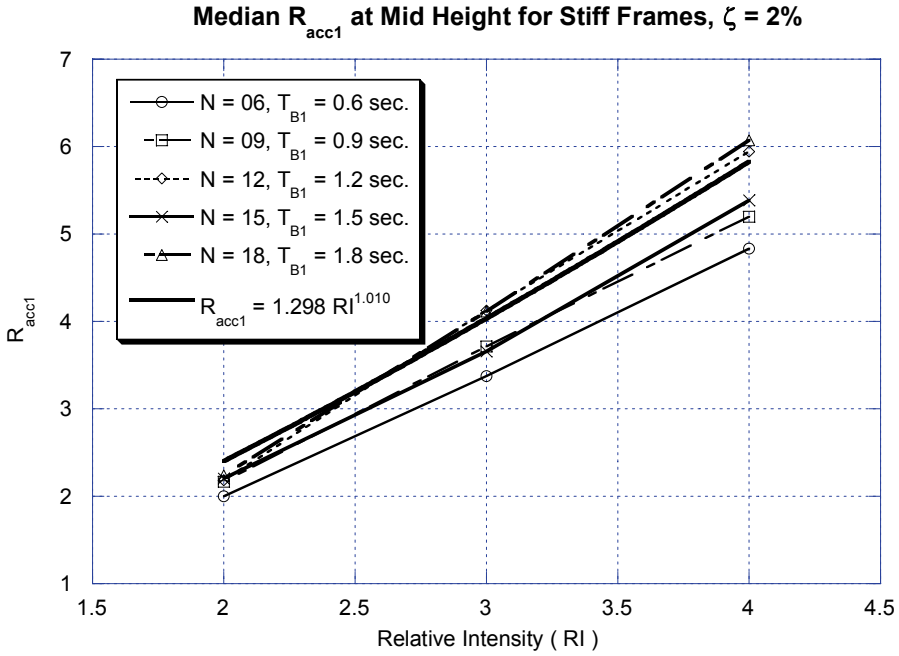

Figure 3.31 Regressed and actual R_{acc1} values at roof and mid-height location for stiff frames; component damping ratio = 2%

3.7.2.3 Short-period Region

The R_{acc} values in the short-period region can be defined by a single parameter namely, $(R_{acc\text{-}HF})_{max}$. This parameter takes into effect the deamplification in inelastic FRS around all the higher modes of the supporting structure. Unlike the R_{acc1} values, this parameter is dependent on the T_{B1} values. Hence, a simple one parameter regression model with RI values will not be sufficient in predicting the $(R_{acc\text{-}HF})_{max}$ values at roof and mid-height locations. A two parameter model that will allow multiple linear regression (SPSS Inc. 2004b; 2004a) with the natural logarithm of R_{acc} values in the short-period region is selected. The proposed $(R_{acc\text{-}HF})_{max}$-$RI$ relationship is of the form:

$$\left(R_{acc-HF}\right)_{\max}(RH, RI, T_{B1}, \zeta) = c\ RI^{d} T_{B1}^{\ e}, \text{where } 2 \le RI \le 4\ ;\ 0.6 \text{ sec.} \le T_{B1} \le 2.4 \text{ sec.} \quad (3.20)$$

The results for the constant c and the power values d and e obtained from regression are provided in Table 3.2. Figure 3.32 shows the $(R_{acc\text{-}HF})_{max}$ data points and the statistical model obtained for frames with fundamental period of 1.2 sec. and NSC damping ratios of 2%. Predicting the $(R_{acc\text{-}HF})_{max}$ values is noticeably harder than for R_{acc1} as this value covers the entire higher modal period region. However, the two parameter model used in this study is sufficiently accurate to predict the deamplification obtained in this region. The correlation coefficients for the above two-parameter models are of the order of 0.65. The standard errors of the estimates are of the order of 0.35.

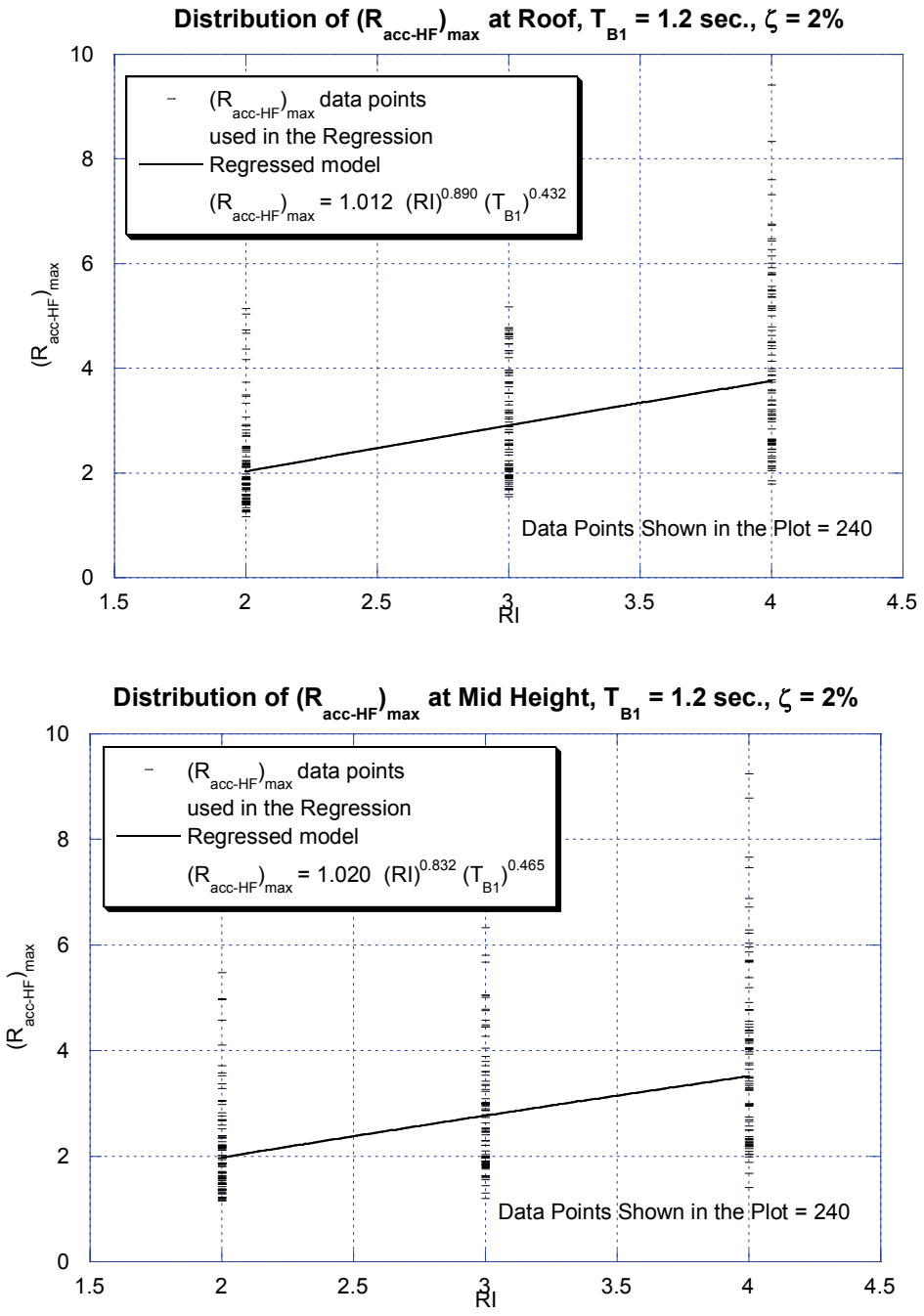

Figure 3.32 Sample regression plot showing the data points and the regressed equation for R_{acc} in low period region for 1.2 sec frames; component damping ratio = 2%

It should be noted that complex mathematical models (nonlinear) were not attempted because the aim of this work is to arrive at a simplified expression that can be more readily implemented in practice. Future studies are necessary to quantify the FRS amplification that can occur in some cases of inelastic structures. Appendix II discusses these effects in detail.

3.8 DISPERSION IN R_{acc}

The statistical models explained above for predicting R_{acc} represents the central values (medians). The R_{acc} values are normally distributed in the natural logarithmic domain. The measure of dispersion or variation in R_{acc} can be represented by studying the standard deviation of the natural logarithm of the R_{acc} values. This value measures the amount by which the R_{acc} values predicted by the recommendations differ from the median values. Figures 3.33 to 3.35 show the dispersion of R_{acc1} and $(R_{acc\text{-}HF})_{max}$ values at roof, mid-height, and bottom-third locations, respectively for RI = 2. The dispersion is similar to the behavior of R_{acc1} and $(R_{acc\text{-}HF})_{max}$ explained before. Higher values of component damping ratio produce larger values. The dispersion in R_{acc} increases for fundamental periods from 0.6 sec. to 1.2 sec.; however, the magnitude of the increase is small. The dispersion in $(R_{acc\text{-}HF})_{max}$ increases with the fundamental period of the buildings. The standard deviation of $ln(R_{acc1})$ at roof, mid-height and bottom-third location, are mostly similar. The dispersion $(R_{acc\text{-}HF})_{max}$ values at bottom-third location are marginally higher than the values at other two relative height locations. Figure 3.36 shows the dispersion of the R_{acc} values at fundamental-period and short-period regions of FRS for RI = 3.

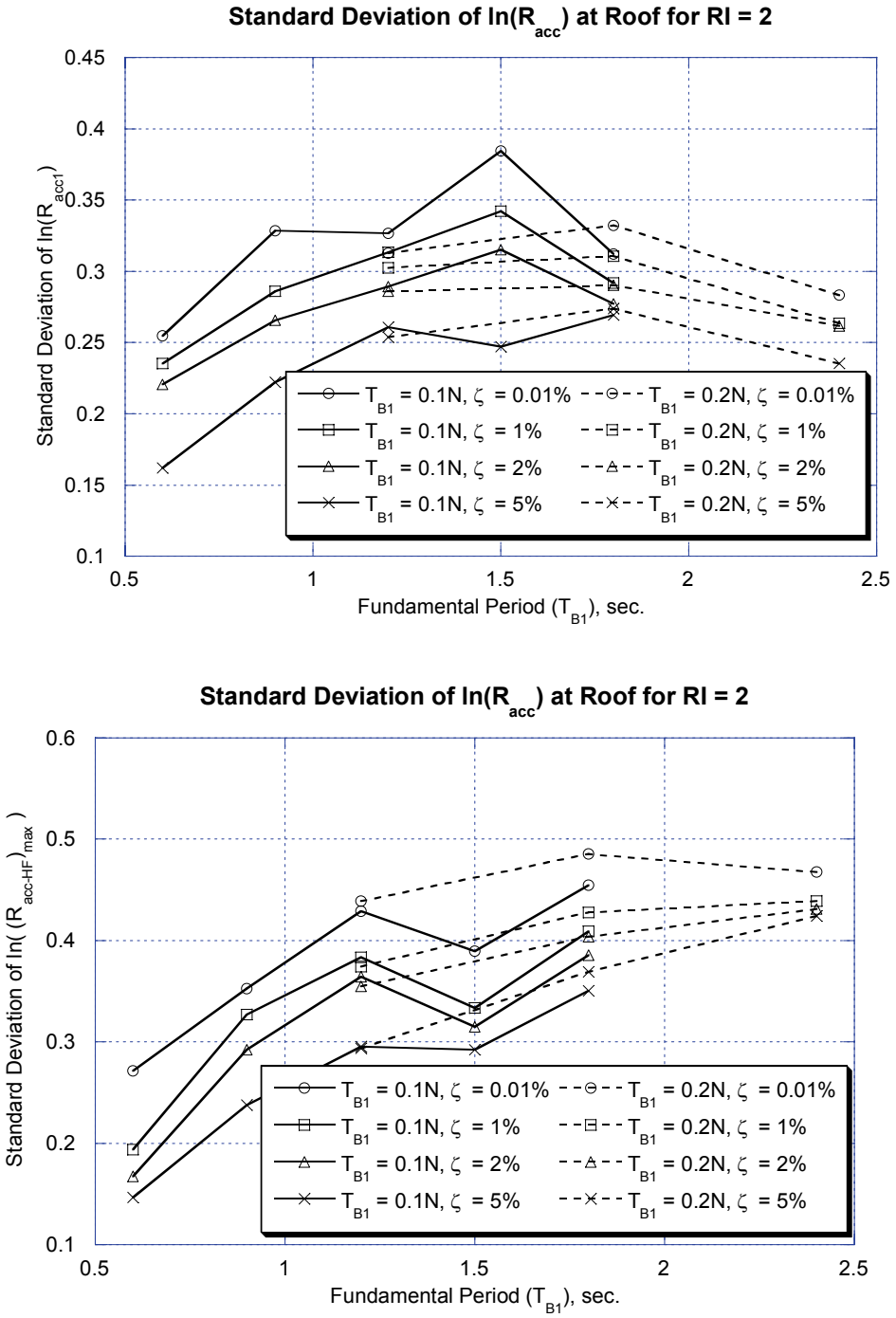

Figure 3.33 Dispersion of ln(R_{acc}) values at roof for RI = 2

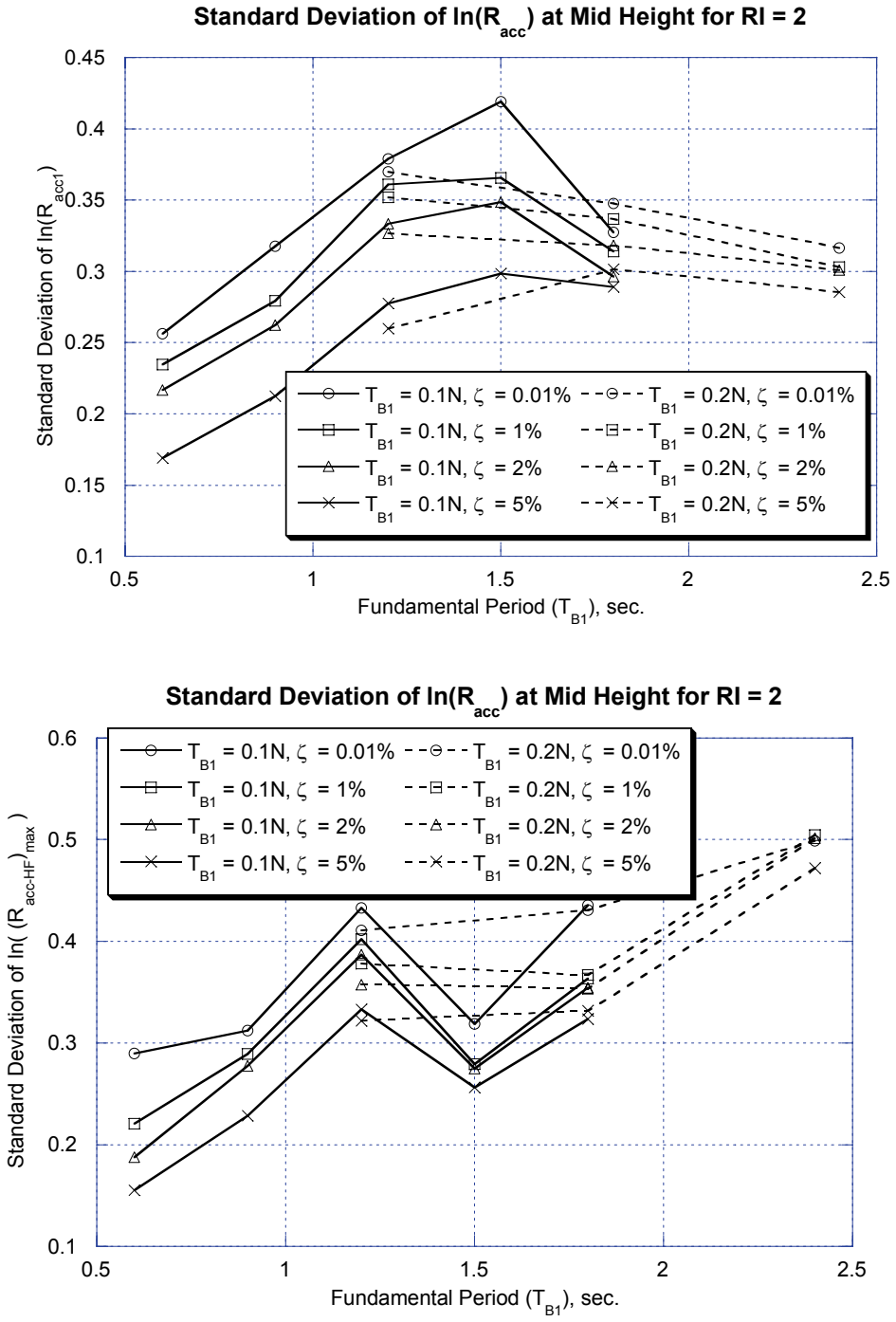

Figure 3.34 Dispersion of ln(R_{acc}) values at mid-height location for $RI = 2$

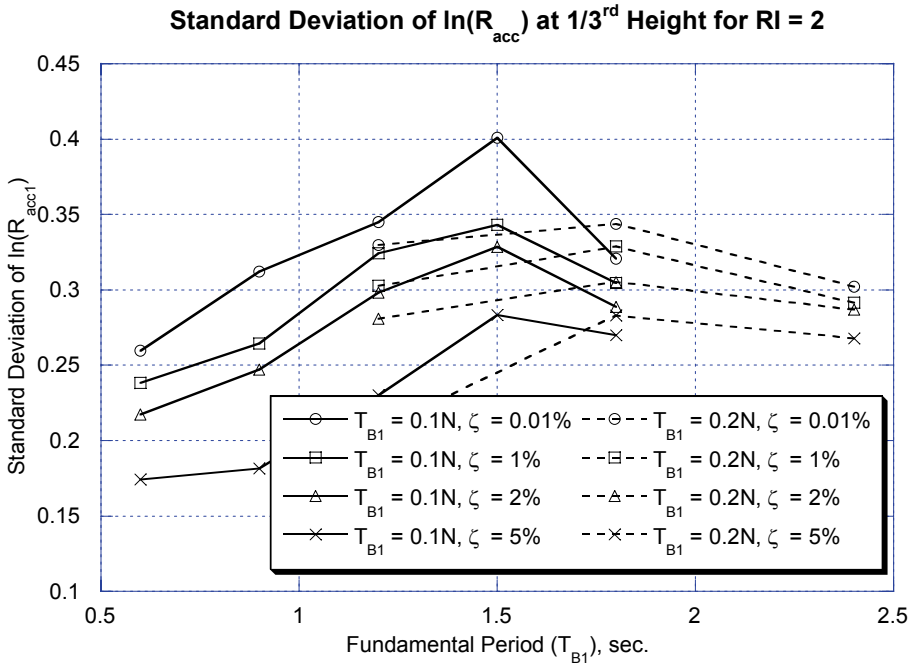

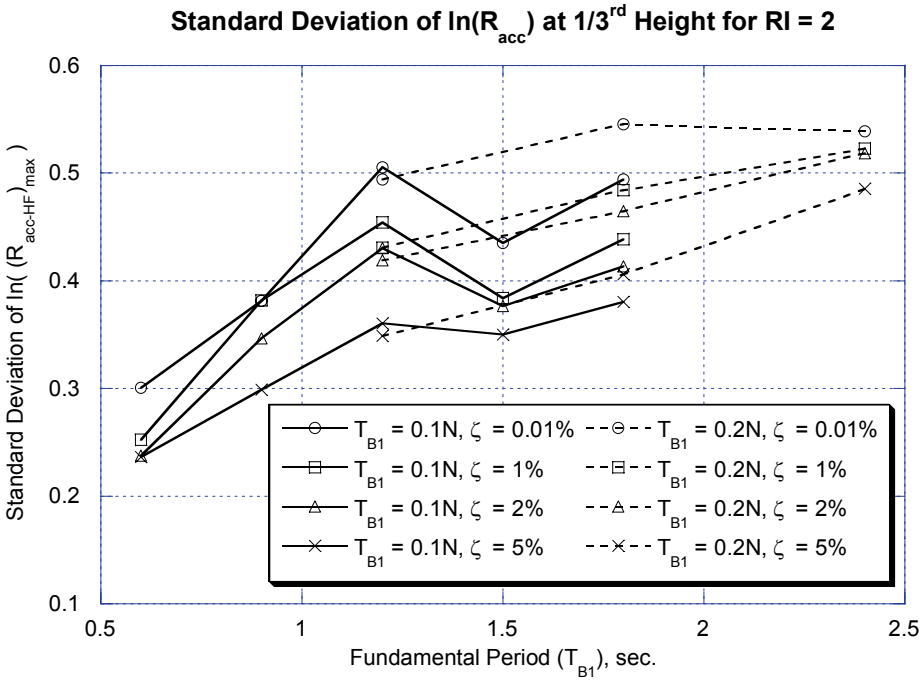

Figure 3.35 Dispersion of ln(R_{acc}) values at bottom-third location for *RI* = 2

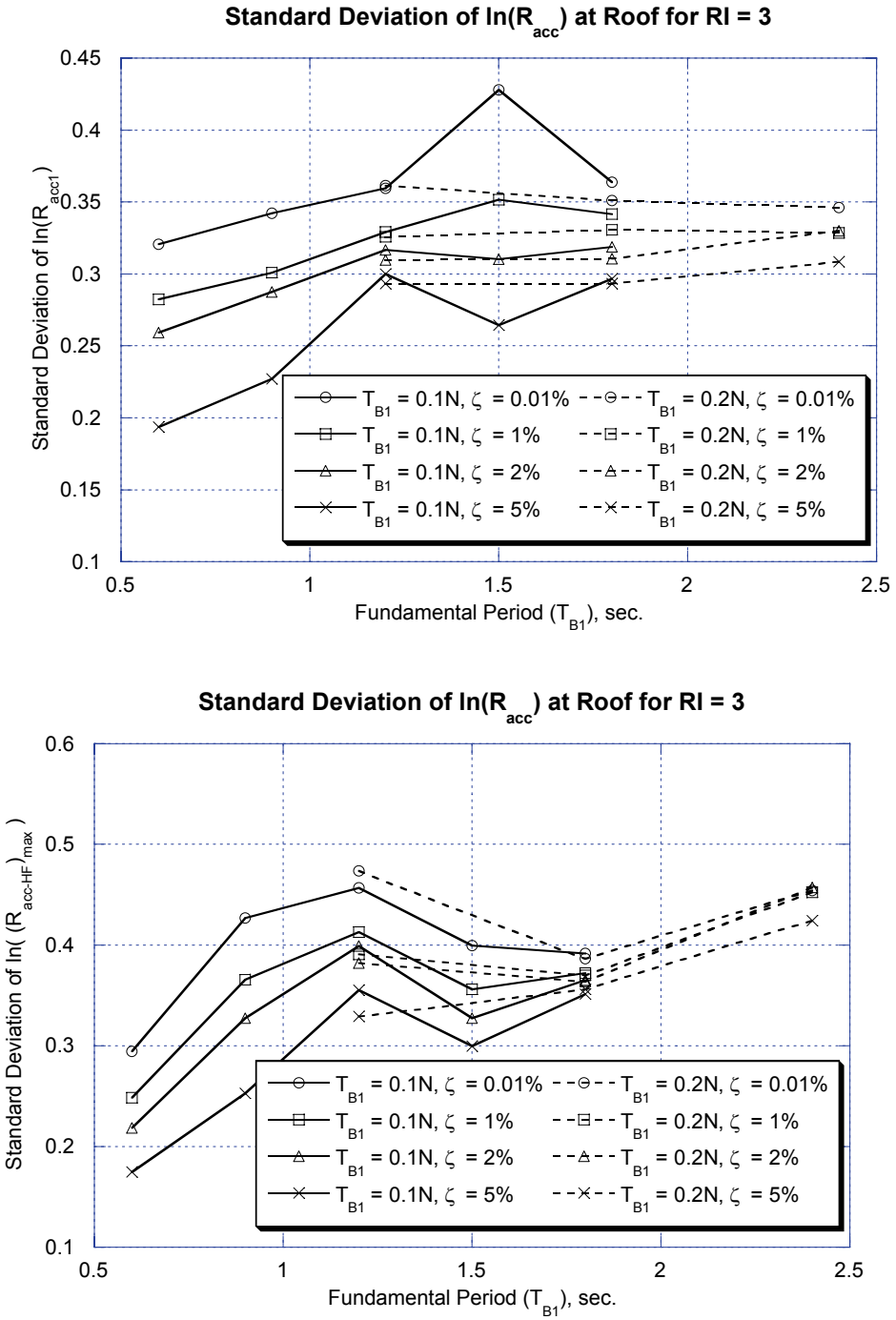

Figure 3.36 Dispersion of ln(R_{acc}) values at roof location for *RI* = 3

The dispersion in R_{acc1} values at roof for higher *RI* values is more uniform and is weakly dependent on T_{B1}. The general behavior of dispersion values is similar to that of *RI* = 2.

3.9 DISPERSION IN a_p*(inelastic)* VALUES

In the methodology proposed for estimating the peak acceleration demands on NSCs, one of the key steps is to determine the component amplification factors for NSCs mounted on inelastic buildings i.e. a_p*(inelastic)*. The R_{acc} factors discussed before help in the process of determining a_p*(inelastic)* from a_p*(elastic)* or S_{aC}*(elastic)* values. This section presents the dispersion in the a_p*(inelastic)* values obtained from the nonlinear time-history analysis independent of R_{acc} (i.e. the a_p*(inelastic)* values are calculated using equation (3.21) and not via the R_{acc} methodology proposed in section 3.6).

$$a_p(inelastic) = \frac{S_{aC}(inelastic)}{PFA_e} \tag{3.21}$$

Figures 3.37, 3.38 and 3.39 present the standard deviation of the natural logarithm of a_p*(inelastic)* values for *RI* = 2. The spread at the roof and bottom-third locations for all the damping values, increases from 0.3 to 0.8 for increase in T_{B1} values. The dispersion of inelastic $(a_{p\text{-}HF})_{max}$ at the three relative height locations is more uniform and is of the order of 0.35. Figure 3.40 presents the corresponding values at roof for *RI* = 3. The a_p*(inelastic)* values at the fundamental-period and short-period regions of FRS are also similar to lower *RI* values.

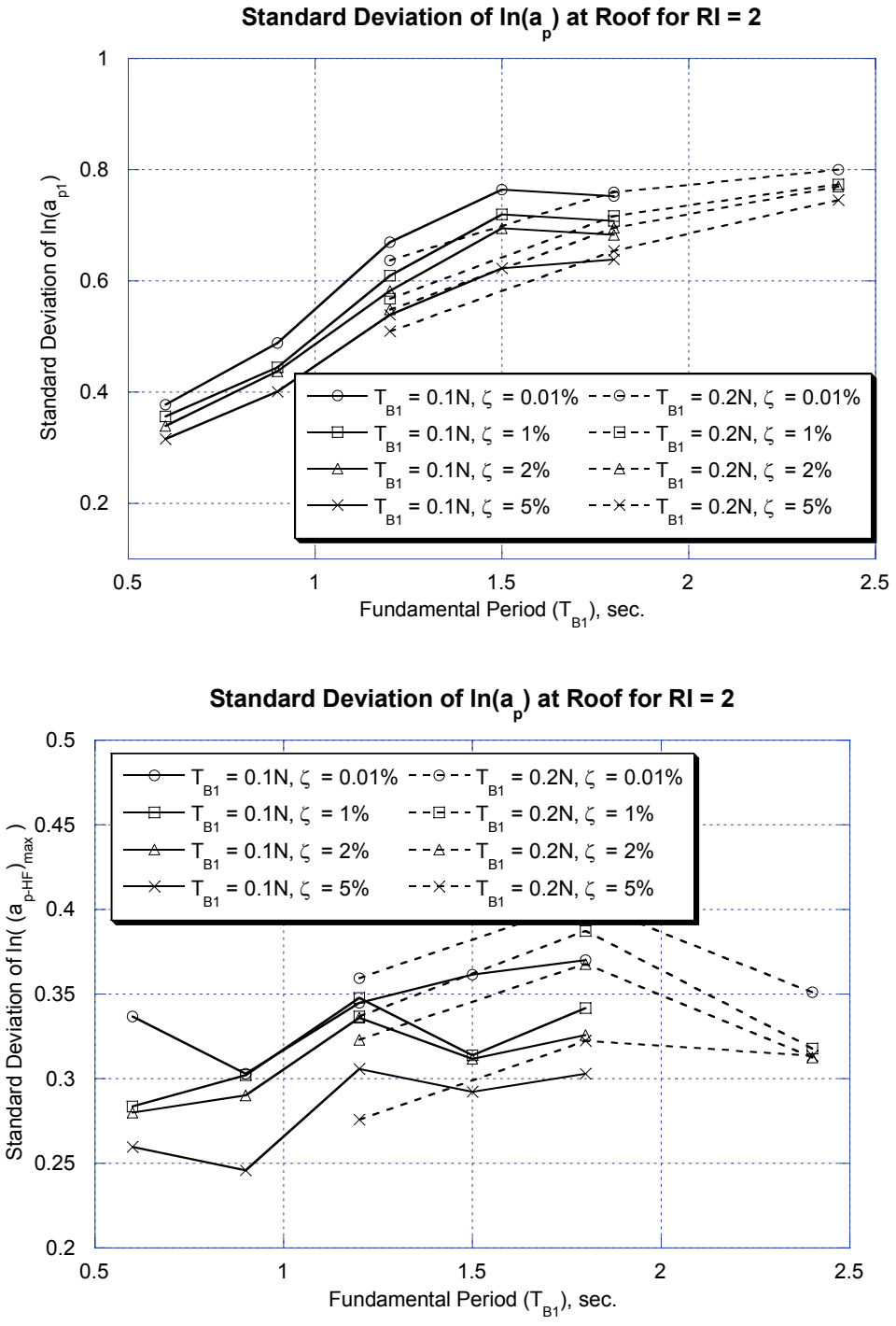

Figure 3.37 Dispersion of ln(a_p) values at roof for *RI* = 2

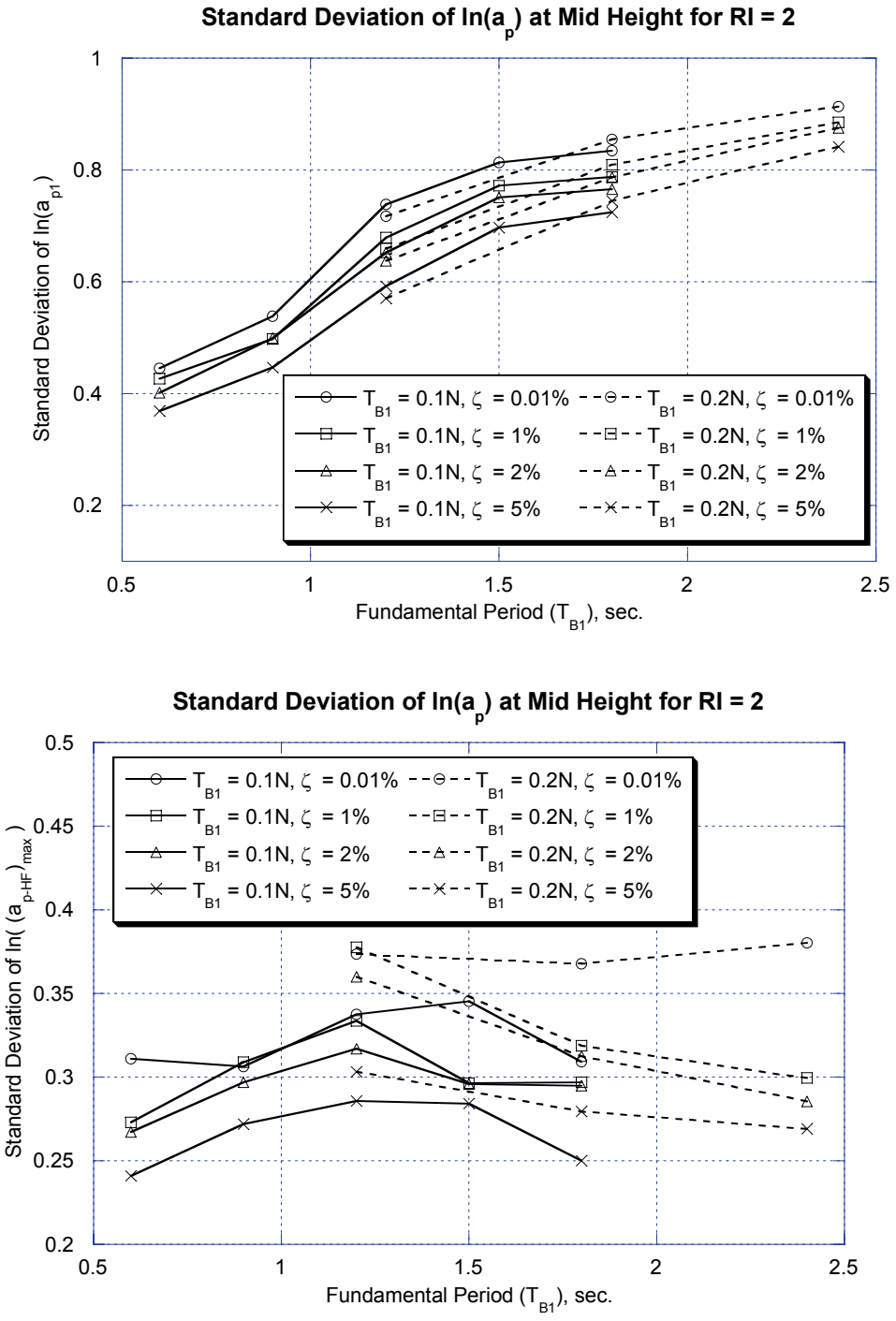

Figure 3.38 Dispersion of ln(a_p) values at mid-height location for *RI* = 2

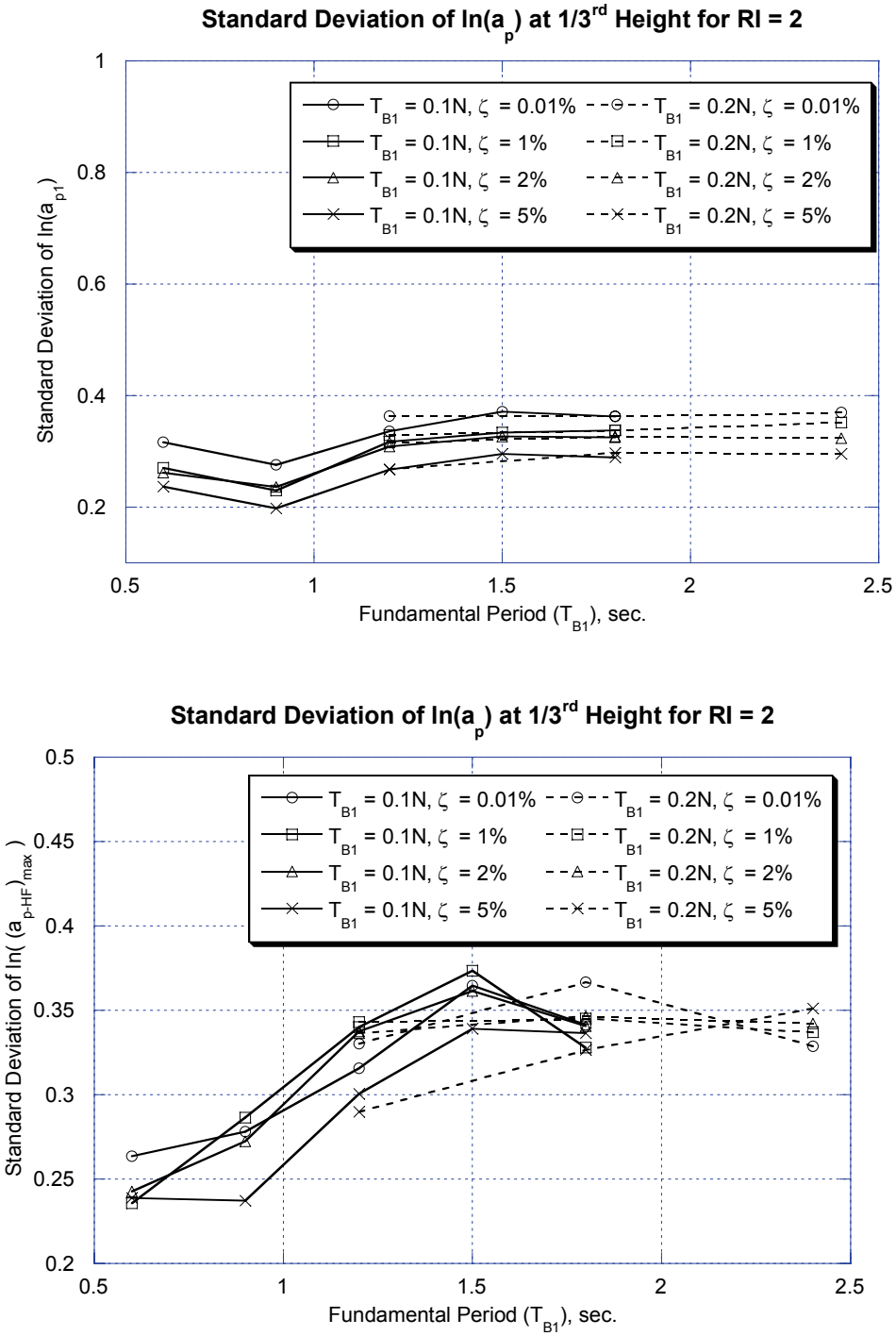

Figure 3.39 Dispersion of ln(a_p) values at bottom-third location for *RI* = 2

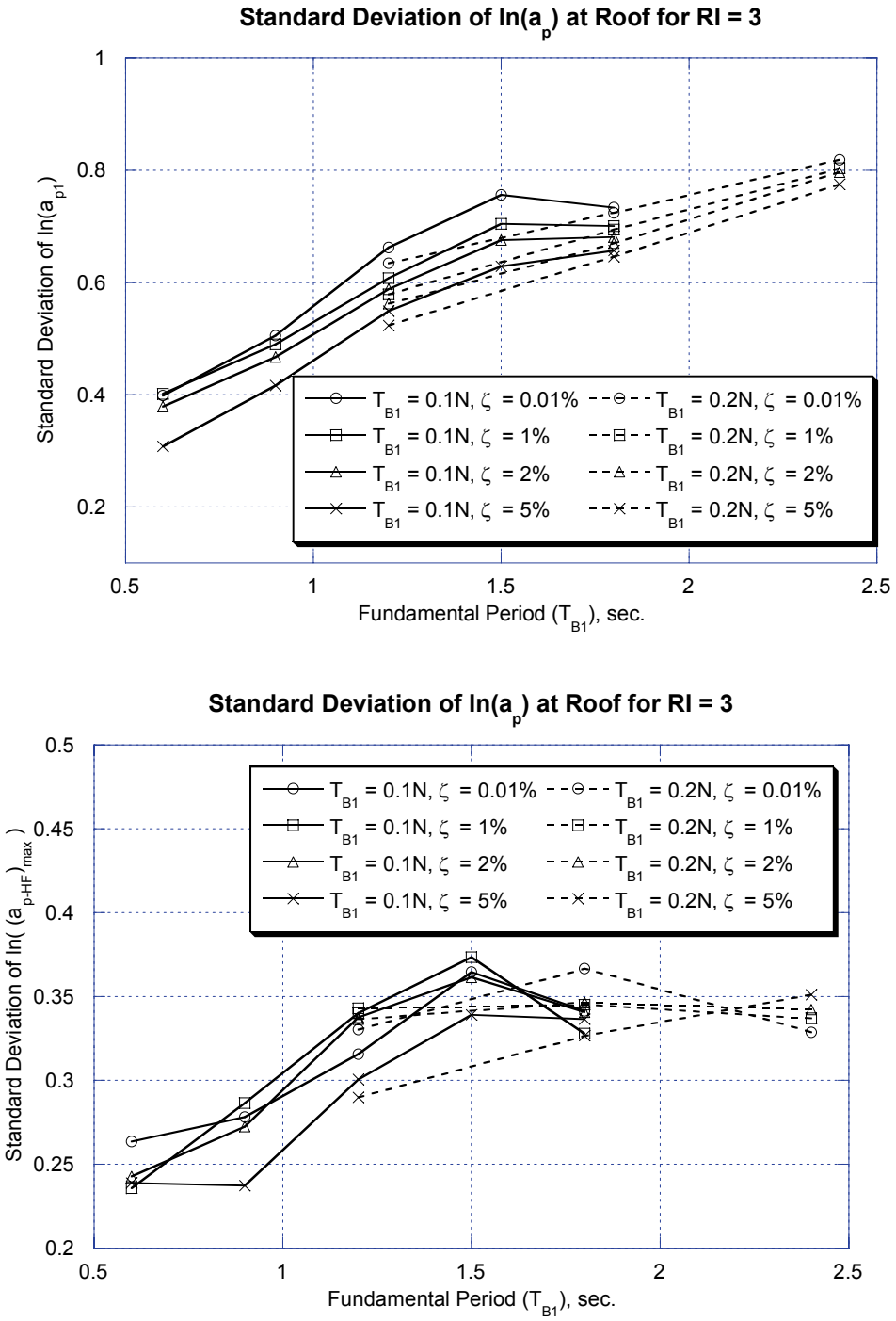

Figure 3.40 Dispersion of ln(a_p) values at roof location for *RI* = 3

3.10 SUMMARY

This chapter discussed the acceleration demands on NSCs mounted on both elastic and inelastic building structures. The design provisions in the current building codes for the estimation of acceleration demands on NSCs are simple and rational. However, they do not account for the inelastic action of the supporting structure and also are not adequate in representing the acceleration demands in the short-period region of the FRS for both elastic and inelastic buildings. Hence, the main focus was on NSCs located in buildings that undergo inelastic action. The component amplification factors (a_p) for elastic frames in the first three modal periods (a_{p1}, a_{p2} and a_{p3}), the maximum over the entire FRS ($(a_p)_{max}$) and maximum value in the region of higher modes $(a_{p\text{-}HF})_{max}$ were presented for buildings with different number of stories (N) and fundamental periods (T_{B1}) varying from 0.3 sec. to 3.6 sec The a_{p1} values vary inversely to the T_{B1} values and the values decrease when the NSC location is shifted from the roof level to the bottom stories. The peak a_p values in the short-period region namely $(a_p)_{max}$ values, are similar for T_{B1} values greater than 0.9 sec. The $(a_p)_{max}$ values are weakly dependent on the location of the NSC or the period of the NSC. The use of this value when the period or the locations of the NSC are not known might be overly conservative in most regions of FRS,

A methodology for estimating the acceleration demands on NSCs mounted on inelastic buildings was proposed based on acceleration response modification factor (R_{acc}). The R_{acc} factor provides an effective way of estimating the peak acceleration demands on NSCs mounted on inelastic frames from the elastic FRS. The properties of the R_{acc} allow the entire FRS to be grouped into three regions namely, long-period,

fundamental-period and short-period regions thus overcoming the difficulties in coming up with a single R_{acc} factor expression for all periods of NSC. The R_{acc} behavior has been consistent in the different regions and along the height of all building models. While the inelastic FRS in the long-period region are close to the elastic FRS values, R_{acc1} and $(R_{acc\text{-}HF})_{max}$ values are characteristic of the deamplification experienced in the fundamental-period and short-period regions respectively. The R_{acc} values are strongly dependent on the level of inelasticity of the supporting structure (*RI*). The R_{acc1} values are weakly dependent on T_{B1} for supporting structure fundamental periods greater than 0.6 sec. Hence, values of R_{acc} in the above regions were presented separately for short period ($T_{B1} \leq 0.6$ sec.) and medium to long period frames ($0.6 \text{ sec.} \leq T_{B1} \leq 2.4$ sec.).

The R_{acc} values were proposed for the fundamental-period and short-period regions based on a regression analysis on a large number of building models with different number of stories (*N*), fundamental periods corresponding to *0.1N* and *0.2N*, different levels of inelasticity (Relative Intensities), NSCs located at different locations in the building and four different NSC damping ratios. Different R_{acc} factor values are provided for NSCs mounted on three distinct locations in the building namely, roof, mid-height location and at a location situated at one third height from the bottom of the building.

The values presented are adequate to provide a complete picture of inelastic FRS from elastic FRS values. For normal equipment mounted on regular moment-resisting frames, R_{acc} provides a simple approach to include the effects of nonlinearity of the supporting structure. The prediction and understanding of R_{acc} values achieved

in this dissertation, comprehend the existing knowledge. The results help address some of the idiosyncrasies of current code provisions that account for the nonlinearity of the equipment but not of the supporting structure. It should be noted that there can be some cases where the calculated force will be underestimated due to the short-period amplification effect in which R_{acc} values are less than one (see Appendix II). Thus, for important equipment in critical facilities (e.g. equipment in nuclear power plant structures) or special equipment (heavy machinery), it may be necessary to conduct a more detailed analysis especially in the short-period region.

Chapter 4: Acceleration Demands on NSCs Mounted on Multi-bay Frames and Validation of Results

4.1 INTRODUCTION

This study makes use of generic single-bay frames that are capable of representing the global behavior of more complex regular multi-bay frames. The regular frames used in this dissertation have adequate representation of strength, stiffness, ductility, and P-delta effects. The models in this study are not geared for rigorous demand prediction for a specific building. An actual building model will have unique characteristics that might deviate from the assumptions used in the development of generic models. The objective of this chapter is to correlate the acceleration demands on NSCs mounted on multi-bay steel / reinforced-concrete frames with that of the results obtained from the generic models used in this study. The R_{acc} values proposed by the regression equations in the previous chapter are compared with the statistical values for multi-bay frames subjected to the set of 40 far-field ground motions.

4.2 DESCRIPTION OF MULTI-BAY FRAME MODELS

Two different multi-bay building models are used to validate the results obtained from the generic models. They are

- SAC steel project LA9 office building (Steel) and
- Van Nuys hotel building (Reinforced-Concrete).

4.2.1 SAC LA9-M1 Building Model

The SAC Joint Venture was formed in 1994 with the specific goal of investigating the damage to welded steel moment frame buildings in the 1994 Northridge earthquake and developing repair techniques and new design approaches to mitigate damage to steel moment frame buildings in future earthquakes. In this study, the SAC LA9-M1 frame model (Gupta and Krawinkler 1999) is utilized to validate the use of single-bay frames to represent the behavior of NSCs mounted on regular multi-bay frames. This model corresponds to one of the steel perimeter moment-resisting frames located in the north-south direction of the design of a standard office building in the Los Angeles area, situated on stiff soil and designed according to the UBC 1994 code. It is based on centerline dimensions; thus, the contribution of the panel zones to the response is neglected. This five-bay frame model has been used extensively in the SAC/FEMA steel project and in other studies (Nakashima et al. 2002). The hysteretic behavior at plastic hinge locations is modeled by using bilinear hysteretic rules with 3% strain hardening. Axial load-bending moment interaction in columns is included as well as second order structure P-delta effects. Strength properties are based on the expected strength of the material and 2% Rayleigh damping is used at the first mode and at a period of 0.2 sec. Figure 4.1 shows a plan view, elevation and the modal properties of this building model. Detailed information about SAC LA9-M1 model and specific model characteristics can be obtained from references (Gupta and Krawinkler 1999; Medina and Krawinkler 2004).

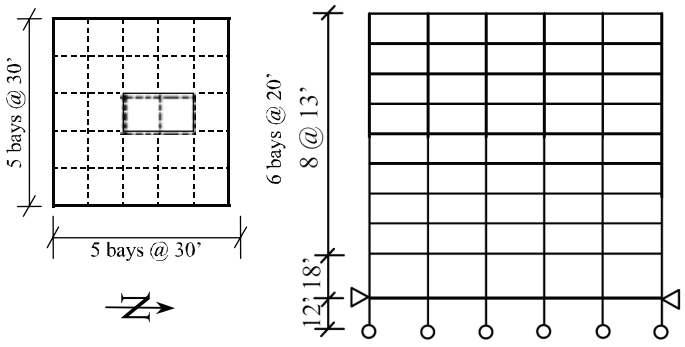

(a) Plan and Elevation (Gupta and Krawinkler 1999)

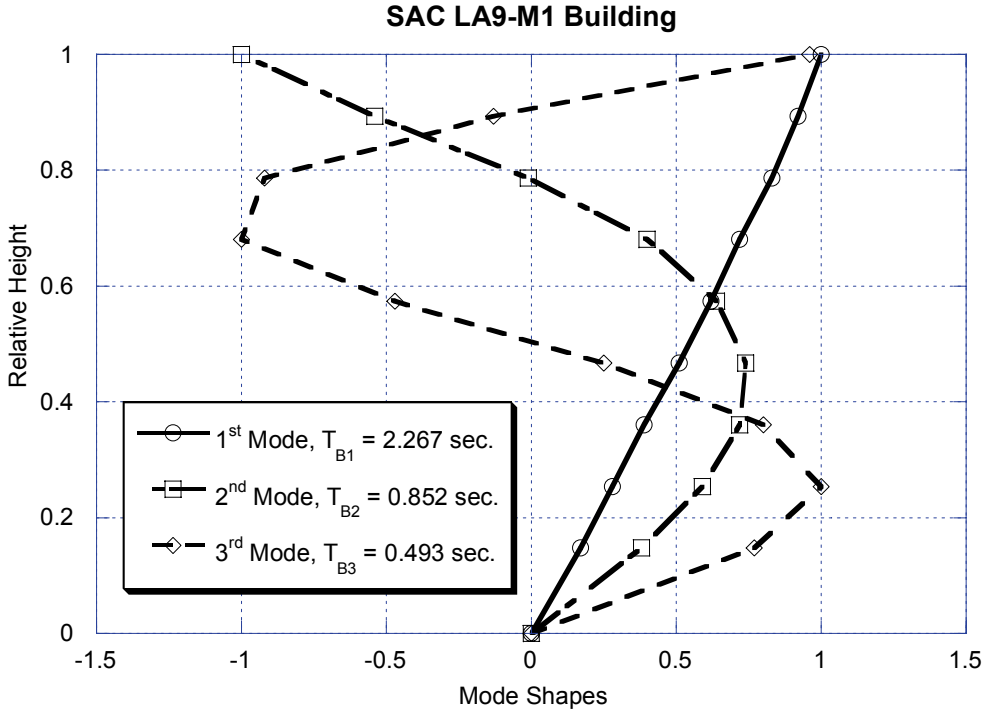

(b) Mode Shapes

Figure 4.1 Perimeter moment-resisting frame of SAC LA9-M1 model and its modal properties

4.2.2 Van Nuys Building Model

This building is a 7-story hotel in Van Nuys, California. The hotel was designed in 1965 according to the 1964 Los Angeles City Building Code, and built in 1966. The structural system is a cast-in-place reinforce-concrete moment-frame building with non-ductile column detailing. Lateral force resistance is provided primarily by the perimeter moment frames. The gravity system comprises 2-way reinforced concrete flat slabs supported by square columns at the interior and the rectangular columns of the perimeter frame. This building has been extensively studied by numerous researchers and detailed information on the structural and architectural characteristics of the building can be obtained from them (Jennings 1971; Islam 1996; Loh and Lin 1996; Li and Jirsa 1998; Trifunac et al. 1999a; Trifunac et al. 1999b; Todorovska et al. 2001; Aslani and Miranda 2005; Krawinkler 2005). This study uses the DRAIN-2DX model whose results have been benchmarked with OpenSees models (Krawinkler 2005). Building acceleration records from the Northridge earthquake indicate that the fundamental period of the building is 1.5 sec. and hence it was taken as the target initial period in the development of models. The building has 5% damping in the 1st and 2nd modes. Figure 4.2 shows the elevation and the modal properties of the Van Nuys building model.

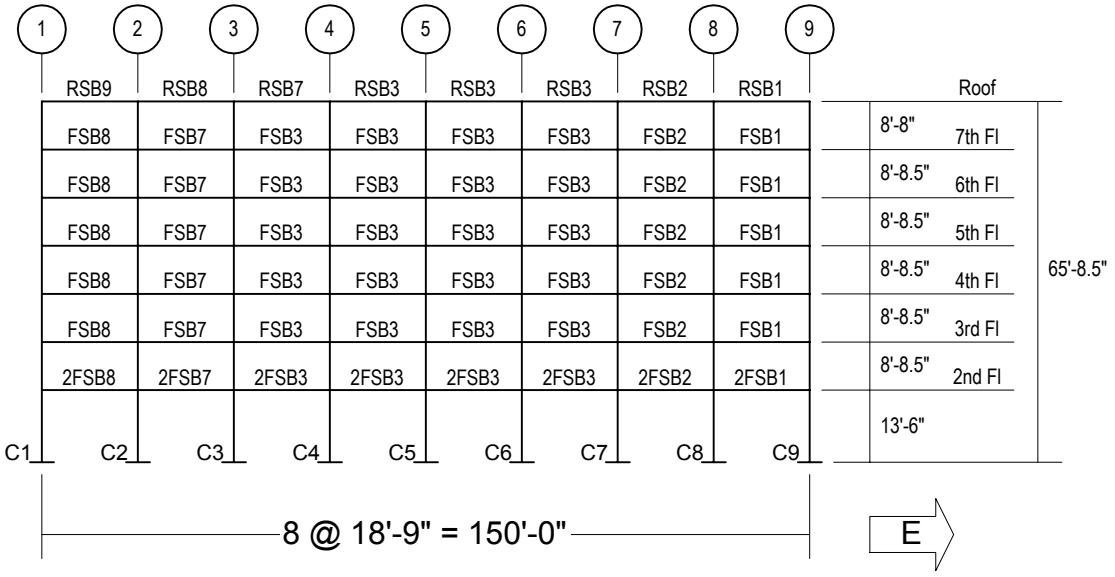

(a) South frame elevation (Krawinkler 2005)

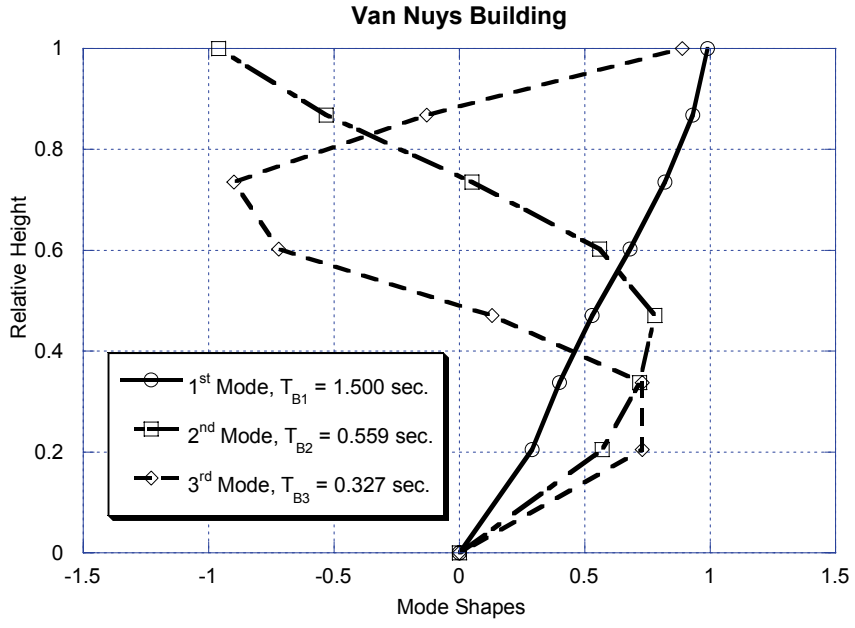

(b) Mode Shapes

Figure 4.2 Elevation of South frame of the Van Nuys building model and its modal properties

4.3 RESULTS

An adequate building model geared towards estimating the demands on NSCs, should be capable of capturing the global behavior of the building, which includes the acceleration time histories at individual floors. Although both these two models do not include panel zones which are aimed mostly to capture localized failure effects (i.e. finite member sizes, shear distortions, plastifications in the panel zones, etc.), the validation models are adequate for current requirements of this study. In the analysis procedure for validation of results, the ground motion intensity is increased by scaling the ground motions while keeping the base shear strength constant. This is different from the methodology used in the development of the R_{acc} recommendations wherein the base shear strength was varied while keeping the ground motion intensity the same. This scaling is appropriate for MDOF systems without axial-force-moment interaction and without second-or-higher-order geometric nonlinearities. More information on the scaling of ground motions versus scaling the model is available in references (Vamvatsikos and Cornell 2002; Medina and Krawinkler 2004). The acceleration demands on NSCs mounted on these two multi-bay frames can further be classified into elastic and inelastic behavior.

4.3.1 Elastic FRS

The elastic a_p values (a_{p1} and $(a_{p\text{-}HF})_{max}$) at roof and mid-height location for the two validation models are shown in Figure 4.3 and Figure 4.4, respectively. For the ease of comparison, the results from the generic frames (discussed in section 3.3) are also shown. The median a_{p1} values at roof and mid-height location for both the

validation frames are close to values obtained from the generic frames used in this study. The fundamental period of the SAC LA9-M1 model and Van Nuys model are 2.3 sec. and 1.5 sec., respectively, which fall under the medium to long period buildings used in this study. For elastic buildings with these fundamental periods, the component amplification factors at the higher modal periods are greater than a_{p1} values i.e. $\underline{(a_p)_{max}}$ values are mainly contributed by $(a_{p\text{-}HF})_{max}$ values.

However, the $(a_{p\text{-}HF})_{max}$ values for the SAC LA9-M1 building are much larger than the values from generic frames while the results for the Van Nuys building model are in the same range as the values from the frames used in this study. This can be attributed to the percentage of critical damping of the SAC LA9-M1 building. The SAC building has 2% critical damping while all the models used in this study and the Van Nuys building model have 5% critical damping. Smaller values of damping of the supporting structure produce sharper spikes in the FRS for a given value of equipment damping. Thus the elastic FRS is very sensitive to the percentage of critical damping. With an increase in the NSC damping, the FRS peaks tend to get blunted and thus the a_p values for higher values of NSC damping are comparable to the results obtained in the previous chapter. A damping value of 0.01% of the equipment is used only as an upper bound to show the maximum values of a_p that can be reached for an equipment with negligible component damping. Actual values of component damping used in other FRS studies fall in the 1%-5% range. For this range the generic frames used in this study represent the elastic FRS adequately.

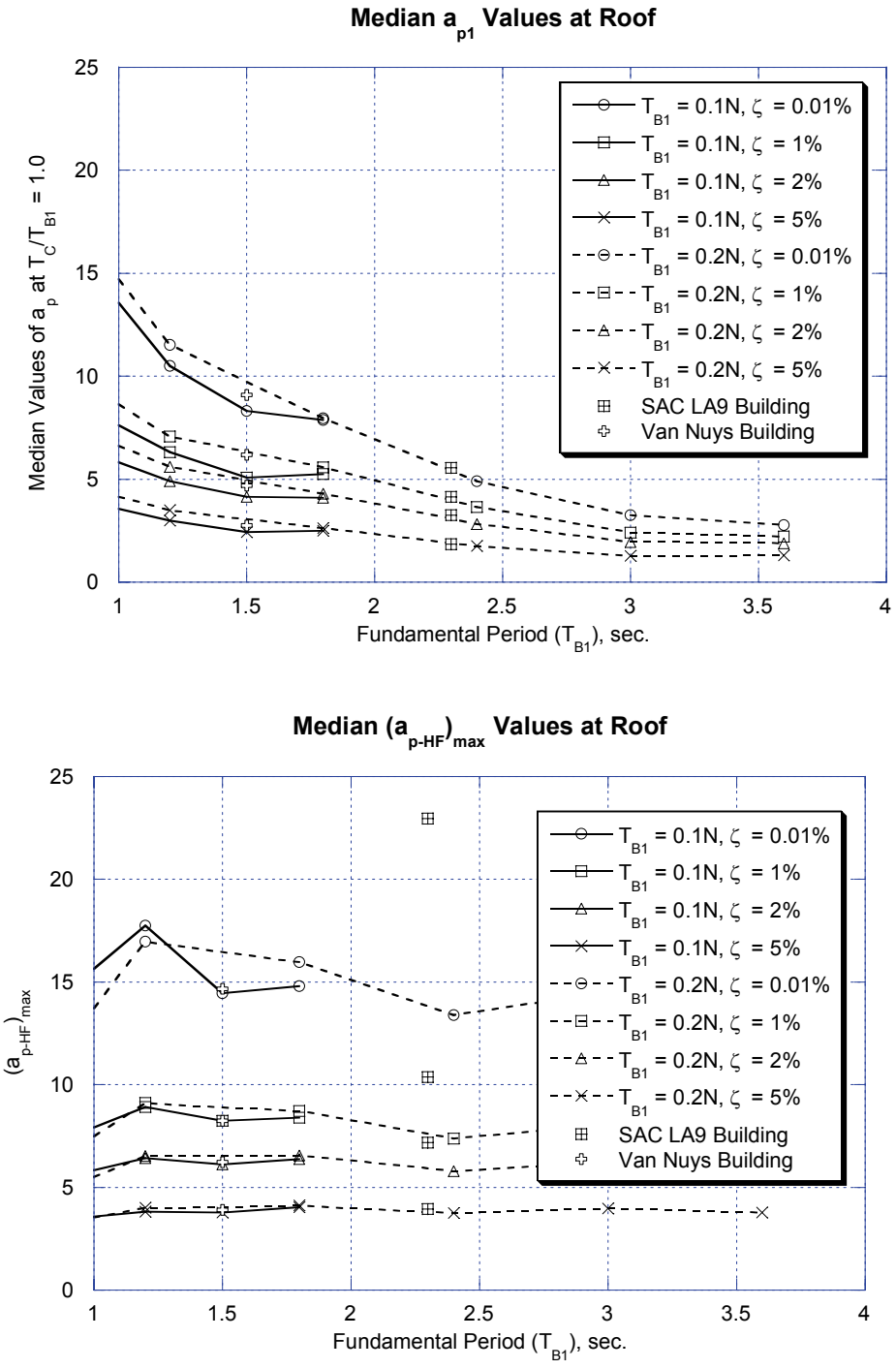

Figure 4.3 a_p values for validation models at roof location

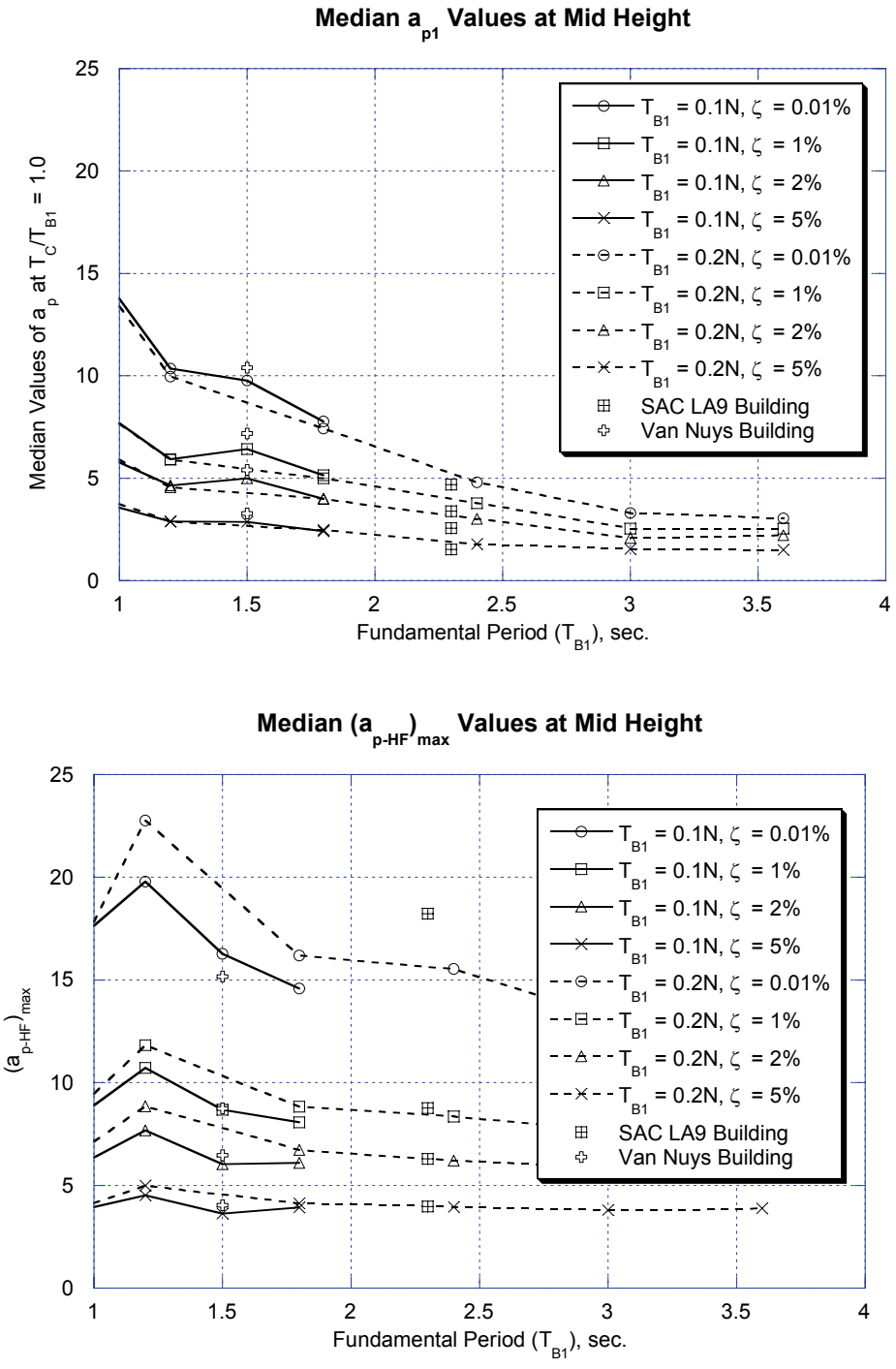

Figure 4.4 a_p values for validation models at mid-height location

4.3.2 Inelastic FRS (R_{acc})

The generic frames whose T_{B1} values are closer to that of multi-bay frames are selected as companion generic frames. The fundamental period of N = 12, T_{B1} = 2.4 sec. flexible frame is close to the T_{B1} value of SAC LA9-M1 frame (T_{B1} for SAC LA9 is around 0.27N). The results of the 9-story multi-bay frame are compared to that of 12-story generic frame. For Van Nuys building, N = 15, T_{B1} = 1.5 sec. stiff frame has the T_{B1} value equal to that of Van Nuys building. Hence for the 7-story Van Nuys building which resembles the flexible frames (the T_{B1} of this building is 0.21N); the results are compared to that of a stiff frame. This is acceptable because of the strong dependence of a_p values on T_{B1} and their weak dependence on the number of stories which has been reported earlier.

Figure 4.5 shows the R_{acc} values at different levels for SAC LA9 building and Van Nuys building for a component damping value of 2%. The shape of the R_{acc} plot in the three regions for the Van Nuys building and SAC LA9 building are similar to the behavior discussed before (see section 3.4.2). Compared to their companion generic frames, greater changes in the shape of the R_{acc} distribution are seen for the SAC LA9 building. Higher values of *RI* are not shown because these frames are prone to experience dynamic instability at lower *RI* values. In the long-period region of the SAC LA9-M1 building, the elastic FRS values, i.e. S_{aC}*(elastic)*, are less than 0.5 times the values for N = 12, T_{B1} = 2.4 sec. frame. Hence, the R_{acc} values slightly larger than one for this particular frame have no significant effect when they are factored to get inelastic FRS.

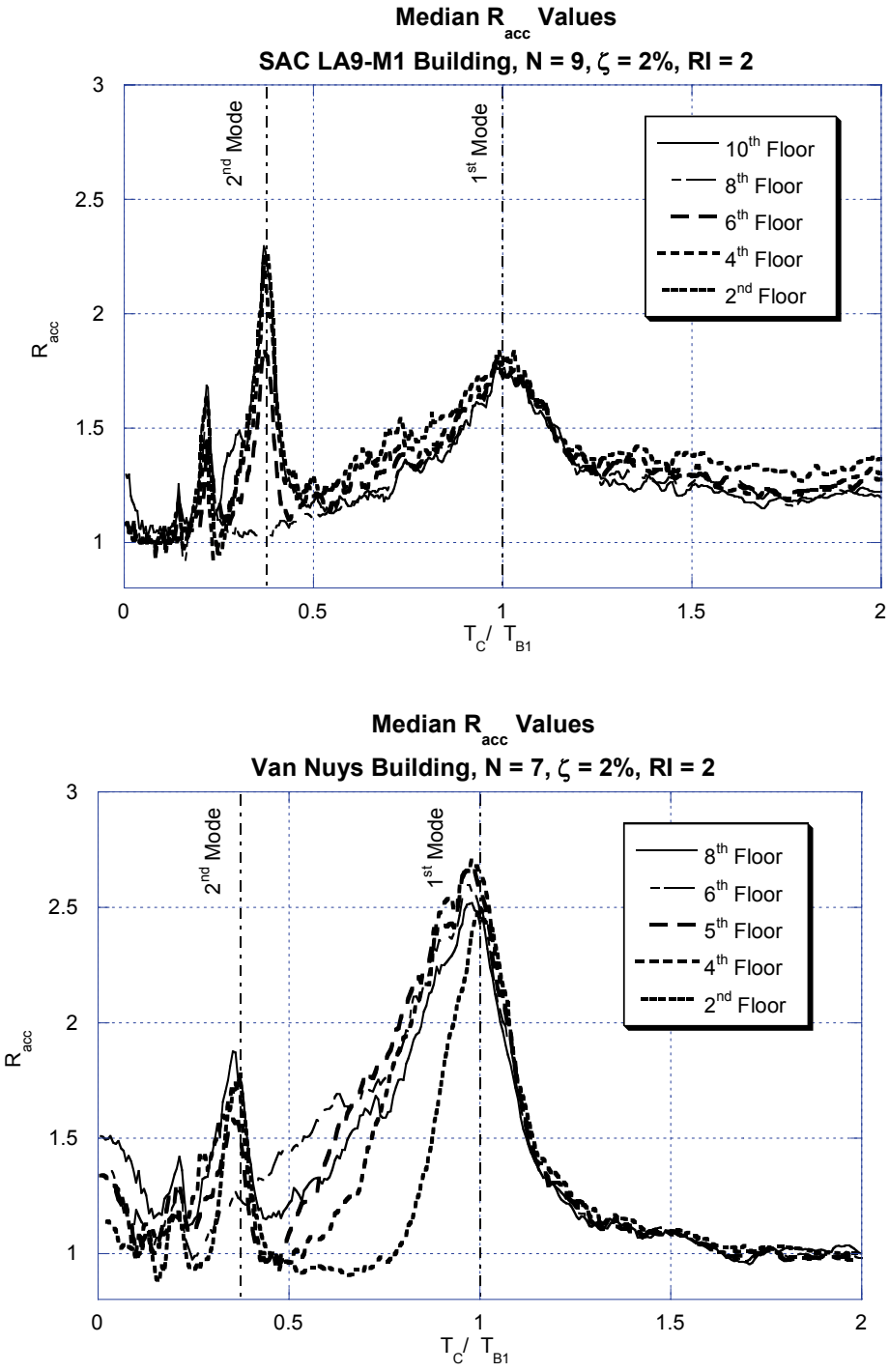

Figure 4.5 R_{acc} factor values for validation models; RI = 2 and component damping ratio = 2%

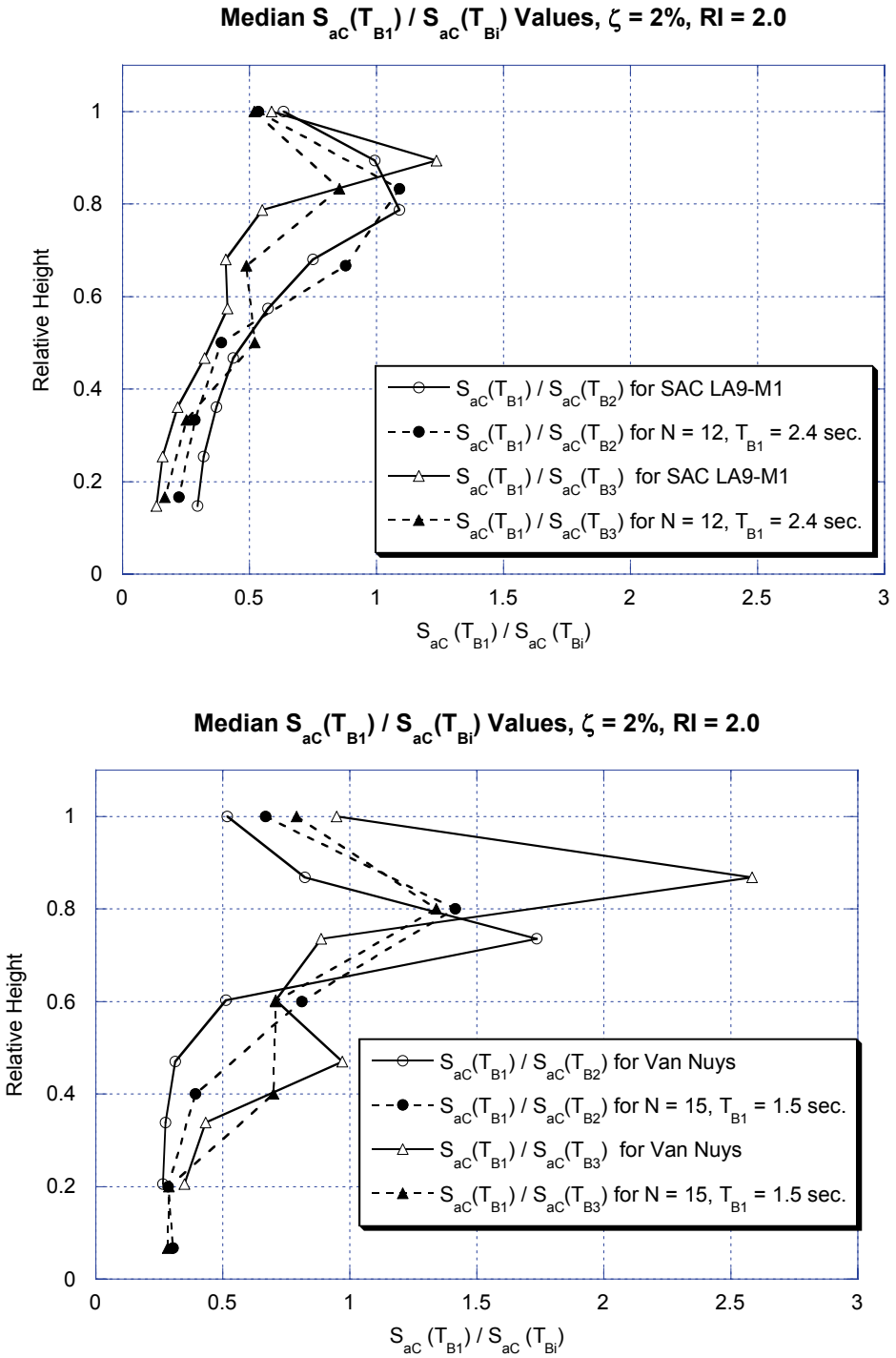

Figure 4.6 Ratio of peak component acceleration at $T_C = T_{B1}$ to the peak component acceleration at 2nd and 3rd modal periods; $RI = 2$ and component damping ratio = 2%

Figure 4.6 shows the ratio of the peaks of the 2nd and 3rd modes to that of the 1st mode. This ratio defines approximately the shape of the FRS. It can be seen that shape of the FRS for multi-bay frame and the generic frames are consistent; however, the values differ slightly due to the differences in modeling (single bay Vs multi-bay) and modal properties. The R_{acc} plots clearly show a deamplification of inelastic FRS around the modal periods when compared to the elastic FRS. It should be noted that R_{acc} values less than one are observed in the short- period region. This is similar to the behavior observed by Sewell (Sewell et al. 1986; Sewell et al. 1987) and Singh (Singh et al. 1993; Singh et al. 1996) wherein a concentration of ductility values tend to increase the amplification in the inelastic FRS in the low period region. This amplification is also shown in R_{acc} plots presented in appendix II.

Table 4.1 and 4.2 show the R_{acc1} and $(R_{acc\text{-}HF})_{max}$ values, respectively. The values predicted by the regression models are compared to the values obtained from the median values of the results from the individual models. Negative values of the percentage difference means that the values from the actual model are lower than the values predicted by the regression equations. Positive values of the % difference mean that the proposed R_{acc} (reduction factors) values are conservative. As seen in the previous plots, the R_{acc1} values for the SAC LA9-M1 model are much lower when compared to that of the predicted values. The R_{acc1} values for the Van Nuys building are in the order of 20% of the predicted values. The model is conservative for Van Nuys building, but not for the SAC LA9 building. The $(R_{acc\text{-}HF})_{max}$ values predicted by the model are higher than the actual value from individual models. The difference in the values between regression models and the multi-bay frames are of the order of

20%. It should be noted that the predicted values are based on the results from numerous stiff and flexible frames and with a large range of values for inelasticity. Moreover, the companion generic frames selected for comparing the values to that of the values predicted by the model have different number of stories and the relative height location used to pick the R_{acc} results are different. The fundamental periods of the buildings used in the study are tuned to match either $0.1N$ (stiff) or $0.2N$ (flexible) and these models are used to predict the behavior of all the frames that have periods in this range. The 20% difference from the multi-bay frames values with that of prediction models are can be considered reasonable when looked in this perspective.

RH	ζ	Median R_{acc1} predicted by the regression model	% difference between predicted and actual value	
			SAC LA9	Van Nuys
1.0	0.01 %	2.72	-23.8	19.8
1.0	1 %	2.43	-19.2	19.2
1.0	2 %	2.27	-14.8	16.8
1.0	5 %	2.00	-10.5	10.3
0.5	0.01 %	2.94	-28.6	15.8
0.5	1 %	2.60	-21.7	15.3
0.5	2 %	2.40	-17.9	15.5
0.5	5 %	2.11	-13.8	16.6
0.33	0.01 %	2.94	-28.2	17.9
0.33	1 %	2.55	-21.0	21.8
0.33	2 %	2.33	-15.9	20.7
0.33	5 %	2.01	-8.1	21.6

Table 4.1 Comparison of R_{acc1} values at roof and mid-height based on regression (see equation (3.19)) with values from multi-bay validation models

RH	ζ	Median $(R_{acc\text{-}HF})_{max}$ predicted by the regression model		% difference between predicted and actual value	
		SAC LA9	Van Nuys	SAC LA9	Van Nuys
1.0	0.01 %	3.65	2.91	-4.4	-17.5
1.0	1 %	2.94	2.42	4.5	-13.7
1.0	2 %	2.67	2.24	2.8	-10.5
1.0	5 %	2.32	1.99	-4.6	-4.7
0.5	0.01 %	3.54	2.82	-16.8	-26.0
0.5	1 %	2.88	2.36	-19.3	-22.5
0.5	2 %	2.66	2.19	-21.2	-20.1
0.5	5 %	2.31	1.97	-24.0	-14.3
0.33	0.01%	4.04	3.11	-26.2	-29.0
0.33	1%	3.19	2.53	-18.0	-22.0
0.33	2%	2.90	2.32	-13.8	-19.4
0.33	5%	2.49	2.03	-20.7	-10.6

Table 4.2 Comparison of $(R_{acc\text{-}HF})_{max}$ values at roof and mid-height based on regression (see equation (3.20)) with values from multi-bay validation models

4.4 SUMMARY

In this chapter, an evaluation of the adequacy of generic frames and proposed statistical models to predict / quantify the acceleration demands for NSCs mounted on real multi-bay structures was made. The results clearly show that the generic frames used in the estimation of acceleration demands on NSCs mounted on buildings in the inelastic range are capable of adequately representing the results from multi-bay frames. The R_{acc} behavior is well captured by the models used in the study and they are similar in behavior to the results obtained by other researchers in earlier studies. Greater deviation in elastic a_p values is seen for the SAC LA9-M1 frame which has 2% damping ratio, while all the other frames have 5% damping ratio. Although the

number of stories of the companion generic frames is different from that of multi-bay frames used in this study, the R_{acc} values from the actual multi-bay models and the predicted equations are very close especially when considering the range of parameters used while developing the models.

Chapter 5: Summary and Conclusions

5.1 SUMMARY

The major objective of the study presented in this dissertation was to develop a methodology for the quantification of acceleration demands on elastic nonstructural components (NSCs) mounted on elastic and inelastic moment-resisting frame structures. An understanding of the important attributes that characterize the acceleration demands was necessary before such an attempt could be made. Hence, the first part of this study focused on identifying the relevant parameters that influence the response of acceleration-sensitive NSCs. The second part was focused on developing a methodology to estimate the acceleration demands on NSCs mounted on inelastic frame structures.

Moment-resisting frame structures with 3, 6, 9, 12, 15 or 18 stories (N) and the same mass at all floor levels were utilized. Two frames were used for a given number of stories with the fundamental period tuned to represent stiff ($T_{B1} = 0.1N$) and flexible ($T_{B1} = 0.2N$) behavior (12 frames in total) and thus the frames had fundamental periods varying from 0.3 sec. to 3.6 sec. The strength of the buildings had been tuned to represent elastic and eight levels of inelastic behavior (RI values from 0.25 to 8). The NSCs were characterized by elastic SDOF systems with single point of attachment mounted on different floor locations of the building and had damping ratios of 0.01%, 1%, 2%, and 5%. The NSCs were assumed to have very

small masses when compared to the supporting structure and hence their responses could be decoupled and the floor response spectrum method was used.

The parameters that were evaluated in order to identify those that are most relevant for the response of acceleration-sensitive NSCs included: modal periods of the supporting structure, location of the NSCs in the building, height of the supporting structure, stiffness distribution of the supporting structure, strength of the supporting structure, and damping ratio of NSCs. The results showed that the maximum acceleration response of NSCs generally occurs when the period of the NSC matches the first or higher modal periods of the supporting structure. Moreover, a reliable quantification and evaluation of FRS for seismic design should address the changes in spectral shape due to the location of the NSC in the structure. For a given fundamental period and relative height, moderate- and long-period frame structures exhibit floor response spectral shapes that are weakly dependent on the number of stories. When the structure behaves inelastically, the acceleration demands on NSCs get reduced. Hence, the nonlinear action of the building is beneficial to NSCs under most situations. The results of this evaluation also concluded that current U.S. seismic design provisions for nonstructural components are in several cases nonconservative.

A methodology to estimate peak acceleration demands for NSCs mounted on inelastic primary structures was developed during the second part of this study. To facilitate this process, a parameter called acceleration response modification factor (R_{acc}) was introduced. This parameter was defined as the floor response spectrum (FRS) for linear elastic structural response normalized by the FRS for a certain level of inelastic structural behavior in the primary structure. Thus, the R_{acc} factor can be

used to scale the FRS for elastic primary structures or component amplification factor values to obtain the FRS for inelastic primary structures. Although the component amplification factors for NSCs whose periods match the first or higher modal period regions of supporting structure are provided for all the frames in this study at different locations in the building, the elastic FRS results from any study (using a different methodology) can be used in conjunction with R_{acc} to obtain the inelastic FRS.

The properties of R_{acc} allow it to be split into three different zones namely long-period, fundamental-period and short-period regions with single R_{acc} values representing the maximum deamplification of FRS in these regions. A sensitivity study on the effect of the modal properties of the supporting structure, height of the frames, location of the NSC in the building, damping ratio of the NSCs, fundamental periods of the building, and level of inelastic behavior of the building, was undertaken to establish the factors affecting R_{acc} in the fundamental-period and short-period regions. Based on the results, a one-parameter model based on level of inelasticity of the supporting structure (*RI*) and a two-parameter model based on both *RI* and T_{B1} were proposed for predicting the R_{acc} values in the fundamental-period, and short-period regions of FRS, respectively. Due to the difference in behavior of the short-period frames ($T_{B1} \le 0.6$ sec.) to that of medium to long period frames, the statistical models were applicable to the region from $0.6 \text{ sec.} \le T_{B1} \le 2.4$ sec. The results for short-period, 3-story frames were presented separately.

An evaluation of the adequacy of generic frames and proposed statistical models to predict / quantify the acceleration demands for NSCs mounted on real multi-bay structures was performed. The results clearly showed that the generic

frames used in the estimation of acceleration demands on NSCs mounted on buildings in the inelastic range are capable of adequately representing the FRS results from multi-bay frames. The R_{acc} values at different locations and for different ratios of component damping falling within 20% of the median values predicted by the statistical models.

5.2 CONCLUSIONS

The conclusions of this study fall into two categories namely general observations and specific results for the current study.

5.2.1 General

- The understanding and quantification of peak acceleration demands experienced by moment-resisting frames and NSCs provides much needed information to develop improved models for seismic design and performance assessment of NSCs in buildings. Such models are necessary in order to implement simple, yet reliable methodologies to estimate and minimize (a) dollar losses and (b) the risk posed by loss of lives and/or injuries due to failure of NSCs.
- A benefit of allowing the primary structure to dissipate energy through inelastic action is the reduction in the maximum acceleration demands experienced by the NSCs. This implies that NSCs and their attachments to the primary structure can be designed based on smaller forces, which translates into more economical connections or attachments. The reduction of peak acceleration demands is larger around the modal periods of the supporting structure. When a building is designed to behave inelastically, great benefit can be achieved by tuning the period of

vibration of the NSC to match that of fundamental period of the building (i.e. flexible NSCs or flexibly attached NSCs). However, this benefit can turn to a detriment when the period of the NSC is in between the higher modal periods of the building (stiff to very stiff NSCs). Due to difficulties in computing the higher modal periods of the primary structure or due to period elongation when the NSC acts inelastically, the period of the NSC may be positioned in one of the narrow short-period regions of FRS wherein the demands on NSCs are amplified due to inelastic action of the building.

- The reduction/amplification in peak acceleration demands due to yielding of the supporting structure depends primarily on the location of NSC in the building, fundamental period (T_{B1}), damping ratio of the NSC, and the amount of inelasticity of the supporting structure (relative intensity). In general, for moderate to long period structures, the demands are strongly dependent on T_{B1} and not on the number of stories of the building (N). The above results are applicable only to regular moment-resisting framed structures. However, it is anticipated that the parameters identified in this study will significantly affect the acceleration demands regardless of the type of later-load resisting system used in the building. Thus, these results can be used to narrow the range of parameters to be considered in future numerical and/or experimental studies that attempt to estimate the NSC acceleration demands on different systems (e.g. dual systems, structural walls, etc.).
- A structural design that distributes damage across all members is better than a design that causes concentration of inelasticity, especially from the perspective of

reducing the seismic demands on acceleration-sensitive NSCs. Some of the old buildings designed according to outdated code provisions have the potential to develop weak-story mechanisms (e.g., tuck-under parking), which implies concentration of inelasticity in one or a few stories. This study shows that these buildings can experience severe amplification in acceleration demands on NSCs due to inelastic action of the buildings and that the amplification is more predominant for bottom stories. In such situations, the NSCs and their attachments at the first-floor are more prone for damage or to cause injuries to building occupants. This highlights the need to conduct seismic retrofitting of existing infrastructure (e.g., old reinforced concrete building) to mitigate not only structural but also nonstructural damage.

- The current code provisions in the United States provide component amplification factor (a_p) values that are not a function of the location of the NSC in the structure. The location of the NSC is considered only when applying the linear scaling for short period spectral acceleration for 5% damping (S_{DS}) while computing the seismic design forces (primarily to account for the PFA variation along height). The results of this study clearly establish the strong influence that location of NSC (in the building) has on both elastic and inelastic a_p values. Hence, a_p and R_{acc} values are provided as a function of relative location in the building. For accurate estimation of seismic design forces on acceleration-sensitive nonstructural components, a_p or other equivalent seismic coefficients should consider location of NSC in the building.

- Component amplification factors for elastic frames are generally larger at higher floors. The corresponding R_{acc} values for inelastic action of the building that represent the reduction in FRS are also larger at higher floors (near the roof). Thus, for moderate levels of inelasticity of the supporting structure ($RI \leq 4.0$), the a_p*(inelastic)* values are more uniformly distributed along the height. For larger levels of inelasticity ($RI > 4.0$), the NSCs at bottom stories experience more acceleration demands than the components at higher locations. These observations also highlight the importance of the location of NSCs on the quantification/estimation of damage to NSCs in buildings.
- This study uses the FRS method wherein the equipment response is decoupled from the behavior of the building and thus the equipment does not offer any dynamic feedback to the building. Results from the study show that this assumption is valid when the mass of the NSCs are in the range of 0.01% to 1% of the mass of the building.
- The major portion of the study uses far-field ground motions that are of broadband type seismic input. When subjected to narrow-band input characteristic of near-fault forward directivity ground motions, the R_{acc} values show similar behavior in all regions of the FRS and also along the height of the building. The R_{acc} methodology is very useful in the sense that it allows for future work on developing a unified methodology based on same principles that is applicable to different ground motions with different frequency content.
- The conclusions and recommendations are based on the results of large number of buildings (number of stories from 3 to 18, stiff and flexible behavior, different

fundamental periods, etc.), a set of 40 far-field ground motions and NSCs with damping values of 0.01%, 1%, 2% and 5%. The recommendations for R_{acc} proposed in this study have been validated with the results of multi-bay frames (SAC LA9-M1 building and Van Nuys building). The results are consistent across a large number of variables. The large amount of data and the statistical results generated as part of the current study can be used in future works to develop a methodology to provide a probabilistic quantification of peak acceleration demands for NSCs. (i.e., generation of peak acceleration hazard curves for various sites).

5.2.2 Specific Results

Peak Acceleration Demands

- The variation of peak floor accelerations (PFA) with height is strongly dependent on the fundamental period of the supporting structure and its strength. Moreover, for a given fundamental period, the variation of PFA with respect to the relative height of the structure is weakly dependent on the number of stories.
- NSC acceleration demands in the fundamental period region are generally higher at the top stories of the frame. However, the acceleration demands at higher modal period region are weakly dependent on the location of the NSCs.
- For a given T_{B1} and relative height, moderate- and long-period frame structures exhibit floor response spectral shapes that are weakly dependent on the number of stories.
- A benefit of allowing the primary structure to dissipate energy through inelastic action is the reduction in the maximum acceleration demands experienced by the

NSCs. This implies that NSCs and their attachments to the primary structure can be designed based on smaller forces, which translates into more economical connections or attachments. This deamplification of component accelerations with a decrease in the strength of the supporting structure is more pronounced for component acceleration values near the modal periods of the supporting structure.

- The maximum amplifications in acceleration demands around the modal periods when compared to the demands obtained for NSCs with 5% component damping ratio are of the order of 1.5 for 2% damping and 2 to 3 for 0.01% damping.
- Although simple and rational, the design provisions in the current building codes (for the estimation of acceleration demands on NSCs) do not account for the inelastic action of the supporting structure and also are not adequate in representing the acceleration demands in the short-period region of the FRS for both elastic and inelastic buildings. Moreover, the variation of PFA along the height of the frame is mostly nonlinear. For longer period structures, the PFA values provided in current provisions are conservative.

Acceleration Response Modification Factor

- The R_{acc} factor provides an effective way of estimating the peak acceleration demands on NSCs mounted on inelastic frames from the elastic FRS. The properties of the R_{acc} allow the entire FRS to be grouped into three regions namely, long-period ($T_C / T_{B1} > 1.5$), fundamental-period ($0.5 \le T_C / T_{B1} \le 1.5$) and short-period ($T_C / T_{B1} < 0.5$) regions thus overcoming the difficulties in coming up with a single R_{acc} factor expression for all periods of NSC. The R_{acc} behavior has

been consistent in the different regions and along the height of all building models. While the inelastic FRS in the long-period region are close to the elastic FRS values, R_{acc1} and $(R_{acc\text{-}HF})_{max}$ values are characteristic of the deamplification experienced in the fundamental-period and short-period regions respectively. These R_{acc} values can be combined with the R_p factor in the current codes, so that both the nonlinearity of the equipment and supporting structures are addressed.

- The internal resonance of higher modes of nonlinear oscillations in the short-period (high frequency) region tends to reduce the values of R_{acci} at higher modes. This sometimes results in R_{acc} values less than one, which means that the acceleration demands due to inelastic action of the supporting structure are higher than the demands on NSCs mounted on corresponding buildings in the elastic domain.
- The R_{acc} values for medium to long fundamental period frames are weakly dependent on the number of stories of the supporting structure.
- The general shape of R_{acc} variation along height is maintained for all component damping ratios in fundamental-period and short-period regions of FRS. Smaller component damping ratios are more prone to producing $R_{acc} < 1$ in narrow regions of FRS in the short-period region.
- R_{acc1} values for medium to long fundamental period buildings are weakly dependent on T_{B1}. However, $(R_{acc\text{-}HF})_{max}$ values increase with the fundamental period of the building.
- Increase in the level of inelastic behavior of the supporting structure (*RI*) reduces the acceleration demands on the NSCs in the fundamental-period and short-period

regions of FRS. The increase of R_{acc} values for a corresponding increase in *RI* values is linear at lower *RI* values. The deviation from the straight line behavior is larger at higher *RI* values.

- An evaluation of the adequacy of generic frames and proposed statistical models to predict / quantify the acceleration demands for NSCs mounted on real multi-bay structures showed that R_{acc} behavior is well captured by the models used in the study. Greater deviation in elastic a_p values is seen for the SAC LA9-M1 frame which has 2% damping ratio, while all the other frames have 5% damping ratio. Although, the validation models have different number of stories as the corresponding generic frames with T_{B1} values close to that of multi-bay frames, the R_{acc} values at the fundamental-period and short-period regions of the FRS predicted by the statistical models fall within 20% of the actual R_{acc} values.

5.2.3 Limitation of the Current Study and Scope for Future Work

The results of the current study are applicable to regular moment-resisting frame structures. The applicability of the current results to NSCs mounted on regular and irregular (both plan and elevation) wall-type structures or braced-frames need to be explored. The decoupling approach used in this study for generating the FRS is applicable only for light equipment. Although a separate computer program that accounts for the interaction between NSCs and buildings was developed as a part of this study, only limited simulations were carried out. Future studies should be attempted to quantify the reduction or increase of NSC acceleration demands due to interaction effects. The current study idealizes the NSCs as elastic SDOF systems with single point of attachment. Hence, future studies should address the estimation

of acceleration demands on NSC with multiple attachments in the building. Studies can also be attempted to arrive at recommendations for R_{acc} factors for buildings subjected near-fault ground motions. A preliminary study conducted as a part of this dissertation explored the R_{acc} behavior for buildings subjected to a set of 64 near-fault forward directivity ground motions. The results of that study are very promising as the R_{acc} behavior is similar to that of results in this dissertation (far-field ground motions).

Appendices

Appendix I – Dynamic Interaction Effects on the Response of NSCs

GENERAL

The FRS approach adopted in this dissertation is applicable to light equipment, which constitute most of the architectural components and equipment in a building. The dynamic responses of these light secondary systems, do not affect the vibration of the building. Thus, the feedback between the NSCs and the building, namely the dynamic interaction effect is not considered. However, some of the heavy equipments and architectural systems that can still be classified as NSCs offer feedback that need to be accounted for in the seismic demand evaluation of such components. The new challenges that occur in evaluating the acceleration demands of these heavy NSCs are referred here as dynamic interaction studies. In most of the interaction cases, the damping ratios of the building and the NSC do not match, which results in nonclassical damping of the combined system. Moreover, when there is tuning between the frequencies of the primary and the secondary system, the spatial coupling effect also needs to be addressed. The purpose of this appendix is to assess to what extent the results based on the FRS method used in this study can be applied to problems that involve dynamic interaction.

INTRODUCTION

Interaction effects are very important when the ratio of the mass of the NSC to the mass of the supporting structure is significant. For example, some researchers have recommended that the coupling between the component and the primary structure need not be considered when the mass of the NSC as a percentage of the total mass of the supporting structure is less than 0.01 (Amin et al. 1971; Singh and Ang 1974). Other studies, state that this interaction may be important even when the nonstructural-to-structural mass ratio is as low as 0.001 (Toro et al. 1989).

Although researchers over the years attempted to study the interaction behavior for the entire range of parameters in the inelastic domain, the practicality of evaluating of the dynamic properties of the combined system several times, made it exigent. Perturbation (Sackman and Kelly 1979; Sackman et al. 1983; Igusa and Derkiureghian 1985; 1992) and stochastic (Saudy et al. 1994b; 1994a; 1995; Dey and Gupta 1998) methods have attempted a simple characterization of the complex behavior of the combined system by means of deriving physically meaningful parameters with closed-form expressions (Gupta 1990; Dey and Gupta 1998). Detailed analysis of full building models have been limited to smaller set of analysis models and are usually used as validation for the mathematical / random-vibration based methods. The new methodology proposed in this dissertation evaluates peak component acceleration (PCA) demands for light NSCs; thus, dynamic interaction effects can be neglected. However, the objective of this appendix is to understand the mass ratio range wherein the decoupling assumptions are valid.

METHODOLOGY AND RESULTS

To study the interaction effects, the frames used in this dissertation were modified to accommodate a NSC element at a single floor level. The NSC element is modeled as an elastic SDOF system composed of point mass m_s, a linear elastic spring and a viscous dashpot damper. Separate building models were created with individual NSCs at specific floor levels of interest. This procedure was repeated to generate interaction models for both stiff and flexible frames of different story heights with NSCs mounted at the floor level of interest.

Depending on the damping ratio of the NSC, the coupled primary-secondary system may be classically or non-classically damped. Only one value of damping (2%) is considered for NSCs. Thus the combined system is non-classically damped. For different mass ratios, the interaction spectra are developed. Fig. I.1 shows the difference in the component amplification factor values for different mass levels for an elastic 9-story frame with first mode period of 0.9 sec. It can be observed that an increase in the mass value of the NSC, reduces the a_p values. Hence the decoupled analyses adopted in the previous tasks of this dissertation, produce conservative results. Greater change in a_p values are observed in the mass range of 0.01% to 1%. This is the range where the interaction effects are negligible to moderate. Based on these results it is apparent that when the mass of the NSC, exceeds 1%, the results are heavily influenced by interaction and thus the interaction effects should not be neglected in the analysis.

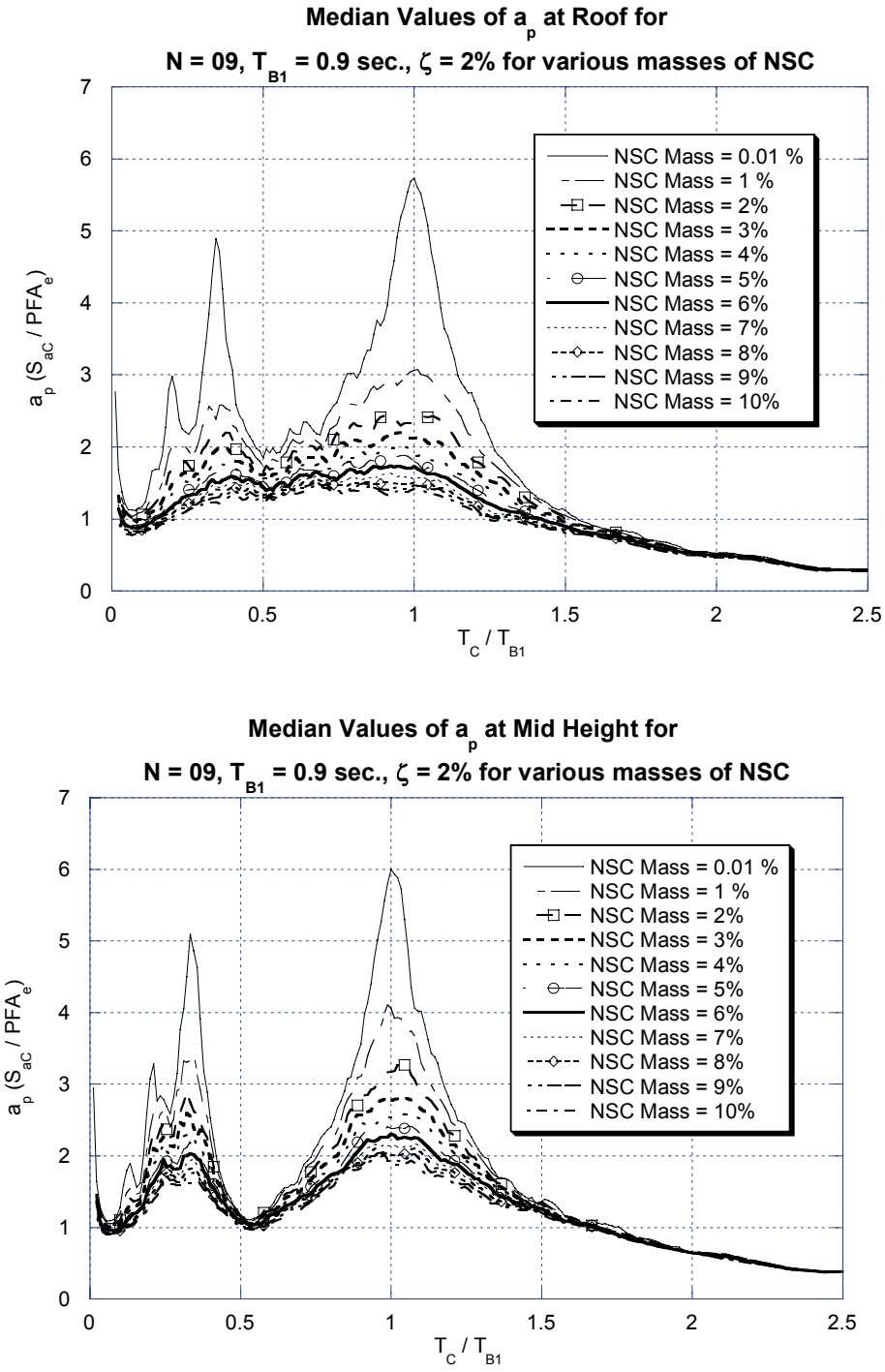

Figure I.1 Median values of component amplification factor for different mass levels for an elastic frame at roof and mid height location

SUMMARY

This appendix attempted to identify the broader mass ratio range in which interaction plays a role. The results show that the main assumption namely the decoupling of the supporting structure and NSCs used in this dissertation is valid when the mass ratio is in the range of 0.01% to 1%.

Appendix II –FRS Amplification due to Localized Yielding of Supporting Structure

GENERAL

The frames used in this dissertation are designed such that simultaneous yielding is attained under a parabolic NEHRP load pattern ($k = 2$). This tuning of strength distribution to a particular lateral load pattern allows a clear demarcation of pre and post-yield states of the supporting structure. Previous research efforts have used different strength distributions and some studies have concluded that distribution of nonlinearity in the structure can have significant impact on the equipment behavior (Sewell et al. 1987; Villaverde 2004). Studies on Nuclear Power Plant structures have pointed out that FRS can increase in magnitude due to yielding of the supporting structure and this effect is more pronounced for concentrated nonlinearity wherein the inelastic action is experience / allowed only in a small region of the building (e.g. one story in a multi-story building). Although FRS values showed some amplification in the high frequency region for the building models used in this dissertation, this effect was pronounced mostly for equipment with very low damping values. This appendix aims to investigate the FRS amplification for regular moment resisting frames by using concentrated inelasticity models wherein the yielding of the building is allowed only at the bottom floor (Weak Story or WS).

DESCRIPTION OF THE MODELS

The Weak Story (WS) models have a strength discontinuity in the first story. In this model the member strengths are tuned so that a story mechanism develops in the first story and all other stories remain elastic. The stiffness of the individual members of each building model has been changed so that first mode period and the shape match with that of the corresponding beam-hinge frames used in this study. All the other properties of the building namely 5% Raleigh damping, peak-oriented hysteretic behavior, 3% strain-hardening, and P-Delta loads are kept the same as original models.

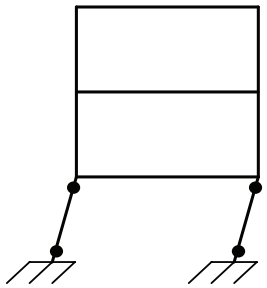

Figure II.1 Weak story (WS) model with the column hinges

Six WS models with number of stories, N, equal to 3, 6, and 9, and fundamental periods, T_{B1}, of $0.1N$ (stiff frames) and $0.2N$ (flexible frames) were generated. The mode shapes of these building models are presented in Fig. II.2 and II.3. Table II-1 presents the first three modal periods of these building models. The WS models are subjected to the set of 40 ordinary ground motions used in this dissertation.

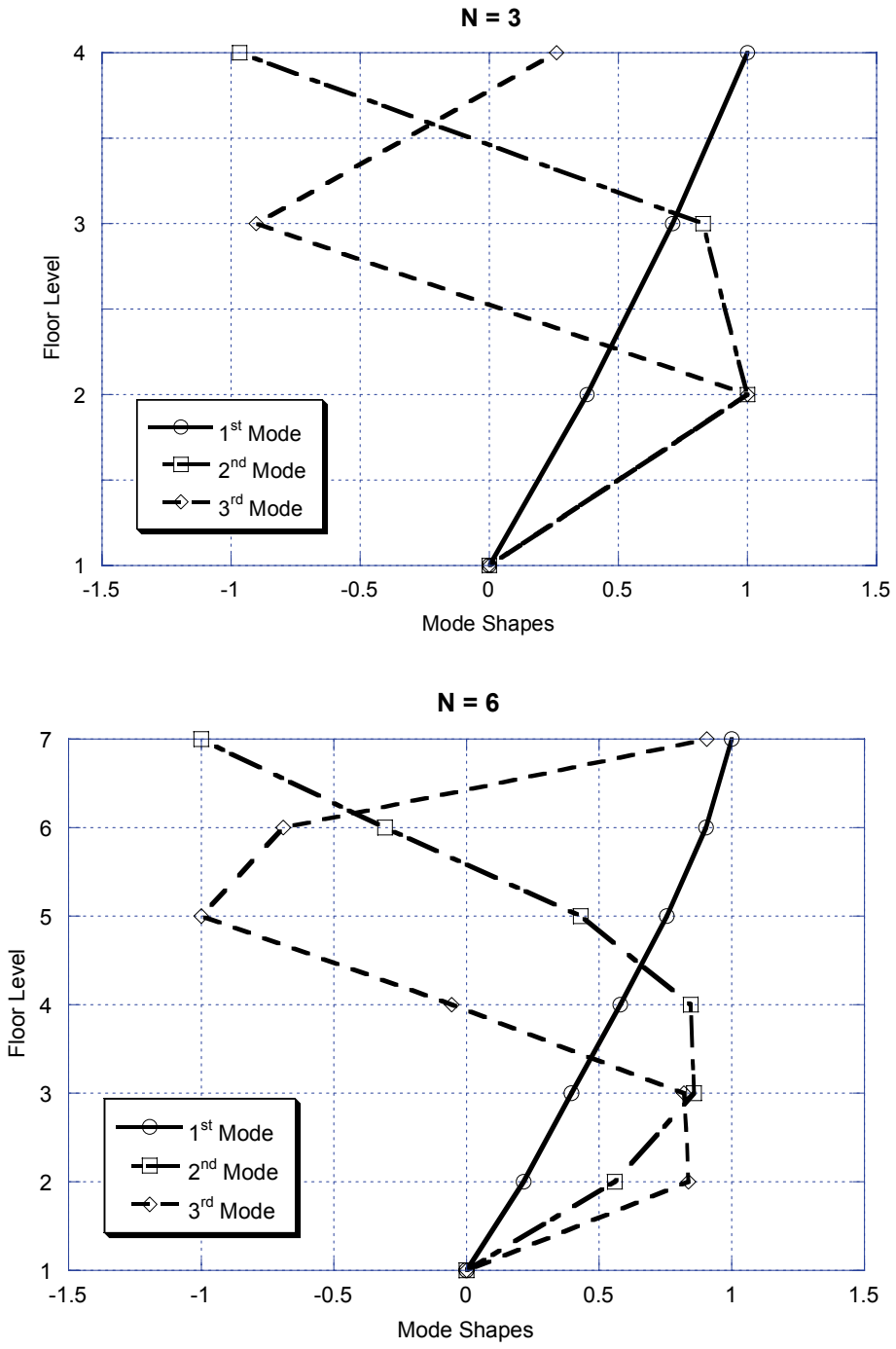

Figure II.2 Mode shapes of 3- and 6-story WS building models

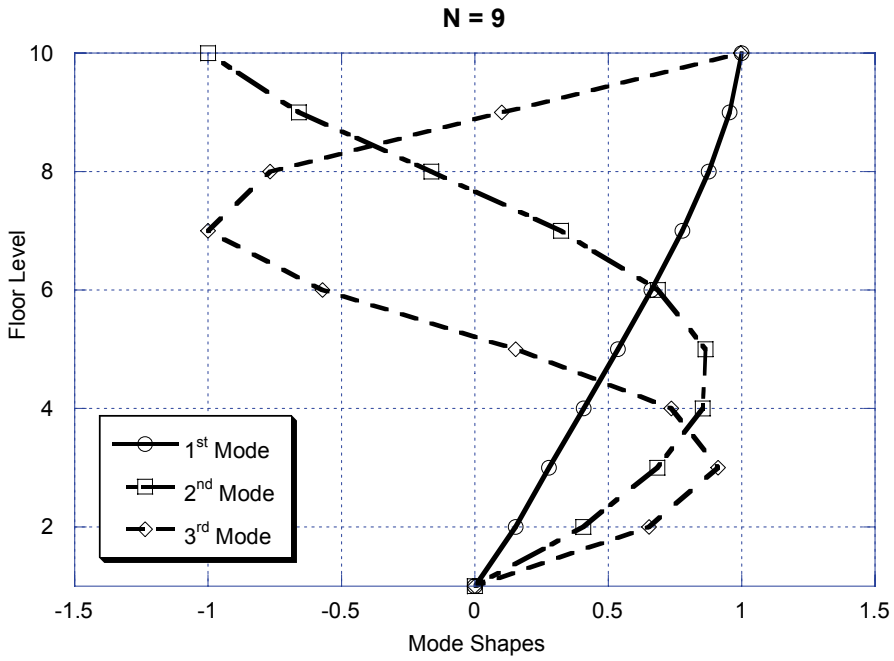

Figure II.3 Mode shapes of 9-story WS building model

# Stories	Stiff frame periods (sec.)			Flexible frame periods (sec.)		
	T_{B1}	T_{B2}	T_{B3}	T_{B1}	T_{B2}	T_{B3}
3	0.300	0.119	0.077	0.600	0.237	0.153
6	0.600	0.223	0.140	1.200	0.446	0.280
9	0.900	0.327	0.201	1.800	0.655	0.403

Table II-1 Modal periods of weak story models

RESULTS

Fig II.4 shows the FRS values at the three locations of the supporting structure namely roof, mid height, and bottom third location respectively. The results are shown for N = 3 and N = 6 stiff frame for RI values of 0.25 (elastic) and 2.0

(inelastic). It should be noted that abscissa for this figure is the frequency of the NSC in Hertz. It can be seen that for the 0.3 sec. frame around the frequency of 7.5 Hz, the inelastic FRS values are higher than the elastic FRS values at all three locations in the building. Moreover at frequencies higher than 10 Hz, the inelastic FRS values at mid-height, and bottom-third location are higher than that of elastic FRS values. For the 0.6 sec. frame at frequencies around 7 Hz, the inelastic FRS values are higher. The amplification in FRS can also be observed for very low-frequency region (long-period) region. These FRS amplifications are better represented by the R_{acc} plots. Fig. II.5 shows the R_{acc} values for the 3- and 6-story stiff frames for RI values of 2.0 and NSC damping values of 1%. It can be seen that the FRS amplification (denoted by $R_{acc} < 1.0$) occurs predominantly in the low period and long period regions. In the long-period region, the R_{acc} values are nearly constant; however, in the short-period region, the FRS amplification occurs around the higher modal periods. The minimum R_{acc} in the low period region and the region till the fundamental period of the building can be represented by the $(R_{acc\text{-}HF})_{min}$ parameter (see equation (II.1)).

$$(R_{acc-HF})_{\min} = \min(R_{acc}) \text{ in the interval } 0 \le T_C \le 0.95T_{B1} \qquad \text{(II.1)}$$

Fig. II.6, II.7 and II.8 show the variation of $(R_{acc\text{-}HF})_{min}$ parameter along the height for all the six frames used in this study for different component damping rations and $RI = 2$. It can be seen that the FRS amplification is more predominant in the bottom stories for all the six stiff and flexible frames used in this study. Lower values of component damping ratio produce more amplification.

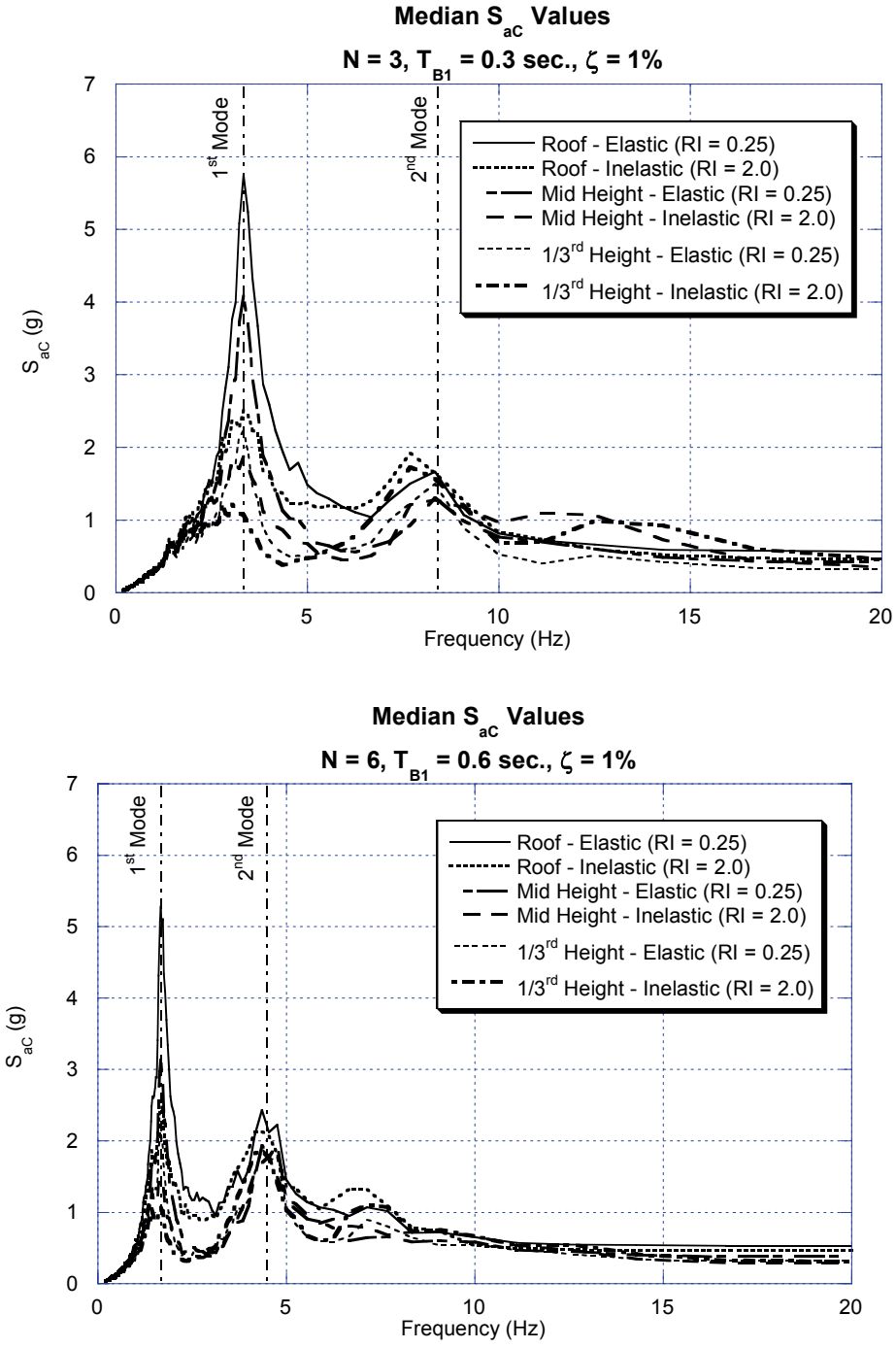

Figure II.4 Elastic and Inelastic (*RI = 2.0*) FRS of *N = 3*, and *N = 6*, WS models with component damping ratio of 1%

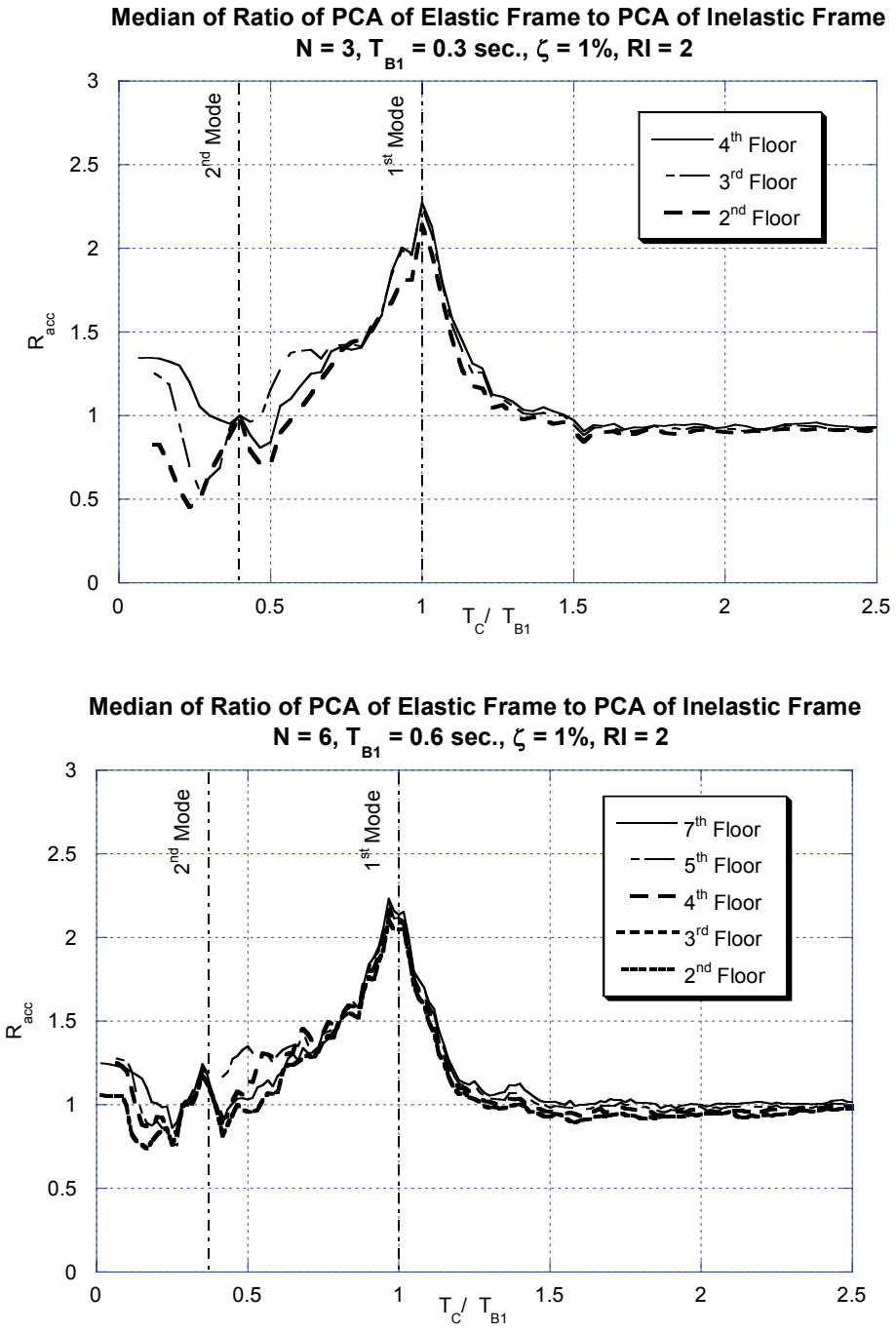

Figure II.5 R_{acc} values for $N = 3$, and $N = 6$, WS models with component damping ratio of 1%

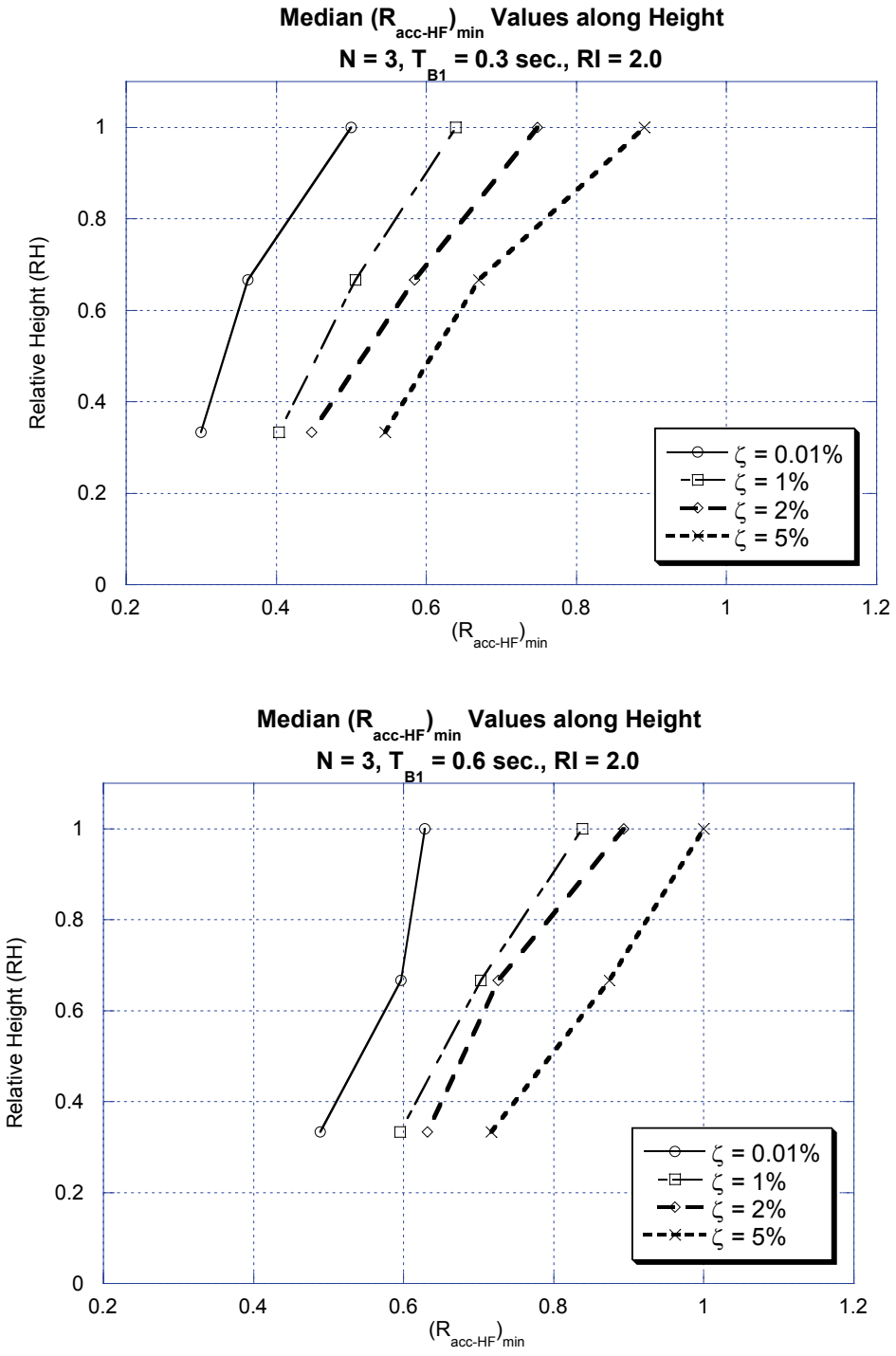

Figure II.6 Minimum R_{acc} values in the low period region for 3-story frames

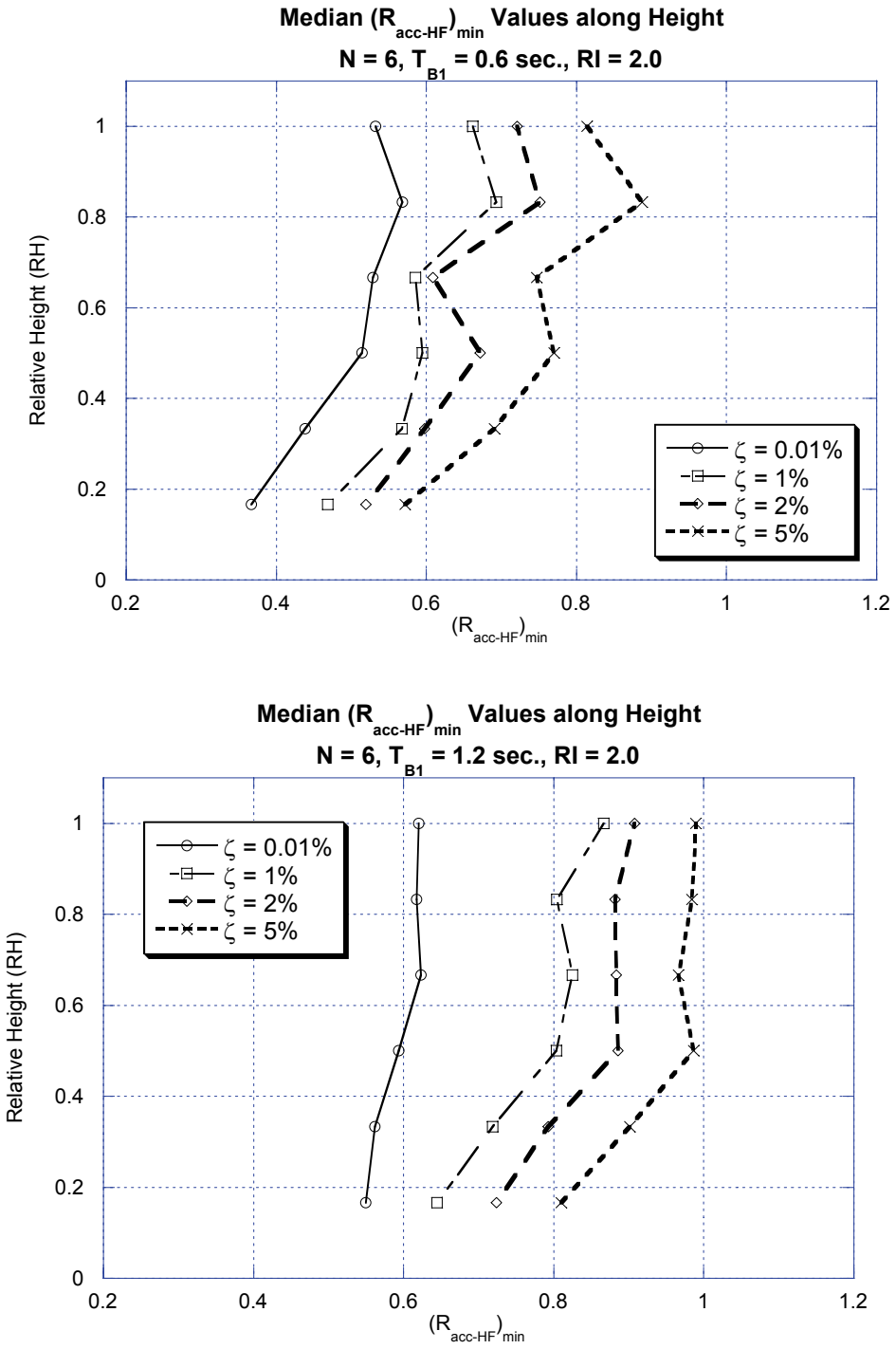

Figure II.7 Minimum R_{acc} values in the low period region for 6-story frames

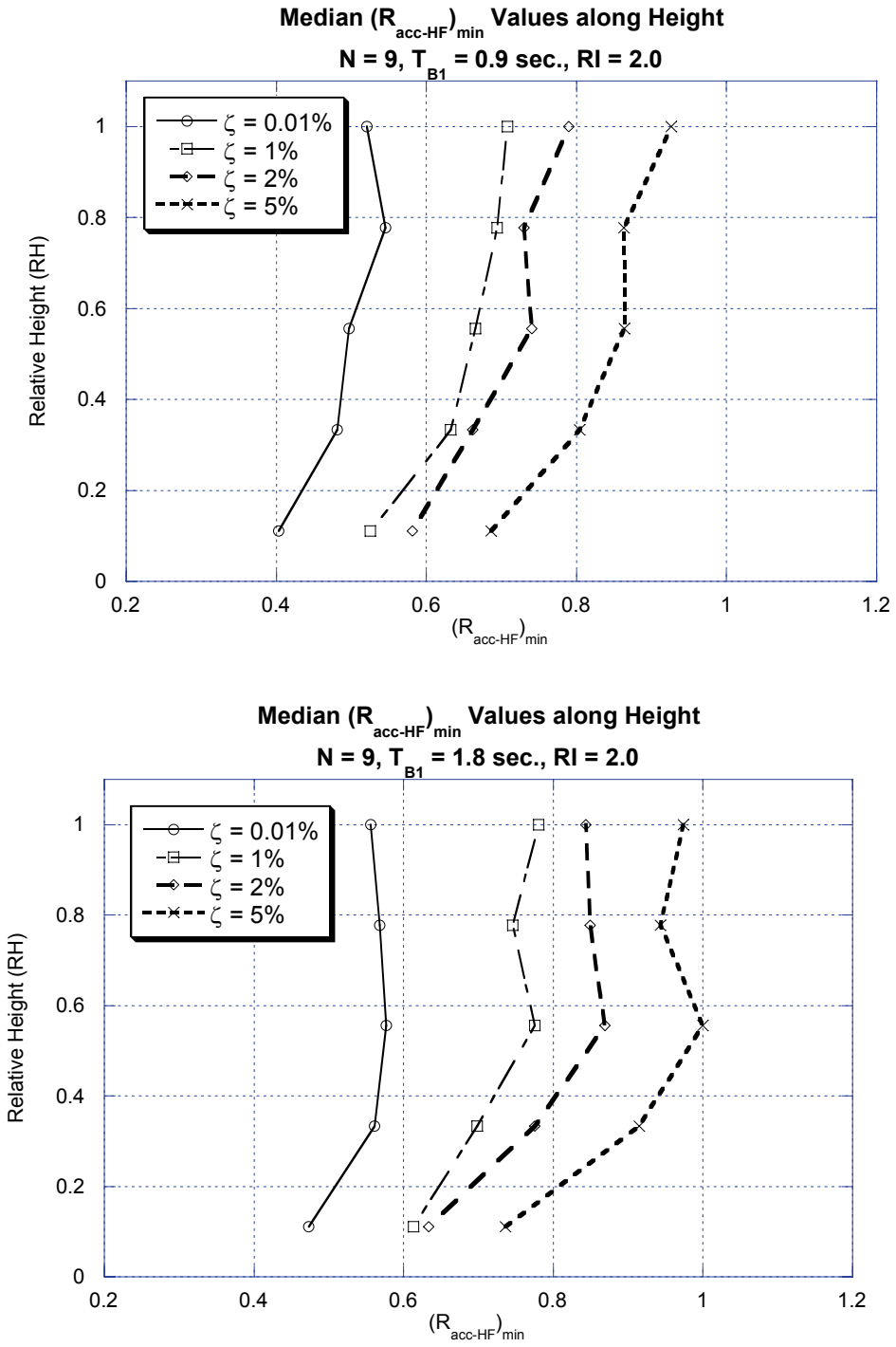

Figure II.8 Minimum R_{acc} values in the low period region for 9-story frames

These results are consistent for all the six frames used in this study. Moreover FRS amplification is higher for short-period frames. For frames with same stories, stiff frames produced greater FRS amplification than flexible frames.

SUMMARY

This appendix evaluated the effect of concentrated inelasticity on the FRS amplification when the building behaves inelastically. This is achieved by developing six new building models (3-, 6- and 9-story stiff/flexible systems) wherein plastification is allowed only at the first story of the building. The results obtained on six building models for the set of 40 far-field ground motions show that FRS amplification, originally reported for Nuclear Power Plant structures, consistently occurs in the low period region of these building models. FRS amplification is more prominent for frames with concentrated inelasticity than that for the original set of frames with distributed inelasticity. The results can be summarized as:

1. FRS amplification is more predominant at the bottom stories than the top stories.
2. Smaller values of NSC damping ratio produce more amplification.
3. FRS amplification for stiffer frames is greater than that of flexible frames.
4. With an increase in period and the number of stories, the magnitude of FRS amplification reduces.

Appendix III – Behavior of NSCs Subjected to Near Fault Ground Motions

Most results in this appendix have been reproduced from the paper presented in 1st European Conference on Earthquake Engineering and Seismology, Geneva, Switzerland (Sankaranarayanan and Medina 2006).

GENERAL

The response of the buildings located within 15 km of the rupturing fault, is distinctly different from the behavior of the buildings located far from the rupture zone. These buildings are subjected to a large amplitude velocity pulse that imparts a large amount of energy to a structure within a short period of time. The damage is often incurred during one or two cycles of severe inelastic deformation that are caused by the sudden influx of energy associated with the velocity pulse. Although the response of building had been evaluated by researchers in the past and present (Iwan 1997; Anderson et al. 1999; Alavi and Krawinkler 2001; Chopra and Chintanapakdee 2001), there have been no significant studies reported in the literature for the demand estimation of acceleration-sensitive NSCs mounted on buildings subjected to near-fault ground motions. It is necessary to mitigate the above by quantifying the acceleration demands of the NSCs when subjected to these special near-fault forward-directivity ground motions vis-à-vis the ordinary / far-field records. This appendix is aimed to sever as a lead up to future work on this topic.

INTRODUCTION

The near-field ground motions when rotated to directions parallel and perpendicular to the strike of the fault yield the "fault-parallel" and "fault-normal" components of the ground motion. The fault-normal component has the distinctive velocity pulse and hence causes the most damage to the structures. Somerville (Somerville et al. 1997; Somerville 2003; Somerville and Graves 2003) identified that this phenomenon is caused by the superposition of seismic shear waves in the direction of the rupture propagation when the rupture velocity is comparable to the shear wave velocity. As a result, at sites located near the fault and in the direction of the rupture propagation, most of the seismic energy arrives in a single large pulse of motion. The radiation pattern of the shear waves causes the pulse to be oriented in the fault-normal direction with lower intensity motions in the fault-parallel direction. Thus, the orientation of the building with respect to fault direction may determine the severity of the ground motion that the structure and NSC in turn will experience.

GROUND MOTIONS AND BUILDING MODELS

The current study uses a set of 64 recorded near-fault ground motions recorded on both soil and rock sites. The fault-normal component of near-fault ground motions with forward directivity is more severe than the fault-parallel component and hence this study uses only the fault-normal component. Fifty-nine of these records are from PEER Strong Motion Database (PEER 2003) and five are from the set of records used by Somerville (Somerville et al. 1997). For this study, only

fault-normal components are utilized. Table III-1 summarizes the main properties of the records along with their pulse periods (T_p) (Fu 2005).

Earthquake	M_w	Station	T_p (s)	Earthquake	M_w	Station	T_p (s)
Parkfield	6.1	Station 2 (Cholame #2)	1.88	Whitter Narrows	6	Santa Fe Springs – E Joslin	0.7
	6.1	Temblor pre - 1969	0.39	Coalinga	6.4	Pleasant Valley P.P.-yard	0.7
Morgan Hill	6.2	Anderson Dam	0.49	San Fernando	6.6	Pacoima dam	1.38
		Gilroy Array # 6	1.04	Northridge	6.7	Canoga Park-Topanga Can	2.02
		Coyote Lake Dam	0.76			Canyon Cty-W Lost Cany	1.89
Imperial Valley	6.5	Brawley Airport	3.43			Jensen Filter Plant	2.83
		EC County Center FF	4.1			Newhall – Fire Station	0.93
		EC Meloland Overpass FF	2.93			Rinaldi Receiving	1.16
		El Centro Array # 3	4.55			Sepulveda VA	2.99
		El Centro Array # 4	4.18			Sylmar Converter	2.88
		El Centro Array # 5	3.66			Sylmar Converter East	3.05
		El Centro Array # 6	3.63			Sylmar Olive View	2.53
		El Centro Array # 7	3.57			Newhall-W.Pico Canyon	2.18
		El Centro Array # 8	4.67			Pacoima Dam Downstreet	0.48
		El Centro Array # 10	4.01			Pacoima Ragel Canyon	0.72
		El Centro Differential Array	4.22			LA Dam	1.42
Superstition Hills	6.7	Holtville Post Office	4.33	Nahanni	6.8	Site 1	3.25
		El Centro Imp. Co. Cent	2.41			Site 2	1.2
		Parachute Test site	2.12	Loma Prieta	6.9	Gilroy-Historic Bldg.	1.54
Erzican	6.9	Erzican	2.31			Gilroy Array #1	4.24
Kobe	6.9	KJMA	0.86			Gilroy Array #2	1.43
		Port Island	2.34			Gilroy Array #3	1.79
		Takatori	2.11			Gilroy Array #4	1.37
		JMA	0.9			Gilroy-Gavilan Coll.	1.77
Landers	7.3	Lucerne Valley	5.54			Saratoga-Aloha Ave.	2.25
Kocaeli	7.4	Duzce	4.59			Saratoga-W Valley Coll.	2.16
		Gebze	6.47			Los Gatos	3.21
		Yarimca	4.27			Lexington Dam	1.81
N. Palm Springs	6	North Palm Springs	1.26	Chi-Chi	7.6	TCU075	5.01
		Desert Hot Sprongs	1.38			TCU129	7.41
		Whitewater Trout Farm	0.63			TCU065	4.73
Whitter Narrows	6	Bell Gardens – Jaboneria	0.71			TCU076	4.15

Table III-1 Fault-normal, near-fault ground motions used in this study

The ground motions have a moment magnitude (M_w) that varies from 6.0 to 7.6, and closest distances to the rupture fault area in the range of 0.1km to 17.0 km.

The behavior of structures subjected to near-fault records depend primarily on the pulse period. The behavior depends on whether the pulse period is greater or lesser when compared to the fundamental period of the building (Alavi and Krawinkler 2001). Ground motion bins are created for each building model based on the ratio of fundamental modal period of the building (T_{B1}) to the pulse period such that only ground motions that correspond to the range $0.35 \le T_{B1} / T_p \le 1.0$ are used. Within this period range the salient characteristics of near-fault ground motions can be represented by simple equivalent pulses and hence the ground motions in this range are grouped into bins. The six structural models namely 3, 6, 9, 12, 15, and 18-story frames explained in the previous chapters have been used in this study. For each period and number of stories, frames with two different base shear strength values are designed – one corresponding to elastic behavior ($RI = 0.25$) and the other one corresponding to moderately inelastic behavior ($RI = 4$).

RESULTS

The peak floor acceleration demands and the floor response spectra characteristics for near-fault forward directivity ground motions are similar to that of the results presented in chapters 2 and 3 for far-field ground motions. Detailed information on these results is available in references (Sankaranarayanan and Medina 2006). The results for component amplification factors (a_p) and acceleration response modification factors (R_{acc}) are presented in this section.

Figure III.1 shows a plot of the median a_p values at the roof level for all the stiff frames used in this study ($T_{B1} = 0.1N$) along with the a_p values from code

provisions based on the NCEER study. Upon reviewing all of the maximum component amplification factors that resulted from the numerous analysis of stiff and flexible frames, the a_p results for near-fault ground motions used in this study consistently exceed the maximum code provided a_p, especially for elastic frames. The median values presented in the plots show the central measure of the results (see Fig. III.1). To provide conservatism, the design values are usually based on statistical measure of mean plus one standard deviation of results. Fig. III.1 also shows that when the primary structure is designed to dissipate energy through inelastic action, the median a_p values in the short-period range are greater for some of the frames when compared to current code provisions. Moreover, this study uses 5% critical damping for NSCs to generate the floor response spectra. Therefore, NSCs with smaller damping values would exhibit much larger component amplifications of 2 to 3 times the current values for 0.01% component damping, especially around the period ratio (T_C/T_{B1}) of 1.0.

Fig. III.2 shows the variation of the median values of a_p with the fundamental period of the supporting structure (T_{B1}). The a_{p1} and a_{p2} values are consistently greater than the code values of 2.5 and 1.0 respectively. As shown in Fig. III.2, it can be seen that second mode effects are dominant for frames with $T_{B1} \geq 0.6$ sec. For a stiff / flexible frame set with the same fundamental period, the a_p values are close. This demonstrates the weak dependence of a_p values on the number of stories of the frame.

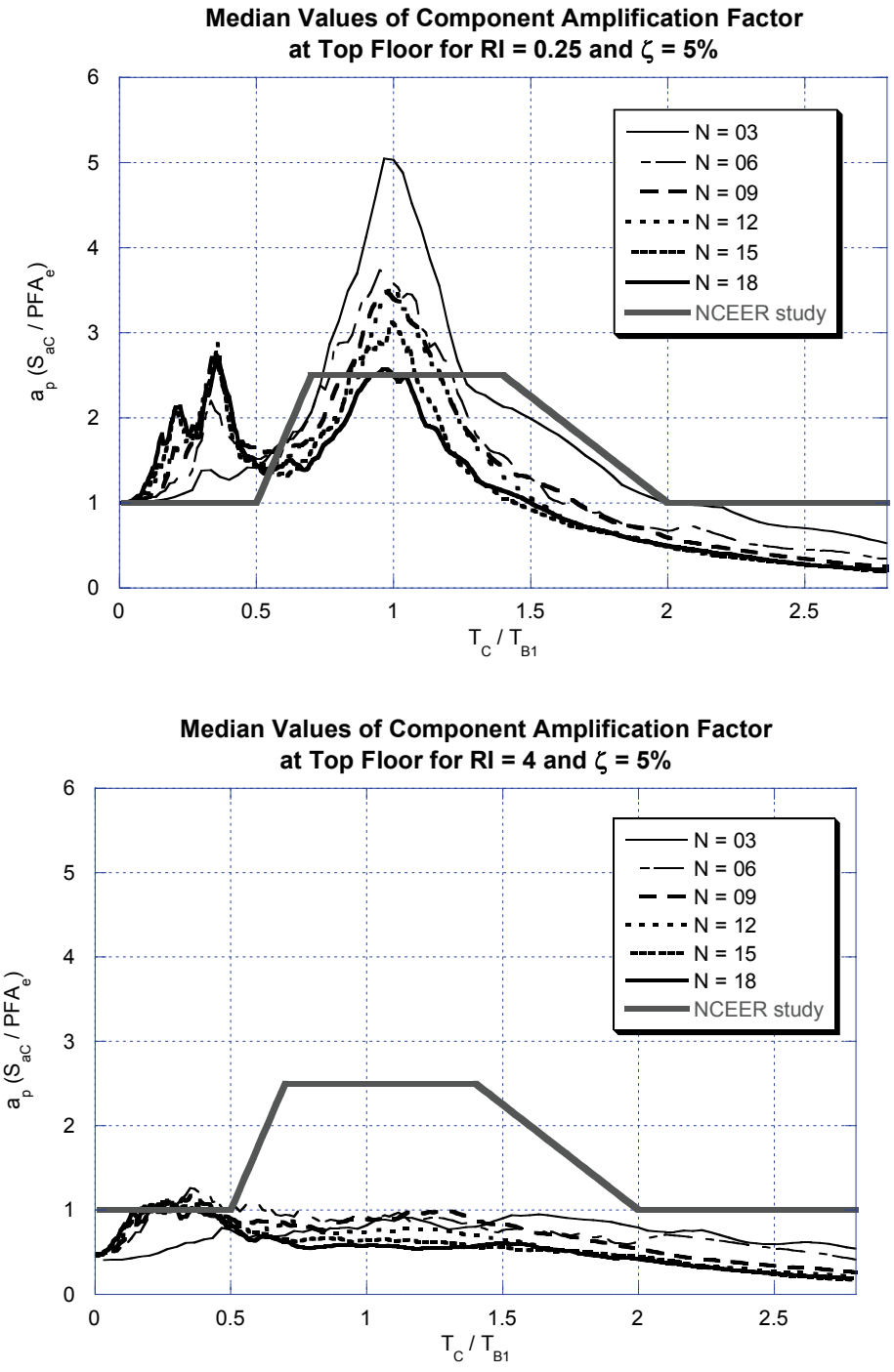

Figure III.1 Median values of component amplification factors at roof for stiff frames ($T_{B1} = 0.1N$)

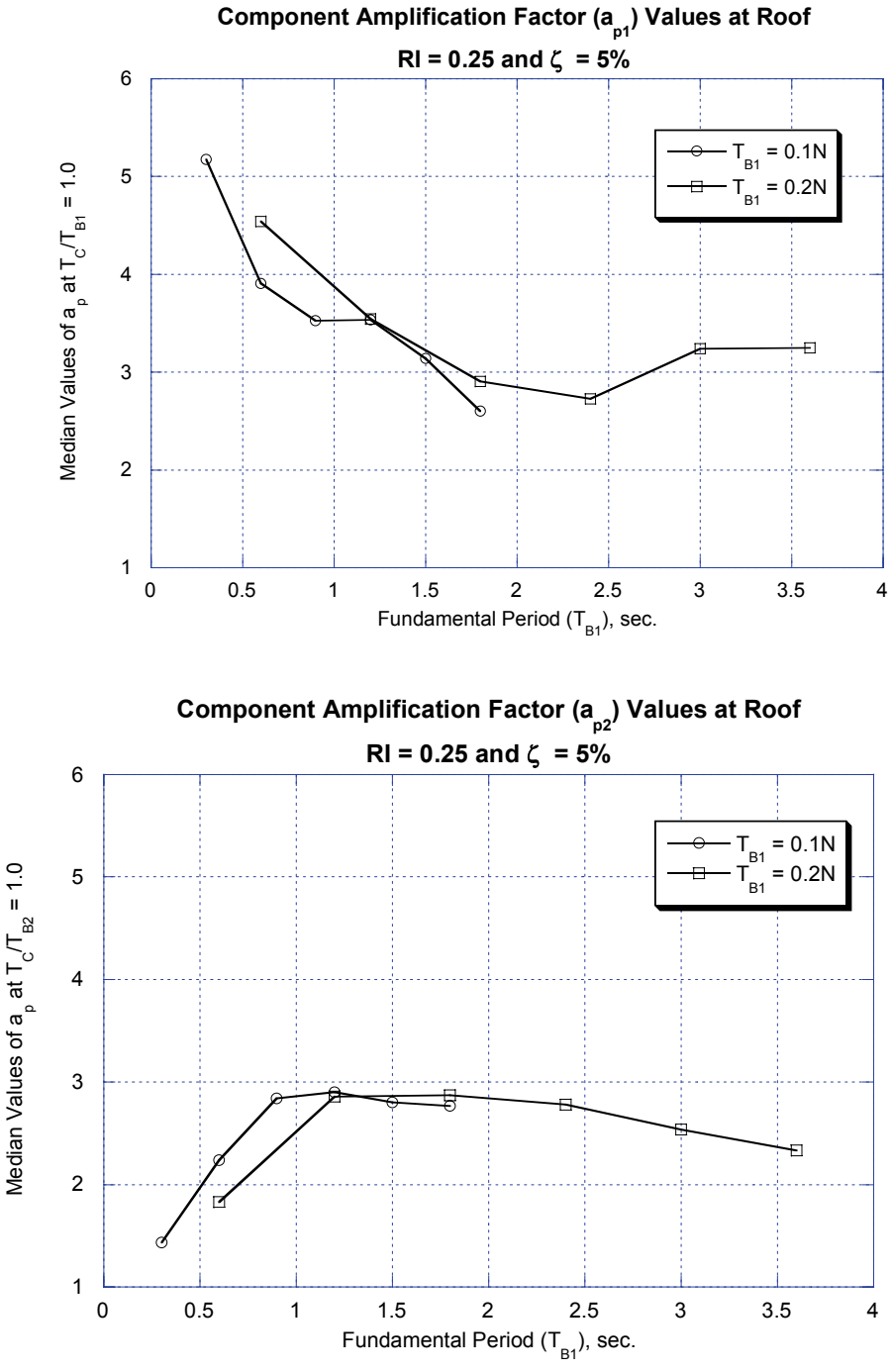

Figure III.2 Median a_{p1} and a_{p2} for elastic frames (RI = 0.25) at roof

Fig. III.3 shows the variation of R_{acc} values along height for 9-story frames when subjected to four levels of inelasticity represented by relative intensity values of 2, 4, 6, and 8. The median values around the fundamental period of the supporting structure are shown in the figure. It can be seen that for stiff frames, greater deamplification of the a_p peaks, as represented by the R_{acc} values, occur at the top two floor levels. The R_{acc} values are closer to the *RI* values at the top two story levels. For stories in the lower third of the building, the R_{acc} values are closer to unity, which represents no deamplification of the a_p values when compared to elastic frames. The variation of R_{acc} values along the height for flexible 9-story frame is similar to that of stiff frames but different in magnitude. The R_{acc} values at the top two story levels are greater than the values of stiff frames. The stiff and flexible frames provide upper and lower bounds for R_{acc} values for a given frame. The R_{acc} factors obtained for $N = 9$ frame in this appendix are similar in behavior to those obtained for ordinary ground motions in chapters 2 and 3. The current results encourage the development of a methodology for estimating the peak acceleration demands of near-fault ground motion sets based on similar principles.

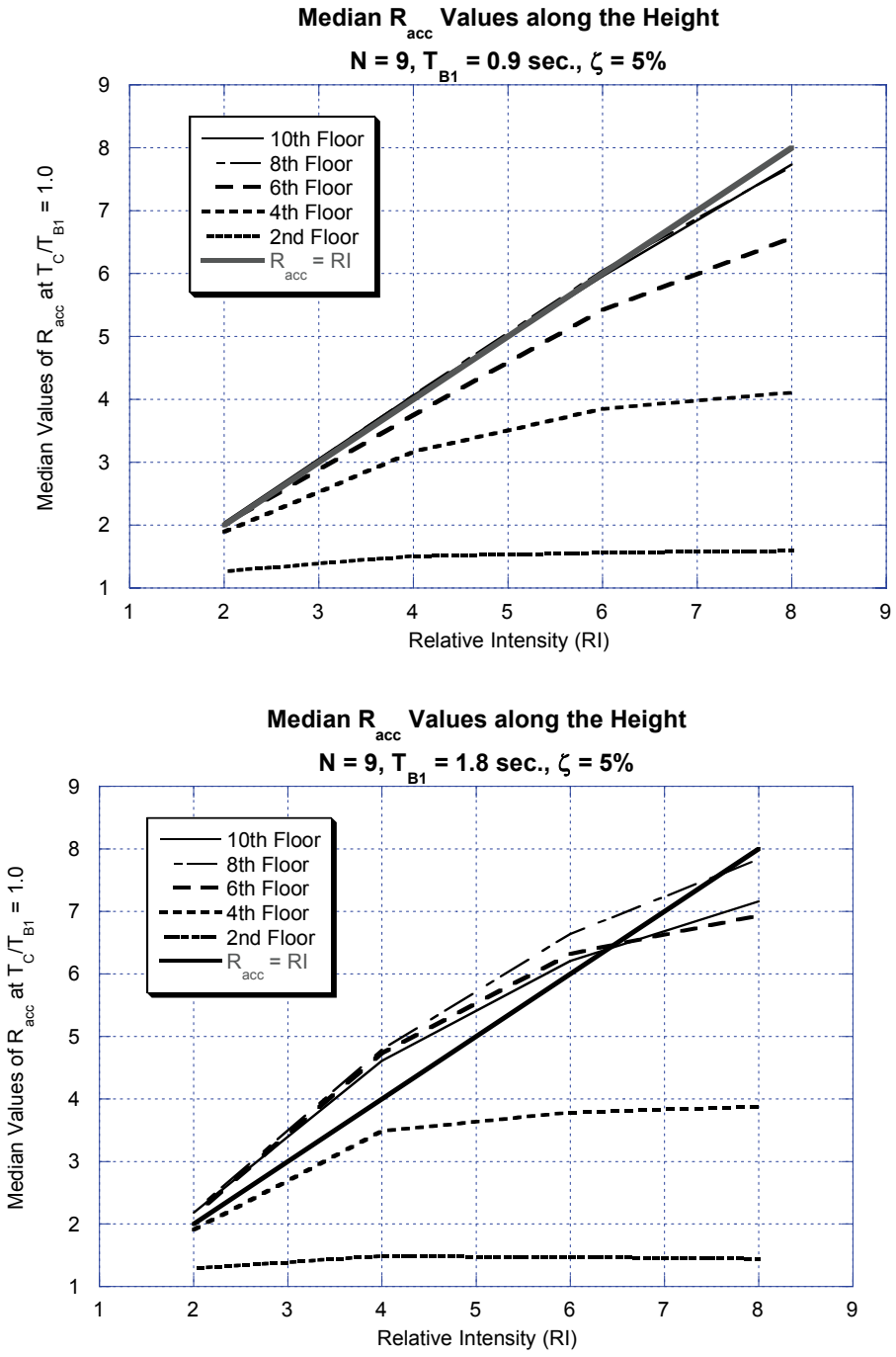

Figure III.3 Median values of R_{acc} along height for $N = 9$ frame

SUMMARY

In this appendix, an evaluation of the acceleration demands on NSCs when subjected to near-field fault-normal ground motions recorded in both soil and rock sites was performed. The focus is on NSCs that can be modeled as elastic SDOF systems and that are mounted on elastic and inelastic moment-resisting frame structures of various heights and periods, i.e., 3, 6, 9, 12, 15, and 18 story frames with periods that vary from 0. 3 seconds to 3.6 seconds. The results showed that similar to far-field ground motions, the FRS is dependent on the modal periods of the supporting structure, degree of inelastic behavior and location of the NSC in the structure. The variation of peak floor accelerations with height is also strongly dependent on the fundamental period of the supporting structure and its degree of inelastic behavior. The current US seismic code provisions underestimate the effects of the higher modes of the supporting structure on the peak acceleration demands experienced by NSCs especially in the short-period region of FRS. The application of the factor R_{acc} originally proposed for ordinary ground motions was also investigated. The R_{acc} values are similar in behavior to that of far-field ground motions. Future studies can attempt to develop unified methodologies that can account for both far-field and near-fault ground motion sets based on the acceleration response modification factor.

Bibliography

1. Adam, C. (2001). "Dynamics of elastic-plastic shear frames with secondary structures: shake table and numerical studies." *Earthquake Engineering & Structural Dynamics* 30(2): 257-277.

2. Alavi, B. and H. Krawinkler (2001). Effects of Near-Fault Ground Motions on Frame Structures. *Blume Report No. 138*. Stanford, CA, The John A. Blume Earthquake Engineering Center, Stanford University.

3. Amin, M., W. J. Hall, N. M. Newmark and R. P. Kassawara (1971). Earthquake response of multiple connected light secondary systems by spectrum methods. *Proceedings of ASME 1st National Congress on Pressure Vessels and Piping*. San Francisco, CA**:** 103 - 129.

4. Anderson, J. C., V. V. Bertero and R. D. Bertero (1999). Performance improvement of long period building structures subjected to severe pulse-type ground motions. *Report No. UCB/PEER 1999/09*. Berkeley, CA, Earthquake Engineering Research Center, University of California.

5. ASCE (2003). Minimum Design Loads for Buildings and Other Structures, SEI/ASCE 7-02. *ASCE Standard No. 7-02*. Reston, VA, American Society of Civil Engineers.

6. Aslani, H. and E. Miranda (2005). "Probability-based seismic response analysis." *Engineering Structures* 27(8): 1151-1163.

7. ATC (1999). Design Example Using Current UBC Requirements Briefing Paper 6 Part B: Design Example Using Current UBC Requirements. *ATC/SEAOC Training Curriculum: The Path to Quality Seismic Design and Construction (ATC-48)*. Redwood City, CA, Applied Technology Council.

8. ATC (2004). ATC-58 Project Task Report, Phase 2, Task 2.3, Engineering Demand Parameters for Nonstructural Components. Redwood City, CA, Applied Technology Council.

9. Bachman, R. (2003). *Session 6: EDPs for nonstructural components: Engineering demand parameters (EDPs) for nonstructural components*. 2003 PEER Annual Meeting, Palm Springs, CA.

10. Bachman, R. E., R. M. Drake and P. J. Richter (1993). 1994 update to 1991 NEHRP provisions for architectural, mechanical, and electrical components and systems. Buffalo, NY, National Center for Earthquake Engineering Research.

11. Biggs, J. M. and J. M. Roesset (1970). Seismic analysis of equipment mounted on a massive structure. *Seismic Design of Nuclear Power Plants*. R. J. Haused, MIT press**:** 319 - 343.

12. BSSC (2003). *The 2003 NEHRP Recommended Provisions For New Buildings And Other Structures Parts 1 and 2: Provisions and Commentary (FEMA 450)*. Washington DC, Federal Emergency Management Agency.

13. Bumpus, S., J. Johnson and P. Smith (1980). Best Estimate Method versus Evaluation Method: A Comparison of Two Techniques in Evaluating Seismic Analysis and Design. *UCRL52746; NUREGCR1489*, Lawrence Livermore National Lab., CA.

14. Chaudhuri, S. R. and T. C. Hutchinson (2004). Distribution of peak horizontal floor acceleration for estimating nonstructural element vulnerability. *13th World Conference on Earthquake Engineering*. Vancouver, BC, Canada.

15. Chen, Y. Q. and T. T. Soong (1988). "Seismic Response of Secondary Systems." *Engineering Structures* 10(4): 218-228.

16. Chopra, A. K. and C. Chintanapakdee (2001). "Comparing response of SDF systems to near-fault and far-fault earthquake motions in the context of spectral regions." *Earthquake Engineering & Structural Dynamics* 30(12): 1769-1789.

17. Chrysanthakopoulos, C., N. Bazeos and D. E. Beskos (2006). "Approximate formulae for natural periods of plane steel frames." *Journal of Constructional Steel Research* 62(6): 592-604.

18. Cornell, C. A. and R. T. Sewell (1989). Equipment response in linear and non-linear nuclear power plant structures: Small-magnitude versus design-type motions. *Proceedings: Engineering Characterization of Small-Magnitude Earthquakes; EPRI NP-6389*, Electric Power Research Institute.

19. Crowley, H. and R. Pinho (2004). "Period-height relationship for existing European reinforced concrete buildings." *Journal of Earthquake Engineering* 8: 93-119.

20. Dey, A. and V. K. Gupta (1998). "Response of multiply supported secondary systems to earthquakes in frequency domain." *Earthquake Engineering & Structural Dynamics* 27(2): 187-201.

21. Drake, R. M. and R. E. Bachman (1996). "NEHRP Provisions for 1994 for Nonstructural Components." *Journal of Architectural Engineering - ASCE* 2(1): 26 - 31.

22. Filiatrault, A., S. Kuan and R. Tremblay (2004a). "Shake table testing of bookcase - partition wall systems." *Canadian Journal of Civil Engineering* 31(4): 664-676.

23. Filiatrault, A., R. Tremblay and S. Kuan (2004b). "Generation of floor accelerations for seismic testing of operational and functional building components." *Canadian Journal of Civil Engineering* 31(4): 646-663.

24. Fu, Q. (2005). Modeling and prediction of fault-normal near-field ground motions and structural response. *Department of Civil and Environmental Engineering*. Stanford, CA, Stanford University. Doctoral Dissertation.

25. Goel, R. K. and A. K. Chopra (1997). "Period formulas for moment-resisting frame buildings." *Journal of Structural Engineering-ASCE* 123(11): 1454-1461.

26. Goel, R. K. and A. K. Chopra (1998). "Period formulas for concrete shear wall buildings." *Journal of Structural Engineering-ASCE* 124(4): 426-433.

27. Gould, N. C. (2003). "Earthquake Performance of Nonstructural Components." Retrieved December 2003, from http://www.irmi.com/Expert/Articles/2003/Gould01.aspx.

28. Griffin, M. J. (2006). Earthquake Performance of Nonstructural Components and Systems: Difficulties in achieving enhanced earthquake performance. *8th U.S. National Conference on Earthquake Engineering*. San Francisco, CA.

29. Gupta, A. and H. Krawinkler (1999). Seismic Demands for Performance Evaluation of Steel Moment Resisting Frame Structures. *JABEEC Report No. 132*. Palo Alto, CA, Department of Civil and Environmental Engineering, Stanford University.

30. Gupta, A. K. (1990). *Response spectrum method in seismic analysis and design of structures*. Boston, Blackwell Scientific Publications.

31. Hosseini, M. (2005). "Behavior of Nonstructural Elements in the 2003 Bam, Iran, Earthquake." *Earthquake Spectra* 21(S1): S439–S453.

32. ICC (2003). *2003 International Building Code*. Falls Church, VA, International Code Council.

33. Igusa, T. and A. Derkiureghian (1985). "Dynamic-Response of Multiply Supported Secondary Systems." *Journal of Engineering Mechanics-ASCE* 111(1): 20-41.

34. Igusa, T. and A. Derkiureghian (1992). "Interaction in Primary-Secondary Systems." *Journal of Pressure Vessel Technology-Transactions of the ASME* 114(1): 53-59.

35. Inel, M., E. M. Bretz, E. F. Black, M. A. Aschheim and D. P. Abrams (2001). USEE 2001: Utility Software for Earthquake Engineering - Report and User's Manual. Urbana, IL, Civil and Environmental Engineering, University of Illinois at Urbana-Champaign.

36. Islam, M. S. (1996). "Analysis of the Northridge earthquake response of a damaged non-ductile concrete frame building." *Structural Design of Tall Buildings* 5(3): 151-182.

37. Iwan, W. D. (1997). "Drift spectrum: Measure of demand for earthquake ground motions." *Journal of Structural Engineering-ASCE* 123(4): 397-404.

38. Jennings, P. C. (1971). Engineering features of the San Fernando earthquake of February 9, 1971. *EERL 71-02*. Pasadena, CA., California Institute of Technology, Earthquake Engineering Research Laboratory.

39. Kawakatsu, T., K. Kitade, T. Takemori, Y. Kuwabara and Y. Ogiwara (1979). Floor Response Spectra Considering Elasto-Plastic Behavior of Nuclear Facilities. *Transactions of the 5th International Conference on Structural*

Mechanics in Reactor Technology. T. Jaeger and B. A. Boley. Berlin, Germany, North-Holland Pub. Co. for the Commission of the European Communities. K9/4.

40. Kennedy, R. P., S. A. Short and N. M. Newmark (1981). The Response of a Nuclear Power Plant to Near-Field Moderate Magnitude Earthquakes. *Transactions of the 6th International Conference on Structural Mechanics in Reactor Technology*. Paris, France, North-Holland Pub. Co. for the Commission of the European Communities. K (a).

41. Krawinkler, H. (2005). Van Nuys Hotel Building Testbed Report: Exercising Seismic Performance Assessment. *PEER Report 2005/11*. Berkeley, CA, Pacific Earthquake Engineering Research Center.

42. Li, Y. R. and J. O. Jirsa (1998). "Nonlinear Analyses of an Instrumented Structure Damaged in the 1994 Northridge Earthquake." *Earthquake Spectra* 14(2): 245-264.

43. Lin, J. and S. A. Mahin (1985). "Seismic Response of Light Subsystems on Inelastic Structures." *Journal of Structural Engineering-ASCE* 111(2): 400-417.

44. LLNL (1980). Seismic Safety Margins Research Program. Executive Summary 1, Best Estimate Versus Evaluation Method - Report LLL-TB-026. Livermore, CA, Lawrence Livermore National Laboratory.

45. Loh, C. H. and H. M. Lin (1996). "Application of off-line and on-line identification techniques to building seismic response data." *Earthquake Engineering & Structural Dynamics* 25(3): 269-290.

46. McKevitt, W. E. (2004). "Reply to the discussion by R.D. Watts on "Proposed Canadian code provisions for seismic design of elements of structures, nonstructural components, and equipment"." *Canadian Journal of Civil Engineering* 31(2): 392-392.

47. Mckevitt, W. E., P. A. M. Timler and K. K. Lo (1995). "Nonstructural Damage from the Northridge Earthquake." *Canadian Journal of Civil Engineering* 22(2): 428-437.

48. Medina, R. A. and H. Krawinkler (2004). Seismic Demands for Nondeteriorating Frame Structures and Their Dependence on Ground Motions. *PEER Report 2003/15*. Berkeley, CA, Pacific Earthquake Engineering Research Center.

49. Medina, R. A., R. Sankaranarayanan and K. M. Kingston (2006). "Floor response spectra for light components mounted on regular moment-resisting frame structures." *Engineering Structures* 28(14): 1927-1940.

50. Miranda, E. and S. Taghavi (2003). Towards the prediction of seismic performance of nonstructural elements. *2003 SEAOC Convention*. Squaw Creek, CA.

51. Miranda, E. and S. Taghavi (2005). "Approximate floor acceleration demands in multistory buildings. I: Formulation." *Journal of Structural Engineering-ASCE* 131(2): 203-211.

52. Moehle, J. P. (2003). *A framework for performance-based earthquake engineering*. Tenth U.S.-Japan Workshop on Improvement of Building Structural Design and Construction Practices, Redwood City, CA, Applied Technology Council, Report ATC-15-9.

53. Myrtle, R. C., S. E. Masri, R. L. Nigbor and J. P. Caffrey (2005). "Classification and prioritization of essential systems in hospitals under extreme events." *Earthquake Spectra* 21(3): 779-802.

54. Naeim, F. (2000). Learning from Structural and Nonstructural Seismic Performance of 20 Extensively Instrumented Buildings. *12th World Conference on Earthquake Engineering*. Auckland, New Zealand.

55. Naeim, F. and R. Lobo (1998). Performance of Nonstructural Components During the January 17, 1994 Northridge Earthquake - Case Studies of Six Instrumented Multistory Buildings. *ATC-29-1 Seminar on Seismic Design, Retrofit, and Performance of Nonstructural Components*. San Francisco, CA.

56. Nakashima, M., K. Ogawa and K. Inoue (2002). "Generic frame model for simulation of earthquake responses of steel moment frames." *Earthquake Engineering & Structural Dynamics* 31(3): 671-692.

57. Nayfeh, A. H. and D. T. Mook (1979). *Nonlinear Oscillations*. New York, Wiley.

58. NRC (1978). Regulatory Guide 1.122 - Development of Floor Design Response Spectra for Seismic Design of Floor-Supported Equipment or Components. Rev. 1, U.S. Nuclear Regulatory Commission.

59. PEER. (2003). "PEER Strong Motion Database." Retrieved December, 2003, from http://peer.berkeley.edu/smcat.

60. Phan, L. T. and A. W. Taylor (1996). State of the Art Report on Seismic Design Requirements for Nonstructural Building Components. *Report NISTIR 5857*, National Institute of Standards and Technology, Gaithersburgh, MD.

61. Prakash, V., G. H. Powell and S. Campbell (1993). DRAIN-2DX: basic program description and user guide. *Report No. UCB/SEMM 93-17*. Berkeley, CA, Department of Civil Engineering, University of California.

62. Retamales, R., G. Mosqueda, A. Filiatrault and A. M. Reinhorn (2006). Experimental Study on the Seismic Behavior of Nonstructural Components Subjected to Full-Scale Floor Motions. *8th U.S. National Conference on Earthquake Engineering*. San Francisco, CA**:** Paper No. 1359.

63. Rodriguez, M. E., J. I. Restrepo and A. J. Carr (2002). "Earthquake-induced floor horizontal accelerations in buildings." *Earthquake Engineering & Structural Dynamics* 31(3): 693-718.

64. Sackman, J. L., A. Derkiureghian and B. Nouromid (1983). "Dynamic Analysis of Light Equipment in Structures - Modal Properties of the Combined System." *Journal of Engineering Mechanics-ASCE* 109(1): 73-89.

65. Sackman, J. L. and J. M. Kelly (1979). "Seismic Analysis of Internal Equipment and Components in Structures." *Engineering Structures* 1(4): 179-190.

66. Sankaranarayanan, R. and R. A. Medina (2006). Estimation of Seismic Acceleration Demands of Nonstructural Components Exposed to Near-Fault Ground Motions. *First European Conference on Earthquake Engineering and Seismology*. Geneva, Switzerland**:** Paper Number: 1248.

67. Saudy, A., T. Aziz and A. Ghobarah (1994a). "A New Stochastic-Analysis for Multiple Supported MDOF Secondary System .2. Tuning and Spatial Coupling Effects." *Nuclear Engineering and Design* 147(3): 251-262.

68. Saudy, A., T. Aziz and A. Ghobarah (1994b). "A New Stochastic-Analysis for Multiple Supported MDOF Secondary Systems .1. Dynamic Interaction Effects." *Nuclear Engineering and Design* 147(3): 235-249.

69. Saudy, A., T. Aziz and A. Ghobarah (1995). "A Stochastic-Analysis for Multiple Supported Mdof Secondary Systems." *Journal of Pressure Vessel Technology-Transactions of the Asme* 117(2): 182-188.

70. Scholl, R. E. (1984). Nonstructural Issues of Seismic Design and Construction. *EERI 84-04*. Oakland, CA, Earthquake Engineering Research Institute.

71. Segal, D. and W. J. Hall (1989). Experimental seismic investigation of appendages in structures. *Civil Engineering Studies, Structural Research Series No. 545*. Urbana, IL, University of Illinois.

72. Seneviratna, G. D. P. K. and H. Krawinkler (1997). Evaluation of Inelastic MDOF Effects for Seismic Design. *JABEEC Report No. 120*. Palo Alto, CA, Department of Civil and Environmental Engineering, Stanford University.

73. Sewell, R. T., C. A. Cornell, G. R. Toro and R. K. McGuire (1986). A study of factors influencing floor response spectra in nonlinear multi-degree-of-freedom structures. *JABEEC Report No. 82*. Palo Alto, CA, Department of Civil and Environmental Engineering, Stanford University.

74. Sewell, R. T., C. A. Cornell, G. R. Toro, R. K. Mcguire, R. P. Kassawara, A. Singh and J. C. Stepp (1987). Factors influencing equipment response in linear and nonlinear structures. *9th International Conference on Structural Mechanics in Reactor Technology*. F. H. Wittmann. Lausanne, Switzerland, AA Balkema, Rotterdam. K2**:** 849-856.

75. Singh, A. K. and A. H. S. Ang (1974). "Stochastic Prediction of Maximum Seismic Response of Light Secondary Systems." *Nuclear Engineering and Design* 29(2): 218-230.

76. Singh, M. P. (1975). "Generation of Seismic Floor Spectra." *Journal of the Engineering Mechanics Division-ASCE* 101(5): 593-607.

77. Singh, M. P. (1990). *An overview of techniques for analysis of nonstructural components*. ATC-29 seminar on seismic design and performance of equipment and nonstructural elements in buildings and industrial structures.

78. Singh, M. P., T. S. Chang and L. E. Suarez (1996). Floor Response Spectrum amplification due to yielding of supporting structure. *Eleventh World Conference on Earthquake Engineering*. Acapulco, Mexico.

79. Singh, M. P., L. M. Moreschi, L. E. Suarez and E. E. Matheu (2006a). "Seismic design forces. I: Rigid nonstructural components." *Journal of Structural Engineering-ASCE* 132(10): 1524-1532.

80. Singh, M. P., L. M. Moreschi, L. E. Suarez and E. E. Matheu (2006b). "Seismic design forces. II: Flexible nonstructural components." *Journal of Structural Engineering-ASCE* 132(10): 1533-1542.

81. Singh, M. P., L. E. Suarez, E. E. Matheu and G. O. Maldonado (1993). Simplified Procedures for Seismic Design of Nonstructural Components and Assessment of Current Code Provisions. *NCEER-93-0013*. Buffalo, NY, National Center for Earthquake Engineering Research, State University of New York at Buffalo.

82. Somerville, P. G. (2003). "Magnitude scaling of the near fault rupture directivity pulse." *Physics of the Earth and Planetary Interiors* 137(1-4): 201-212.

83. Somerville, P. G. and R. W. Graves (2003). "Characterization of earthquake strong ground motion." *Pure and Applied Geophysics* 160(10-11): 1811-1828.

84. Somerville, P. G., N. F. Smith, R. W. Graves and N. A. Abrahamson (1997). "Modification of Empirical Strong ground Motion Attenuation Relations to Include the Amplitude and Duration Effects of Rupture Directivity." *Seismological Research Letters* 68(1): 199-222.

85. Soong, T. T. (1994). Seismic behavior of nonstructural elements state-of-art report. *10th European Conference on Earthquake Engineering*. Vienna, Austria.

86. Soong, T. T., G. Shen, Z. Wu, R. H. Zhang and M. Grigoriu (1993). Assessment of the 1991 NEHRP provisions for nonstructural components and recommended revisions. *NCEER-93-0003*. Buffalo, NY, National Center for Earthquake Engineering Research, State University of New York at Buffalo.

87. SPSS Inc. (2004a). *SPSS base 13.0 user's guide*. Chicago, IL, SPSS Inc.

88. SPSS Inc. (2004b). *SPSS regression models 13.0*. Chicago, SPSS Inc.

89. Taghavi, S. and E. Miranda (2003). Probabilistic Study of Peak Floor Acceleration Demands in Linear Structures. *Ninth International Conference*

on Applications of Statistics and Probability in Civil Engineering. San Francisco. 2**:** 1565-1572.

90. Taghavi, S. and E. Miranda (2005). "Approximate floor acceleration demands in multistory buildings. II: Applications." *Journal of Structural Engineering-ASCE* 131(2): 212-220.

91. Todorovska, M. I., S. S. Ivanovic and M. D. Trifunac (2001). "Wave propagation in a seven-story reinforced concrete building I. Theoretical models." *Soil Dynamics and Earthquake Engineering* 21(3): 211-223.

92. Toro, G. R., R. K. McGuire, C. A. Cornell and R. T. Sewell (1989). Linear and nonlinear response of structures and equipment to California and Eastern United States earthquakes. *EPRI Report NP-5566*. Palo Alto, CA, Electric Power Research Institute.

93. Trifunac, M. D., S. S. Ivanovic and M. I. Todorovska (1999a). Instrumented 7-Storey Reinforced Concrete Building in Van Nuys, California: Description of the Damage from the 1994 Northridge Earthquake and Strong Motion Data. *Report CE 99-02*. Los Angeles, CA., Department of Civil Engineering, University of Southern California.

94. Trifunac, M. D., S. S. Ivanovic, M. I. Todorovska, E. I. Novikova and A. A. Gladkov (1999b). "Experimental evidence for flexibility of a building foundation supported by concrete friction piles." *Soil Dynamics and Earthquake Engineering* 18(3): 169-187.

95. Vamvatsikos, D. and C. A. Cornell (2002). "Incremental dynamic analysis." *Earthquake Engineering & Structural Dynamics* 31(3): 491-514.

96. Villaverde, R. (1991). "Approximate formulas to calculate the seismic response of light attachments to buildings." *Nuclear Engineering and Design* 128(3): 349-368.

97. Villaverde, R. (1997a). "Method to improve seismic provisions for nonstructural components in buildings." *Journal of Structural Engineering* 123(4): 432-439.

98. Villaverde, R. (1997b). "Seismic design of secondary structures: State of the art." *Journal of Structural Engineering-ASCE* 123(8): 1011-1019.

99. Villaverde, R. (2004). Seismic Analysis and Design of Nonstructural Components. *Earthquake Engineering: From Engineering Seismology to Performance-Based Engineering*. Y. Bozorgnia and V. V. Bertero, CRC.

100. Villaverde, R. (2005). "Approximate Procedure for the Seismic Nonlinear Analysis of Nonstructural Components in Buildings." *Journal of Seismology and Earthquake Engineering* 7(1): 9-24.

101. Villaverde, R. (2006). "Simple method to estimate the seismic nonlinear response of nonstructural components in buildings." *Engineering Structures* 28(8): 1209-1221.

102. Wang, Q. F. and L. Y. Wang (2005). "Estimating periods of vibration of buildings with coupled shear walls." *Journal of Structural Engineering-ASCE* 131(12): 1931-1935.

103. Watts, R. D. (2004). "Discussion of "Proposed Canadian code provisions for seismic design of elements of structures, nonstructural components, and equipment"." *Canadian Journal of Civil Engineering* 31(2): 391-391.

104. Wesley, D. A. and P. S. Hashimoto (1981). Nonlinear Structural Response Characteristics of Nuclear Power Plant Shear Wall Structures. *Transactions of the 6th International Conference on Structural Mechanics in Reactor Technology*. Paris, France, North-Holland Pub. Co. for the Commission of the European Communities. K (a).

105. Ye, L. P. and S. Otani (1999). "Maximum seismic displacement of inelastic systems based on energy concept." *Earthquake Engineering & Structural Dynamics* 28(12): 1483-1499.